UCRL-9065

UNIVERSITY OF CALIFORNIA

Ernest O. Lawrence Radiation Laboratory

TWO-WEEK LOAN COPY

This is a Library Circulating Copy which may be borrowed for two weeks. For a personal retention copy, call Tech. Info. Division, Ext. 5545

BERKELEY, CALIFORNIA

DISCLAIMER

This document was prepared as an account of work sponsored by the United States Government. While this document is believed to contain correct information, neither the United States Government nor any agency thereof, nor the Regents of the University of California, nor any of their employees, makes any warranty, express or implied, or assumes any legal responsibility for the accuracy, completeness, or usefulness of any information, apparatus, product, or process disclosed, or represents that its use would not infringe privately owned rights. Reference herein to any specific commercial product, process, or service by its trade name, trademark, manufacturer, or otherwise, does not necessarily constitute or imply its endorsement, recommendation, or favoring by the United States Government or any agency thereof, or the Regents of the University of California. The views and opinions of authors expressed herein do not necessarily state or reflect those of the United States Government or any agency thereof or the Regents of the University of California.

UCRL-9065

UNIVERSITY OF CALIFORNIA

Lawrence Radiation Laboratory
Berkeley, California

Contract No. W-7405-eng-48

A REVIEW OF NUCLEAR FISSION

PART TWO - FISSION PHENOMENA AT MODERATE AND HIGH ENERGY

Earl K. Hyde

February 1960

Crystal structure transformations in inorganic
nitrites, nitrates, and carbonates
QD921 Rao, Chintamani Nagesa Ramachandra.
R215 Crystal structure transformations in
1975 inorganic nitrites, nitrates, and carbonates
[by] C.N.R.Rao, B. Prakash and M. Natarajan.
[Washington] National Bureau of Standards, 1975.
48 p. (NSRDS-NBS 53)

1. Crystals. 2. Phase rule and equilibrium.
I. Prakash, Brahm, 1912- II. Natarajan,
M III. Title. IV. Series: U.S.
National Bureau of Standards. National Stan-
dard Reference Data Series, NSRDS-NBS 53.

A REVIEW OF NUCLEAR FISSION

PART TWO - FISSION PHENOMENA AT MODERATE AND HIGH ENERGY

Earl K. Hyde

February 1960

Author's note: Part One of this review entitled, "Fission Phenomena at Low Energy" has appeared as the report UCRL-9036. Both reports are self-contained reviews which may later be incorporated in a larger work covering many other aspects of the nuclear physics of the heavy elements. This larger work is being prepared under the authorship of E. K. Hyde, I. Perlman and G. T. Seaborg. This material is being given limited circulation at this time in hope that it will provide a useful review in its present form. The author would be grateful for comments on the material, for notification of errors, or for new information concerning the topics discussed herein.

A REVIEW OF NUCLEAR FISSION

PART TWO - FISSION PHENOMENA AT MODERATE AND HIGH ENERGY

12.1 FISSION PHENOMENA AT MODERATE EXCITATION ENERGY

12.1.1 General Comments on Fission Induced by Charged Particles

12.1.2 Fission Cross Sections at Moderate Excitation Energy

12.1.3 The Application of a Statistical Model to Compound Nucleus Reactions in Non-Fissile Heavy Elements

12.1.4 Competition of Fission and Neutron Emission in the Interaction of Charged Particles with Heavy Elements $Z \geqq 90$.

12.1.5 Competition of Fission and Neutron Emission in the Interaction of Charged Particles with Target Elements below Thorium

12.1.6 Fission Product Yield Distributions as a Function of Energy

12.1.7 Angular Distribution of Fission Fragments

12.1.8 Fission Induced by Heavy Ions

12.2 NUCLEAR REACTION PHENOMENA INCLUDING FISSION AT HIGH BOMBARDMENT ENERGY

12.2.1 The Serber Model

12.2.2 Monte Carlo Calculations of Nuclear Cascade

12.2.3 Monte Carlo Calculations of the Evaporation Cascade

12.2.4 Spallation-Fission Competition in the Evaporation Cascade

12.2.5 Summary Comments on Serber Model of High Energy Reactions

12.2.6 Fission Cross Sections at High Energy

12.2.7 Photoemulsion Studies of High Energy Fission

12.2.8 Radiochemical Study of Bismuth Fission Induced by High Energy Particles

12.2.9 Radiochemical Study of Uranium and Thorium Fission Induced by High Energy Particles

12.3 FISSION INDUCED BY MESONS

12.4 PHOTOFISSION

12.4.1 Photofission Probability

12.4.2 Fission Product Yield Distributions in Photofission

12.4.3 Photofission Probability at Very High Photon Energies - Photomesonic Fission

A REVIEW OF NUCLEAR FISSION

PART TWO - FISSION PHENOMENA AT MODERATE AND HIGH ENERGY

12.1 FISSION PHENOMENA AT MODERATE EXCITATION ENERGY

12.1.1 General Comments on Fission Induced by Charged Particles. It is interesting to consider the changes which occur in the fission reaction as we turn from spontaneous fission or slow-neutron-induced fission on the one hand to fission induced at moderate excitation energy on the other. We shall talk first about the fission of heavy nuclei ($Z \geq 90$) induced by charged particles of moderate energy. By "moderate" energy we shall mean an energy range of a few Mev up to roughly 50 Mev - a range in which compound nucleus formation is the chief mechanism for the nuclear reaction. We shall first briefly summarize what is known of fission in nuclear reactions of this type and we shall then proceed to a more detailed examination of the experimental data. It is impossible to discuss fission induced by charged particles without at the same time considering the competing reactions which we group together under the term "spallation."

The primary reaction usually involves the initial formation of a compound nucleus excited to an energy which is the sum of the kinetic energy of the bombarding particle plus the Q-value for the incorporation of this particle into the compound nucleus. This excitation energy is assumed to be rapidly distributed back and forth over all the possible degrees of freedom of the compound nucleus and is eventually disposed of by ejection (evaporation) of particles, by nuclear fission, or by gamma ray emission. For the heavy nuclei in which we are interested, neutron emission is so much more probable than emission of charged particles that we can often neglect charged particle evaporation. Also gamma ray emission is a slow process and does not compete significantly with neutron emission or fission except at an excitation energy below the thresholds for both these processes. The de-excitation of highly excited heavy nuclei reduces for the most part to a competition between neutron emission and fission. A typical evaporation chain is shown in the Figure 12.1.

Fission is a very unlikely process when lead or bismuth is bombarded with protons, deuterons or helium ions and de-excitation occurs chiefly by neutron emission. The chief reaction products of proton, deuteron and helium ion bombardment are the (p,xn), (d,xn) and (α,xn) products, respectively where x specifies

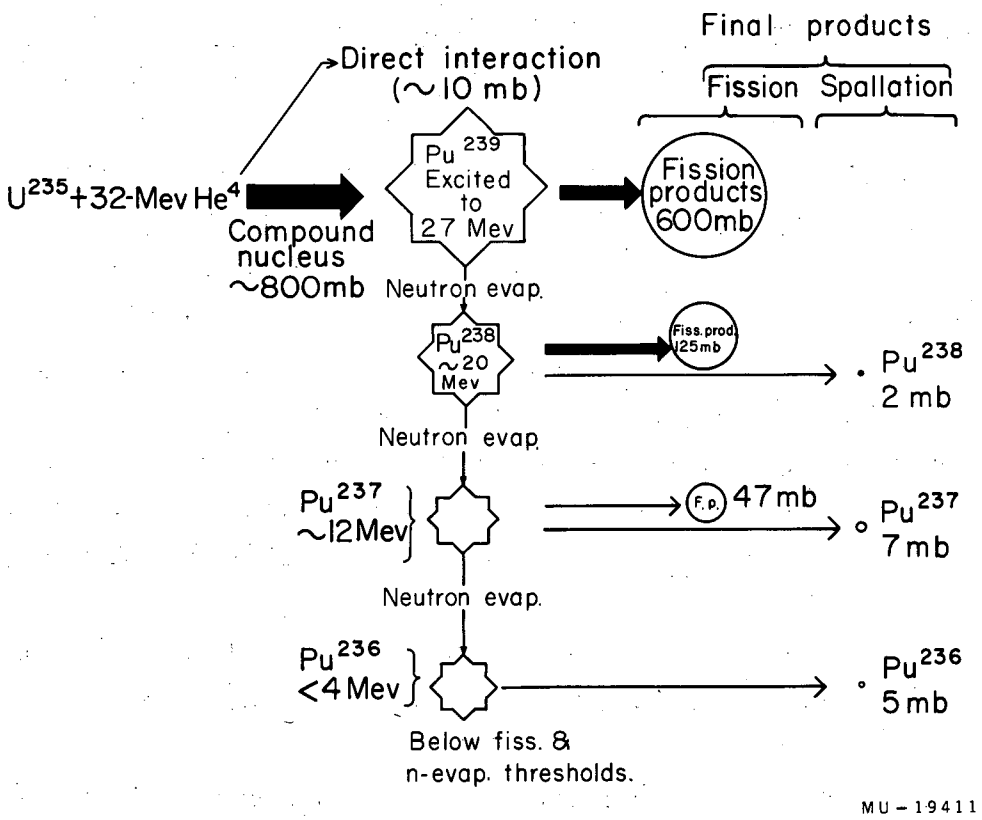

Fig. 12.1 The interaction of U^{235} with 30 Mev helium ions used as an illustration of the origin of fission products and spallation products via the compound nucleus route when a heavy element is caused to fission by bombardment with charged particles of moderate energy.

the number of evaporated neutrons. The yield of each specific product has a characteristic rise and fall as a function of the bombarding energy. There is a threshold at the point where enough energy becomes available for the evaporation of x neutrons, a rise to a maximum, and then a fall as a new threshold is passed for the evaporation of x + 1 neutrons. A typical example of such excitation functions is shown in Fig. 12.2 where the (p,xn) products of the bombardment of bismuth are displayed. From statistical considerations, from reasonable assumptions on the energy spectrum of evaporated neutrons, and from nuclear reaction radii of heavy nuclei, it is possible to develop mathematical expressions to fit such data as those shown in the figure and to predict cross sections for unmeasured products. We shall later discuss such a reaction model developed by JACKSON.[1]

When the target element is thorium, or uranium, or some element of higher atomic number, the fission probability is at least comparable with the probability of neutron emission. Hence it is necessary to consider fission competition at each step in the neutron evaporation chain. Fission may occur before any neutrons are emitted, or after one neutron is emitted, after two neutrons are emitted, etc. The (p,xn), (d,xn), and (α,xn) reaction cross sections still show the characteristic rise and fall as the energy of the bombarding particle is increased and the positions of the maxima in the cross section peaks are nearly the same as they would be without fission competition. However, the cross section curves are markedly reduced and the observed peak heights of the successive products along the evaporation chain are smaller and smaller because of additional losses to fission at each successive evaporation step.

It is still possible to use a statistical evaporation model to describe the experimental results, but only after modification of the model to include fission competition. We consider such a modified model below.

From a consideration of the experimental data one can reach certain tentative conclusions on the relative probability for neutron emission and fission as a function of various parameters. This probability is often expressed in terms of the "widths" for neutron emission or fission. The ratios

---

1. J. D. Jackson, Can. J. Phys. 34, 767 (1956).

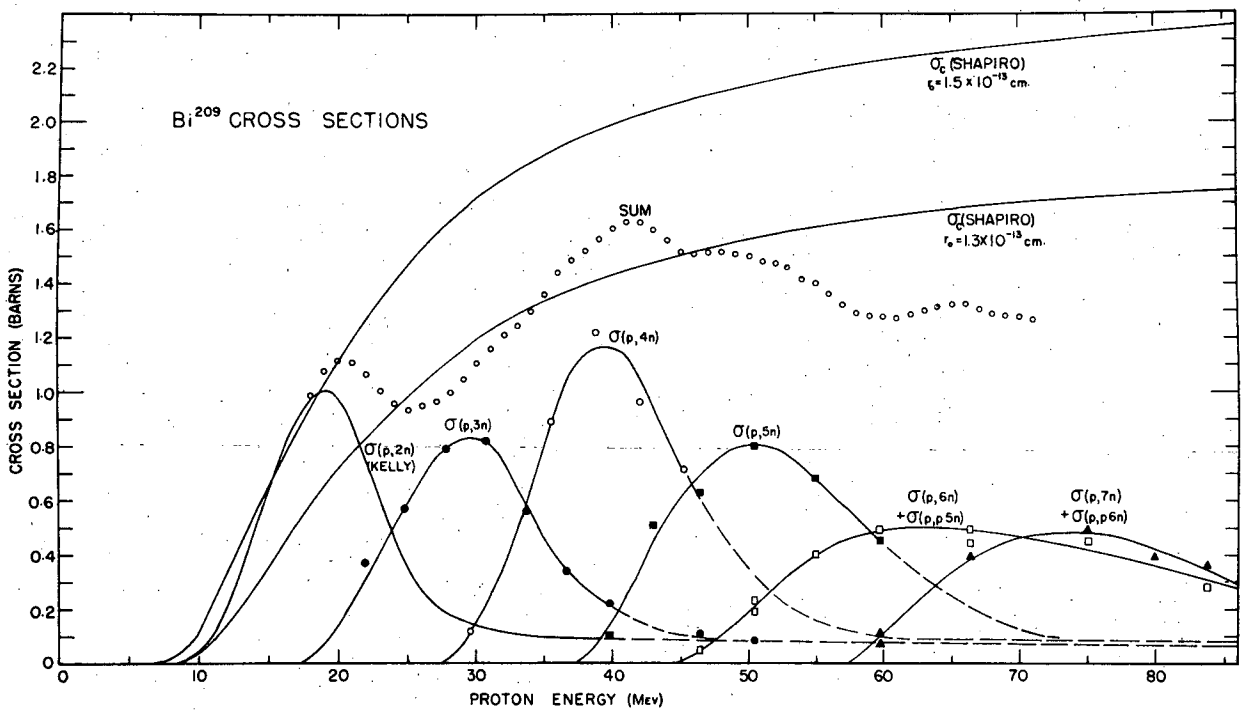

MU-19328

Fig. 12.2 A typical example of the excitation functions for (p,xn), (d,xn), and (α,xn) products when the target element is from the lead-bismuth group of elements. This particular figure is taken from the work of BELL and SKARSGARD and shows the excitation functions for Bi^{209}(p,xn) reactions. Can.J.Phys. 34, 745 (1956).

$\frac{\Gamma_n}{\Gamma_n + \Gamma_f}$ or $\frac{\Gamma_n}{\Gamma f}$ are those of chief interest. It has been concluded that for the heaviest elements (Z = 90 or greater) the ratio $\frac{\Gamma_n}{\Gamma_f}$ decreases as the atomic number increases but is also subject to a strong mass number dependence (fissionability decreases with increasing A). There is no marked dependence of the $\frac{\Gamma_n}{\Gamma_f}$ ratio on excitation energy, although there are differing interpretations as to the exact nature of the trends which may be discernible in the data.

The pattern of fission product yields as a function of energy of the bombarding particles undergoes a uniform change which seems to be largely independent of the target element or the bombarding particles. This typical change is illustrated in Fig. 12.3. At low bombarding energy, a twin-peaked curve resembling that observed in slow-neutron induced fission is found. At higher energies the yields corresponding to symmetric fission increase rapidly and the valley fills in. It is important to note, however, that the positions of the asymmetric fission peaks do not appear to change appreciably with excitation energy. The peaks appear to shift slightly to lower mass because of the emission of more neutrons but the increase in symmetric fission is not a result of the two asymmetric peaks moving together. In fact, the overall width of the mass yield distribution <u>increases</u> as the excitation energy is raised; the relative yield of very asymmetric fission increases at the same time that the relative yield of symmetric fission rises. The twin-peaked distribution characteristic of low-energy fission gives way to a broad single-humped curve with a rather flat top when the energy of the deuterons reaches about 20 Mev and the energy of helium ions reaches about 40 Mev.

The overall fission product distribution is often interpreted as the superposition of two fundamentally different types of fission, an asymmetric and a symmetric mode.* The probability for each type of fission and other characteristics of each type of fission, such as the details of the mass division, undergo independent changes as a function of the excitation energy. To make the situation even more complex, the radiochemical results in many cases reflect an average distribution for two or more fissioning nuclei at varying

---

* One of the first suggestions that it was meaningful to discuss the mass yield curve in terms of an asymmetric and a symmetric fission mode was made by TURKEVICH AND NIDAY, Phys. Rev. <u>84</u>, 52 (1951).

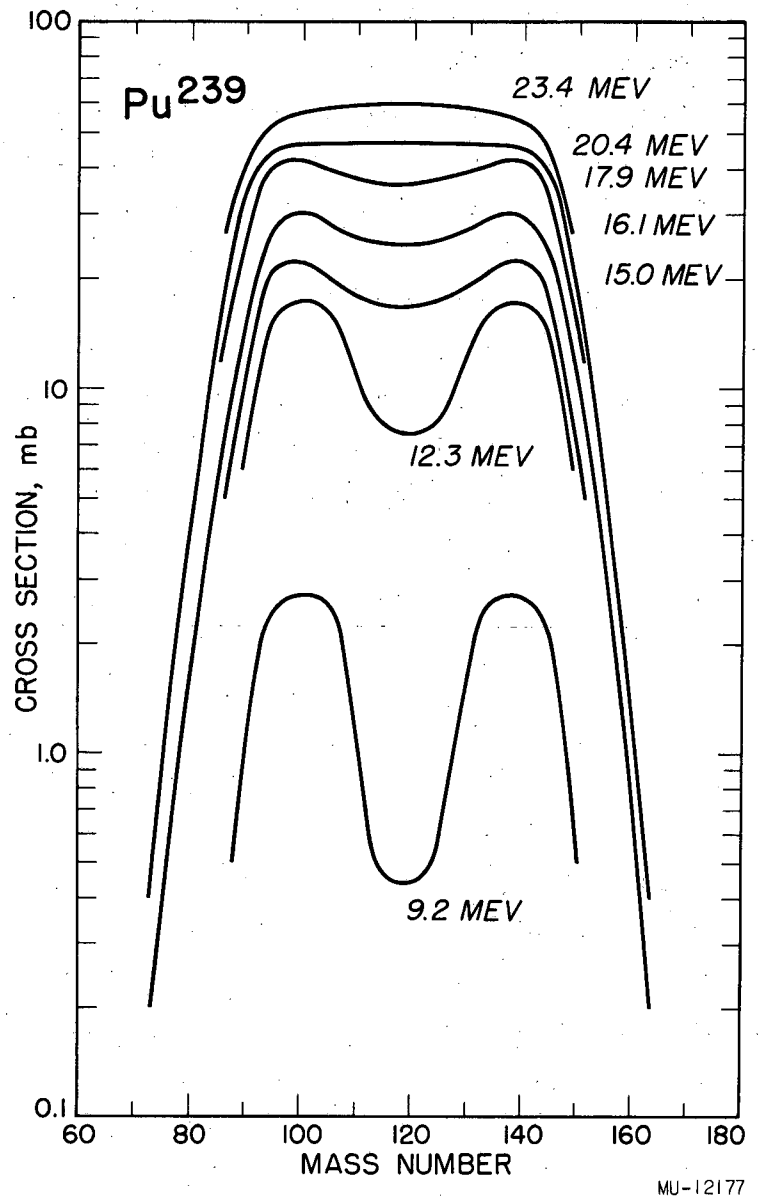

Fig. 12.3 Variation of fission yield curves with energy for deuteron induced fission of Pu^{239}. From GIBSON in report UCRL-3493. Similar sets of curves have been found for fission caused by other charged particles, by photons and by neutrons.

levels of excitation because of the occurrence of fission at more than one stage of the evaporation chain. In the study of many other features of fission as for example the angular distribution of the fission fragments one runs into the same problem that the results are an average for a mixture of fissioning nuclei so that the exact behavior of a specific fissioning nucleus excited to a specific energy has to be extracted from the data in an indirect fashion.

The mass distribution of the fission products observed in the bombardment of lead or bismuth targets with deuterons or helium ions of moderate energy is decidedly different. A symmetric distribution in mass is observed and the width of the distribution is much smaller than observed in any other case of symmetric mass splitting. The results probably represent mainly a single nuclear species excited only slightly above the fission threshold. This fission threshold may refer to a symmetric saddle point quite different from the saddle point which leads to the asymmetric division of heavier nuclei. As the excitation energy increases the width of the mass division increases until at very high energies the appearance of the mass yield curve is similar to that for very high energy fission of uranium. The ratio $\frac{\Gamma_f}{\Gamma_n}$ is extremely low for near-threshold fission in the lead-bismuth group of targets but, contrary to the thorium-uranium group of targets, this ratio increases rapidly as a function of energy. There is some evidence that it levels off at high excitation energy.

The mass yield curves for fission of intermediate nuclei such as radium and actinium are intermediate in character. In the fission of radium bombarded with 11 Mev protons, for example, one sees a three-humped, mass-yield curve which receives its most direct interpretation as a superposition of symmetric and asymmetric fission types occurring with about equal probability. At higher bombarding energies the mass yield curve soon turns into an overall broad symmetric distribution with no indication of three peaks. This shows that the probability for the symmetric type of fission increases more rapidly with energy.

We summarize these general observations on the mass distribution of fission products in the schematic diagram Fig. 12.4. It is tempting to interpret the experimental data as suggested above in terms of an asymmetric and a symmetric mode of fission. The fission threshold for asymmetric fission lies lower in the heaviest elements and higher in the lead-bismuth region. In an intermediate group of elements centering around radium and actinium the two fission thresholds are apparently quite close.

	Fission Probability	Shape of Mass Yield Curve: Near threshold	Exc. energy 10-40 Mev	Exc. energy > 40 Mev
HIGHLY-FISSILE ELEMENTS (Thorium and heavier elements)	Asymmetric fission threshold lies lower Γ_f/Γ_n moderate to high σ_f approaches σ_{TOTAL}. Not strongly dependent on excitation energy	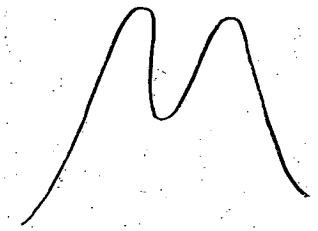		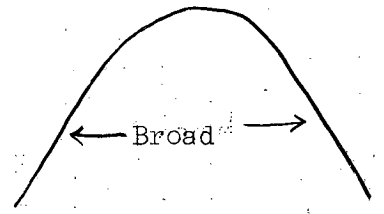
INTERMEDIATE ELEMENTS (Actinium, radium, etc.)	Symmetric and asymmetric fission thresholds about equal Γ_f/Γ_n low. Asymmetric fission does not increase with excitation. Symmetric fission increases rapidly and soon washes out asymmetric fission	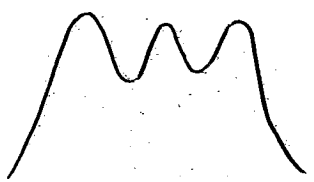	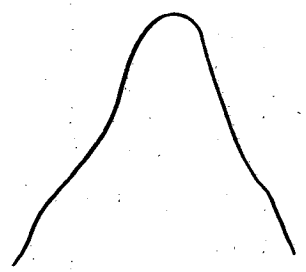	
SLIGHTLY-FISSILE ELEMENTS (Lead-Bismuth)	Symmetric fission threshold lies lower Γ_f/Γ_n very low but increases markedly with energy; but σ_{fiss} never approaches σ_{TOTAL} Symmetric fission predominant Γ_f/Γ_n levels off at high excitation	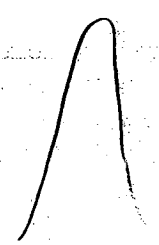	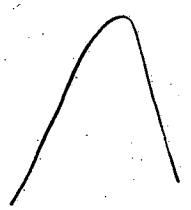	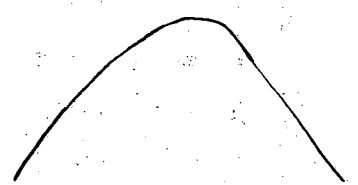

Fig. 12.4 Characteristics of fission.

In the moderate energy range which we are now considering, the majority of reactions involve the initial formation of a compound nucleus but there are a significant number of events which go by other reaction mechanisms which we can consider together under the general heading of direct interactions.

The strong competition by fission for the de-excitation of the compound nucleus and the intermediate nuclei in the evaporation chain has the obvious consequence that the cross sections for the (α,xn) processes are greatly reduced. It has another consequence, not so clearly anticipated, that other nuclear reaction types not proceeding by a compound nucleus mechanism become evident. For example, the (α,pxn) reaction cross sections are of the same order of magnitude (a few millibarns) as those for the (α,xn) reaction when uranium or plutonium targets are bombarded. The (α,pxn) reaction products cannot be produced by the compound nucleus mechanism because proton evaporation is strongly repressed by the Coulombic barrier in the heavy elements. Furthermore, the (α,pxn) excitation functions do not show a peak characteristic of an evaporation process but rise steadily. Hence the (α,pxn) reactions involve direct interaction processes. The same comments apply to (d,pxn) and (p,pxn) reactions.

Even in the (α,xn), (d,xn) and (p,xn) type reactions there is evidence of a sizable contribution to the total cross section by non-compound nucleus mechanisms. The (α,n), the (d,n), and (p,n) reactions never have cross sections above a few millibarns, do not show a peak of the type predicted by compound nucleus theory, and decrease only slowly at high beam energy. Hence, a major fraction of the cross section is attributed to direct interaction. The excitation functions for the (α,2n) and (d,2n) reactions have peaks characteristic of compound nucleus formation but in addition, have high energy extensions ("tails") which must be attributed to other mechanisms. Such a mechanism, for example, might involve the following in the case of the (α,2n) reaction: The incoming helium ion strikes a neutron in the nucleus ejecting it with a sizable amount of the initial energy of the helium ion. The helium ion is amalgamated with the nucleus and residual energy is removed by the evaporation of a second neutron.

In the (α,p2n) or (d,p2n) cases, the reactions are more properly described as (α,t) or (d,t) reactions as has been shown by the work of WADE, GONZALEZ-VIDAL, GLASS AND SEABORG.[2] These investigators studied the yield of

2. W. H. Wade, J. Gonzlez-Vidal, R.A. Glass, and G.T. Seaborg, Phys. Rev. 107 1311, (1957).

tritium in heavy element targets and found it large enough to account for the entire (α,p2n) or (d,p2n) cross section as determined by measuring the heavy element product. The energy and angular distribution of the tritons were those expected of a direct interaction ("stripping" or "pick-up") process and quite unlike those predicted by a compound nucleus mechanism.

The total cross section for all reactions of the non-compound nucleus type is not a large fraction of the total reaction cross section. It probably is not much greater than it is in the case for bismuth and other non-fissionable heavy element targets. In the latter case, however, these reactions are not very apparent because the (α,xn), (d,xn), or (p,xn) cross sections are so huge. For the fissionable elements the large (α,xn), (d,xn) and (p,xn) reaction probabilities are reduced markedly so that they are comparable in magnitude to those resulting from less probable reactions. This feature lends a great deal of interest to the detailed study of the spallation reactions in the fissionable elements. It has not been possible to be very specific about the mechanism of the direct interaction processes since these are not well understood; some more specific discussion of the spallation reactions under consideration here are given in the references cited, but the relative importance of stripping, knock-on, pick-up and "local excitation" reactions is not established.

It may be worth mentioning at this point that the study of the interaction of heavy ions with heavy element targets will be quite interesting since there is some evidence that non-compound nucleus reactions are of appreciable magnitude. Such mechanisms may be of considerable importance in by-passing the severe fission competition which tends to eliminate transuranium element nuclides produced by compound-nucleus-type reactions.

12.1.2 Fission Cross Sections at Moderate Excitation Energy. Shortly after the discovery of slow neutron fission, it was observed that fission could be induced in uranium by its bombardment with charged particles, but it was some years before quantitative measurements were made.

JUNGERMAN AND WRIGHT[3] measured fission excitation functions in thorium and uranium when these were bombarded with deuterons of energy ranging up to 18.8 Mev and by helium ions of energy up to 37.6 Mev. The basis of the method was a determination of gross fission product beta activity. This somewhat inaccurate method was improved upon by JUNGERMAN[4] who developed an ion chamber method for direct measurement of fission pulses in charged particle beams. Using Th^{232}, U^{235} and U^{238} targets, he showed that there was a fission threshold at about 7 Mev for deuterons and at about 18 Mev for helium ions. Above these thresholds the fission cross sections rose rapidly with beam energy to values representing a high percentage of the total geometric cross section for these elements. A sampling of JUNGERMAN'S results is given in Table 12.1. An extension of these measurements to higher energies is reviewed in Section 12.2.6 below. MC CORMICK AND COHEN[5] bombarded the same target nuclides with protons ranging up to 22 Mev in energy. A sampling of their results is also given in the table. In all cases a major fraction of the total reaction cross section went into fission, but this percentage was appreciably less for thorium than for uranium.

It is also possible to measure fission cross sections radiometrically by quantitative analysis of individual fission products and by suitable integration of the mass-yield curve. A number of determinations of this type are listed in Table 12.1 for thorium, uranium, neptunium and plutonium targets. Values of the fission cross section at other bombardment energies than those listed as well as values of individual spallation cross sections can be found in the reference listed.

Values of the fission cross section for neutron induced fission as a function of the neutron energy were covered in Section 11.3 of the previous chapter. (UCRL-9036) Photofission probability is covered later in this chapter in Section 12.3.1.

3. J. Jungerman and S. C. Wright, Phys. Rev. 74, 150 (1948)
4. J. Jungerman, Phys. Rev. 79, 632 (1950)
5. G. H. McCormick and B. L. Cohen, Phys. Rev. 96, 722 (1954).

Table 12.1 Fission Cross Sections for Fission Induced by Protons, Deuterons or Helium Ions of Energy Less than 50 Mev*

Target Nucleus	Bombarding Particle	Energy (Mev)	Fission Cross-section (barns)	% Spallation	Method	Reference**
Rh	α	40.8	2.1×10^{-6}	100	Radiochemistry	21a
Bi	d	15	1.6×10^{-7}	~100	Radiochemistry	20
		22	1×10^{-5}	~100	Radiochemistry	
Ra^{226}	p	11	~.002	99		6
Ra^{226}	d	22	.050	96		20,21
Ra^{226}	n	3.3	.0004			21a
		7	.003			21a
		23	.037			21a
Th^{232}	d	7.7	2×10^{-4}			
		10	.04		Ionization chamber	4
		15	.28			
		17	.40			
Th^{232}	α	18.2	4×10^{-4}			
		25	.17		Ionization chamber	4
		30	.55			
		34	.75			
Th^{232}	α	37.5	~0.6		Radiochemistry	7
Th^{232}	p	21.5	0.83	35	Radiochemistry	8
Th^{232}	α	15.6-19.6	9×10^{-4}			
	α	19.8	0.021			
	α	25.7-28.9	0.560±0.140		Radiochemistry	9
	α	34.9-37.7	0.88±0.22			
	α	43.4-45.9	1.6±0.40			
U^{233}	α	23.5	0.184	98.8		
	α	35.3	1.27	98.8	Radiochemistry	10,11
	α	44	1.99	98		
U^{233}	d	9.0	0.125			
		12.1	0.60	97		
		15.4	1.1	97	Radiochemistry	14,15
		23.4	1.9	98		
U^{233}	p	22.8	1.29	10	Prop. ctr.	21c

Table 12.1 (cont'd.)

Target Nucleus	Bombarding Particle	Energy (Mev)	Fission Cross-section (barns)	% Spallation	Method	Reference
U^{235}	α	20.5	.010	9	[illegible]	[illegible]
		23.1	.087	7.4		
		25.9	.310	5.5		
		28.2	.580	3.3	Radiochemistry	21b
		33.8	1.030	1.9		
		39.9	1.380	1.4		
		21.9	0.58			
		26.8	0.42		Radiochemistry	10,12
		34.1	1.29			
		45	1.84			
U^{235}	p	21.5	1.31		Radiochemistry	8
		22.8	1.28	11	prop. ctr.	21c
U^{235}	d	8.2	.003			
		10.0	.06		Ion-chamber	4
		15.0	0.6			
		17	0.85			
U^{235}	α	19.5	.004			
		22.8	.10		Ion-chamber	4
		25	.22			
		30	.65			
U^{238}	α	22.6	0.13			
		27.1	0.89		Radiochemistry	10,13
		38.6	1.48			
		45.4	1.50			
U^{238}	p	22.8	1.22	12	prop. ctr.	21c
		21.5	1.28		Radiochemistry	8
		10	0.029		Radiochemistry	16a
		32	1.47			
U^{238}	α	18.0	.001	~70		
		20	.011	~41	Radiochemistry and mass spectroscopy	18
		32.5	.790	10.7		
		43	.986	9		

Table 12.1 (cont'd.)

Target Nucleus	Bombarding Particle	Energy (Mev)	Fission Cross-section (barns)	% Spallation	Method	Reference
U^{238}	d	8	.001		Ion-chamber	4
		10	.06			
		15	.40			
U^{238}	α	19	.001		Ion-chamber	4
		25	.20			
		30	.60			
		35	.83			
U^{238}	d	5	0.0035		Radiochemistry	19a
		10	0.086			
		13.6	0.430			
		20	1.03		Radiochemistry	16a
		50	1.61			
Np^{237}	α	19.8	0.013		Radiochemistry	14,15
		22.7	0.13	93		
		31.5	0.72	97		
		45.7	1.36	97		
Pu^{239}	d	9.2	0.05		Radiochemistry	14,15
		15.0	0.59	93		
		20.2	1.4	96		
		23.4	1.8	97		
Pu^{239}	α	20.2	.005	18	Radiochemistry	16,17
		24.5	0.125	6.1		
		34	0.31	6.6		
		40.7	0.78	3.2		
		47.5	1.9	1.3		
Pu^{238}	α	25.2	0.430	4.4	Radiochemistry	16,17
		30.2	0.98	2.3		
		47.4	1.40	2.3		
Pu^{240}	d	12.4	0.367		Radiochemistry	19
		15.4	0.995			
		21.2	1.3			

* $\sigma_{fission}$ for high energy neutrons and protons are given in Tables 12.19-12.22, Section 12.2.6.

** Fission cross sections are given for a number of other energies and fission cross section curves as a function of energy are given in the original references. Reference numbers refer to footnote entries in text.

References

6. R. C. Jensen and A. W. Fairhall, Phys. Rev. 109, 942 (1958).

7. A. S. Newton, "The Fission of Thorium with Alpha Particles", Phys. Rev. 75, 17 (1949).

8. G. H. McCormick and B. L. Cohen, "Fission and Total Reaction Cross Sections for 22 Mev Protons on Th^{232}, U^{235} and U^{238}", Phys. Rev. 96, 722 (1954).

9. B. M. Foreman, "Spallation Fission Competition in Thorium Bombarded with Helium Ion", Ph.D. Thesis, University of California Radiation Laboratory Report UCRL-8223 (1958).

10. R. Vandenbosch, T. D. Thomas, S. E. Vandenbosch, R. A. Glass and G. T. Seaborg, "Spallation Fission Competition in Heaviest Elements; Helium-Ion Induced Reactions in Uranium Isotopes", Phys. Rev. 111, 1358 (1958).

11. T. D. Thomas, "Spallation-Fission Competition from the Compound System U^{233} plus He^{4}", Ph.D. Thesis, University of California Radiation Laboratory Report, UCRL-3791 (1957).

12. R. Vandenbosch, "Fission and Spallation Competition in Ra^{226}, Th^{230}, U^{235} and Np^{237}", Ph.D. Thesis, University of California Radiation Laboratory Report, UCRL-3858 (1957).

13. S. E. Ritsema, "Fission and Spallation Excitation Functions of U^{238}", University of California Radiation Laboratory Report, UCRL-3266 (1956).

14. W. M. Gibson, "Fission and Spallation Competition from the Intermediate Nuclei Am^{241} and Np^{235}", University of California Radiation Laboratory Report, UCRL-3493 (1957).

15. B. M. Foreman, W. M. Gibson, R. A. Glass and G. T. Seaborg, "Spallation Fission Competition in Heavy Element Reactions; Th^{232}+He^{4} and U^{233}+ d", Phys. Rev. 116, 382 (1959).

16. R. A. Glass, R. J. Carr, J. W. Cobble and G. T. Seaborg, "Spallation Fission Competition in Heaviest Elements; Helium Ion Induced Reactions in Plutonium Isotopes", Phys. Rev. 104, 434 (1956).

16a. P. C. Stevenson, H. G. Hicks, W. Nervik and D. R. Nethaway, Phys. Rev. 111, 886 (1958).

17. R. A. Glass, "Studies in the Nuclear Chemistry of Plutonium, Americium and Curium", University of California Radiation Laboratory Report, UCRL-2560, April, 1954.

18. J. Wing, W. J. Ramler, A. L. Harkness and J. R. Huizenga, "Excitation Functions of U^{235} and U^{238} Bombarded with Helium and Deuterium Ions", Phys. Rev. 114, 163 (1959).

19. E. V. Luoma, "Deuteron-Induced Spallation and Fission Reactions in Plutonium Isotopes", University of California Radiation Laboratory, UCRL-3495, November, 1956.

19a. T. T. Sugihara, P. J. Drevinsky, E. J. Troianello and J. M. Alexander, Phys. Rev. 108, 1264 (1957).

20. A. W. Fairhall, "Fission of Bismuth with 15 and 22 Mev Deuterons", Phys. Rev. 102, 1335 (1956). A. W. Fairhall, R. C. Jensen and E. F. Neuzil, Paper P/677, Chapter 15, Proceedings of the Second United Nations Conference on the Peaceful Uses of Atomic Energy, Geneva, 1958.

21. A. W. Fairhall and E. F. Neuzil, Phys. Rev.

21a. R. D. Griffioen and J. W. Cobble, Unpublished, see thesis by R. D. Griffioen, Purdue University, 1960.

21b. R. Gunnick and J. W. Cobble, Phys. Rev. 115, 1247 (1959).

21c. C. B. Fulmer, Phys. Rev. 116, 418 (1959).

12.1.3. The Application of a Statistical Model to Compound Nucleus Reactions in Non-Fissile Heavy Elements. There have been a number of experimental studies of the yields of the principal heavy element nuclides produced by the bombardment of lead and bismuth targets with charged particles of moderate energy: bismuth + deuterons (KELLY AND SEGRÈ[22,23] RAMLER[24]); bismuth + helium ions (KELLY AND SEGRÈ[22,23] RAMLER[24]; bismuth + protons (KELLY[22], ANDRE[25]); lead + protons (BELL AND SKARSGARD[26]); lead + helium ions (JOHN[27]). The data from several of these studies are summarized in Section 7.4.1 of Chapter 7. The excitation functions for the (p,xn), (d,xn) and (α,xn) products are all very much alike and it has been possible to fit the data rather satisfactorily with a statistical model developed by JACKSON[28] which we now discuss.

Let us consider a nucleus excited to energy E and assume that this nucleus will de-excite only by neutron emission as long as this is energetically possible. Let us assume further that the neutron spectrum is given by

$$P(n) = E \exp \quad -E/T \qquad (12.1)$$

where the nuclear temperature T is taken to be constant. This assumption of constant nuclear temperature is contrary to the assumptions inherent in most nuclear models but it is doubtful that any large errors are introduced by this approximation.

---

22. E. Kelly, Ph.D. Thesis, University of California; see also University of California Radiation Laboratory Report, UCRL-1044, Dec. 27, 1950.
23. E. L. Kelley and E. Segrè, Phys. Rev. 75, 999 (1949)
24. W. J. Ramler, J. Wing, D. J. Henderson and J. R. Huizenga, Phys. Rev. 114, 154 (1959).
25. Andre, Huizenga, Mech, Ramler, Rauk, and Rochlin, Phys. Rev. 101, 645 (1956).
26. R. E. Bell and H. M. Skarsgard, Can. J. Phys. 34, 745 (1956).
27. W. John, Phys. Rev. 103, 704, (1956).
28. J. D. Jackson, Can. J. Phys. 34, 767 (1956).

With these assumptions JACKSON then shows that the probability that a nucleus with initial excitation E will evaporate exactly x neutrons is given by

$$P(E,x) = I(\Delta_x, 2x-3) - I(\Delta_{x+1}, 2x-1) \qquad (12.2)$$

where I(z,n) is Pearson's incomplete gamma function,

$$I(z,n) = (1/n!)\int_0^z y^n e^{-y}\, dy, \text{ and } \Delta x = (E-\sum_i^x B_i)/T \qquad (12.3)$$

B_i is the binding energy for the ith neutron and T is the nuclear temperature. The first term of these Pearson functions (equation 12.2) gives the probability that at least x neutrons will be evaporated from the compound nucleus, and the second term gives the probability that at least (x+1) neutrons will be evaporated. The difference of these two terms gives the probability that the compound nucleus will emit only x neutrons.

Figure 12.5 shows how the function P(E,x) appears as a function of E/T. To construct these curves $\bar{B}/T$ was set equal to 4.0; $\bar{B}$ is the average neutron binding energy. In the lower range of bombarding energies where all the interactions of the bombarding particle with the target nucleus involve the initial formation of a compound nucleus the cross section for the (p,xn), (d,xn), and (α,xn) products are given by simple functions of the type

$$\sigma_{(p,xn)} = \sigma_c\,(E_o)\, P(E,x) \qquad (12.4)$$

where P(E,x) is given in expression 12.2 and $\sigma_c(E_o)$ is the reaction cross section for an incident proton of energy E_o as given by the curves of SHAPIRO[29]; this evaluation involves a choice of a nuclear radius for which the best choice appears to lie in the range $R = 1.35 - 1.50 \times 10^{-13} A^{1/3}$ from the curve-fitting trials of several authors using the JACKSON model. The energy E in Eq. 12.4 is approximately equal to the kinetic energy of the incoming particle corrected for the Q-value of compound nucleus formation.

At somewhat higher energies not all reactions go by the compound nucleus reaction since a certain fraction go by the SERBER[30] mechanism involving primary interactions of the incoming particles with individual nucleons in the

29. M. M. Shapiro, Phys. Rev. 90, 171 (1953)

30. R. Serber, Phys. Rev. 72, 1114 (1947)

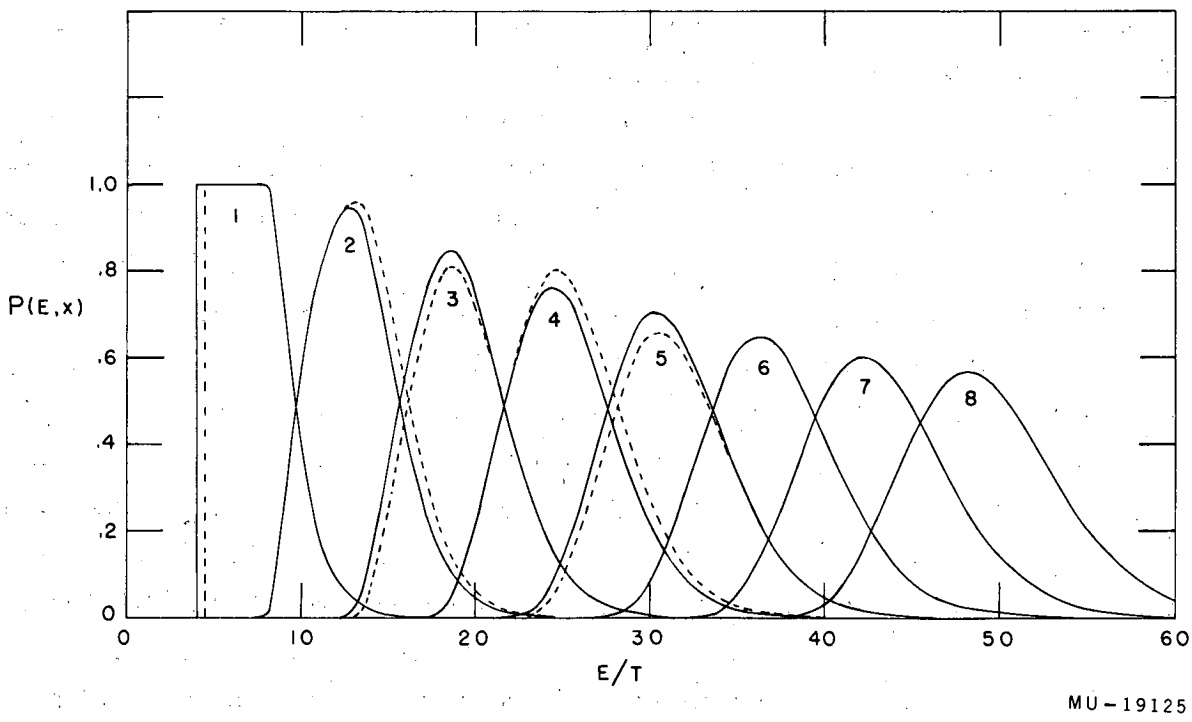

Fig. 12.5 The probabilities P(E,x) that a nucleus with excitation energy E will evaporate exactly x neutrons as a function of E/T where T is the nuclear temperature. The curves are for $\bar{B}/T = 4.0$, $\bar{B}$ is the average neutron binding energy. The effect of the alternation of the successive neutron binding energies is shown by the dotted curves (appropriate for even neutron number targets). From JACKSON.[28]

nucleus in a series of quasi-free two-body collisions. The incident particle may pass through the nucleus without any interaction or it may make a few collisions with nucleons in the nucleus knocking some of them out and perhaps escaping itself. Hence the primary interaction may involve the emission of a few prompt particles, random in number and in amount of kinetic energy. The residual nuclei may be left with a wide range of different excitations. The second step of the reaction is the evaporation of further particles mostly neutrons from the excited residual nucleus.

This reaction mechanism is very prominent at high ranges of bombarding particle energies - say 100 Mev or greater - and we shall have more to say about it in Section 12.2 below. In the energy range below 50 Mev, which we are now discussing, it enters only as a minor correction. JACKSON[28] discusses how Monte Carlo calculations of the prompt knock-on cascade process can be incorporated with his evaporation model to predict cross sections of the (p,xn) reaction types for protons of energy ranging up to 100 Mev. Figure 12.6 is his curve showing (p,xn) cross sections as a function of incident proton energy for x = 1,2 ...8 with the constants appropriate for Bi^{209} targets. The binding energy of the incident proton is 5.0 Mev, the average neutron binding energy is 7.3 Mev, and the nuclear temperature is approximately 1.8 Mev. The nuclear radius constant was set equal to 1.35×10^{-13} cm. As the energy increases the effects of the internal multiple collision cascade become apparent. A given cross section has the usual compound nucleus peak but has a "tail" extending up to higher energies. The magnitude of this tail goes up as the number of evaporated neutrons increases while the peak height goes down.

Comparison of these curves with the experimental results of BELL AND SKARSGARD[26], who analyzed the products from (p,xn) reactions in targets of Pb^{206}, Pb^{207}, Pb^{208} and Bi^{209}, showed good general agreement of theory and experiment as far as the general features of the reactions are concerned. RAMLER, WING, HENDERSON, AND HUIZENGA[31] compared their experimental results for the reactions Bi^{209} (α,2n), Bi^{209} (α,3n), Bi^{209} (α,4n) and Bi^{209} (d,n), Bi^{209} (d,2n) and Bi^{209} (d,3n) with the predictions of the JACKSON model and got good agreement except for a high energy "tail" on the (d,n) experimental curve, which they attributed to a stripping process.

---

31. W. J. Ramler, J. Wing, D. J. Henderson and J. R. Huizenga, Phys. Rev. 114, 154 (1959).

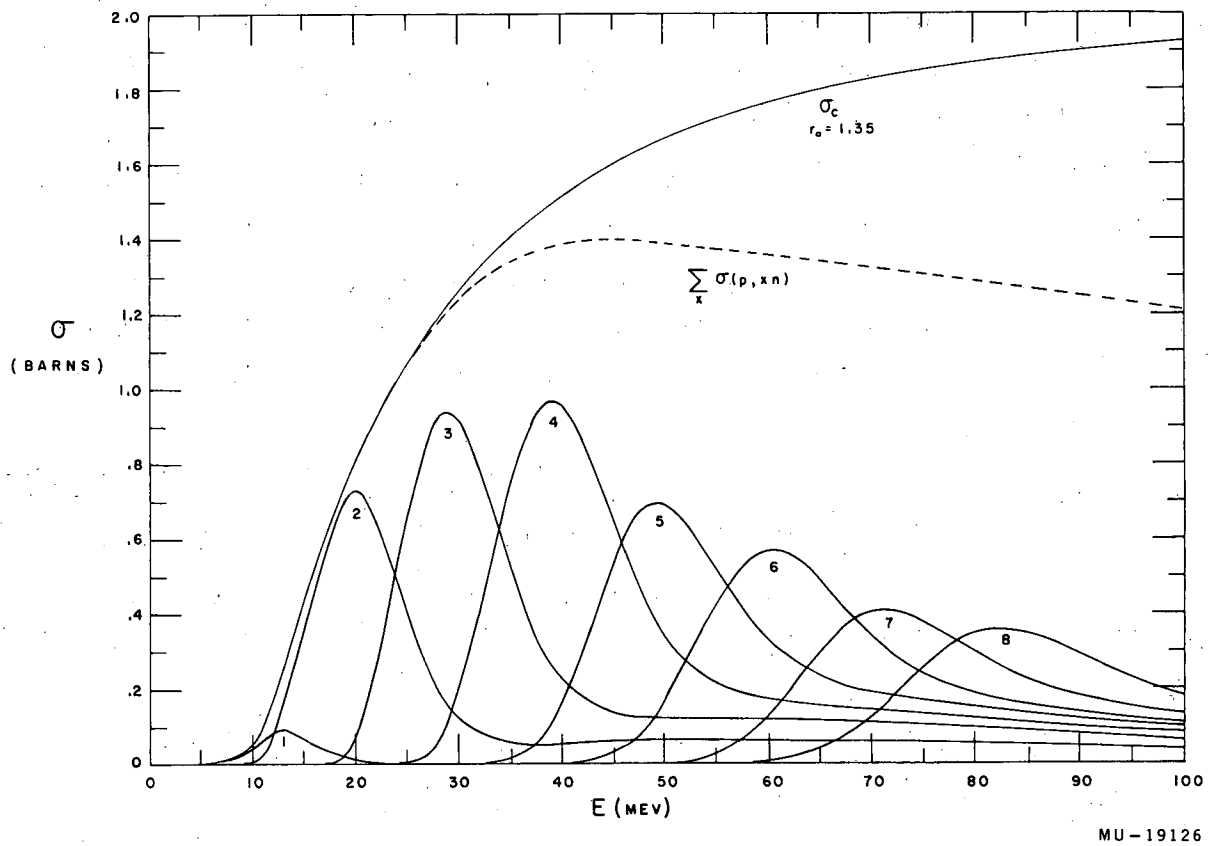

Fig. 12.6. JACKSON's calculated (p,xn) cross sections in barns for heavy elements as a function of incident proton energy in Mev. The curves are drawn for Bi^{209} as target with $R = 8.0 \times 10^{-13}$ cm, $\overline{B} = 7.3$ Mev, $T = 1.8$ Mev. Also shown are the sums of the (p,xn) cross sections and the "geometrical" cross section σ_c; the deviation of these two curves at higher bombarding energies is a result of the onset of the internal prompt cascade process.

12.1.4 Competition of Fission and Neutron Emission in the Interaction of Charged Particles with Heavy Elements ($Z \geq 90$). There have been many radiochemical studies of the interaction of charged particles of moderate energy in which fission cross sections and characteristics have been determined directly by analysis of the fission product yields or in which fission probability has been measured indirectly by analysis of the spallation products.[7,8,10,11,13,14,17,18,19,19a,32-40] (see especially 10,15,16,39,40). We shall have space to consider only a few selected examples from these studies.

As a first example, let us consider the bombardment of U^{235} with helium ions. Figures 12.7 and 12.8 show the excitation functions for the (α,xn) products and for the (α,pxn) products. The yields of the (α,xn) products are

---

32. H. A. Tewes and R. A. James, "Proton Induced Reactions of Thorium-Fission Yield Curves", Phys. Rev. 88, 860 (1952); H. A. Tewes, "Excitation Functions for Some Proton-Induced Reactions of Thorium", Phys. Rev. 98, 25 (1955).

33. R. J. Carr, "Spallation-Fission Competition in the Nuclear Reactions of Plutonium Induced by Alpha Particles", University of California Radiation Laboratory Report, UCRL-3395, April 1956.

34. T. T. Sugihara, P. J. Drevinsky, E. J. Troianello and J. M. Alexander, "Fission Yields of Natural Uranium with Deuterons of 5,10 and 13.6 Mev: Deuteron Capture and Competition with Stripping", Phys. Rev. 108, 1264 (1957).

35. J. M. Alexander and C. D. Coryell, "Nuclear Charge Distribution in the Fission of Uranium and Thorium with 13.6 Mev Deuterons", Phys. Rev. 108, 1274, (1957).

36. G. E. Gordon, "The Cross Section of the Reaction U^{234} (α,4n) Pu^{234}", University of California Radiation Laboratory Report, UCRL-8215, April 1958.

37. R. M. Lessler, "Spallation-Fission Competition in Neptunium Compound Systems", University of California Radiation Laboratory Report, UCRL-8439, October 1958.

38. D. L. Eads, "Spallation Reactions of Pu^{240} with Helium Ions and Pu^{242} with Deuterons", University of California Radiation Laboratory Report, UCRL-8561, January 1959.

39. R. Vandenbosch and J. R. Huizenga, "Competition Between Fission and Neutron Emission as a Function of Excitation Energy and Nuclear Type," Paper P/688, Proceedings of the Second International United Nations Conference on the Peaceful Uses of Atomic Energy, Volume 15, Geneva 1958.

40. T. D. Thomas, B. G. Harvey and G. T Seaborg, "Spallation Fission Competition in the Heaviest Elements", Paper P/1429, Volume 15, ibid.

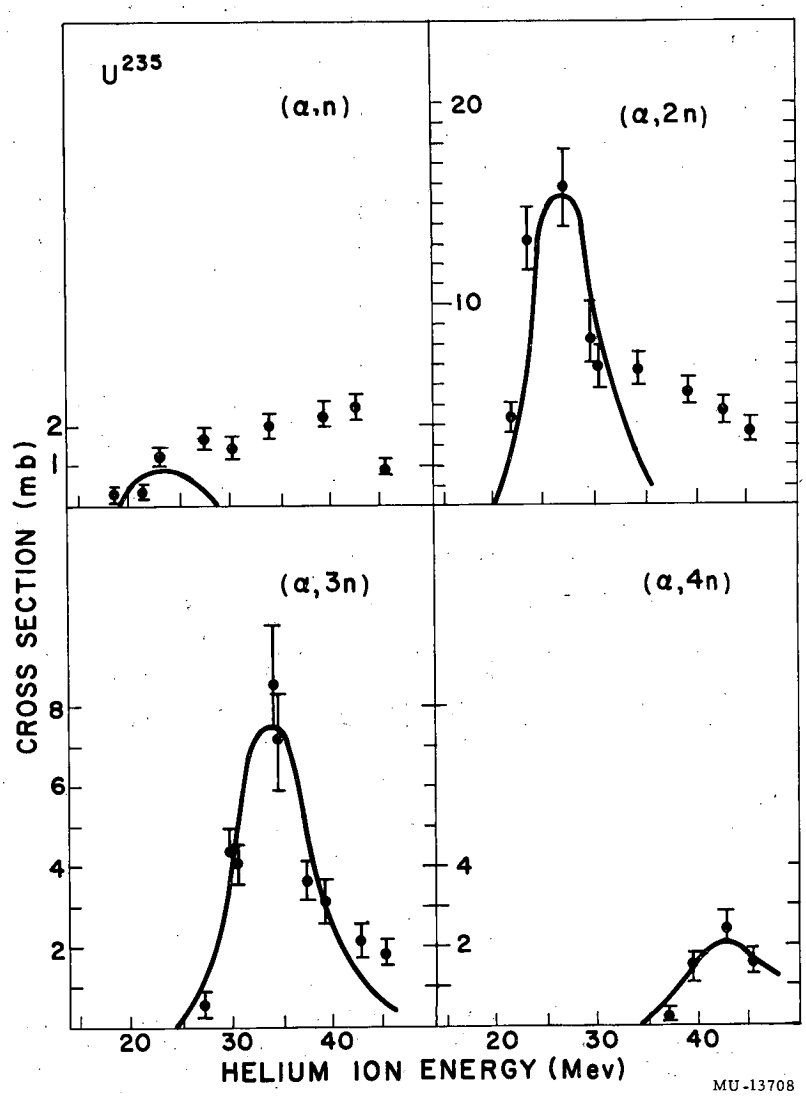

Fig. 12.7 Yield of (α,xn) products as a function of helium ion energy for U^{235} targets. Points are experimental and curves are a modified Jackson model calculation with fission competition included in the model. From Vandenbosch et al.[10]

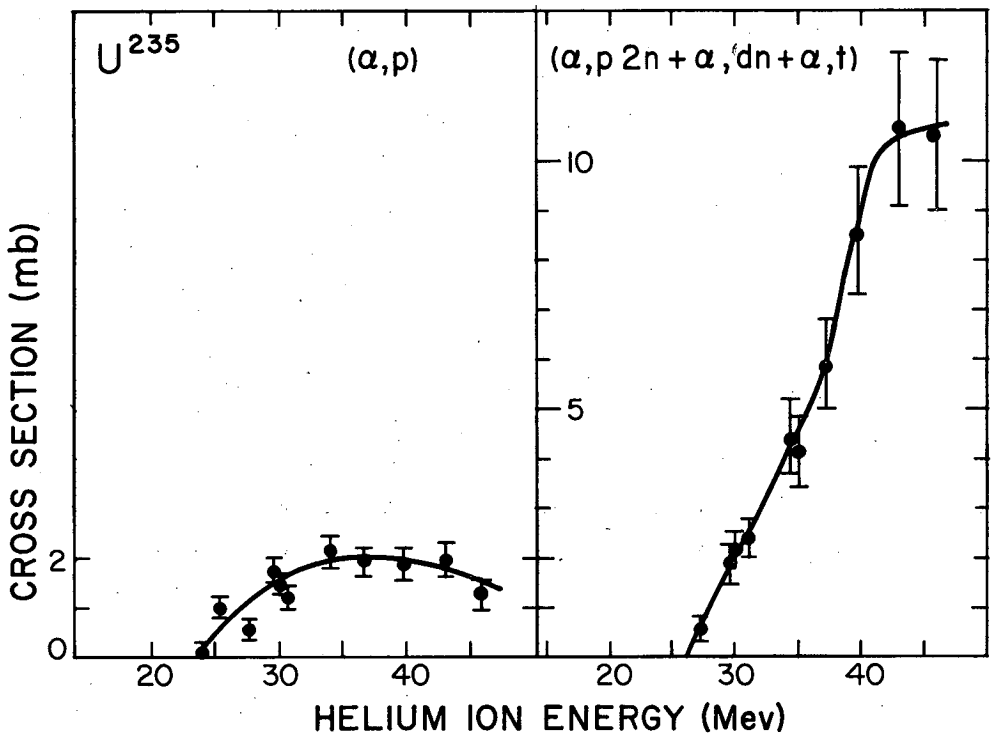

MU-13640

Fig. 12.8 Yield of "proton-out" reactions as a function of helium ion energy for U^{235} targets. From Vandenbosch et al.[10]

very markedly reduced because of fission competition in the evaporation chain. The peak heights are a few millibarns instead of about 1000 millibarns as they would be without this competition. The peak heights decrease in magnitude as x increases for x greater than 1.

The decrease in the peak heights for the successive (α, xn) reactions has been interpreted to mean that fission is competing successfully at each stage of the evaporation chain in a compound-nucleus reaction. See Fig. 12.1. Thus the peak cross section of the $(\alpha, 3n)$ reaction is lower than the peak cross section of the $(\alpha, 2n)$ reaction because in the former case fission has had three chances to compete with neutron emission compared with two chances in the latter case. The long "tail" on the (α, xn) excitation functions and the relatively high cross sections for the reactions involving the emission of charged particles suggest direct interactions of the projectile with the nucleons on the nuclear surface. The direct interaction processes are probably not subject to as much fission competition because of the transfer of lesser amounts of excitation energy to the struck nucleus.

The fission cross section was measured directly by radiochemical analysis of a sufficient number of individual fission products to define the mass yield curve, as shown in Fig. 12.9. The fission product mass-yield curve in the U^{235} case shows the same shape changes with increasing energy mentioned above in connection with the discussion of Fig. 12.3 The total spallation cross section is compared with the total fission cross section in Fig. 12.10 from which we note that fission takes up more than 90 percent of the reaction cross section. The total fission cross section is so high, in fact, for targets of uranium and heavier elements that it is not useful to look for changes in fissionability from nuclide to nuclide by examining the small percentage changes in the total fission cross section. A much more sensitive gauge of fissionability is the yield of the spallation products whose peak values are a sensitive measure of fission competition.

For example, let us compare some spallation data for U^{233}, U^{238} and for Pu^{239} with the U^{235} data we have just seen. See Fig. 12.11 through Fig. 12.16. The yield of corresponding (α, xn) products decreases steadily as the mass number of the uranium target isotopes decreases. This mass number effect was also noted by GLASS, CARR, COBBLE AND SEABORG[16] in a study of plutonium isotope targets. In fact, this mass number effect on fissionability is so strong that

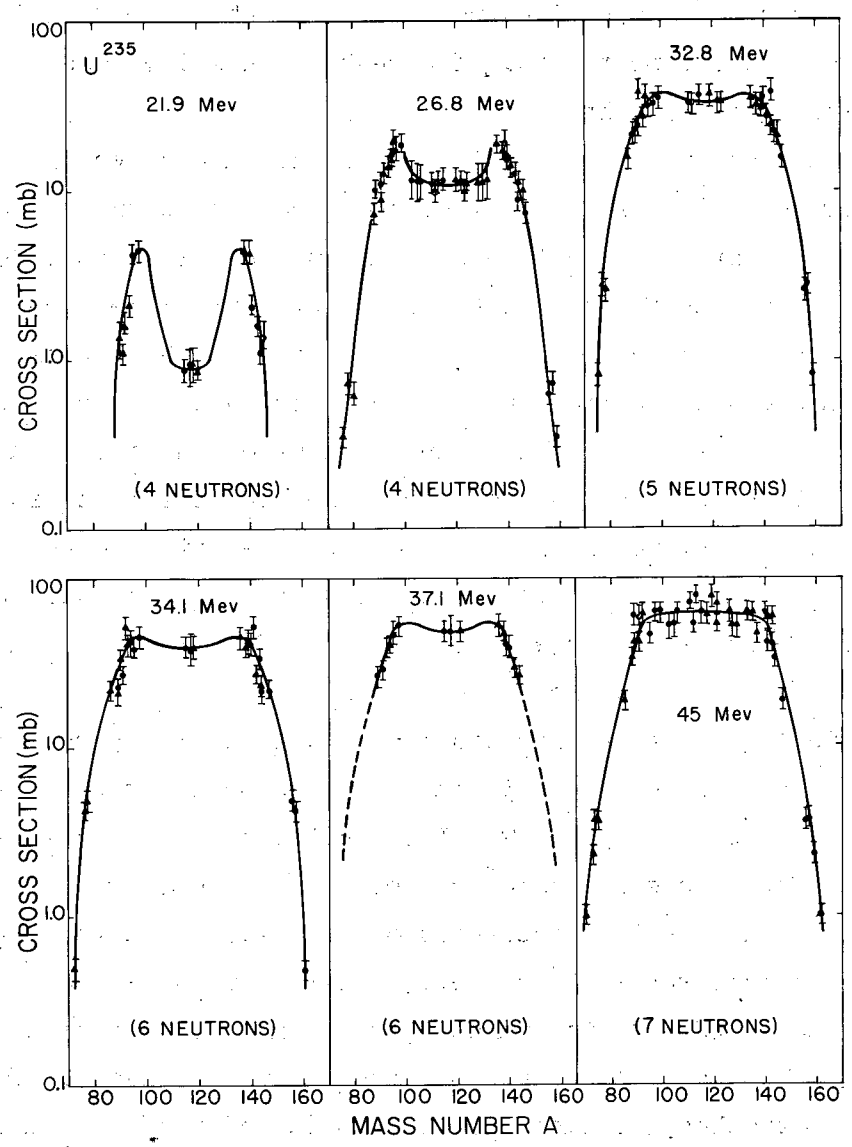

MU-13591

Fig. 12.9 Fission yield curves for helium-ion induced fission of U^{235}. The circles represent experimental points and the triangles represent reflected points. The number of neutrons $\bar{\nu}$ assumed in fixing the position of the reflected points are indicated for each energy. From Vandenbosch et al.[10]

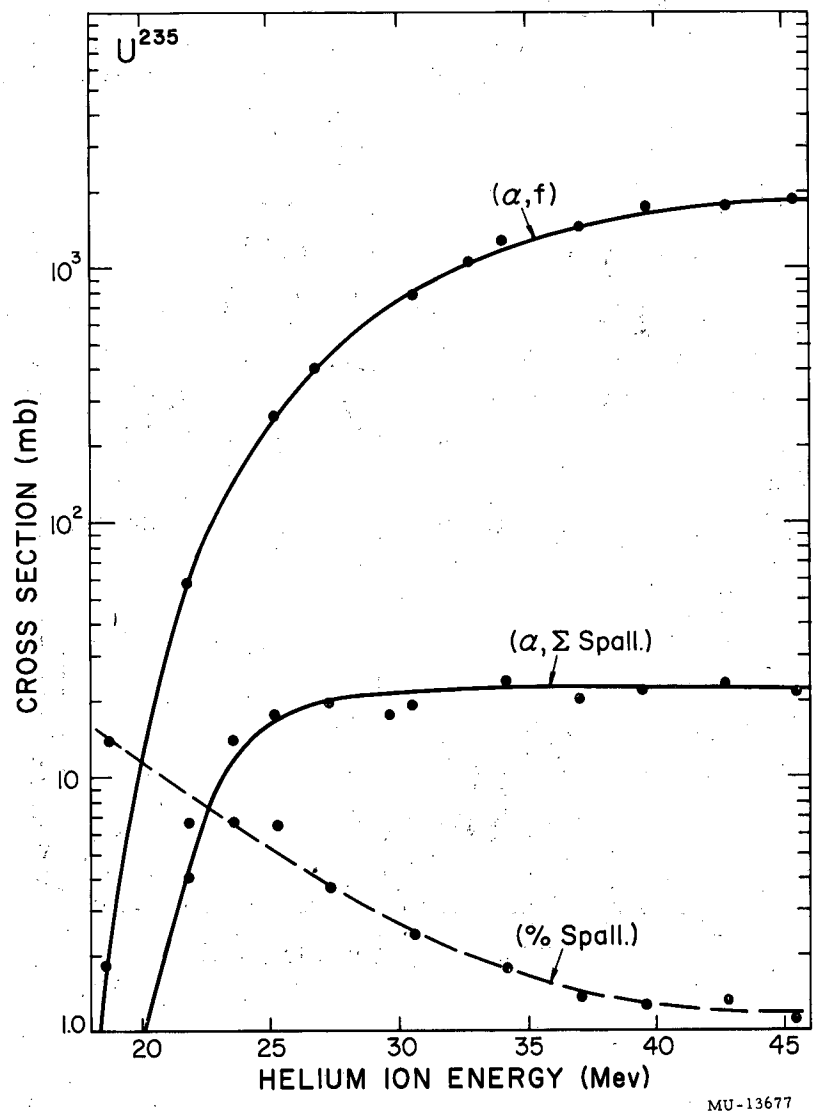

Fig. 12.10 Excitation functions for fission and summed spallation reactions in U^{235}. The dashed line shows the percent of the total reaction cross section going into spallation. From Vandenbosch et al.[10]

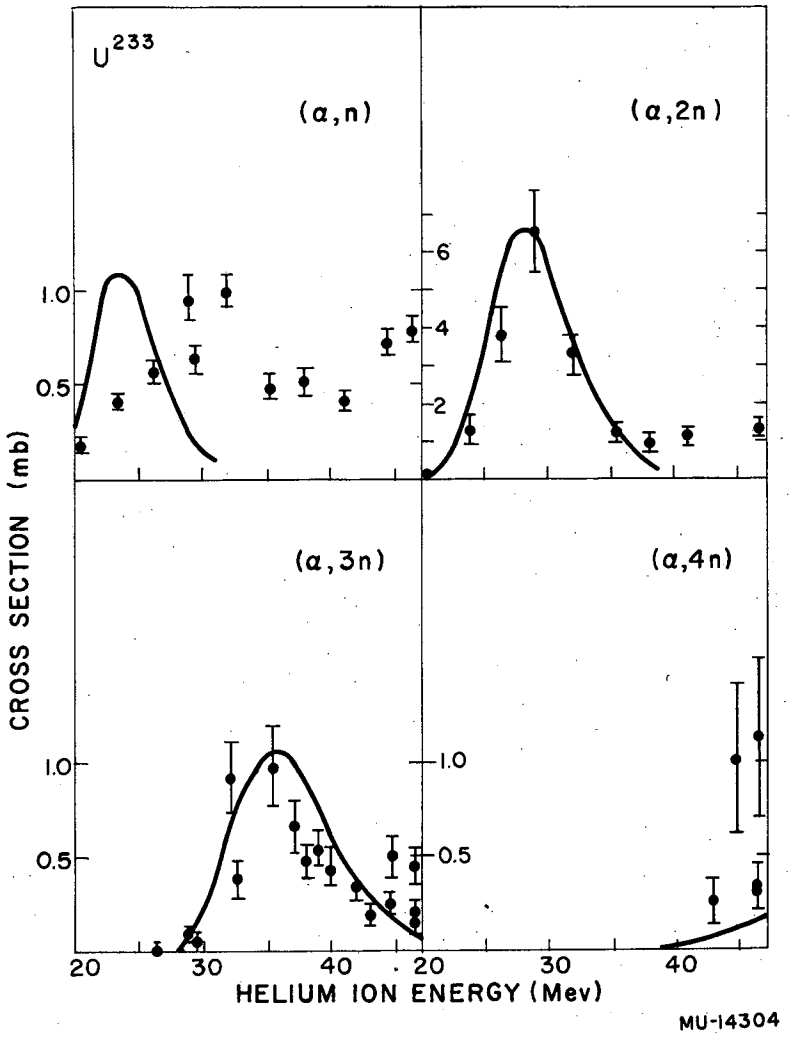

Fig. 12.11 Yield of (α,xn) products as a function of helium ion energy for U^{233} targets. Points are experimental and curves are a modified Jackson model calculation. From Vandenbosch et al.[10]

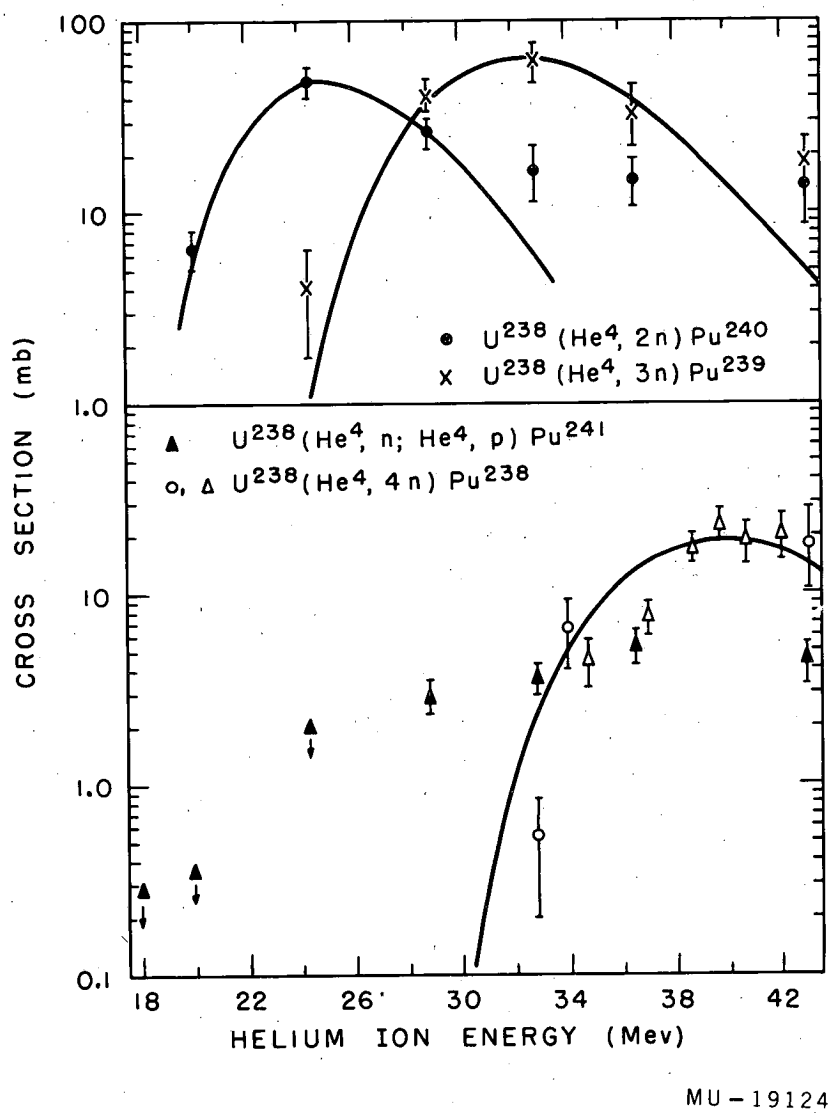

Fig. 12.12 Yield of (α,xn) products as a function of helium ion energy for U^{238} targets. Points are experimental and curves are a modified Jackson model calculation. From Wing et al.[18]

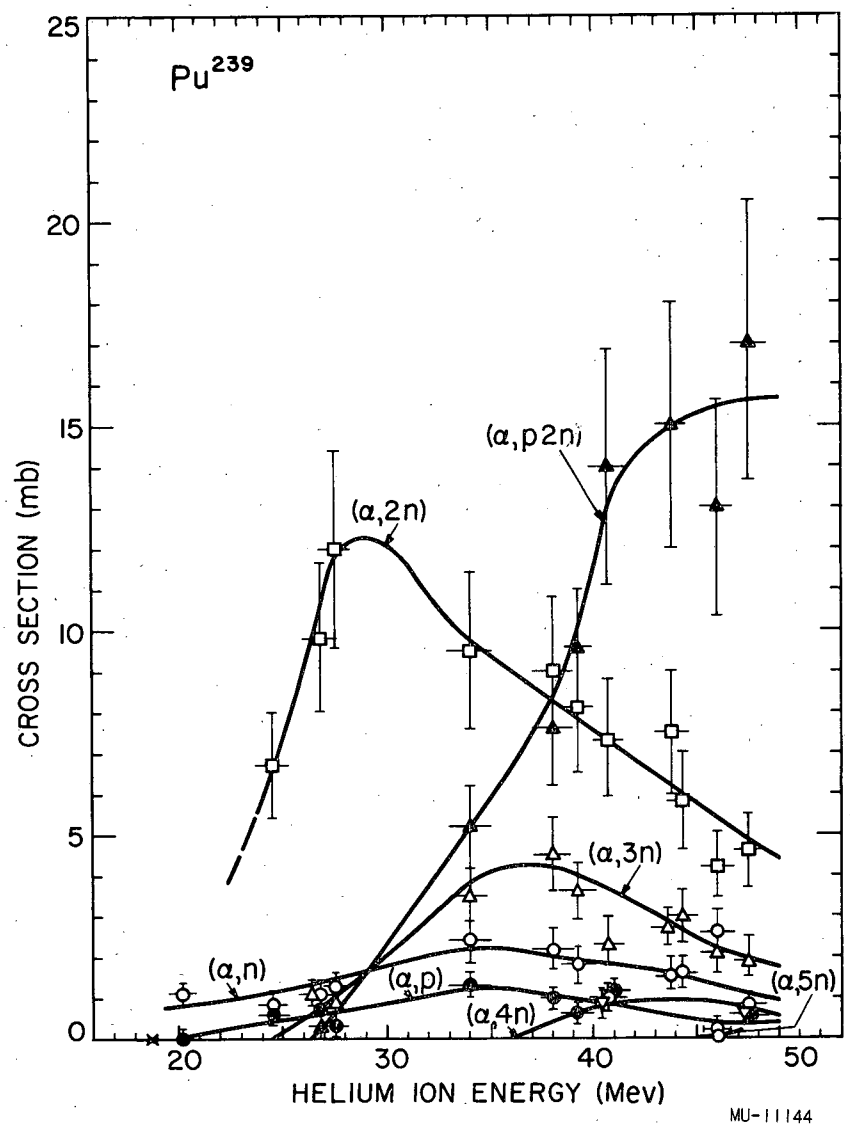

Fig. 12.13 Yield of (α,xn) products as a function of helium ion energy for Pu^{239} targets. From Glass et al.[16]

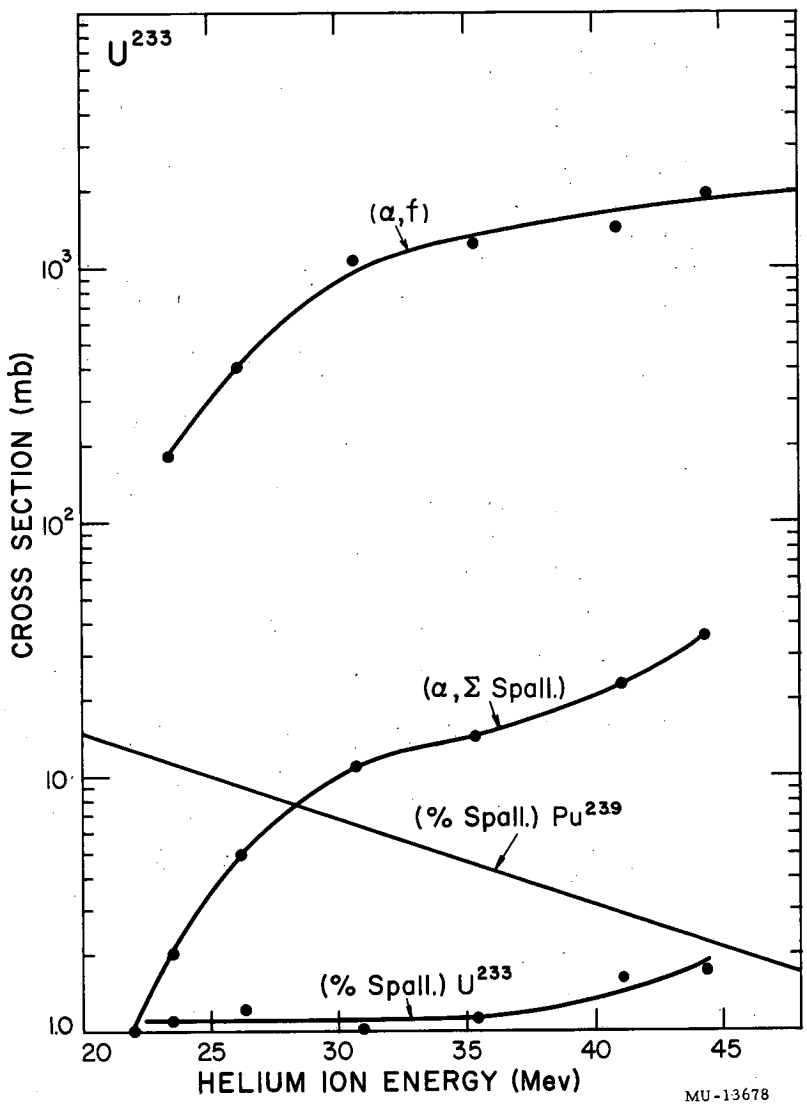

Fig. 12.14 Excitation functions for fission and summed spallation reactions in U^{233}. Also shown is the total-reaction cross section going into spallation for U^{233} and also for Pu^{239}, for comparison. From Vandenbosch et al.[10]

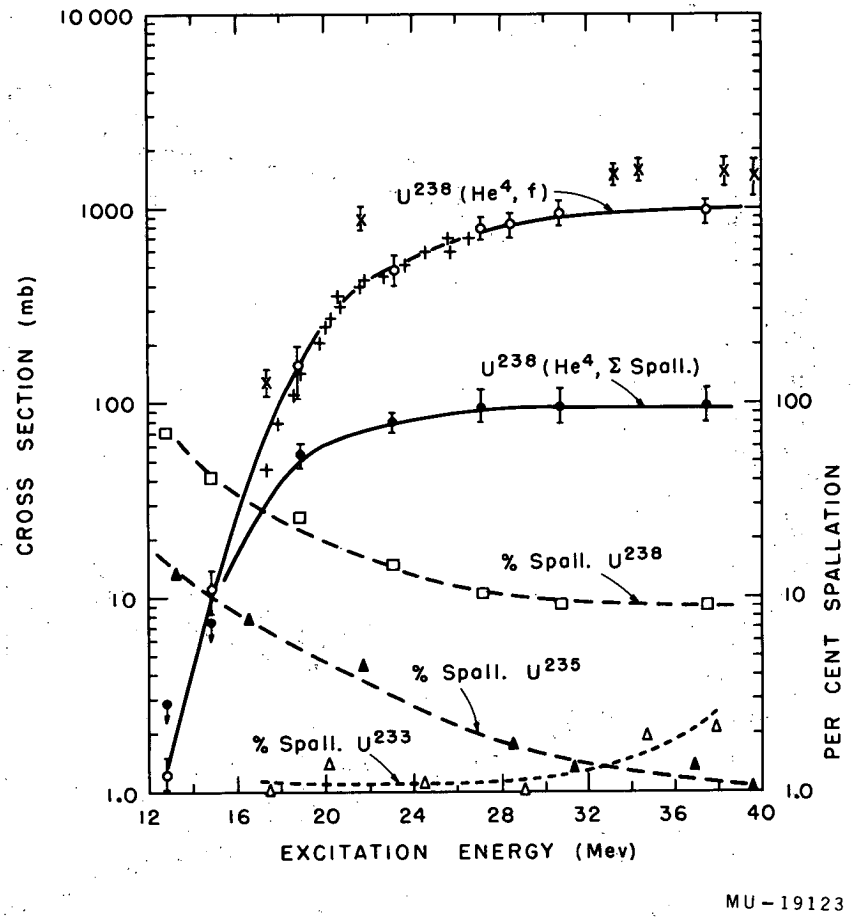

Fig. 12.15 Excitation functions for fission and sum of spallation reactions of U^{238} bombarded with He^4. The dashed lines represent the percent of spallation reactions in the helium-ion induced reactions of U^{233}, U^{235} and U^{238} and show the increase of percent spallation with mass number. Figure reproduced from WING et al.[18]

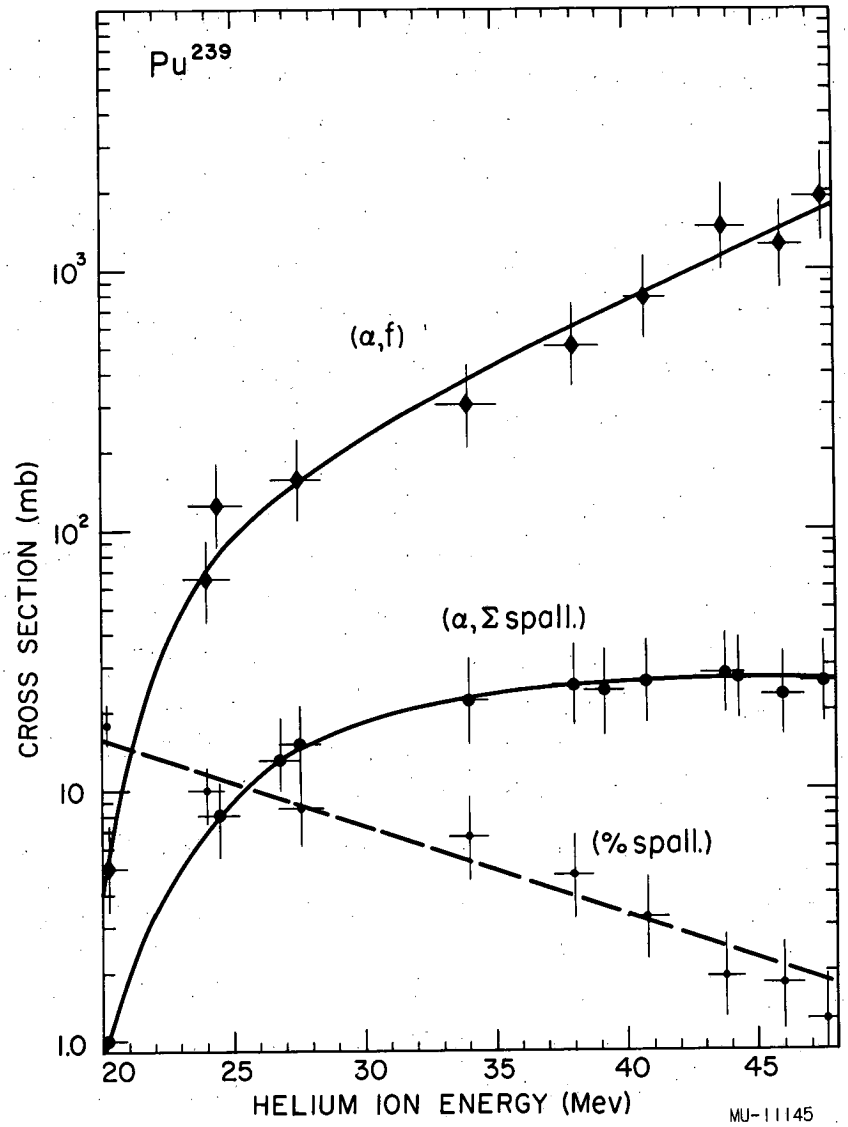

Fig. 12.16 Excitation functions for fission and sum of spallation reactions of Pu^{239} bombarded with He^4. From GLASS et al.[16]

U^{233} exhibits a greater fissionability with helium ions than does Pu^{239} (see Fig. 12.14) in spite of the fact that Z^2/A is greater for Pu^{239}. There are two factors at work to account for these changes: the relative fissionability of corresponding compound nuclei and the ease with which neutrons are evaporated from corresponding compound nuclei. Fissionability increases as Z^2/A increases; the curium isotopes produced by the bombardment of Pu^{239} have higher values of Z^2/A than do the corresponding plutonium isotopes produced by the bombardment of U^{233}. The ease of neutron evaporation increases with decreasing neutron binding energy; the neutron binding energies of the curium isotopes produced by bombardments of Pu^{239} are lower than the neutron binding energies of the corresponding plutonium isotopes produced by bombardment of U^{233}. Hence the higher fissionability of the curium isotopes is apparently more than offset by the greater ease of neutron evaporation from these isotopes.

The strong effect of the mass number, A, on the relative probability of neutron emission and fission in a series of isotopes of one element can be explained similarly. The most extensive data are available for a series of uranium and plutonium target isotopes. Z^2/A decreases as A increases and the ease of neutron evaporation increases. Furthermore, fission thresholds are lower than neutron binding energies in the nuclides considered, with the result that a nucleus that has survived fission long enough to evaporate all the neutrons allowed by the original excitation energy may still have sufficient residual excitation to undergo fission. Thus fission has an additional chance to occur when neutron emission can no longer compete. The higher the neutron binding energy and the lower the fission threshold, the larger will be the excitation energy range in which such fission can occur. Since neutron binding energies decrease and fission thresholds increase as A increases, such fission will compete less effectively as A increases. Thus the three factors mentioned all contribute to decreasing competition from fission as A increases.

If the picture of the fission mechanism being presented here is correct then the yield of some product well along in the neutron evaporation chain should serve as a good gauge of the overall fissionability observed in these charged particle reactions. Figure 12.17 is an interesting case of this since it shows the steady decrease in the $(\alpha,4n)$ yield when uranium isotopes of lower mass number are bombarded.[41]

---

41. R. Vandenbosch gives a good discussion of the relation of $(\alpha,4n)$ cross sections to fissionability in his thesis, University of California Radiation Laboratory Report, UCRL-3858, July 1957. See also R. Vandenbosch and G.T. Seaborg, Phys. Rev. 110, 507 (1958).

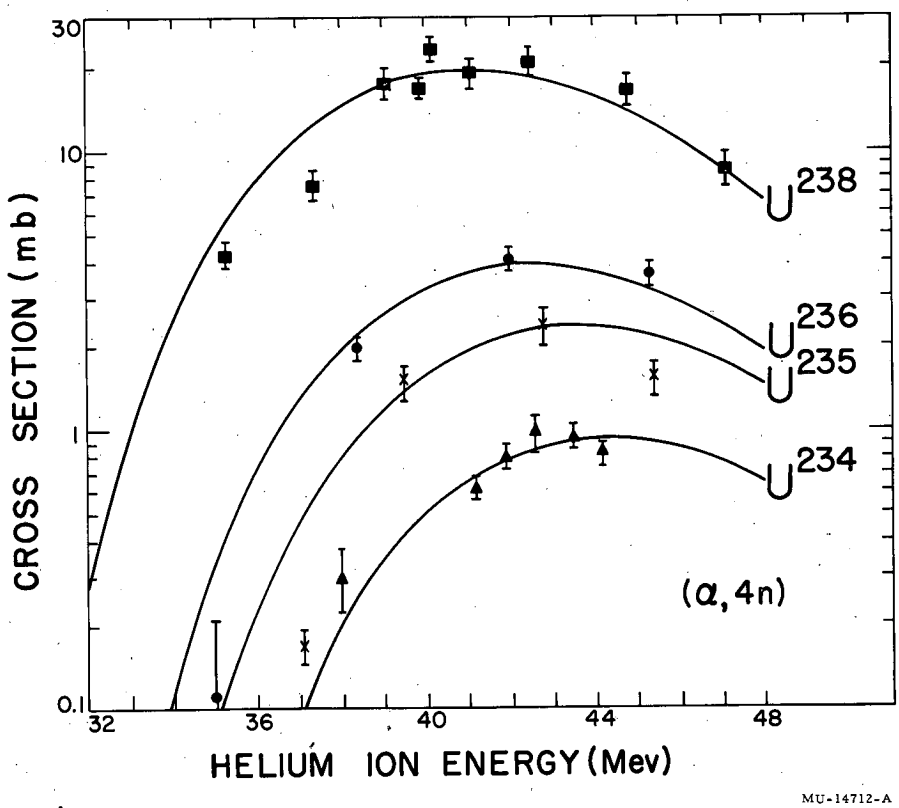

Fig. 12.17 Excitation functions for (α,4n) reactions of uranium isotopes. Decreasing yield with decreasing mass number is a consequence of increased fission competition in the neutron evaporation chain. From THOMAS, HARVEY and SEABORG.[40]

Conclusions of a somewhat more quantitative nature can be obtained by means of calculations based on a modified form of JACKSON'S[28] statistical model for spallation reactions. We have presented this model in Section 12.1.3 above, but before this model can be applied to elements as heavy as thorium, uranium or plutonium it must be changed to include the effect of fission competition. In this we follow closely the paper of VANDENBOSCH, THOMAS, VANDENBOSCH, GLASS AND SEABORG.[10]

The fission competition will be considered in the framework of compound nucleus formation followed by competition between neutron emission and fission at each stage of the evaporation chain. There are two effects to consider: first, fission occurs while neutron emission is energetically possible, thus destroying nuclei during the early stages of the evaporation chain, and, second, some fission occurs after all of the possible neutrons have been evaporated, thus destroying nuclei whose excitation energy is less than the binding energy of the last neutron, and which would otherwise have de-excited by gamma emission.

The probability that an excited nucleus will emit a neutron is given by its branching ratio (level width ratio) for neutron emission $\Gamma_n/\Sigma_i \Gamma_i$ (henceforth designated as Gn). Similarly the branching ratio for fission is given by $\Gamma_\gamma/\Sigma_i \Gamma_i$, or G_f, and the branching ratio for gamma ray de-excitation by $\Gamma_\gamma/\Sigma_i \Gamma_i$ or G_γ. The denominator, $\Sigma_i \Gamma_i$, contains terms for all the possible modes of decay of the compound nucleus. However, the assumptions will be made that the widths for proton evaporation and for gamma-ray de-excitation are negligible wherever neutron emission or fission is energetically possible. However, the gamma-ray branching ratio is taken as unity wherever neither fission nor neutron evaporation is energetically possible. When the excitation energy is greater than the fission threshold and less than the binding energy of the last neutron, G_f is taken to be unity. Hence to take into account the fission competition along the evaporation chain, we multiply the probability, P (E,x), (see Eq. 12.1) by terms, G_{ni}, to give a new probability that the original compound nucleus will not only evaporate x neutrons but will also survive fission during the evaporation process.

After all of the neutrons have been evaporated, the residual nucleus may either undergo fission or may de-excite by gamma emission. As stated above, we make the somewhat arbitrary assumption that if the residual nucleus has an excitation energy greater than the activation energy for fission it will undergo

fission and that if the nucleus has an excitation energy less than the activation energy for fission it will de-excite by gamma emission. In JACKSON'S model, the first incomplete gamma function of Eq. (12.2) gives the probability that the original compound nucleus will emit at least x neutrons; the second the probability that the residual nucleus will have an excitation greater than the binding energy of the last neutron. Therefore, to account for fission competition at the final stage, we replace the last incomplete gamma function of JACKSON by one giving the probability that the residual nucleus will have an excitation greater than the activation energy for fission. The result is a narrowing of the peak of the theoretical excitation functions, in better agreement with experiment.

Using these considerations, one can express the cross section for a reaction following compound nucleus formation as

$$\sigma(\alpha, xn) = \sigma_c G_{n_1} \; G_{n_2} \text{---} G_{n_x} \; [\, I\,(\Delta_x, 2x-3) - I\,(\Delta^f_x, 2x-1)\,] \qquad (12.5)$$

where $\Delta^f_x = (E - \sum_i^x B_i - E_{th})\,/T$.

E_{th} is the activation energy for fission for the residual nucleus. The subscripts 1, 2--x on the G_n factor refer to the branching ratio for emission of the 1st, 2nd, --, xth neutron from the compound nucleus. σ_c is the cross section for the formation of the compound nucleus at the particular energy considered. The neutron binding energies can be taken from such tables as those given in Chapter 8. (See Table 8.3). The fission activation energies can be taken from Table 11.4 in Chapter 11, Section 11.3.1.

It is necessary to evaluate the G_n quantities and to choose a value of the nuclear temperature. Not a great deal is known about the variation of Γ_n/Γ_f with excitation energy and nuclear type (Z, A, even-odd character, etc.) The following assumptions about Γ_n/Γ_f will be made:

(1) Γ_n/Γ_f is independent of excitation energy for excitation energies well above the neutron emission threshold.

(2) Γ_n/Γ_f for even-even nuclei is twice as great as Γ_n/Γ_f for even-odd nuclei. (It will not be necessary to consider odd-odd products in the present calculations.)

(3) Aside from even-even and even-odd effects, there is a general trend for Γ_n/Γ_f to increase with increasing mass number.

The first assumption as a first approximation obtains support from the shape of excitation functions for fast neutron-induced fission and also from an analysis by BATZEL[42] of high energy spallation excitation functions.≠ The same conclusion was reached by GLASS AND COWORKERS from analysis of spallation excitation functions.[16] There is, however, some evidence that Γ_n/Γ_f increases with increasing excitation.[43] The second assumption arises from the belief that the odd-mass product of the evaporation of a neutron from an even-mass nucleus has a higher level density than the even-mass product from an odd-mass nucleus; the factor of two used was taken from an estimate by WEISSKOPF.[44] The variation of Γ_n/Γ_f with mass number has been evaluated from a plot of the neutron to fission width ratios obtained from an analysis of $(\alpha,4n)$ reactions in various uranium isotopes.[41] The quantity Γ_n/Γ_f was found to increase by a factor of 1.3 per unit increase of mass number A.

Using the above considerations, one needs to choose only two parameters to calculate excitation functions for all of the possilbe (α,xn) reactions. These are the nuclear temperature T and a mean value of Γ_n/Γ_f. Calculations have been made for the (α,xn) reaction cross sections of U^{233} and U^{235}. A mean (geometric) value for Γ_n/Γ_f of 0.11 for U^{233} and 0.21 for U^{235} and nuclear temperatures of 1.41 Mev and 1.35 Mev respectively were found to give the best fit to the experimental data. The neutron branching ratios derived from the mean values of Γ_n/Γ_f are illustrated in Table 12.2*.

42. R. F. Batzel, University of Calif. Radiation Laboratory Report, UCRL-4303, February 1954 (unpublished).

43. C. T. Coffin and I. Halpern, Paper P/642, Volume 15, Proceedings of the Second United Nations Conference on the Peaceful Uses of Atomic Energy, Geneva (1959) and unpublished results.

44. V. F. Weisskopf, Lecture series in Nuclear Physics, MDDC-1175 ,U.S. Gov't Printing Office, Washington D. C., 1947.

≠ Refer to the description of a similar analysis by Lindner and Turkevich in Section 12.2.4.

* Glass and co-workers[16,17] have shown how the G_n factor for a certain nucleus at a certain excitation may be derived from the spallation cross sections in a few favorable cases without introducing any assumptions about level density effects. Consider the Pu^{238} $(\alpha,2n)$ and the Pu^{239} $(\alpha,3n)$ reactions for which Cm^{240} is the product nuclide and for which intermediate nuclei possess similar excitation energies if the respective peak energies are considered. The ratio of cross sections is given by the expression

$$\frac{\sigma\ (\alpha,2n)_{238}}{\sigma\ (\alpha,3n)_{239}} = \frac{G_{n_2}\ G_{n_1}\ \sigma_t\ 238}{G_{n_3}\ G_{n_2}\ G_{n_1}\ \sigma_t\ 239} \qquad (12.4)$$

The G_{n_2} and G_{n_1} factors cancel out. The ratio of the total cross sections is close to 1 and the (α,xn) cross section ratio can be evaluated from the

(see next page)

Table 12.2

Neutron branching ratios used in calculating U^{233} and U^{235} (α,xn) cross sections. The numerical subscripts refer to the emission of the 1st, 2nd ... ith neutron. From Vandenbosch et al.[10]

Ratio	U^{233}	U^{235}
$\left(\frac{\Gamma_n}{\Gamma_t}\right)_1$	0.12	0.23
$\left(\frac{\Gamma_n}{\Gamma_t}\right)_2$	0.17	0.32
$\left(\frac{\Gamma_n}{\Gamma_t}\right)_3$	0.07	0.15
$\left(\frac{\Gamma_n}{\Gamma_t}\right)_4$	0.10	0.21
$\left(\frac{\Gamma_n}{\Gamma_t}\right)_5$	0.04	0.09

The calculated curves are compared with the experimental points in figures 12.7 and 12.11. Considering the simplicity of the model, the agreement with those features of the excitation functions believed to result from compound nucleus formation is good. The agreement with the peak cross section values for the $(\alpha,2n)$, $(\alpha,3n)$ and $(\alpha,4n)$ reactions supports the assumed variation of Γ_n/Γ_f with mass number and nuclear type.

In view of the success in reproducing certain features of the spallation excitation functions using the branching ratios shown in Table 12.2 it seems justifiable to use these branching ratios to calculate the fraction of the fission that occurs before the emission of various numbers of neutrons. Given an initial excitation energy of the compound nucleus, we can also calculate the average excitation energy at which fission occurs. It is assumed that the average excitation energy of a residual nucleus after the emission of a neutron is given by the initial excitation energy minus the binding energy of the neutron and minus 2T, where the nuclear temperature T has been taken as 1.41 Mev for U^{233} and 1.35 Mev for U^{235}.

In Table 12.3 the percentage of total fissions occurring after the evaporation of various numbers of neutrons are listed for three helium-ion bombardment energies. The second row gives the initial excitation energy corresponding to the helium ion energy. The last row gives the average excitation energy at which fission is occurring for each of the three initial excitation energies in the case of each isotope. Calculations by COFFIN AND HALPERN give results which are in substantial agreement with those reported here.[43]

According to the assumption that Γ_n/Γ_f does not vary much with energy the increased probability for fission observed when the energy of the compound nucleus is increased is to be attributed not to an increasing relative probability of fission with increasing excitation energy, but rather to the increased number of chances for fission to occur as the length of the evaporation chain increases with increasing excitation energy.

Several authors [10,16,39,40,45,46] have carried through analyses of the

---

* (cont'd) experimental data. Hence it is possible to evaluate G_{n3}, the neutron emission branching ratio, of Cm^{243} excited to about 30 Mev. The opportunities to use this method are very limited.

45. R. Vandenbosch and G. T. Seaborg, Phys. Rev. 110, 507 (1958)

46. J. R. Huizenga, Phys. Rev. 109, 484 (1958)

Table 12.3

The percentage of total fissions occurring after the evaporation of various numbers of neutrons in the helium-ion induced fission of U^{233} and U^{235}. Calculations for three different initial excitation energies are listed in each case. From Vandenbosch et al.[10]

	U^{233}			U^{235}		
Helium-ion energy (Mev)	46	36	29	42	32	23
Excitation energy (Mev)	40	30	23	37	27	18
Neutrons emitted before fission						
0	88%	88%	90%	77%	78%	83%
1	9.6%	10%	10%	16%	16%	17%
2	1.8%	2%		6%	6%	
3	0.1%			1%		
Average excitation energy of fission (Mev)	38.3	28.4	22.2	34.2	24.6	16.6

type outlined here using all the available experimental data on spallation reactions with heavy element targets. We reproduce here in Table 12.4 a summary prepared by VANDENBOSCH AND HUIZENGA[39]. This table lists an average value of the quantity Γ_n/Γ_f for all nuclei in the evaporation chain leading to a particular spallation product, rather than Γ_n/Γ_t for individual nuclei as given in Table 12.2. The entries in column 4 are the intermediate (or average) fissioning nuclei half way along the evaporation chain. These authors also found it of interest to examine Γ_n/Γ_f values deduced from experimental data on the fission cross section of heavy nuclei for fission induced by 3 Mev neutrons and by 12 Mev Bremsstrahlung beams; we reproduce these summaries here as Tables 12.5 and 12.6. In discussing the conclusions from these tables we quote from the paper of VANDENBOSCH AND HUIZENGA.[39]

Several correlations of the data summarized in Tables 12.4 through 12.6 can be made. In Fig. 12.18 the neutron-emission-to fission-width ratios are plotted as a function of mass number. The data fall into rather distinct groups which define almost straight parallel lines for different values of the atomic number of the compound nucleus. There is no obvious systematic deviation between the Γ_n/Γ_f values derived either from the different types of experiments or from compound nuclei with different excitation energy. There is a slight change in the variation of Γ_n/Γ_f with atomic number at Z of approximately 93. For higher atomic numbers Γ_n/Γ_f does not depend as strongly on the atomic number or on Z^2/A as for lower atomic numbers. This is an important practical point in connection with the preparation of higher transuranium elements by spallation reactions.

As stated above, the strong variation with mass number for a given atomic number can be explained by the following two experimental observations: (1) neutron binding energies increase as the mass number decreases, making it increasingly difficult to evaporate a neutron, and (2) fission thresholds decrease with decreasing mass number as the fissionability parameter Z^2/A increases (neglecting the reversal in E_f for the very heavy isotopes of a particular element). It might be expected that on a plot of this type, even-even and even-odd compound nuclei would define separate lines, particularly for the cases where only one competition step occurs. Examination of the data from photofission and 3-Mev neutron induced fission of uranium isotopes, however, shows no systematic deviations from a single line even though both nuclear types are represented.

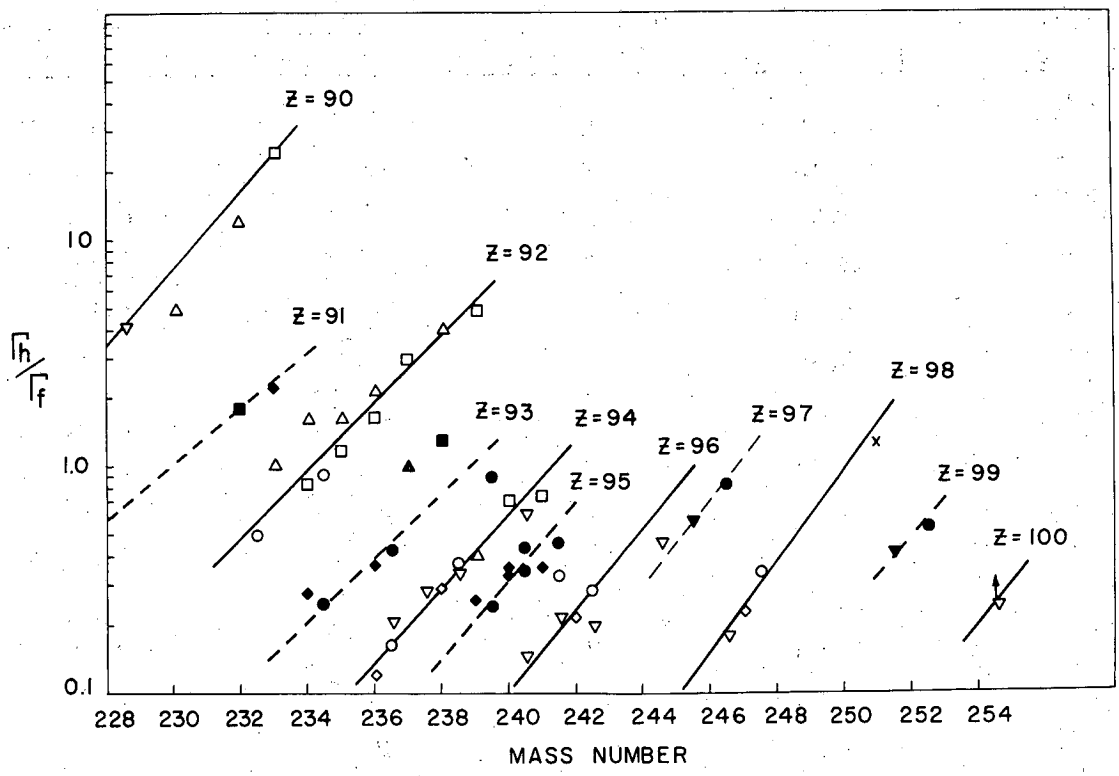

MU-19340

Fig. 12.18 Neutron emission to fission width ratios are plotted as a function of mass number. Open and closed symbols refer to fissioning nuclei with even and odd atomic number, respectively. Triangles (△) refer to data obtained from photoneutron and photofission experiments and correspond to an excitation energy of 8-12 Mev. Squares (□) refer to data derived from 3-Mev neutron fission cross sections and correspond to an excitation energy of 8-10 Mev. Circles (○), diamonds (◇), and inverted triangles (▽), refer to mean values of Γ_n/Γ_f obtained from spallation excitation functions and correspond to average excitation energies of approximately 13, 18, and 23 Mev, respectively. Figure reproduced from VANDENBOSCH AND HUIZENGA.[39]

Table 12.4
Geometric Mean Values of Neutron Emission to Fission Width Ratios Deduced from Charged Particle Induced Spallation Reactions.
From Vandenbosch and Huizenga[39].

Target nucleus	Reaction	Cross section Reference	Average fissioning nucleus	$\overline{(\Gamma_n/\Gamma_f)}$
Ra^{226}	α,4n	1	$Th^{228.5}$	4.2
Th^{232}	p,3n	2	Pa^{232}	2.2
Th^{230}	α,4n	1	$U^{232.5}$	0.50
Th^{232}	α,4n	3	$U^{234.5}$	0.92
U^{233}	d,2n	4	$Np^{234.5}$	0.25
U^{233}	d,3n	4	Np^{234}	0.28
U^{235}	d,2n	5	$Np^{236.5}$	0.43
U^{235}	d,3n	5	Np^{236}	0.37
U^{238}	d,2n	5	$Np^{239.5}$	0.89
U^{233}	α,2n	6	$Pu^{236.5}$	0.16
U^{233}	α,3n	6	Pu^{236}	0.12
U^{234}	α,4n	7	$Pu^{236.5}$	0.21
U^{235}	α,4n	6	$Pu^{237.5}$	0.28
U^{235}	α,3n	6	Pu^{238}	0.29
U^{235}	α,2n	6	$Pu^{238.5}$	0.38
U^{236}	α,4n	1	$Pu^{238.5}$	0.34
U^{238}	α,4n	8	$Pu^{240.5}$	0.61
Np^{237}	α,2n	4	$Am^{240.5}$	0.34
Np^{237}	α,3n	4	Am^{240}	0.33
Pu^{238}	d,2n	8	$Am^{239.5}$	0.24
Pu^{238}	d,3n	8	Am^{239}	0.26
Pu^{239}	d,2n	4	$Am^{240.5}$	0.44
Pu^{239}	d,3n	4	Am^{240}	0.35
Pu^{240}	d,2n	8	$Am^{241.5}$	0.46
Pu^{240}	d,3n	8	Am^{241}	0.36
Pu^{238}	α,2n	9	$Cm^{241.5}$	0.33
Pu^{238}	α,4n	9	$Cm^{240.5}$	0.15
Pu^{239}	α,2n	9	$Cm^{242.5}$	0.28

Table 12.4 (cont'd.)

Target nucleus	Reaction	Cross section Reference	Average Fissioning nucleus	$\overline{(\Gamma_n/\Gamma_f)}$
Pu^{239}	α,3n	9	Cm^{242}	0.22
Pu^{239}	α,4n	9	$Cm^{241.5}$	0.22
Pu^{240}	α,4n	10	$Cm^{242.5}$	0.20
Pu^{242}	α,2n	9	$Cm^{245.5}$	2.8
Pu^{242}	α,4n	9	$Cm^{244.5}$	0.46
Am^{243}	α,2n	11	$Bk^{246.5}$	0.81
Am^{243}	α,4n	11	$Bk^{245.5}$	0.57
Cm^{244}	α,2n	12	$Cf^{247.5}$	0.34
Cm^{244}	α,3n	12	Cf^{247}	0.23
Cm^{244}	α,4n	12	$Cf^{246.5}$	0.18
Bk^{249}	α,2n	13	$E^{252.5}$	0.53
Bk^{249}	α.4n	13	$E^{251.5}$	0.41
Cf^{252}	α,4n	14	$Fm^{254.5}$	0.24[a]

(a) Lower limit.

1. R. Vandenbosch and G. T. Seaborg, Phys. Rev. 110, 507 (1958).
2. H. A. Tewes, Phys. Rev. 98, 25 (1955).
3. Foreman, Gibson, Glass and Seaborg, Phys. Rev. 116, 382 (1959)
4. W. M. Gibson, University of California Radiation Laboratory Report UCRL-3493, November, 1956; see also 3.
5. J. Wing, W. J. Ramler, A. L. Harkness and J. R. Huizenga, Phys. Rev. 114, 163 (1959).
6. R. Vandenbosch et al., Phys. Rev. 111, 1358 (1958).
7. G. E. Gordon, unpublished data.
8. J. A. Coleman, T. D. Thomas and G. T. Seaborg, Bull. Am. Phys. Soc. Series II, 2, 386 (1957).
9. R. A. Glass et al., Phys. Rev. 104, 434 (1956).
10. D. L. Eads, unpublished information.
11. R. J. Silva, unpublished information.
12. A. Chetham-Strode, Jr., G. R. Choppin and B. G. Harvey, Phys. Rev. 102, 747 (1956).
13. B. G. Harvey et al., Phys. Rev. 104, 1315 (1956).
14. T. Sikkeland, S. Amiel and S. G. Thompson, Phys. Rev. 112, 543 (1958).

Table 12.5

3-Mev Neutron Fission Cross Sections and Derived Values of Neutron Emission to Fission Width Ratios. From Vandenbosch and Huizenga[39]

Target nucleus	σ_f (barns)	Fissioning nucleus	Γ_n/Γ_f
Ra^{226}	0.0003	Ra^{227}	10^4
Th^{232}	0.13	Th^{233}	24.3
Pa^{231}	1.16	Pa^{232}	1.85
U^{233}	1.78	U^{234}	0.85
U^{234}	1.52	U^{235}	1.17
U^{235}	1.25	U^{236}	1.64
U^{236}	0.82	U^{237}	33.01
U^{238}	0.54	U^{239}	5.13
Np^{237}	1.42	Np^{238}	1.32
Pu^{239}	1.94	Pu^{240}	0.70
Pu^{240}	1.90	Pu^{241}	0.74

Table 12.6

Neutron Emission to Fission Width Ratios Deduced from 12-Mev Bremsstrahlung Photofission and Photoneutron Yield Experiments. Table prepared by Vandenbosch and Huizenga[39]

Target nucleus = fissioning nucleus	Γ_n/Γ_f
Th^{230}	4.9
Th^{232}	12
U^{233}	1.0
U^{234}	1.6
U^{235}	1.6
U^{236}	2.1
U^{238}	5.0
Np^{237}	1.0
Pu^{239}	0.4

An even-even compound nucleus has a larger neutron binding energy than an even-odd nucleus, but the even-odd product nucleus (following neutron evaporation from an even-even nucleus) has a larger level density than the even-even product nucleus (following neutron evaporation from an even-odd nucleus). The influence of these two factors on Γ_n/Γ_f cancel each other to a first approximation.

Previous correlations of photofission[46] and fast neutron fission cross sections[42,46] have been made with the fissionability parameter Z^2/A. Figure 12.19 (a) is a plot presenting such correlations. The nuclides with lower atomic number are observed to fit the correlations satisfactorily, but for nuclides with atomic number greater than 94 the correlation fails. For example, plutonium isotopes formed by helium-ion induced reactions of U^{233} have lower neutron emission to fission width ratios than fermium isotopes formed from helium-ion induced reactions of Cf^{252}, although the latter have much larger values of Z^2/A than the former.

HENKEL AND BARSCHALL[47] found that fast neutron fission cross sections can be correlated with the parameter $Z^{4/3}/A$. (See Fig. 11.29). in Part I of this review, UCRL-9036. A related plot containing all known values of Γ_n/Γ_f is shown here in Fig. 12.19 (b). The correlation of the data, particularly for higher atomic number nuclides is slightly improved over the Z^2/A correlation. The parameter $Z^{4/3}/A$ has no known theoretical significance although the improvement in the correlation can be attributed to the increase of the mass number dependence relative to the atomic number dependence resulting from the fact that neutron binding energy trends, as well as fission thresholds, are of importance.

Perhaps a more fundamental parameter for correlating Γ_n/Γ_f values is the difference between the fission threshold and the neutron binding energy. FUJIMOTO AND YAMAGUCHI[48], by an extension of the BOHR-WHEELER theory, have derived the following approximate equation:

$$\Gamma_n/\Gamma_f \cong (TA^{2/3}/10) \exp (E_f - B_n)/T \qquad (12.6)$$

JACKSON[49] has suggested that in making a correlation of this type, one should use effective values for the difference between fission thresholds and neutron

---

47. R. L. Henkel and H. H. Barschall, Los Alamos Report LA-2122, March 1957.

48. Y. Fujimoto and Y. Yamaguchi, Prog. Theor. Phys. 5, 76 (1950).

49. J.D. Jackson in Proceedings of the Symposium on the Physics of Fission held at Chalk River, Ontario, May 1956, report CRP-642 A, July 1956.

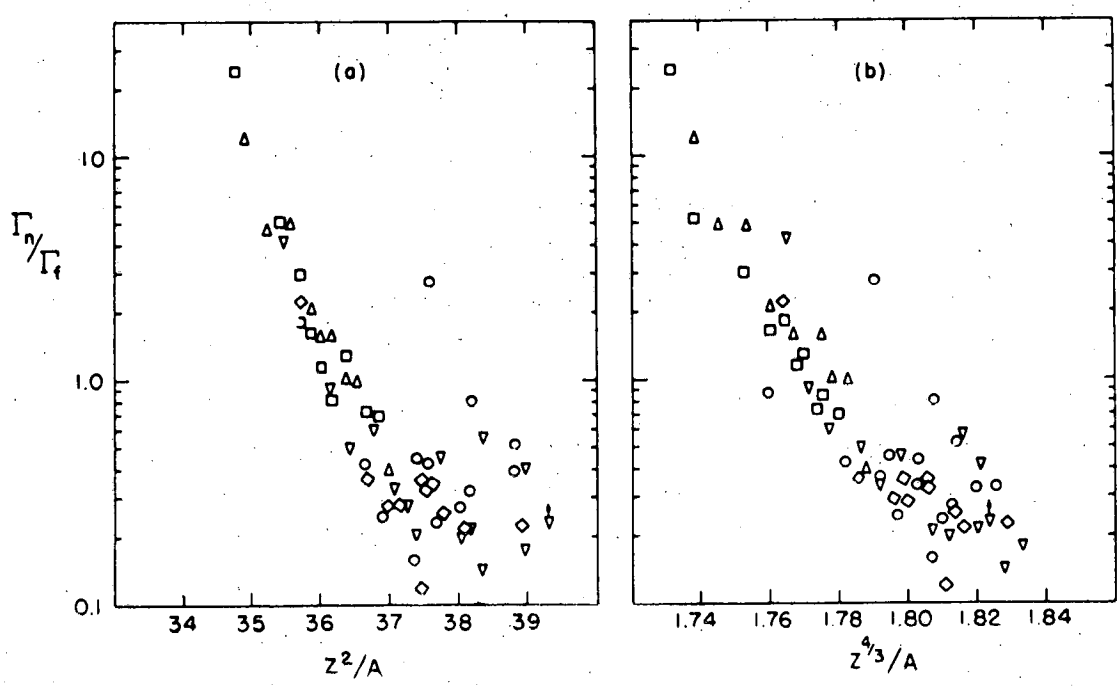

MU-19443

Fig. 12.19 Neutron emission to fission width ratios are plotted as a function of (a) Z^2/A and (b) $Z^{4/3}/A$. The shapes of the symbols have the same meanings as in Fig. 12.18. From VANDENBOSCH and HUIZENGA.[39]

binding energies. These effective values differ from the true values because of the dependence of level density on nuclear type. It is assumed that the exponential level density dependence on excitation energy is determined from a reference mass surface[50] which differs from actual ground state masses due to pairing energies, etc. In particular, odd-A ground state masses are taken as the reference mass surface, with the masses of the even-even and odd-odd ground states 0.72 Mev below and above the reference mass surface, respectively. The average difference between the even-even and odd-odd surfaces was experimentally found to be 1.44 Mev in the heavy element region.[51] This point is discussed in Chapter 1. From similar arguments the saddle-point surfaces for fission of even-even and odd-odd nuclei were chosen to lie 0.4 Mev below and 0.3 Mev above, respectively, the corresponding odd-A surface.

The dependence of Γ_n/Γ_f on nuclear type is dramatically demonstrated in Figs. 12.20 (a) and 12.20 (b) where all of the plotted Γ_n/Γ_f values are derived from data in which only a single competition occurred between neutron emission and fission. In Fig. 12.20 (a) the abscissa represents the actual difference between the fission threshold and the neutron binding energy ($E_f - B_n$). The fission thresholds for this particular comparison were derived from the equation of SWIATECKI[52] since this formula probably gives the best systematic values of fission thresholds in the limited mass region under investigation. In Fig. 12.20 (b) the effective difference between the fission threshold and the neutron binding energy ($E'_f - B'_n$) is plotted on the abscissa and the excellent agreement between values of Γ_n/Γ_f for different type nuclei supports the assumptions made above concerning ground state masses and fission saddle-point surfaces.

An examination of all the Γ_n/Γ_f data for these heavy elements by several authors[10,16,45] has led to the conclusion that there is no obvious dependence of this ratio on the excitation energy.

We can summarize our knowledge of the Γ_n/Γ_f ratios for the elements thorium and above in the following statements.

---

50. H. Hurwitz, Jr., and H.A. Bethe, Phys. Rev. 81, 898 (1951).

51. R. A. Glass, S. G. Thompson, and G. T. Seaborg, J. Inorg. and Nuc. Chem. 1, 3 (1955).

52. W. J. Swiatecki, Phys. Rev. 101, 97 (1956).

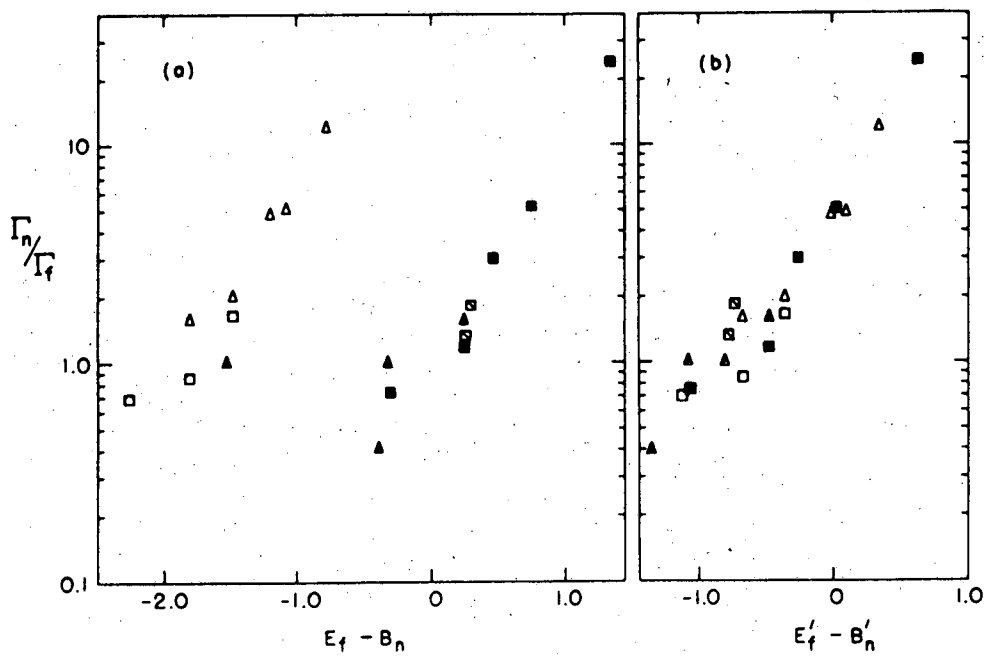

MU-19440

Fig. 12.20 Neutron emission to fission width ratios derived from data in which only a single competition occurred are plotted as a function of the difference between (a) the actual values of fission threshold and neutron binding energy (E_f-B_n), (b) the effective values of the fission threshold and neutron binding energy (E_f'-B_n'). Open symbols refer to even-even compound nuclei, closed symbols to even-odd compound nuclei, crossed triangle (△) to an odd-even compound nucleus, and crossed squares (⧅) to odd-odd compound nuclei. From VANDENBOSCH and HUIZENGA.[39]

(1) Γ_n/Γ_f is Z dependent (see Fig. 12.18)
(2) Γ_n/Γ_f is A dependent (see Fig. 12.17 and 12.18)
(3) Γ_n/Γ_f is independent or only weakly dependent on excitation energy $E_x < 40$ Mev.
(4) Γ_n/Γ_f is correlated with the quantity $B'_n - E'_f$

12.1.5 Competition of Fission and Neutron Emission in the Interaction of Charged Particles with Target Elements Below Thorium. When we examine the data for the fission of elements below thorium we find rather different systematic trends. FAIRHALL and his co-workers [53-56] have been chiefly responsible for the experimental data and interpretation in this mass region.

As mentioned above and discussed more fully below, the fission product distribution in the fission of spearated isotopes of lead and of bismuth bombarded with low energy deuterons or helium ions is highly symmetric; the fission mode for these elements at moderate excitation energies is a symmetric rather than an asymmetric mode. The probability for fission is quite small but it increases rapidly with excitation energy; Γ_f/Γ_{Total} is a rapidly increasing function of the excitation energy of the nucleus, at least up to about 40 Mev of excitation. There is no indication of an atomic number effect on the fissionability of the separated isotopes of lead. Thereis a definite Z-affect on fissionability.≠ Some data illustrating these points are summarized in Fig. 12.21. The fissionability trends observed for these cases are markedly different from those observed in the heavy elements above thorium.

The ratio , Γ_f/Γ_n, does not continue to rise indefinitely with excitation energy but must flatten out quite sharply for excitation energies above 35 Mev; this conclusion follows from the observed fission cross sections in the bombardment of targets in this mass region with charged particles in the energy range 50-100 Mev.

---

53. A. W. Fairhall, Phys. Rev. 102, 1335 (1956).
54. R. C. Jensen and A. W. Fairhall, Phys. Rev. 109, 942 (1958).
55. E. F. Neuzil, A. W Fairhall (to be published).
56. A. W. Fairhall, R. C. Jensen and E. F Neuzil, Paper P/677, Volume 15, Proceedings of the Second United Nations Conference on the Peaceful Uses of Atomic Energy, Geneva, 1958.

≠ Griffioen and Cobble, Purdue University, 1959, have studied fission cf targets lighter than lead. They report a fission cross section of 2 microbarns for rhenium bombarded with 41 Mev helium ions.

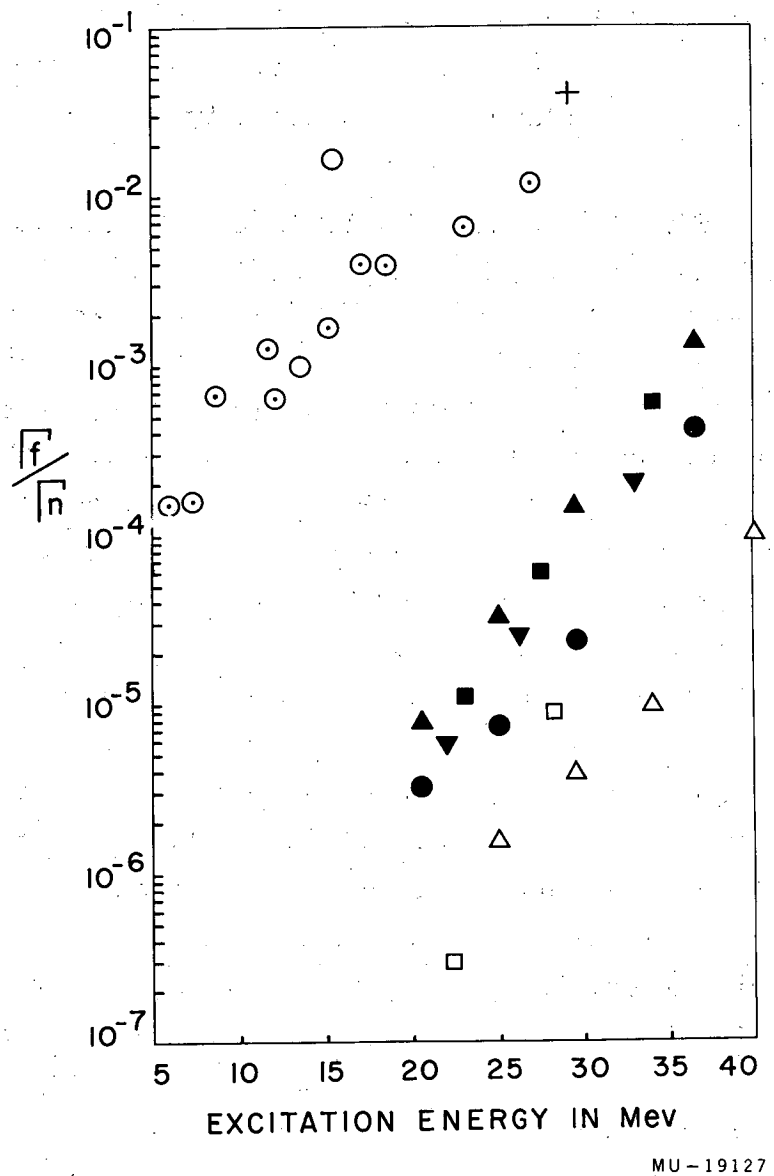

Fig. 12.21 Ratio of fission width and neutron emission width for target nuclei Z <90 plotted as a function of excitation energy. The values of Γ_f/Γ_n for the reactions Pb^{204}, Pb^{206}, Pb^{207}, Pb^{208} and Au^{197} with helium ions were calculated with the assumption that the fission yield of Y^{93} is 7%. Data from FAIRHALL.[56] Figure drawn by VANDENBOSCH and HUIZENGA.[39]

Moving up the atomic number scale to radium, JENSEN AND FAIRHALL[54] found a three-humped mass yield distribution when radium was caused to fission with 11 Mev protons. (See Fig. 12.26 below). This indicated separate symmetric and asymmetric fission modes of roughly equal probability. When the fission was induced in the same target with 22 Mev deuterons the yield of the products of symmetric fission was much greater. (See Fig. 12.27 below) From a consideration of the cross sections for fission in the two cases (about 2 mb for 11 Mev protons and 50 mb for the deuterons) and the estimated total reaction cross sections of 170 mb and 1200 mb, respectively, FAIRHALL, JENSEN AND NEUZEIL[56] conclude that there is considerably more symmetric fission but only about the same amount of asymmetric fission in the deuteron bombardment compared with the proton bombardment. The increasing yield of symmetric fission with increasing excitation energy is again apparent. Evidence for a similar type of behavior has also been obtained in fission induced by fast-neutron bombardment of radium using neutrons ranging in energy from 3 to 21 Mev.[57]

With this as a background, FAIRHALL, JENSEN AND NEUZIL[56] re-examined the question of fissionability trends in the region of thorium and heavier elements and came to somewhat different conclusions on the systematic trends than those summarized above. They conclude that it is important to emphasize that fission of these elements with charged particles of moderate energy is a mixture of symmetric and asymmetric fission modes and that one should first decompose the fission yield curve into a symmetric and asymmetric contribution and then treat separately the behavior of fission cross sections and Γ_f/Γ_n ratios as a function of energy for the two modes. A strong piece of evidence that this point of view is correct comes from the 3-humped mass-yield curves obtained by COLBY AND COBBLE[57a] for the helium-ion-induced fission of U^{233}. This is shown in figure 12.22.

By making the assumption that the shape of the fission product distribution for a pure symmetric fission mode in element above radium is similar in width to that seen in the fission of radium Fairhall, Jensen and Neuzil make a preliminary attempt

57. R. A. Nobles and R. B. Leachman, Nuclear Phys. 5, 211 (1958)

57a. L. J. Colby, Jr., and J. W. Cobble, unpublished results; see thesis study by L. J. Colby, Jr., Purdue University, 1960.

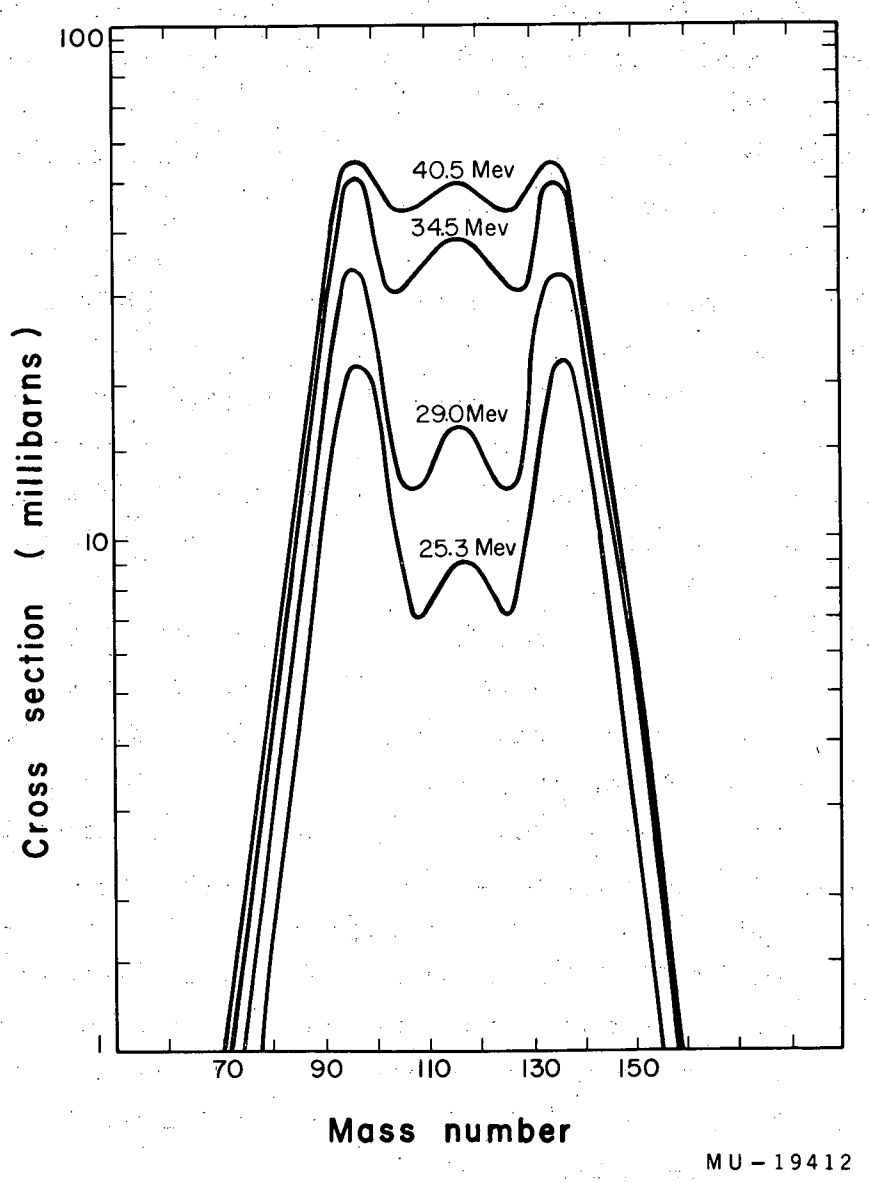

Fig. 12.22 Variation of the fission yield curves for U^{233} with energy of bombarding helium ions. From COLBY and COBBLE.[57a]

to decompose the published mass yield curves of the type shown in Fig. 12.3 into a symmetric and asymmetric component. They then show that the probability for symmetric fission in the elements above thorium also shows a very steep rise with excitation energy of the compound nucleus, the rise leveling off sharply above 25 Mev of excitation. Also as in the case of the lead isotopes there is no A-dependence of the fission probability in the symmetric mode. At the same time these authors conclude that the probability of asymmetric fission is highest for low excitation energies (above the fission threshold) and then drops off with increasing excitation energy, perhaps even becoming zero for excitation energies of 20 Mev.

This two-fission-mode view of fission has the virtue of applying equally well in all mass regions. It will remain a speculative interpretation until the resolution of mass-yield data into a symmetric and an asymmetric contribution can be done with more certainty and until more experimental data become available to define more precisely the characteristics of both types of fission.

12.1.6 Fission Product Yield Distribution as a Function of Energy. As early as 1940 NISHINA and CO-WORKERS[58] irradiated uranium with fast neutrons produced in the Li-D reaction and observed products of symmetrical fission which had not been found in thermal fission. SEGRÈ and SEABORG[59] did a similar study at the same time. Somewhat later, ENGELKEMEIR and CO-WORKERS[60] observed that the yield of Pd^{109} from fission of Pu^{239} with neutrons of roughly 600 kev was 50% higher than the corresponding yield in thermal fission. TURKEVICH and NIDAY[61] measured the mass-yield curve for Th^{232} irradiated with fission spectrum neutrons (average energy 2.6 Mev). A two-humped distribution was observed but the ratio of peak to trough yields was only 110 compared to the U^{235} thermal fission ratio of 600. TURKEVICH, NIDAY and TOMPKINS[62] irradiated thorium with neutrons from the Li + D reaction. In their experiment most of the fission was caused by neutrons in the energy range 6 to 11 Mev. The trough to peak yield ratio in this case was 0.09 or ten times greater than in the study just quoted. This increase of trough to peak yield ratios as a function of neutron energy follows the general trend summarized above in Fig. 12.4.

In more recent years there have been a number of radiochemical studies in which enough fission products were analyzed to delineate the shape of the mass-yield curve as a function of the energy of the bombarding particles.

---

58. Nishina, Yasaki, Kimura and Ikawa, Phys. Rev. 58, 660 (1940).
59. E. Segrè and G. T. Seaborg, Phys. Rev. 59, 212 (1941).
60. Engelkemeir et al., Paper 204, 219 in "Radiochemical Studies; The Fission Products", National Nuclear Energy Series, McGraw-Hill Book Company, Inc., New York, 1951.
61. A. Turkevich and J. B. Niday, Phys. Rev. 84, 52 (1951).
62. A. Turkevich, J. B. Niday and A. Tompkins, Phys. Rev. 89, 552 (1953).

Examples of such studies are given in Fig. 12.3, 12.9 and 12.22 above. A rather complete list of literature references to other radiochemical studies of this type is given in Table 12.7.

None of these studies is as detailed as the careful studies of the mass yield curve for fission of U^{235} induced by slow neutrons reviewed in the previous chapter (Report UCRL-9036). Because of the very great labor involved in a complete study most investigators have been obliged to limit themselves to the measurement of a few yields and from these data to sketch in only the broad features of the mass yield curves. The derivation of a mass-yield curve from the experimental data requires the introduction of assumptions or deductions on the charge distribution in the fission process and various investigators have individual preferences on the correct assumptions. For example, GIBSON[63] and later GUNNICK AND COBBLE[63a] decided on the basis of a consideration of their data that charge distribution in fission induced by charged particles comes close to preserving the charge-to-mass ratio of the fissioning nucleus while ALEXANDER AND CORYELL[64] conclude that the equal charge displacement assumption (see Section 11.5 in Chapter 11) gives a better fit. CHU[63b] also has interesting comments to make on this point. These differences do not alter the main conclusions to be drawn from the fission product yields as a function of energy. In connection with a brief discussion of Fig. 12.3 in the introductory section we mentioned the most obvious changes such as the gradual change from the two-humped distribution to a broad symmetric hump as the "valley" yields corresponding to a symmetric fission rapidly rise.

---

63. W. M. Gibson, University of California Radiation Laboratory Report, UCRL-3493, November 1956; see also B. M Foreman, W. M. Gibson, R. Glass and G. T. Seaborg, Phys. Rev. 116, 382 (1959).

63a. R. Gunnick and J. W. Cobble, Phys. Rev. 115, 1247 (1959).

63b. Y. Y. Chu, Thesis, University of California Radiation Laboratory Report, UCRL-8926, November 1959.

64. J. M. Alexander and C. D. Coryell, Phys. Rev. 108, 1274 (1957).

Table 12.7

Published Radiochemical Studies of Mass Yield Curves for Heavy Element Targets Induced to Fission with Particles or Photons of Moderate* Energy

Target	Energy of Particles or Photons	Report or Journal Reference
Re	41 Mev α	Griffioen and Cobble, Purdue University thesis.
Au	40 Mev α	Fairhall, unpublished.
Pb	20-42 Mev α	Neuzil and Fairhall, unpublished.
Bi	15-22 Mev d	Fairhall, Phys. Rev. 102, 1335 (1956).
Ra	23 Mev γ	Duffield et al., Geneva Conf. Proceedings, (1958) 15, 202.
Ra	11 Mev p	Jensen and Fairhall, Phys. Rev. 109, 942 (1958).
Ra	23, 43 Mev α	Jensen and Fairhall, unpub.; Geneva Report P/677 (1958)
Ra	22 Mev d	Jensen and Fairhall, unpub.; Geneva Report P/677 (1958)
Th^{232}	6.7-21 Mev p	Tewes and James, Phys. Rev. 88, 860 (1952).
Th^{232}	38 Mev α	Newton, Phys. Rev. 75, 17 1209 (1949).
Th^{232}	15-46 Mev α	Foreman, UCRL-8223 (1958); Phys. Rev. 116, 382 (1959).
Th^{232}	14 Mev d	Alexander, Phys. Rev. 108, 1274 (1957).
U^{233}	9-23 Mev d	Gibson, UCRL-3493 (1956); Phys. Rev. 116, 382 (1959)
U^{233}	23-44 Mev α	Thomas, Phys. Rev. 111, 1358 (1958).
U^{233}	20-40 Mev α	Colby, Purdue University thesis, (1960).
U^{235}	14 Mev n	Spence and Ford, Ann. Rev. Nuc. Sci. 2, 399 (1953). and AECD-2625 (1949); Wahl, Phys. Rev. 99, 730 (1955).
U^{235}	12-20 Mev p	Jones et al., Phys. Rev. 99, 184 (1955).
U^{235}	20-45 Mev α	Vandenbosch et al., Phys. Rev. 111, 1358 (1958).
U^{235}	20-40 Mev α	Gunnick and Cobble, Phys. Rev. 115, 1247 (1959).
U^{238}	14 Mev n	Cunninghame, J. Inor. Nucl. Chem. 5, 1 (1957).
U^{238}	16 Mev e	Richter and Coryell, Phys. Rev. 95, 1550 (1954).
U^{238}	22-45 Mev α	Vandenbosch et al., Phys. Rev. 111, 1358 (1958).
U^{238}	12-20 Mev p	Jones et al., Phys. Rev. 99, 184 (1955).
U^{238}	5-14 Mev d	Sugihara, Phys. Rev. 108, 1264 (1957).
U^{238}	14 Mev d	Alexander, Phys. Rev. 108, 1274 (1957).
U^{238}	48 Mev γ	Schmitt and Sugarman, Phys. Rev. 95, 1260 (1954).
U^{238}	5.5-8.0 Mev γ	Duffield et al., Geneva Conf. 1958, Vol.15, p.202.
U^{238}	22 Mev γ	L. Katz et al., Phys. Rev. 99, 98 (1955).

Table 12.7 (cont'd.)

Target	Energy of Particles or Photons	Report or Journal Reference
U^{238}	31 Mev γ	Dahl and Pappas, unpublished.
U^{238}	44 Mev α	Y. Chu, UCRL-8926 (1959).
U^{238}	20-40 Mev α	Lasalle, Purdue University thesis (1960).
Np^{237}	14-46 Mev α	Gibson, UCRL-3493 (1956).
Pu^{238}	30-42 Mev α	Carr, UCRL-3395 (1956); Glass et al., Phys. Rev. 104, 434 (1956).
Pu^{239}	20-47 Mev α	Glass, UCRL-2560 (1954); Glass et al., Phys. Rev. 104, 434 (1956).
Pu^{239}	9-23 Mev d	Gibson, UCRL-3493 (1956). Phys. Rev. 116, 382 (1959)
Pu^{240}	10-23 Mev d	Luoma, UCRL-3495 (1956).

* The term "moderate" is taken here to mean bombarding energies of <50 Mev.

The interesting mass yield curves seen in the fission of bismuth and radium were discussed earlier and are discussed in more detail a few pages later.

One piece of information that one can obtain from the radiochemically determined mass yield curve is the average number of neutrons, $\bar{\nu}$, emitted in fission. This is found by doubling the mass number of the midpoint of the fission product yield distribution, and subtracting this number from the mass of the presumed fissioning nucleus. Some sample values of $\bar{\nu}$ obtained in this fashion are listed in Table 12.8. These values for $\bar{\nu}$ are much less precisely known than those reviewed in the previous chapter for the case of slow neutron fission. Nonetheless it is interesting to note the rough trends in $\bar{\nu}$ as a function of the type and the energy of the particles causing fission in a variety of nuclei.

Since it has not been possible to obtain complete data on fission product distributions for all fissioning systems it has proved useful to draw conclusions from an examination of more restricted data. Frequently, for example, the yields of a few products from symmetric fission (trough yields) are measured and compared to the yields of a few of the most probable products of asymmetric fission (peak yields). The trough to peak yield ratio can be taken as a crude estimate of the relative contribution of symmetric and asymmetric fission. TURKEVICH, NIDAY AND TOMPKINS[62] showed how such yield ratios could be plotted against excitation energy to show a rather smooth increase in symmetric fission with increase of excitation energy. Other modifications of this plot have been suggested.

Figure 12.23 was prepared by GIBSON[63] according to a relationship suggested by FOWLER, JONES AND PAEHLER.[64a] The logarithm of the trough to peak yield ratio is plotted as the ordinate. The abscissa is $(E_x-5)^{-1/2}$ where E_x is the sum (in Mev) of the bombarding particle energy plus the energy with which it is found in the compound nucleus. The 5 Mev is subtracted to correct for the energy expended in distorting the nucleus to the point of fission. The square root of the quantity (E_x-5) is thus of the nature of nuclear temperature T and $(E_x-5)^{-1/2}$ is proportional to the reciprocal temperature of the distorted nucleus.

64a. J. L. Fowler, W. H. Jones and J. H. Paehler, Phys. Rev. 88, 71 (1952).

Table 12.8

Average Number of Neutrons, $\bar{\nu}$, Emitted During Fission Induced by Charged Particles of Moderate Energy as Deduced from Mass-Yield Curve

Target Nucleus	Particles	Energy of Particles (Mev)	$\bar{\nu}$	Reference
Bi^{209}	d	22	4	Fairhall, Phys. Rev. 102, 1335 (1956).
Ra^{226}	p	11	3-5	Jensen and Fairhall, Phys. Rev. 109, 942 (1958).
Th^{232}	α	15-19	3	Foreman et al., Phys. Rev. (1959).
		20	4	
		26	4	
		35-42	6	
		44	7	
U^{233}	α	23	4	Vandenbosch et al., Phys. Rev. 111, 1358 (1958).
		31	6	
		41	7	
U^{233}	d	9-14	3	Foreman et al., Phys. Rev. (1959).
		5-19	4	
		22	5	
U^{235}	α	22	4	Vandenbosch et al., Phys. Rev. 111, 1358 (1958).
		33	5	
		34	6	
		45	7	
		23	4.0±0.5	Gunnick and Cobble, Phys. Rev. 115, 1247 (1959).
		39.9	5.5±1	
U^{238}	α	23	4	Vandenbosch et al., Phys. Rev. 111, 1358 (1958).
		27	5	
		39	6	
		44	7	
U^{238}	d	10	4.0±1.5**	Sugihara et al., Phys. Rev. 108, 1264 (1957).
			5.0±0.7***	
			5.0±0.7****	
		13.6	3.3±0.7*	
			5.2±0.9**	
			5.2±1.0***	
			4.7±0.8****	
Pu^{238}	α	30.2	3	Carr, UCRL-3395
Pu^{238}	α	42.2	4	Carr, UCRL-3395
Pu^{242}	α	30.2	3	Carr, UCRL-3395
		42.2	4	

In the work of Sugihara et al., $\bar{\nu}$ was estimated as a function of mass ratio of the products. The asterisks designate the fission mode characterized by the following masses for the light fragment *77, **83, ***89, ****105.

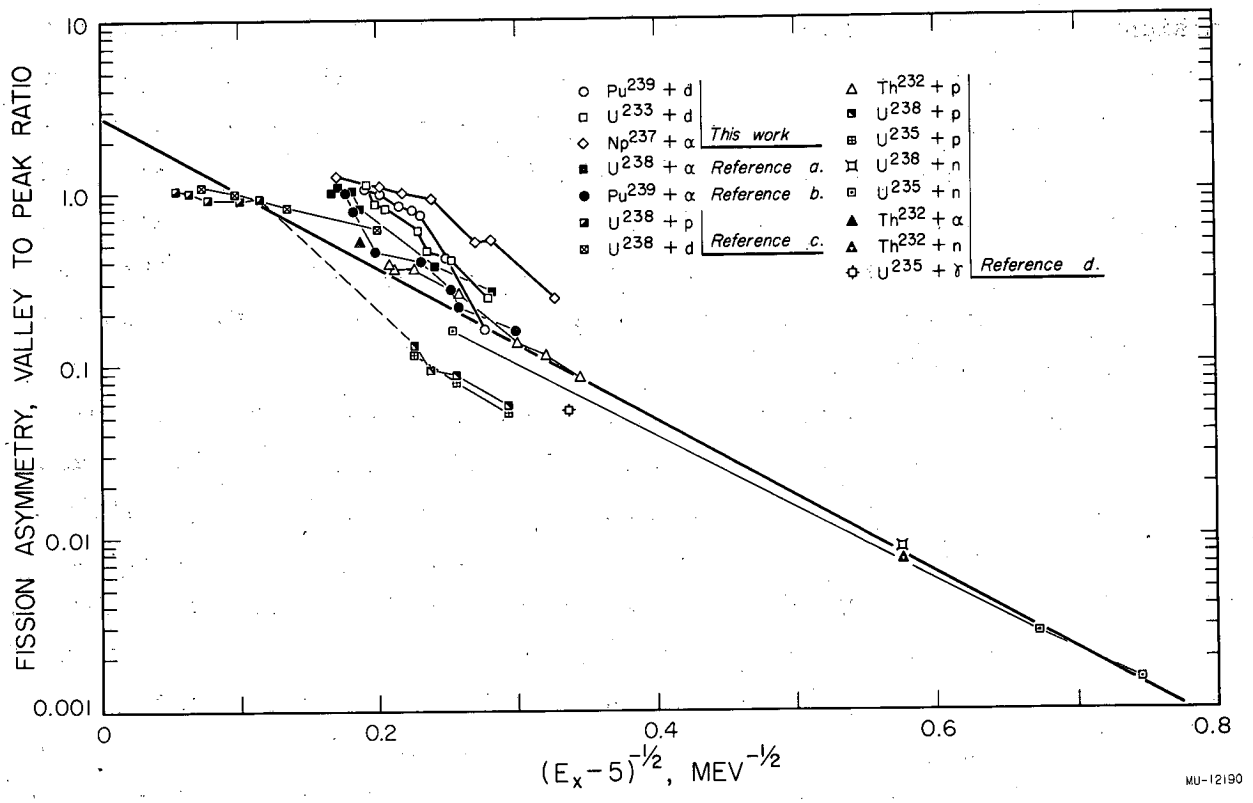

Fig. 12.23 Fission asymmetry (valley to peak) vs. $(E_x - 5)^{-1/2}$ for the fission of various heavy element nuclides excited by charged particles, neutrons and protons.

The references are (a) RITSEMA, UCRL-3266, (b) GLASS, UCRL-2560, (c) HICKS and GILBERT, Phys. Rev. 100, 1286 (1955), (d) JONES, TIMNICK, PAEHLER and HANDLEY, Phys. Rev. 99, 184 (1955). The heavy solid line is from reference d. This figure was prepared by GIBSON[63] and displays a relationship introduced by FOWLER, JONES and PAEHLER, Phys. Rev. 88, 71 (1952).

The proportionality constant can be determined if the level density can be assumed to be of the form given by the Weisskopf formula $W(e) = C \exp [2(E/a)^{1/2}]$. JONES, TIMNICK, PAEHLER AND HANDLEY[65] have used this approach to derive the relation $Y_{trough}/Y_{peak} = 2.8 \exp [-2.9/T]$ which corresponds to the diagonal straight line in Fig. 12.23. Since the relative probability of two states differing in energy by an amount ΔE is $\exp [- \Delta E/T]$ it is thus suggested that 2.9 Mev is the additional energy required to produce symmetrical in preference to asymmetrical fission. The data show a definite trend with the quantity $(E_x-5)^{-1/2}$ although it is evident that significant deviations occur from the above simple relationship.* This is not very surprising since, for one thing, the energy level formula may not be accurate for these deformed heavy elements at the excitation energies involved.

Another quite interesting study based on the measurement of peak to trough yields was carried out by BOWLES, BROWN AND BUTLER.[66,67] These authors studied the rise in the ratio of symmetric to asymmetric fission in thorium, uranium and plutonium targets bombarded with protons of increasing energy. The two nuclides Ag^{113} and Ba^{139} were selected as reliable indicators of these two modes of fission. Extreme care was taken in the measurement of the ratio of Ag^{113} to Ba^{139} (symmetric/asymmetric) and in the determination of the peak energy and energy spread of the protons striking the target.

The results of this study are summarized in Fig. 12.24. There is a general overall rise of the valley/peak ratio with increasing energy but superimposed on this rise are a number of dips rather pronounced in the lower energy regions, but becoming less pronounced at higher energies. These dips are most prominent for the thorium case and the interpretation in that case is as follows.

---

65. W. H. Jones, A. Timnick, J. H. Paehler, and T. H. Handley, Phys. Rev. 99, 184 (1955).

66. B. J. Bowles, F. Brown and J. P. Butler, Phys. Rev. 107, 751 (1957).

67. J. P. Butler, B. J. Bowles and F. Brown, Paper P/6, Vol. 15, Proceedings of the Second United Nations International Conference on the Peaceful Uses of Atomic Energy, Geneva, 1958.

* Sugihara, Drevinsky, Troianello and Alexander (Phys. Rev. 108, 1264, 1957) find that their data on the deuteron fission of uranium do not fit this straight line relationship at all well. See also the comments of Katz et al., Phys. Rev. 99, 98 (1955).

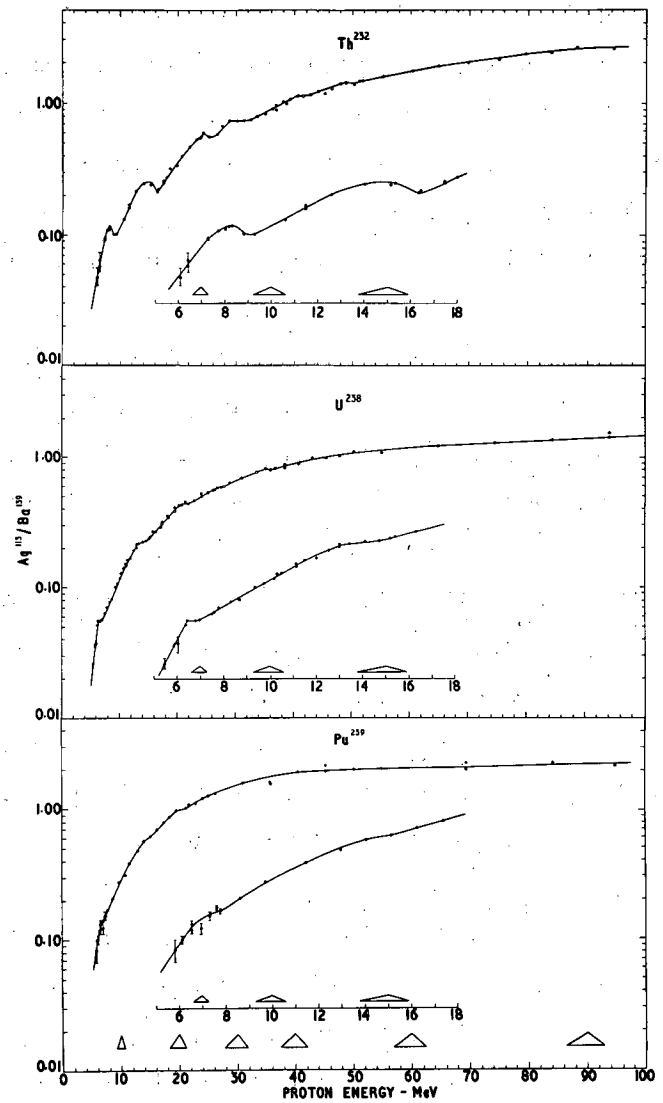

MU-19378

Fig. 12.24 BUTLER, BOWLES and BROWN's study of the ratio of Ag^{113} to Ba^{139} yield versus photon energy for Th^{232}, U^{238} and Pu^{239}. (1) The size of the circles shows the experimental precision of about 2 percent; (2) the crosses represent duplicate or triplicate points which were reproduced within 2 percent; (3) the spread in the energy of the protons is indicated by the open triangles.

"The excitation energy of the compound nucleus Pa^{233} is the kinetic energy of the proton plus 5.51 Mev, the proton binding energy. While the excitation energy is in the range 6-14 Mev the principal reactions will be (p,f) and (p,n); the energy of the fissioning nucleus Pa^{233} increases with increasing proton energy and the Ag^{113}-Ba^{139} ratio increases likewise (most of this energy range is not accessible experimentally because of the Coulomb barrier). At an excitation energy of approximately 14 Mev the reaction (p,nf) becomes possible, the energy required for this process being composed of the neutron binding energy (6.74 Mev), the kinetic energy of the emitted neutron (about 2 Mev) and the energy required to cause fission in the residual Pa^{232} nucleus (5-6 Mev). The fissions in Pa^{232} [the (p,nf) reaction] occur with an excitation energy approximately 8.74 Mev lower than those in Pa^{233} [(p,f) reaction] and the Ag^{113}-Ba^{139} ratio is lower. The observed Ag^{113}-Ba^{139} ratio corresponding to a mixture of the two fission reactions, thus falls at around this energy. A further increase in proton energy causes both the (p,f) and the (p,nf) reaction to occur with higher energies and the Ag^{113}-Ba^{139} ratio thus rises again until the (p,2nf) reaction sets in, whereupon another fall occurs, and so on." The spacings between the dips is in good agreement with what is known about nucleon binding energies and the kinetic energy of evaporated neutrons.

In the thorium case six discontinuities are observed at proton energies of 8.0, 14.0, 23.6, 29.5, 40 and 48 Mev. The dips in the U^{238} curve are not nearly as pronounced but five were noted at proton energies of 6.5, 13.0, 20.5, 27.0, and 35 Mev. The Pu^{239} curve rises much more rapidly and no discontinuities are noted with certainty. These differences in the appearance of the three curves is readily understood in terms of the relative fissionability of the three target isotopes. Plutonium-239 is so highly fissionable (high Γ_f/Γ_n) that fewer excited nuclei undergo neutron emission before fission; i.e. (p,nf) and (p,2nf) fission has a small probability compared to (p,f) fission. In the Th^{232} case the situation is quite different; BUTLER, BOWLES AND BROWN[67] estimate the (p,nf) fission is 1.40 times as probable as (p,f) fission. There is an appreciable probability that some of the protactinium compound nuclei will survive long enough to emit four or more neutrons.

This evidence and interpretation fits in neatly with the compound-nucleus model of fission developed previously in this chapter with fission and neutron emission competing at each stage of the evaporation chain. It also fits it with the suggestion of FAIRHALL that symmetric fission rises with increase of excitation energy in a particular fissioning nucleus.

Radiochemical investigations of the fission product distribution in the case of elements lighter than thorium caused to fission with charged particles of moderate energy have led to some striking results and to some new ideas about the fission process. The first study of this type was carried out by FAIRHALL[68] who studied the fission of bismuth with 15 and 22 Mev deuterons. The fission cross sections are extremely small in these cases, being only 1×10^{-29} cm^2 and 4×10^{-31} cm^2 respectively. Nonetheless, FAIRHALL[68] was able to measure the mass yield curve shown in Fig. 12.25. This curve is strikingly different from the two humped distribution seen in the low-energy fission of the heaviest elements. The distribution is single-humped, symmetric about mass 103.5 and has no pronounced fine structure. The width of the distribution is small; at half the maximum it is only 17 mass units.

NEUZIL AND FAIRHALL[69,70] have investigated the fission products of the separated isotopes of lead caused to fission with helium ions of various energies up to 42 Mev. In every case the mass distributions are narrow like that of Fig. 12.25, the only significant differences being that the axis of symmetry is displaced toward a lower mass value for the lighter isotope Pb^{204} relative to Pb^{208}.

JENSEN AND FAIRHALL[71] bombarded radium with 11 Mev protons and found the striking three-humped distribution of fission product yields shown in Fig. 12.26. The cross section for fission is only 2 millibarns at this proton energy. This curve is interpreted to mean that fission of radium with 11 Mev

---

68. A. W. Fairhall, Phys. Rev. 102, 1335 (1956).

69. E. F. Neuzil and A. W. Fairhall, unpublished results cited in ref. 70.

70. A. W. Fairhall, R. C. Jensen and E. F. Neuzil, Paper P/677, Vol. 15, Proceedings of the Second United Nations International Conference on the Peaceful Uses of Atomic Energy, Geneva, 1958.

71. R. C. Jensen and A. W. Fairhall, Phys. Rev. 109, 942 (1958).

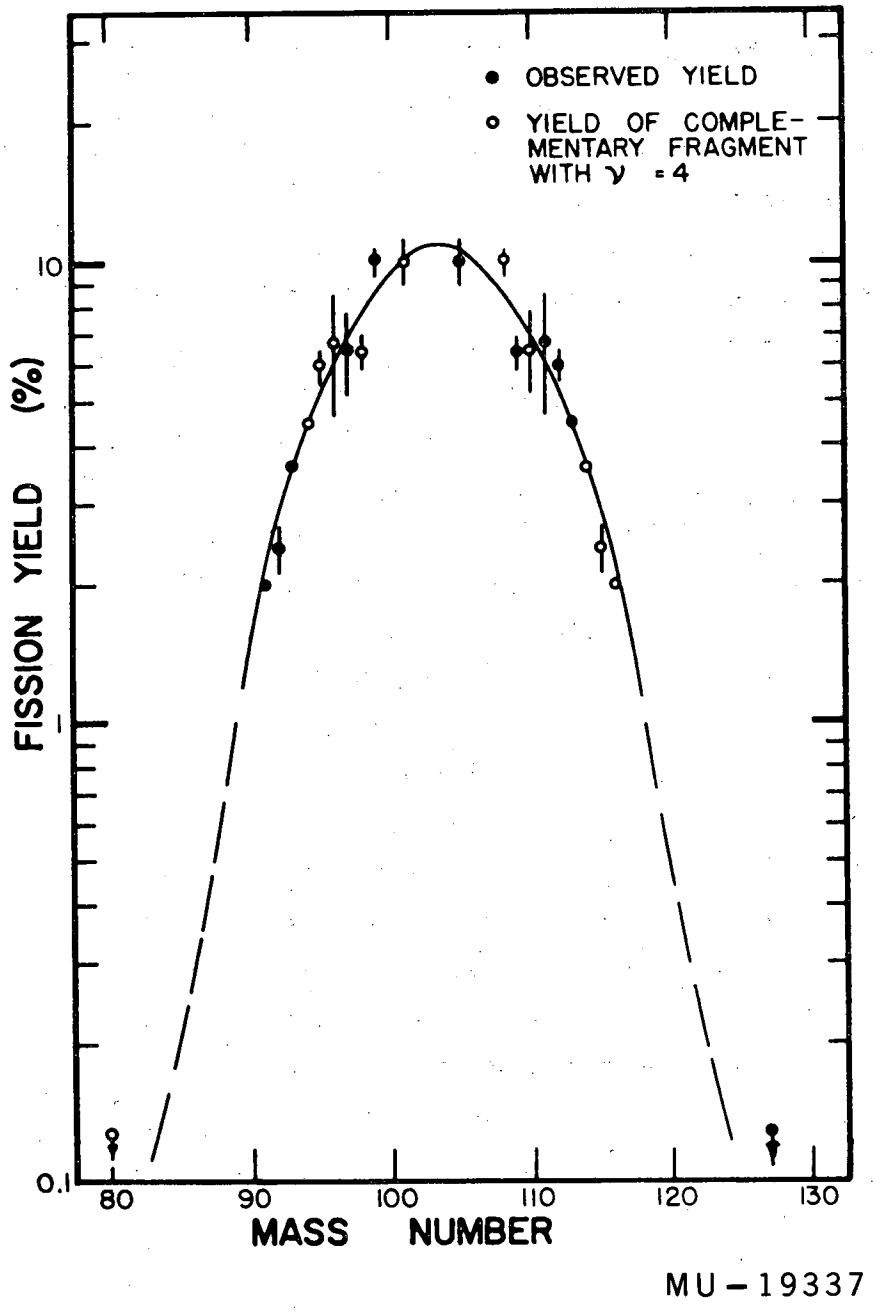

Fig. 12.25 Fission yield versus mass number for bismuth bombarded with 22 Mev deuterons. The fissioning species is probably Po^{211} excited to about 27 Mev. FAIRHALL.[68]

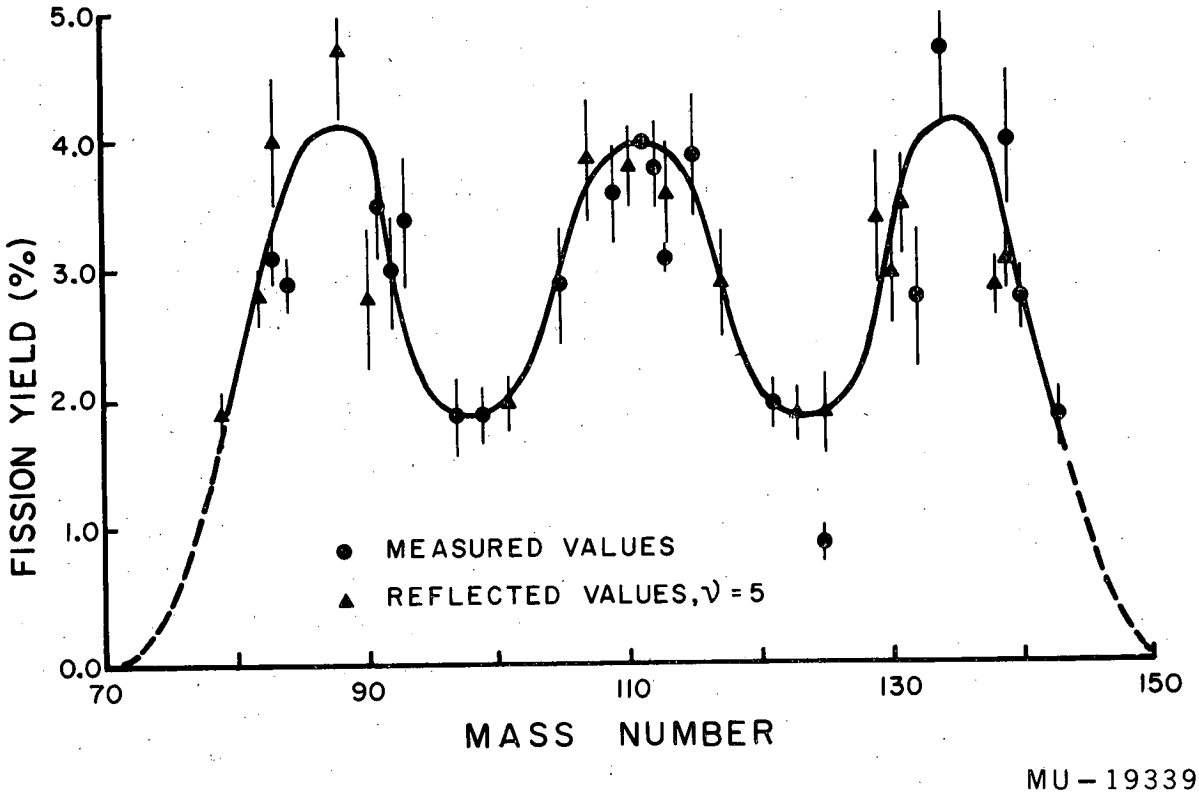

Fig. 12.26 JENSEN and FAIRHALL's fission yield curves for 11 Mev proton-induced fission of Ra^{226}. The compound nucleus is Ac^{227} excited to 16 Mev. The three-humped curve probably represents a mixture of symmetric and asymmetric fission.

protons occurs by two distinctly different fission modes: typically asymmetric fission and symmetric fission characterized by a narrow range of fission product masses.

The heavy "wing" of the asymmetric fission mode observed for radium fission is very similar to those observed in the asymmetric fission-yield curves of other elements. Within experimental error it is of the same width at half the maximum yield as the curve for thermal-neutron-induced fission of uranium. It is also interesting that the peak occurs in the same mass region as it is observed to occur for the other elements which undergo asymmetric fission. Thus the observation (see Section 11.4.2 of Chapter 11) that the location of the heavy-fragment "wing" stays fixed and the light-fragment "wing" shafts compensatingly as one goes to lighter fissioning elements also applies to the asymmetric fission of radium.

Fig. 12.27 shows the results of radium fission induced with 22 Mev deuterons which proceeds through the compound nucleus Ac^{228} excited to about 30 Mev. In this case the curve represents primarily symmetric fission with a much broader mass distribution associated with it. In addition, there is a suggestion of two small peaks at the positions of the maximas of the asymmetric mass division as in the case of fission induced by 11 Mev protons. The total fission cross section is about 50 millibarns. From a comparison of the fission cross sections and the mass yield curves in the two studies it is clear that the symmetric fission mode increases rapidly with energy.

Evidence for a similar type of behavior has also been obtained in fission of Ra^{226} caused by irradiation with fast neutrons. NOBLES AND LEACHMAN[72] did not measure yields radiochemically but measured the kinetic energies of single fragments in a scintillation counter of xenon gas. They observed that the fission cross section rose rapidly with neutron energy from 4 to 21 Mev. The fragment energy distribution (and hence the mass distribution) was twin-peaked corresponding to asymmetric fission at the lowest energies (3.3-4.6 Mev) and rapidly changed over to a single peaked distribution with increasing neutron energy. The excitation function for fission rises steadily and does not show the stepwise plateaus characteristic of the elements above thorium (See for

72. R. A. Nobles and R. B. Leachman, Nuclear Phys. 5, 211 (1958).

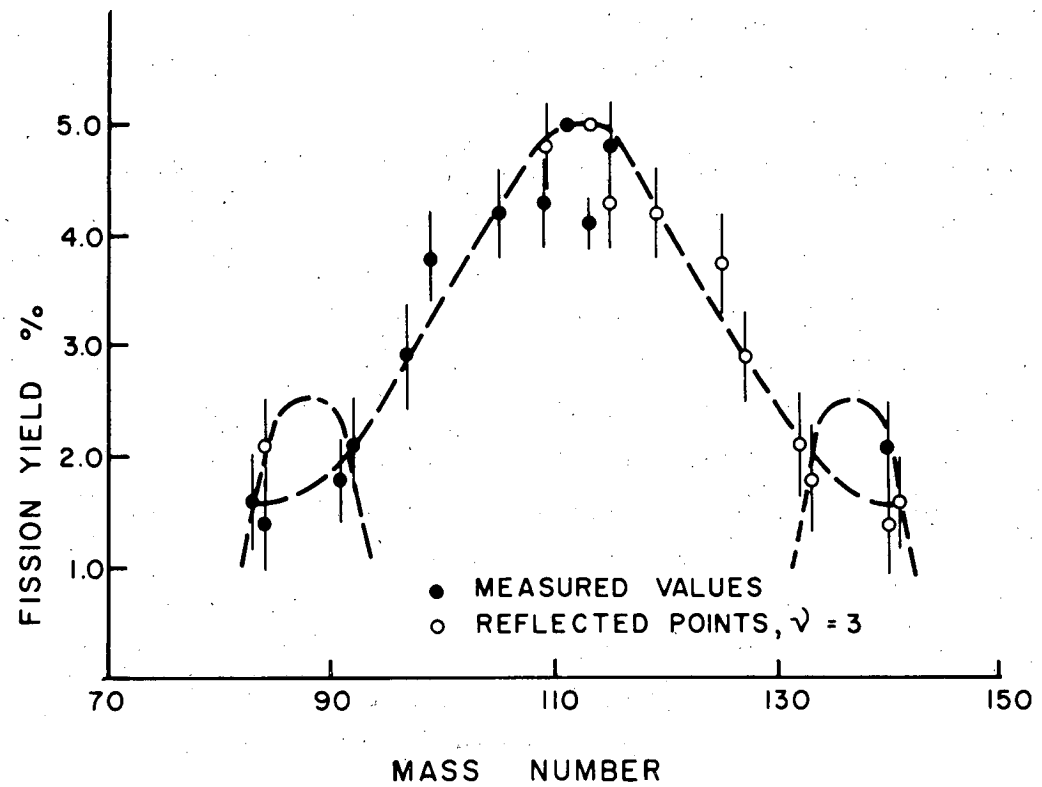

MU-19338

Fig. 12.27 Mass yield curve of fission products from Ra^{226} bombarded with 22 Mev deuterons. The compound nucleus is Ac^{228} excited to about 30 Mev. From FAIRHALL, JENSEN and NEUZIL.[70]

example Section 11.3.5 in the previous chapter). This may indicate that Γ_f/Γ_n increases rapidly with excitation energy for the symmetric mode of fission in radium.

DUFFIELD, SCHMITT AND SHARP[73] irradiated radium with 23 Mev x-rays and by radiochemical analysis were able to measure a three-humped fission product distribution similar to that shown in Fig. 12.26 corresponding to fission induced by 11 Mev protons.

JENSEN AND FAIRHALL[74,70] studied the fission products of radium in targets bombarded with 23.5 Mev and 43 Mev helium ions. The compound nuclei were Th^{230} excited to 18.5 Mev and 38 Mev, respectively. The shapes of the distributions for these thorium compound nuclei were very similar to those for other heavy element nuclei; at the lower energy the mass division looked like a typical heavy element asymmetric distribution while at the higher energy it had the appearance of a broad flat mass distribution.

A significant contribution was made by GRIFFIOEN AND COBBLE[74a] who studied the fission of rhodium with helium ions of incident energies of 31, 36 and 44 Mev. Because of the extremely low fission cross section it was necessary to use thick targets so that the effective average energies of the helium ions was somewhat less. The cross section values deduced from the mass yield curves were ~200 millimicrobarns, 000 millimicrobarns and 2.1 microbarns, respectively, for the three energies. It was a difficult radiochemical problem to isolate specific fission products so only a few were taken out. These were enough, however, to show that the fission of rhenium with 31 Mev helium ions results in a 3-humped fission product distribution rather like that of radium (Fig. 12.26) caused to fission with 11 Mev protons. At this energy the two peaks of the asymmetric distribution are higher than the peak representing symmetric mass division. When 36 Mev helium ions are incident on the target the symmetric fission peak is somewhat higher. When 44 Mev helium ions are used the mass-yield distribution looks almost symmetric although slight "bumps" on the sides

---

73. R. B. Duffield, R. A. Schmitt and R. A. Sharp, Paper P/678, Vol. 15, Proceedings of the Second United Nations Conference on the Peaceful Uses of Atomic Energy, Geneva, 1958.

74. R. C. Jensen and A. W. Fairhall, unpublished results.

74a. R. D. Griffioen and J. W. Cobble, unpublished results; See thesis study by R. D. Griffioen, Purdue University, 1960.

of the symmetric peak reveal a small contribution of asymmetric fission. In short, the fission product distribution and its change with increase of bombarding energy are similar to those seen by JENSEN AND FAIRHALL[71] in the fission of radium.

GRIFFIOEN AND COBBLE point out that this result indicates that asymmetric fission must in some way be associated with nuclei which have deformed nuclear shapes in the ground state. As one considers the character of fission across a large range of elements one discerns the following trends. In the heaviest elements beyond thorium low energy fission is predominantly asymmetric. The nuclei of these elements are known from many lines of evidence to be highly deformed. (See Chapter 9). Around the lead-bismuth region the atomic nuclei are stabilized in a spherical shape under the influence of the 82 proton and 126 neutron shells. The low or moderate energy fission of these elements is symmetric. As we drop down to lighter elements like rhenium nuclei again become stabilized in a deformed shape and asymmetric fission reappears. This hypothesis of a close connection between asymmetric fission and the deformation of the nucleus in the ground state can be tested further by additional studies of fission product yield distributions in other elements. Further work is being done in spite of the difficulties imposed by the extremely small fission cross sections.

12.1.7 Angular Distribution of Fission Fragments. It has been observed experimentally that fission fragments are emitted preferentially in certain directions when neutrons, charged particles, or photons of moderate energy are used to induce fission. The precise form of this anisotropy depends upon the fissioning nucleus, the mass ratio of the fragments and the nature and energy of the particles or photons initiating the fission. It is useful to divide the discussion of these anisotropy effects into three parts, corresponding to photofission in the threshold region and to particle-induced or neutron-induced fission in the region of moderate energy and the region of high energy.

(a) Fragment Angular Correlations in Photofission Near Threshold

WINHOLD, DEMOS AND HALPERN[75] were the first to call attention to anisotropic distribution of fission fragments in any fissioning system. They studied the photofission of thorium and uranium using x-rays from the 16 Mev electron linear accelerator at M.I.T. Fragments were collected at several angles and found to be emitted preferentially at 90° to the photon beam for Th^{232} and U^{238} targets. The observed distributions were compatible with an expression of the form, $a + b \sin^2 \theta$. In the case of U^{235} no anisotropy was noted. The anisotropy, expressed as the ratio b/a, was greater for Th^{232} than for U^{238} but this ratio dropped rapidly as the energy of the gamma rays increased to a value a few Mev above the fission threshold. In the region of the giant resonance (centered at 14 Mev) the anisotropy was small if not zero. In some experiments the fragment intensities in various directions were determined by radiochemical analysis so that fragment angular distributions could be measured as a function of mass asymmetry. A strong correlation was found; mass-symmetric fission was essentially isotropic but anisotropy increased monotonically, perhaps linearly, with the mass ratio. The most asymmetric products had a b/a ratio of about 0.6.

KATZ, BAERG AND BROWN[76] extended these studies. They found no evidence for anisotropy in the emission of fragments from odd-A nuclei U^{233}, U^{235}, Np^{237} Pu^{239}, and Am^{241} even though they concentrated on the lower photon energies where

---

75. E. J. Winhold and I. Halpern, Phys. Rev. 103, 990 (1956); preliminary results reported by Winhold, Demos, and Halpern, Phys. Rev. 85, 728 (A) (1952); Phys. Rev. 8, 1139 (1952) and Fairhall, Halpern and Winhold, Phys. Rev. 94 33 (1954). E. J. Winhold, Ph. D. Thesis, Massachusetts Institute of Technology, Sept. 1953.

76. L. Katz, A. P. Baerg and F. Brown, Paper P/200, Volume 15, Proceedings of the Second UN Conference on the Peaceful Uses of Atomic Energy, Geneva, 1958; also reproduced as Canadian report AECL-610.

any anisotropy might be expected to be greatest. Strong anisotropies were noted for the fragments of Th^{232} and U^{238} fission, the former having the higher anisotropy. Table 12.9 summarizes the results. The last column in the table gives the empirical value of α needed to fit the data to a formula of the type $1 + \alpha \sin^2 \theta$. Figures 12.28 and 12.29 show the sharp decrease in anisotropy as a function of the maximum bremsstrahlung energy. The most extreme anisotropy value was found for Th^{232} bombarded with a photon beam of maximum energy 6.5 Mev where 20 times as many fragments came off at 90° to the beam as were ejected at 0°. One might judge from the trends in the data that the true value of α as a function of monoenergetic photons would indicate fragment distributions peaked even more strongly at the lower photon energies.

BAZ AND CO-WORKERS[77] concluded from their studies of photofission that there is a sizable electric quadrupole component in the angular distribution of U^{238} fission fragments for synchrotron energies of 9.4 Mev. KATZ, BAERG AND BROWN[76] were able to get a good fit with formula of the form $1 + \alpha \sin^2 \theta$ and found no clear reason to assume any quadrupole contribution.

When these effects were first observed it seemed difficult to account for them since it seemed likely that any angular momentum brought into the nucleus by the photon would be distributed between the orbital motion of the fragments around each other and the internal motion of the nascent fission fragments. If any distribution of this type occurred there would be little or no anisotropy in the emission of the final fragments. The strong peaking of the experimental distribution is strong evidence that none of the angular momentum is passed on to the internal motion of the fission fragments.

A reasonable explanation for this exclusion of angular momentum from the internal motion of the fragments was provided by A.BOHR[78] in his 1955 Geneva paper. He suggested that a compound nucleus with an excitation energy not very much above the fission threshold would have to bind up most of its energy content in potential energy of deformation in order to reach a saddle point shape. At the saddle point the nucleus is relatively unexcited and the quantum states available to the nucleus are few in number and widely separated. If the reason-

---

77. A.I. Baz, N. M. Kulikova, L. E. Lazareva, N.V. Nikitina, V. A. Semenov, Paper P/2037, Second U.N. International Conference on the Peaceful Uses of Atomic Energy, Geneva, 1958

78. A. Bohr, Paper P/911, Vol. 2, Proceedings of the UN International Conference on the Peaceful Uses of Atomic Energy, Geneva, 1955.

Table 12.9

Relative Fission-Fragment Yields[a] as a Function of Peak Bremsstrahlung Energy, E_o, and Angle to X-ray Beam, Θ. Katz, Baerg and Brown.

	Angle Θ					Value of α in $W(\Theta) = 1 + \alpha \sin^2 \Theta$
E_o(Mev)	0°	25°	45°	60°	90°	
			Th^{232}			
6.5	1.0 ±0.3				20 ±5	> 25
7.0	1.00±0.04		4.1±0.2	6.7±0.3	8.4±0.3	13 ±1
7.5	1.0 ±0.1		5.1±0.4	6.0±0.4	8.8±0.5	7.2±0.7
8.0	1.00±0.09		2.4±0.2	3.6±0.3	5.1±0.3	6.7±0.7
9.0	1.0 ±0.1				3.4±0.3	2.8±0.4
10.0	1.00±0.04	1.16±0.05	1.67±0.08	1.97±0.08	2.4±0.1	1.63±0.06
14.0	1.00±0.05				1.43±0.08	0.46±0.09
20.0	1.00±0.05				1.13±0.06	0.14±0.06
			U^{238}			
6.0	1.0 ±0.3				6.0±1.4	6.6 ±2
6.3	1.0 ±0.1		3.6±0.4		5.9±0.6	5.8 ±1
6.5	1.0 ±0.2				4.5±0.7	4.4 ±1
7.0	1.00±0.08	1.5±0.1	2.0±0.2	2.4±0.2	2.9±0.2	1.84±0.2
8.0	1.00±0.06				2.1±0.1	1.3±0.1
9.4	1.00±0.04		1.22±0.06		1.43±0.06	0.46±0.06
10.0	1.00±0.04				1.38±0.04	0.41±0.05
14.0	1.00±0.04				1.08±0.04	0.09±0.04
20.0	1.00±0.03				1.05±0.03	0.05±0.03

[a] All values quoted are counts observed for unit X-ray dose and normalized to unit yield at $\Theta = 0^o$.

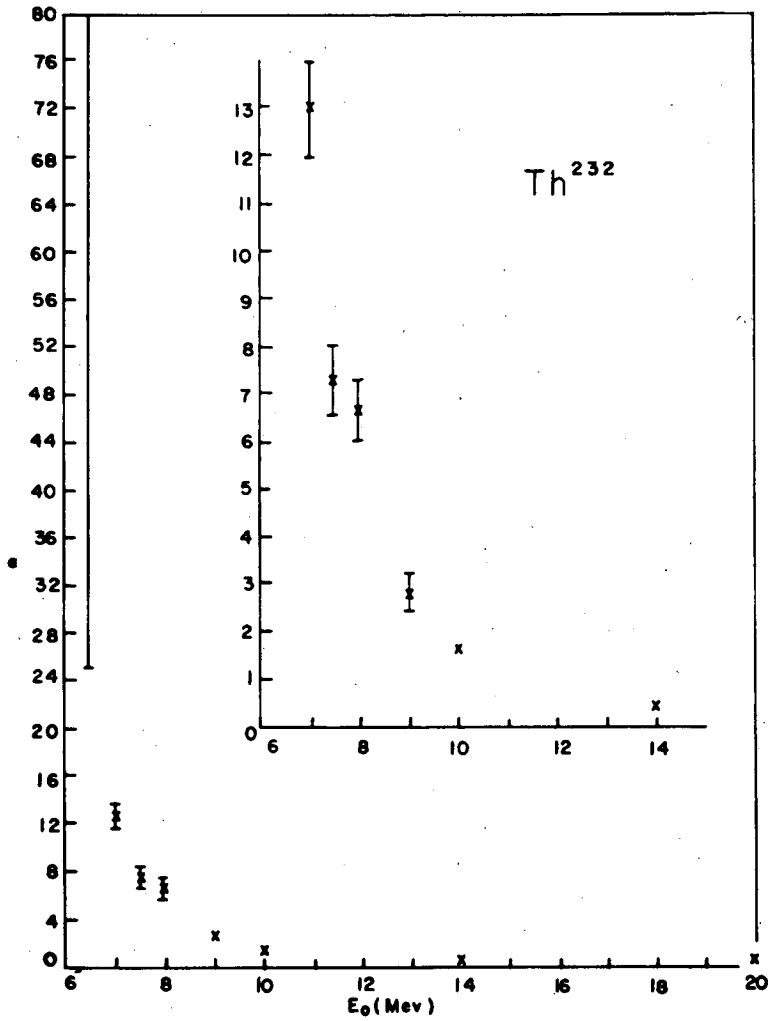

MU-19442

Fig. 12.28 Anisotropy of fission product distribution in Th^{232} versus maximum bremsstrahlung energy. The ordinate is α in the expression $1 + \alpha \sin^2\theta$. The values are corrected for resolution. From KATZ, BAERG and BROWN.[76]

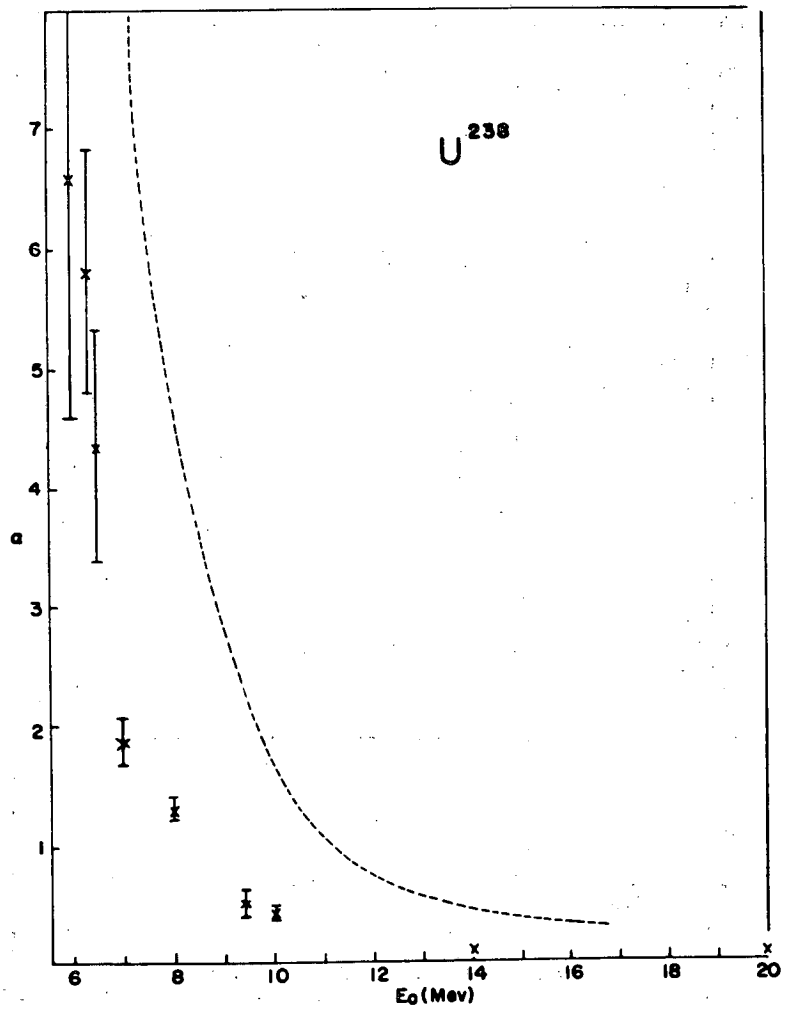

MU-19441

Fig. 12.29 Anisotropy of fission product distribution in U^{238} versus maximum bremsstrahlung energy. The ordinate is α in the expression $1 + \alpha \sin^2\theta$. The values are corrected for resolution. The dotted line represents the results for Th^{232} and corresponds to the data given in Fig. 12.28. From KATZ, BAERG and BROWN.[76]

able assumption is made that the nucleus is axially symmetric at the saddle point then the low-lying quantum states might well resemble those seen in the ground state of the same nucleus which is also known to be somewhat deformed. (See discussion of unified model in Chapter 9). In even-even nuclei the nucleons are coupled (K-quantum number = 0) and about one Mev is required to uncouple a nucleon pair and excite nucleonic states with a higher K-number. The low-lying excitations are rotational in character and the prominent states form a 0+, 2+, 4+ ... sequence. In addition, there is a low-lying I = 1- state believed to result from collective quadrupole vibrations of the nucleus. (See sections 9.3.4 and 9.5.3 of Chapter 9).

In terms of this model the photofission effects of even-even nuclei are rather easy to explain in a qualitative way. The chief photon absorption is electric dipole in character so the compound nucleus is always produced in a 1- state. The lowest 1- state at the saddle point corresponds to the K = 0 configuration with the nuclear angular momentum taken up by the rotational motion. For photon energies close to the fission threshold the great majority of the fissioning nuclei must pass through this particular saddle point quantum state. Since the rotation of the elongated nucleus is perpendicular to the angular momentum in this state and the angular momentum vector is lined up along the direction of the photon beam (M-quantum number ± 1) the fragments should fly off perpendicular to the photon beam. This statement tacitly assumes that no significant interchange of angular momentum between rotational and intrinsic motion occurs during the final stages of fission as the nucleus moves down from the saddle point into two separated fragments; any such interchange would tend to wash out the fragment anisotropy.

For excitation energies even a few Mev above threshold many other 1- states become available at the saddle point distortion. In these states the nuclear symmetry axis has various orientations with respect to the nuclear angular momentum and the angular distribution tends to become isotropic. Anisotropic photofission is expected to be observable only within a few Mev of threshold.

The experimental fact that the anisotropy is larger in Th^{232} than in U^{238} might indicate a larger gap in Th^{232} between the first collective 1- state and the lowest -lying intrinsic excitations with spin and parity 1- at the saddle point. This is in accord with Fig. 9.14 (Chapter 9) which shows that

the lowest 1- state increases in energy in going from thorium to uranium for ground state deformations.

If an 1- state of collective motion is indeed involved in low energy photofission and if this 1- state is correctly described as a vibration of the nucleus into asymmetric (pear-shaped) configurations then one might expect that a nucleus in this state could not undergo symmetric mass division.[78] As mentioned above, FAIRHALL, HALPERN AND WINHOLD[75] have observed just this effect. The anisotropy disappears when specific fission products of symmetric mass division are examined and increases strongly with the ratio of the fragment masses.

In odd-A nuclei one expects to find a greater concentration of low-lying levels at the saddle point configuration in which the angular momentum is carried by the nucleonic motion instead of only by collective oscillations. In addition, when a sample of an odd-A nucleus like U^{235}, which has a large spin in its ground state, undergoes dipole absorption a collection of excited nuclear states is produced with angular momentum vectors almost isotropically oriented with respect to the beam. Hence one expects an isotropic distribution of fragments in the photofission of odd-A nuclei and this is what is found experimentally.

(b) Fragment Angular Distributions in Fission Induced by Neutrons or Charged Particles of Moderate Energy

Pronounced anisotropy is also noticed in certain cases when fissionable nuclei are bombarded with neutrons. BROLLEY, DICKINSON AND HENKEL[79-81] bombarded thin foils of uranium, thorium and neptunium with monoenergetic neutrons obtained from the $T(p,n)He^3$, $D(d,n)He^3$ and $T(d,n)He^4$ reactions using protons or deuterons from an electrostatic accelerator. The neutron energy was varied from 1.26 Mev to 20.3 Mev. The fissile material was mounted in back-to-back ionization chambers and suitable collimation was provided to define the angle of emission of the fragments which were detected in the chamber. In some experiments, the energy peaks of the heavy and light groups were separated by pulse height analysis of the ionization chamber output.

---

79. J. E. Brolley, W. C Dickinson and R. L. Henkel, Phys. Rev. 99, 159 (1955).
80. J. E. Brolley and W. C. Dickinson, Phys. Rev. 94, 640 (1954).
81. R. L. Henkel and J. E. Brolley, Phys. Rev. 103, 1292 (1956).

Some striking effects were observed. Table 12.10 summarizes $0^\circ/90^\circ$ yield ratios for fragment emission for U^{238} and Th^{232}. The observed ratios are not as extreme as those observed in the threshold region for photofission but values different from unity are very definite nonetheless. At most energies the favored direction of emission is along the direction of the neutron beam but there are strong fluctuations in the magnitude of this forward peaking. Even more striking is the reversal of the anisotropy in the Th^{232} case. In Fig. 12.30 we notice that the fragments are emitted preferentially at 90° to the beam when the neutron energy is 1.6 Mev. At a little higher energy the angular distribution shifts drastically so that at 2.26 Mev neutron energy the beam direction is favored by 1.74 to 1. Figure 12.30 also shows the fission cross section as a function of neutron energy for Th^{232}. There appears to be a strong correlation between the resonance peak in the cross section curve at 1.6 Mev and the minimum in the $0^\circ/90^\circ$ yield ratio of the fragments.

The angular distribution was measured at several angles in addition to 0° and 90° for a few selected neutron energies. The resulting curves could be fitted with an expression of the type

$$1 + \Sigma A_n \cos^{2n\theta} \qquad (12.7)$$

provided that terms through $A_3 \cos^{6\theta}$ were included. This suggests that neutrons with ℓ-values up to 3 may be participating in the reaction. Figure 12.31 is a polar plot of the angular distributions observed in several cases.

SIMMONS AND HENKEL[82] extended these studies to Th^{230}, U^{234} and U^{236} using a multiangle gas-filled counter to measure the angular distributions. Neutrons of energy between 0.6 Mev and 9 Mev were used to induce fission. At 6 Mev the anisotropy increased sharply as in the previous studies of Th^{232} and U^{238} showing that this effect is general for even-even targets. The highest anisotropy values occurred for Th^{230}; the ratio of yields attained a value of approximately 2.3 ($0^\circ/90^\circ$) at 7 Mev. Near the fission thresholds the anisotropies showed considerable variation. For the case of U^{236} in particular near 0.85 Mev the preferred emission was at 90° to the beam.

The resonance character of the energy dependence of the angular distributions illustrated for Th^{232} in Figure 12.30 suggests that only one or a

---

82. J. E. Simmons and R. L. Henkel, Bull. Amer. Phys. Soc. (II) 4, 373 (1959).

Table 12.10

Ratio of the fission fragment yield at 0° to the neutron beam, to the yield at 90°. The values have been corrected for the finite angular resolution of the apparatus.

Neutron energy	$0^{\circ}/90^{\circ}$ Ratio of fragments
U^{238}	
1.260±0.071	0.989±0.32
1.348±0.081	1.09±0.16
1.474±0.103	1.70±0.12
1.979±0.060	1.36±0.06
2.498±0.056	1.40±0.06
3.246±0.061	1.18±0.05
4.870±0.215	1.25±0.09
6.008±0.140	1.47±0.08
7.265±0.105	1.69±0.08
14.5±0.500	1.40±0.14
17.77±0.300	1.26±0.12
20.28±0.120	1.36±0.10
Th^{232}	
1.400±0.072	0.68±0.10
1.607±0.067	0.10±0.05
1.607±0.067	0.15±0.07
1.800±0.064	0.98±0.20
2.260±0.057	1.74±0.17
2.400±0.054	1.65±0.21
3.00±0.046	1.39±0.14
4.00±0.038	1.15±0.08
6.00±0.028	1.12±0.16
6.230±0.140	2.21±0.22
7.147±0.113	2.41±0.23
7.777±0.100	2.20±0.22
9.562±0.054	1.79±0.16
14.5±0.30	1.96±0.38
14.5±0.30	1.85±0.80
16.36±0.252	1.34±0.16
17.86±0.150	1.79±0.37
20.32±0.085	2.10±0.46

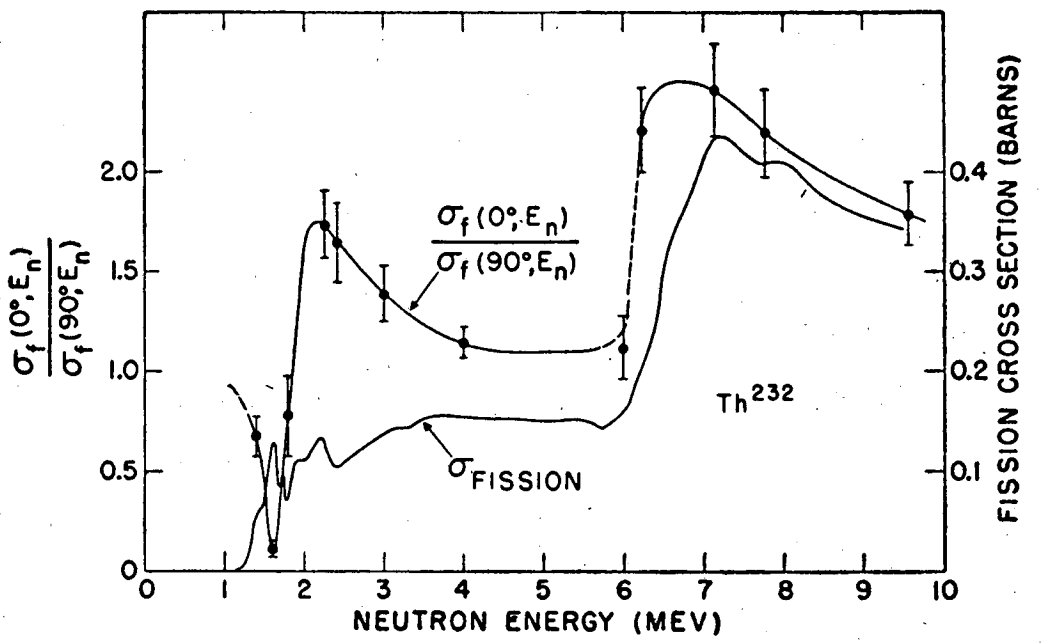

MU-19436

Fig. 12.30 Variation in the anisotropy of fission fragment distribution with the energy of neutrons for Th^{232} targets. Anisotropy is defined as the ratio of fragments ejected in the direction of the beam to those ejected at 90° to the beam. The fission cross section is also shown. From HENKEL and BROLLEY, Phys. Rev. 103, 1292 (1956).

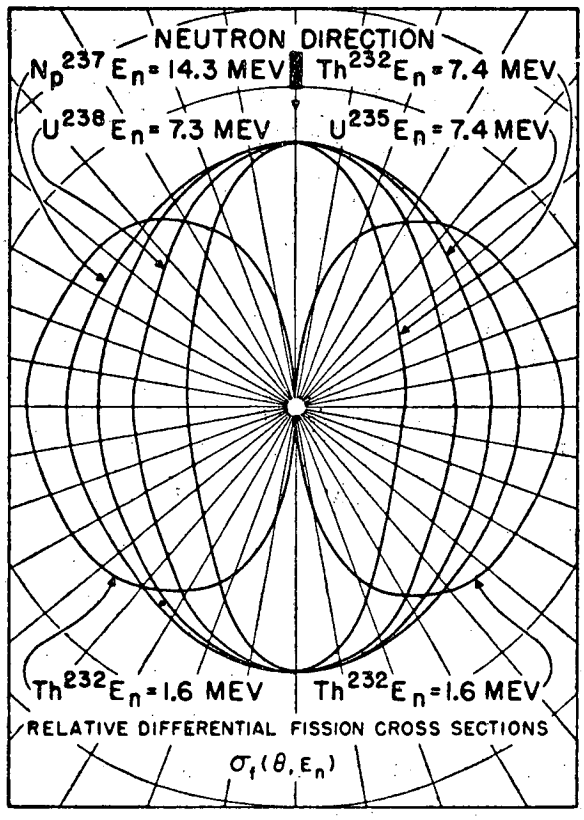

MU-19437

Fig. 12.31 Angular distributions of fission fragments. In the upper right hand section of the figure $E_n = 7.4$ should read $E_n = 7.2$ Mev. From HENKEL and BROLLEY.[81]

few quantum states are involved in the passage of the fissioning nucleus through the saddle point deformation region. The unified model of the nucleus and the suggestions of BOHR[78] can again be used to account for a few features of the experimental distributions. WILETS AND CHASE[83] have contributed to the discussion of the angular distributions at threshold within the framework of the BOHR model. They interpret the Th^{232} results of BROLLEY AND HENKEL[81] in the following way.

Regarded classically the angular momentum vector of the incident neutron points approximately normal to the incident direction ($m_L = 0$, $m_s = \pm 1/2$). The compound nucleus formed of an even-even target and an incident neutron also has its angular momentum vector oriented approximately normal to the beam direction. Most of the excitation energy of the compound nucleus is used in deforming the nucleus to the saddle point shape and only the lowest nuclear state is occupied. The lowest state is that for which the rotational angular momentum (and energy) is lowest. Hence the angular momentum vector and nuclear symmetry axis are nearly parallel and both nearly normal to the beam direction. The fragments then emerge at 90° to the beam. For higher energies the nuclear symmetry axis rotates nearly normal to the angular momentum vector and forward peaking results. WILETS AND CHASE develop some quantitative expressions and apply them to the data on Th^{232} at neutron energy 1.6 Mev. They conclude that the important saddle point state has $K = 3/2$ and odd parity.

Several measurements of these effects have been made for target nuclei of odd mass. Part of the interest in such measurements stems from the suggestion by Bohr that target spin might have a strong effect on the observed distribution and in particular that an even-odd nucleus of low spin such as Pu^{239} might show an especially strong forward-peaking. HENKEL AND SIMMONS[85] investigated U^{233}, U^{235} and Pu^{239} at a series of neutron energies from 0.5 Mev to 5.0 Mev using a multiangle gas-filled counter to detect the fragments. The cross section ratio, $\sigma_{10^o}/\sigma_{90^o}$, differed only about 10 percent from unity at the most and Pu^{239} (spin 1/2) showed a lesser anisotropy than U^{233} (spin 5/2) or U^{235} (spin 7/2).

---

83. L. Wilets and D. M. Chase, Phys. Rev. 103, 1296 (1956).

84. J. W. T. Dabbs, L. D. Roberts, and G. W Parker, Bull. Amer. Phys. Soc., Series II, 3, 6 (1958); ibid II, 5, 22 (1959)

85. J. E. Simmons and R. L. Henkel, Bull. Amer. Phys. Soc. (II) 4, 233 (1959); ibid (II) 4, 373 (1959).

These results were confirmed and extended by BLUMBERG AND LEACHMAN[86] who used a catcher foil technique to determine the angular distribution of fragment β activity from Pu^{239} and U^{233}. Their results are summarized in Figure 12.32. The dependence of the anisotropy on the initial spin I_o is obtained from a comparison of the anisotropy from the high-spin U^{233} and the low-spin Pu^{239} in the region $E_n < 6$ Mev where only (n,f) fissions are energetically possible. The relative anisotropies of U^{233} and Pu^{239} is the reverse of that expected. This indicates the possibilities that I_o does not affect the anisotropy of any fissions or that more detailed applications of theory are required.

In Figure 12.32 large increases in anisotropy occur just above 6 Mev and just above 12 Mev. These result from the enhanced contributions of "last chance" fissions at energies for which the threshold for (n,nf) is lower than for (n,2n') and for (n,2n'f) is lower than for (n,3n'). These fission events are highly anisotropic as a result of the combination of large angular momentum of the incident neutron and the low excitation energy following neutron emission. These authors discuss the application of the theory of STRUTINSKII[94] (see below) to their results.

COHEN AND COWORKERS[8-88] studied the angular distribution of specific fission products identified radiochemically in the fission of thorium and uranium isotopes with 22 Mev protons. A pronounced peaking in the forward and backward directions was noted. The anisotropy was more pronounced for fission products resulting from asymmetric fission then for products resulting from symmetric fission. The results are summarized in Figure 12.33. The anisotropy for symmetric fission is about the same for all nuclides studied; for asymmetric fission it seems to be appreciably larger for the thorium than for the uranium isotopes. Among the uranium isotopes U^{233} seems to show the least variation of anisotropy with mass ratio. FULMER[88a] has measured angular distributions of the whole fission product spectrum by a counter technique in the case of uranium isotopes bombarded with 22.8 Mev protons. He reports the following

---

86. L. Blumberg and R. B. Leachman, Phys. Rev. 116, 102 (1959).

8 . B. L. Cohen, W. H. Jones, G. H. McCormick and B. L. Ferrell, Phys. Rev. 94, 625 (1954).

88. B. L. Cohen, B. L. Ferrell.Bryan, D. J. Coombe and M. K. Hullings, Phys. Rev. 98, 685 (1955).

88a. C. B. Fulmer, Phys. Rev. 116, 418 (1959)

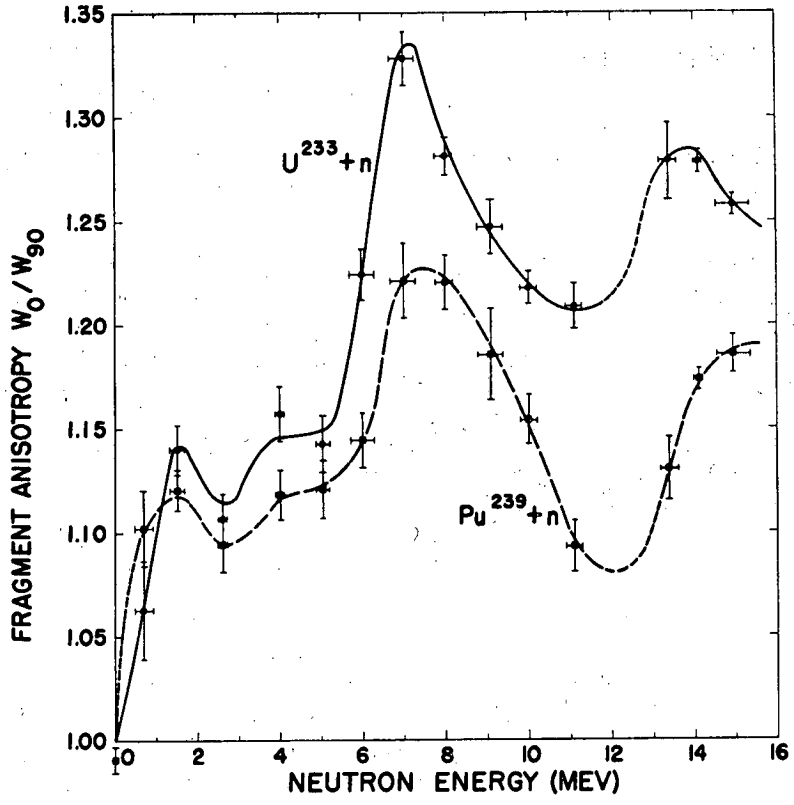

MU-19435

Fig. 12.32 Fission fragment anisotropy in the fission of U^{233} and Pu^{239} as a function of neutron energy. Anisotropy is defined as W_{0^o}/W_{90^o}. Fragment activities were measured on catcher foils by BLUMBERG and LEACHMAN.[86]

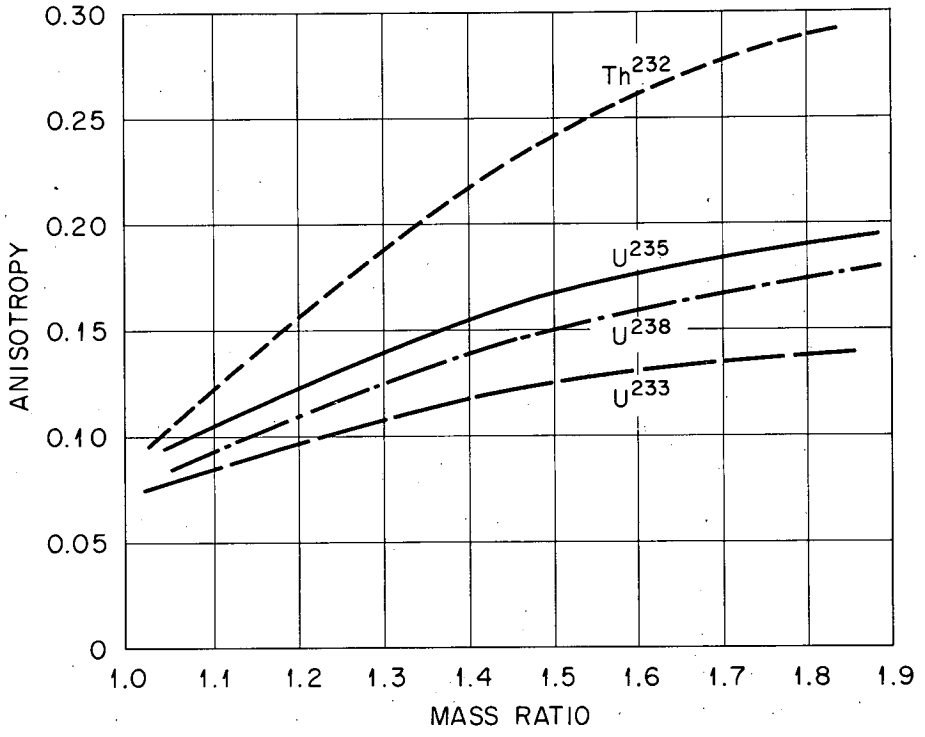

MU-19292

Fig. 12.33 Anisotropy (b/a) of fission fragment emission in the fission of uranium and thorium induced by 22 Mev protons. Angular distribution described by the expression $I(\theta) = a + b\cos^2\theta$. Specific products measured radiochemically by COHEN and co-workers.[88]

values of the anisotropy ratio b/a where the angular distribution is given by the expression, $I(\theta) = a + b \cos^2 \theta$.

For U^{233} $(b/a) = 0.23 \pm 0.04$
For U^{235} $(b/a) = 0.21 \pm 0.03$
For U^{238} $(b/a) = 0.22 \pm 0.02$

These values are higher than those found by the radiochemical analysis of specific fission products (Figure 12.33).

HALPERN AND COFFIN[89-90] used the radiochemical method to study fragments ejected at various angles from targets of Pu^{239}, Np^{237}, U^{235}, U^{238}, Th^{232}, Ra^{226} and Bi^{209} bombarded with 43 Mev helium ions and 22 Mev deuterons. The general character of each of the observed angular distributions was the same. Most fragments were emitted at 0° and 180° to the beam. The differential cross section fell smoothly from these angles to a minimum at 90°. Table 12.11 gives the observed anisotropies for the different bombardments. The anisotropy for the purpose of this table is defined as the ratio of the differential cross section at 0° compared to 90°.

THOMAS AND VIOLA[91] have studied fission fragment angular distribution in gold targets, caused to fission by bombardment with heavy ions. They counted gross fission fragment activity recoiling in various directions. GORDON, LARSH AND SIKKELAND[92] have done similar studies by ion-chamber techniques. They find a stronger forward-backward peaking of the distribution than was obtained by HALPERN AND COFFIN with lighter bombarding projectiles. These particular results are discussed further in the next section. (Section 12.1.8)

Another type of experimental information that would be exceedingly valuable would be the angular distribution of fragments from aligned nuclei. Some preliminary experiments of this kind are reported by DABBS, ROBERTS AND PARKER[84].

Most of the results from all of these studies can be summarized as follows:[93]

---

89. I. Halpern and C. T. Coffin, Paper P/642, Vol. 15, Proceedings of the Second UN Conference on the Peaceful Uses of Atomic Energy, Geneva, 1958.

90. C. T. Coffin and I. Halpern, Angular Distributions in Fission Induced by Alpha Particles, Deuterons and Protons, Phys. Rev. 112, 536 (1958).

91. T. D. Thomas and V. Viola, unpublished results, University of California, 1959.

92. G. E. Gordon, A. E. Larsh and T. Sikkeland, unpublished results, University of California Report, UCRL-9003, 1959; Submitted for publication in Phys. Rev. Let, 1960.

93. I. Halpern, "Nuclear Fission", Ann. Rev. Nucl. Sci. 9, 245 (1959).

Table 12.11

Anisotropies ($0^{\circ}/90^{\circ}$) for fission induced by alpha particles and deuterons (Halpern and Coffin[89,90])

Target nucleus	43 Mev alphas	22 Mev deuterons	10 Mev protons
Pu^{239}	1.37 ± 0.03	1.17 ± 0.04	1.03 ± 0.03
Np^{237}	1.40 ± 0.03	1.19 ± 0.04	1.05 ± 0.03
U^{235}	1.44 ± 0.03	1.21 ± 0.04	1.09 ± 0.03
U^{238}	1.54 ± 0.03	1.25 ± 0.04	1.07 ± 0.03
Th^{232}	1.76 ± 0.03	1.42 ± 0.04	1.12 ± 0.03
Ra^{226}	2.04 ± 0.05	1.28 ± 0.04	---
Bi^{209}	2.02 ± 0.07	---	---

(1) The fragments come off with greatest probability forward and backward along the beam.

(2) The anisotropies increase in the order of the size of the particle inducing fission.

(3) The anisotropies are roughly as large in odd-A targets as in even-even targets in contrast to the situation in low energy photofission.

(4) In fission induced by fast neutrons the anisotropy increases sharply whenever a threshold is reached where it becomes energetically possible for fission to occur in the residual nucleus which is left behind after the evaporation of some definite number of neutrons.

(5) As the bombarding energy increases the average anisotropy changes only slowly.

(6) The anisotropy is largest for the most asymmetric mass ratios.

(7) The anisotropy decreases as the value of Z^2/A of the target increases.

HALPERN AND STRUTINSKI[94] AND GRIFFIN[95] used the suggestions of BOHR[78] as a starting point for a semi-quantitative explanation of these observations. The angular distribution of the fragments depends upon the angular momentum I introduced by the projectile and on the fraction of it converted into orbital momentum between the fragments which is characterized by the quantum number K. K is the projection of I on the separation axis between fission fragments; if we assume an axially symmetric saddle point shape we can also identify it with the K quantum number applied in the unified model description of nuclear ground states. For an axially symmetric nucleus and K = 0 the fragments will necessarily be emitted at right angles to I.

The general characteristics of the angular distributions summarized above suggest that the distribution in K is determined largely by the nucleus itself and not very much by the way the energy and angular momentum are brought into the compound nucleus. One may infer that during the relatively long life time of the compound nucleus the excitation energy is exchanged back and forth among many degrees of freedom and that the nucleus distorts many times with

---

94. I. Halpern and V.M. Strutinski, Paper P/1513, Vol 15, Proceedings of the Second UN Conference on the Peaceful Uses of Atomic Energy, Geneva, 1958; See also I. Halpern, ref. 93; see also V.M. Strutinski, Atomic Energy (English translation) 2, 621, (1957).

95. J.J. Griffin, Phys. Rev. 116, 107 , 1959.

many choices of K without quite making it over the saddle point. The values of K for the nuclei which actually pass through the saddle point will depend on the K spectrum of the states in the saddle point region with the one restriction that K can never exceed I.

It is necessary to have some way of specifying the K-spectrum and the most general way of doing this is to start from elementary statistical mechanics or from classical arguments. STRUTINSKI[94], for example, suggests that the distribution in K should be controlled by a Boltzmann factor, $\exp(-E_{ROT}/T)$, where $E_{ROT} = \frac{\hbar^2 K^2}{2\,\mathfrak{J}_{parallel}} + \frac{\hbar^2 (I^2 - K^2)}{2\,\mathfrak{J}_{perpend.}}$ and where the $\mathfrak{J}$'s are the moments of inertia of the deformed nucleus in its saddle point shape for rotation parallel and perpendicular to the axis of symmetry. If T is constant the distribution in K is Gaussian and the average value of K^2 is

$$K_o^2 = T \frac{\mathfrak{J}_{parallel} \quad \mathfrak{J}_{perpend.}}{\mathfrak{J}_{perpend.} - \mathfrak{J}_{parallel}} \frac{1}{\hbar^2} \tag{12.7}$$

In this expression K_o^2 is independent of I^2 except for the limitation that K may not exceed I.

Let us now consider the angular distribution of fragments from a nucleus with a given I and K. The form of the distribution can be obtained from the simple geometrical considerations of Fig. 12.34. The fragments emitted from the nucleus with spin I come off with equal probability on the circle formed by the intersection of the cone and the sphere. The half angle of the cone is $\cos^{-1} K/L$. The vector I can point in any direction in the plane perpendicular to the beam direction so we must rotate I and its associated circle uniformly around the beam axis. The distribution of fragments becomes

$$W_{I,K} = \frac{2I}{4\pi^2} \left(I^2 \sin^2 \theta - K^2\right)^{-1/2} \tag{12.8}$$

where θ is the angle between the direction of the fragment motion and the incident beam. The distribution is normalized to unit value when integrated over the sphere.

The next step is to integrate $W_{I,K}$ over the Gaussian K-distribution. The distribution for some fixed I and a given K_o^2 is given by HALPERN AND STRUTINSKI[94] as

$$W(\theta)_{I,K_o} = \sqrt{\frac{2}{\pi}} \; \frac{N}{2\pi} \; \frac{1}{2K_o} \exp\left(-I^2 \sin^2\theta/4K_o^2\right) \; J_o\left(iI^2 \sin^2\theta/4K_o^2\right) \tag{12.9}$$

where J_o is the zero-order Bessel function and N is a normalization constant (close to unity for $I > K_o$).

Finally the distribution W_{I,K_o} must be integrated numerically over I from zero up to the maximum value I_m. The resultant angular distribution W_{I_m,K_o} is peaked forward and backward along the beam. The functions W_{I_m,K_o} all behave like $(\sin \theta)^{-1}$ at 90° but depart from this behavior at smaller angles as can be seen in Fig. 12.34. Each of the functions W_{I_n,K_o} can be characterized by a single parameter $P = (I_m/2K_o)^2$. The larger the value of P, the larger the anisotropy, and the longer the distribution resembles $(\sin \theta)^{-1}$ as one moves from 90° to smaller angles.

It should be particularly interesting to study angular distributions of fragments from targets bombarded with heavy ions because of the very large values of I_{max} in such cases. Some experimental data are discussed in the next section.

In order to apply the above equations it is necessary to have some basis for estimating the I and K distributions and the nuclear temperature T. A crude classical estimate of the I distribution would be a uniform distribution from zero up to a maximum set by the ratio of the radius of the nucleus to $1/2\pi$ times the projectile wave length just outside the nucleus. More realistic estimates based on calculations of particle transmissions into the nucleus as a function of I give somewhat larger values of I_{max} and a non-linear distribution.[94] The most uncertain quantity is the K distribution. One does know that K_o should increase with excitation energy above the fission barrier and from this fact alone one can draw the important conclusion that the fragment anisotropy should decrease with increase in energy <u>for a specific fissioning nucleus.</u> HALPERN AND STRUTINSKI[94] made some preliminary deductions about the forms of the K_o^2 versus excitation energy curve by an examination of the experimental data on angular distributions particularly those cases where good data were available at small angles. Their paper should be consulted for details. In the future the collection of more extensive data and the development of better nuclear models for description of nuclear shapes and excitation spectra at the saddle point should make it possible to obtain a more reliable estimate of the K-distribution. ≠

≠ See reference 86 for a discussion of this point.

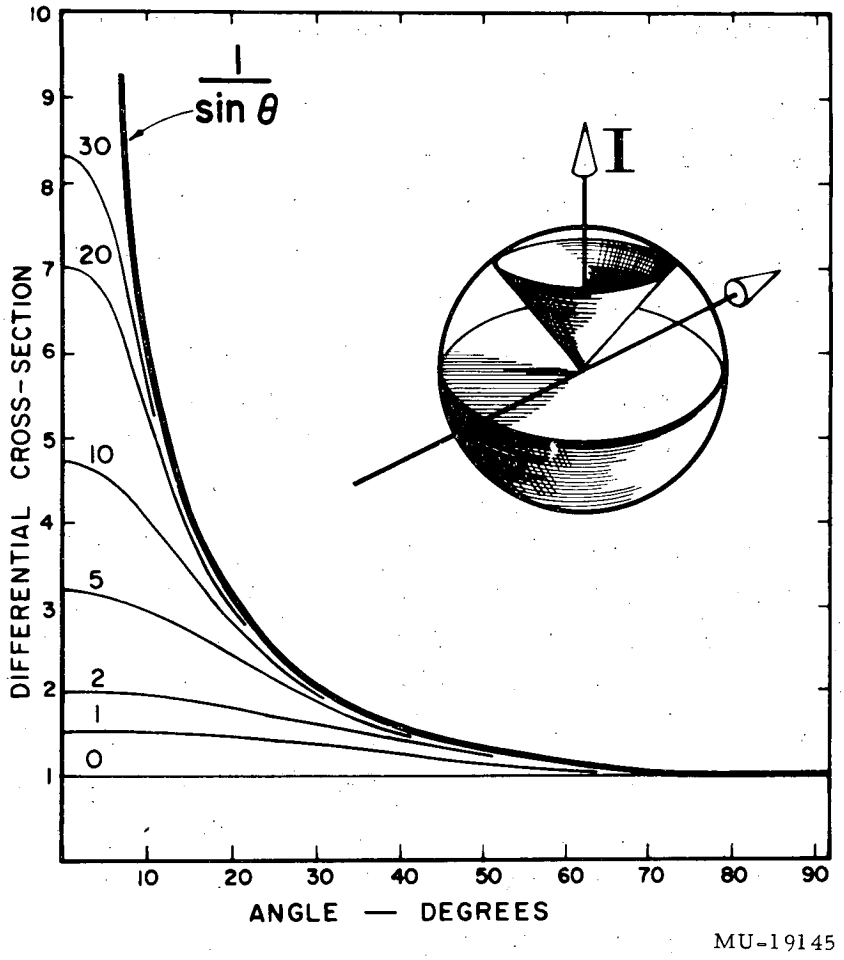

Fig. 12.34 Angular distributions of fission fragments. If a beam of particles is incident upon a target from left to right (see insert) it introduces into nuclei angular momenta $\vec{I}$ which are oriented at right angles to the beam. If these nuclei undergo fission in such a way that the projection of $\vec{I}$ on the fission direction is K, the fragments will come off in a cone whose half angle is $\cos^{-1} K/L$. To obtain the angular distribution for a given species one must average over the K and $\vec{I}$ distributions in the problem. Typical angular distributions are shown. These are characterized by the parameter $P = 1/2\ (I_o^2/K_o^2)$ where I_o^2 and K_o^2 are average values of I^2 and K^2. HALPERN and STRUTINSKI.[94] Figure reproduced from Halpern, Rev. Modern Phys. 9 (1959).

HALPERN AND STRUTINSKI[94] point out that the interpretation of the observed fragment distributions is complicated by the fact that in most cases a collection of different fissioning nuclei at different excitation energies are contributing to the observed products. To make a complete and meaningful analysis one must make use of the trends in the competition between neutron emission and fission which we have reviewed earlier in this chapter to determine the percentage contributions to the total fission products of two or more nuclei in the neutron evaporation chain and the excitation energy of each of these fissioning nuclei. It can be shown that the I distribution is not disturbed greatly by evaporation of a few neutrons but the excitation energy drop causes a great change in the K_o values as we proceed down the neutron evaporation chain. Knowing, as we do, the general characteristics of the variation in neutron emission versus fission competition with nuclear type we can make some very general statements about the angular distributions. For example, we have noted above that fragment anisotropy decreases as Z^2/A increases. This can be attributed to higher fissionability for higher Z^2/A. The major part of the fission then occurs in the early stages of de-excitation of the compound nucleus, hence K_o^2 is greater, hence $P = \frac{I^2}{K_o^2}$ is lower, hence anisotropy is less. In neutron-induced fission a sharp increase in anisotropy occurs when the neutron energy increases past a threshold for the evaporation of some definite number of neutrons. This can be attributed to the fact that above this threshold some fission is occurring at a much lower energy in the nucleus resulting from the emission of this number of neutrons. This lower excitation energy means a lower K_o^2 value and hence an increased peaking of fragment emission along the beam of incoming neutrons. The increase in anisotropy as a function of the complexity of the bombarding particle is just a reflection of the fact that the average value of I is going up while the value of K_o (to a first approximation) is left the same. The fact that the observed anisotropy is not the same for all fragment mass ratios is explained if one assumes that low energy fission is much more asymmetric than fission at moderate energies. Hence those fission events which occur late in the evaporation chain give a more asymmetric mass distribution of products and, because the excitation energy is low, the anisotropy of the fragment emission is increased. It remains an open question whether there are any differences in the angular distributions as a function of mass ratio for a <u>single</u> fissioning species at a definite excitation energy. Finally, the uniform general appearance of the angular distributions as a function of nuclear type reflects the fact that the

I_o and K_o values in most of the cases studied are large compared to the spin of the odd-A target nuclei. Geometrical considerations show that random orientations of the target spin cannot have much effect on the angular distributions of the fragments.

c) Fragment Angular Distributions when Bombardment Energy is High

When the energy of the bombarding particles is raised beyond the moderate energy region (i.e. beyond tens of Mev for light particles) the direct interaction processes begin to replace the compound nucleus reaction mechanism and the degree of orientation of the total spin I should become steadily less. Experimental data, however, have revealed some curious unexpected results.

LOZHKIN, PERFILOV AND SHAMOV[96] have investigated anisotropy effects in the fission of uranium with 660 Mev protons using photo emulsion techniques. They found a preference for emission of fragments in a direction perpendicular to the proton beam as given by the function $1 + 0.29 \sin^4$. The anisotropy increases as the energy of excitation of the fissioning nucleus increases. See Table 12.12. This implies a well oriented spin at the time of fission but in an unanticipated direction.

OSTROMOV AND PERFILOV[97] studied angular distributions of fragments from fissioning nuclei produced by bombardment of uranium with high energy neutrons. The anisotropy was studied as a function of the number of evaporated charged particles accompanying fission. The results (Table 12.13) indicate that the anisotropy increases strongly as the excitation energy increases. The neutrons were produced by charge exchange in a beryllium target bombarded with 680 Mev proton protons.

PORILE AND SUGARMAN[98] studied radiochemically the relative amounts of specific fission products ejected parallel to and perpendicular to the high energy proton beam. For bismuth targets bombarded with 450 Mev protons, the favored direction is parallel to the beam. If the distribution is assumed to

---

96. O. V. Lozhkin, N. A. Perfilov and V. P. Shamov, J.E.T.P. 29, 292 (1955); Soviet Physics 2,116 (1956).

97. V. I. Ostromov and N. A. Perfilov, J.E.T.P. 31, 716 (1956); Soviet Physics 4, 603 (1957).

98. N.T. Porile and N. Sugarman, Phys. Rev. 107, 1410 (1957).

Table 12.12

Anistropy of fission fragments of uranium with respect to direction of proton beam (660 Mev). Ref. 96

Excitation energy	~60	~150	~320
Anisotropy = $\frac{N_{>60^\circ}}{N_{<30^\circ}}$	1.13	1.31	1.35

Table 12.13

Anistropy in the emission of fission fragments from uranium bombarded with high energy neutrons

Anisotropy defined as

$$\frac{\text{no. fragments at } 45^\circ\text{-}90^\circ}{\text{no. fragments at } 0^\circ\text{-}45^\circ}$$

no. fragments at 0°-45°	Number of prongs
0.90	0
1.15	1
1.13	2
1.50	3-6

be of the type

$$a + b \cos^2 \theta \qquad (12.10)$$

the ratio of the asymmetry parameters, b/a is about 0.1 for typical fission products. On the other hand, when fission is induced in tantalum targets the fragments favor the plane perpendicular to the beam. If the distribution is assumed to be

$$a + b \sin^2 \theta \qquad (12.11)$$

then b/a ranges from 0.370 to 0.026. The most asymmetric fission fragments are emitted most anisotropically.

WOLKE AND GUTMAN[99] studied fission fragments from bismuth bombarded with 450 Mev protons. Fragments escaping from a small spherical bismuth target were caught on an aluminum cone which was subsequently cut into pieces corresponding to various recoil angles and subjected to radiochemical analysis for Ga^{72-73}, Sr^{91-92} and $Cd^{115, 117}$. These fragments were ejected according to the law

$$a + b \cos^2 \theta \qquad (12.10)$$

and the values of b/a were found to be 0.10, 0.115 and 0.09 respectively, for the three groups of products.

MEADOWS[100] studied the fragments emitted in thorium and uranium fission induced by bombardment with 45, 80 and 155 Mev protons. At 45 Mev the fragments were preferentially emitted forward and backward in agreement with other published results in the moderate energy region. The anisotropies were less at 80 Mev and at 155 Mev the favored distribution had shifted over to favor the 90° direction to the beam. This result is in agreement with the high-energy Russian work quoted above.

The HALPERN-STRUTINSKI[94] analysis quoted above does not lead to this result and it is clear that some overlooked factor becomes important in the very high energy region. HALPERN[93] quotes unpublished work by himself and independent unpublished work by STRUTINSKI which may provide some explanation for the reversal. In the high energy region a prominent reaction in the fast "cascade" step of the reaction is the passage of the fast particle through the heavy nucleus hitting one or two nucleons and projecting them with rather low energies

---

99. R. L. Wolke and J. R. Gutman, Phys. Rev. 107, 850 (1957).

100. J. W. Meadows, Phys. Rev. 110, 1109 (1958).

into a direction at right angles to its path. These "soft" nucleons travel through the nucleus playing the role of a beam of particles which is "incident" at right angles to the original beam. They therefore give "inverted" anisotropies.

It is clear that further experimental work is needed on angular distributions of fission fragments and that more detailed nuclear model predictions of excited states in the saddle point region would be helpful.

12.1.8 Fission Induced by Heavy Ions. Fission induced by bombardment of heavy element targets with energetic charged particles with atomic number greater than 2 resembles in many respects that induced by protons, deuterons and helium ions but in some ways heavy ion induced fission has some special characteristics which give it unusual interest. By proper choice of the target nucleus and the heavy ion projectile it is possible to make a wide variety of compound nuclei many of which cannot be made in any other way. Another advantage is that the excitation energy of the compound nucleus may be made quite high at the same time that the compound nucleus is well specified in atomic number and mass. This fortunate situation is to be distinguished from the nuclear reactions induced by lighter particles, particularly protons. In the latter case as the energy of the incident particle rises above 40 Mev the compound nucleus reaction mechanism begins to give way to the high-energy cascade mechanism which can leave the intermediate nucleus at the end of the first stage of the reaction in a variety of forms with a spread in Z, A and excitation energy. When the cascade mechanism accounts for an appreciable fraction of the total reaction cross section it becomes difficult to make a clean cut interpretation of experimental results. Heavy ion reactions go primarily by the compound nucleus mechanism up to a much higher range of excitation energies so that our term "charged particles of moderate energy" can mean energies of 100 to 200 Mev for heavy ions rather than 50 Mev or less. Another advantage of reactions induced by heavy ion bombardments is the opportunity they afford for studying the influence of high angular momentum on the course of the de-excitation of compound nuclei. The average angular momentum of the compound nucleus formed by the bombardment of U^{238} with C^{12} ions of 100 Mev energy is 36 units; it is not unusual to transmit angular momentum as high as 100 units to the compound nucleus in heavy ion reactions. It is

an interesting experimental and theoretical matter to determine how such large amounts of angular momentum affect fission probability, the angular distribution of fission fragments, the emission of gamma radiation during and after fission, and other characteristics of fission.

A good part of what we have to say about the reactions induced by heavy ions is contained in Section 2.4 of Chapter 2. In addition, the production of heavy ion beams and important quantitative details such as Coulombic barrier energies, compound nucleus formation cross sections, etc. are discussed there. In this chapter we wish to mention briefly how the observed trends in mechanism, probability and characteristics of fission induced in heavy ions fit in with the picture of fission induced by charged particle as this picture has been developed so far in this chapter.

In the case of target elements lying in or above the rare earth region of elements the compound nucleus de-excites primarily by neutron emission or fission. If we take C^{12} and N^{14} as representative heavy ions then we can state that the (C^{12},xn) and (N^{14},xn) reactions show a variation of cross section with energy of the bombarding particle very similar to that seen in (p,xn), (d,xn) and (α,xn) reactions. Each individual reaction has a threshold, a rise to a peak value and then a drop as the energy of the compound nucleus passes the threshold for the emission of an additional neutron. When the target element is gold or a heavier element the probability for fission becomes appreciable and the (C^{14},xn) and (N^{14},xn) type reactions reflect this by a marked reduction in the peak heights in their excitation function. This fission-neutron emission competition can be analyzed by use of the modified Jackson model developed in Section 12.1.4 above. The (C^{14}, xn) reactions with U^{238} targets have been analyzed in this way by SIKKELAND, THOMPSON AND GHIORSO[101], and by FLEROV AND CO-WORKERS.[102] A similiar analysis has been made of the Au^{197} (C^{14},xn) reaction cross sections by BARABOSHKIN, KARAMIAN AND FLEROV[103]. All these analyses indicate that the

---

101. T. Sikkeland, S. G. Thompson and A. Ghiorso, Phys. Rev. 112, 543, (1958). [illegible] and A. Ghiorso in Paper [illegible] Vol. [illegible] Proceedings of the Second UN Conference on the Peaceful Uses of Atomic Energy, Geneva, [illegible].

102. As reported by Polikanov in seminar talk "Nuclear Fission of Heavy Elements During Interaction with Carbon, Nitrogen and Oxygen Nuclei", Copenhagen, 1957, See also, S.M. Polikanov and V.A. Druin, Sov. Phys. JETP, 36, 522 (1958).

103. Baraboshkin, Karamian, Flerov, Soviet Physics, J.E.T.P. 5, 1055 (1957).

fission-modified Jackson model is as applicable to heavy ion reactions as to reactions with lighter particles.

As this is being written the absolute cross section for fission is being measured in many laboratories for a variety of targets bombarded with heavy ions, but only a few published values are available for discussion. A Russian group under the direction of FLEROV[102,104] has published quantitative work on the total fission cross sections. Figures 12.35 and 12.36 show the observed cross section for fission in uranium and bismuth targets bombarded with carbon, nitrogen and oxygen ions. Fission fragments were counted in a specially constructed differential ionization chamber which could discriminate fission pulses from "pile-up" pulses from the heavy ion beam. In all cases the fission cross sections are described within experimental error by the formula

$$\sigma = \pi r_o^2 \left(A^{1/3}_{\text{target nucleus}} + A^{1/3}_{\text{projectile nucleus}}\right) \left(1 - \frac{B}{E}\right)$$

where

r_o = 1.4 to 1.55 x 10^{-13} cm

E = energy of bombarding particles

B = energy of the Coulomb barrier

Since the BLATT AND WEISSKOPF formula given above is a reasonable expression of the total reaction cross section it can be concluded that almost the entire reaction cross section goes into fission. This is confirmed by the extremely low cross sections for the reaction products of the (C^{12},xn) type reaction; see for example Fig. 2.4 of Chapter 2 which shows a peak cross section of a few microbarns for products of this type in uranium targets.

Figure 12.37 shows fission cross sections for bismuth, gold, rhenium and ytterbium placed in a nitrogen beam. In these cases, except for bismuth, the total fission cross section is definitely less than the compound nucleus cross section. The fission cross section drops rapidly as the atomic number of the target nucleus decreases. This is shown more clearly in Fig. 12.38 which shows the fraction of the total cross section taken up by fission as a function of the compound nucleus and its excitation. From this figure we can

104. V. A. Druin, S. M. Polikanov, G. N. Flerov, Soviet Physics, JETP, 5, 1059 (1957)

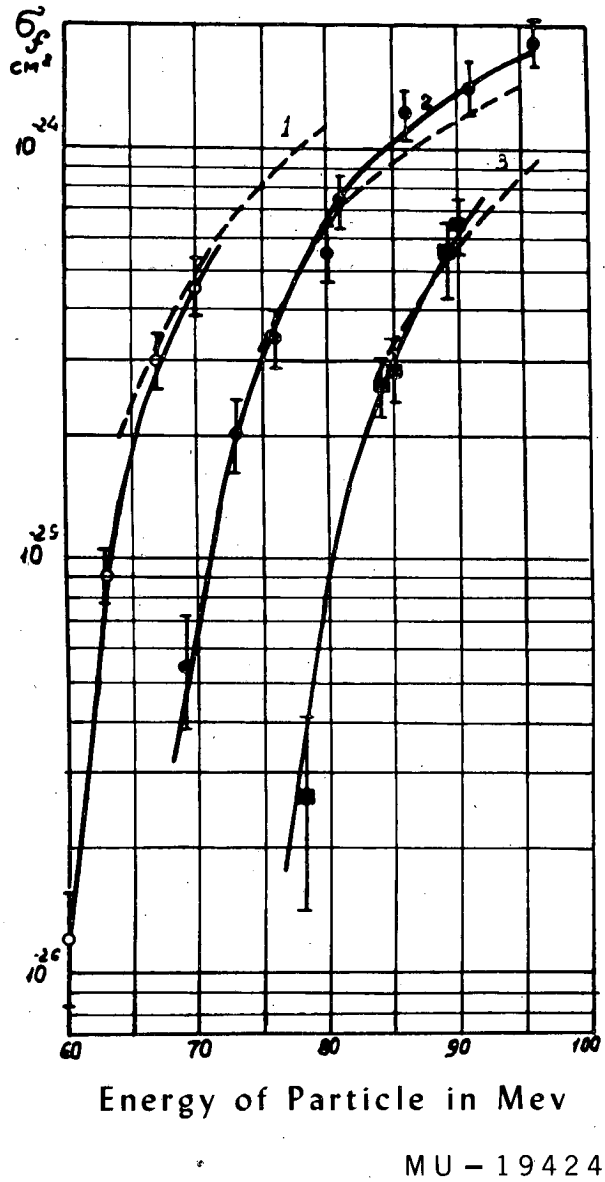

Fig. 12.35 Dependence of cross section for fission of bismuth on energy of carbon ions (1), nitrogen ions (2), and oxygen ions (3). Solid lines - experimental curves, broken lines - calculated according to the formula $\sigma = \sigma_o(1 - B/E)$ for values of r_o equal to 1.5f (1), 1.55f (2 and 3).) Reference 102.

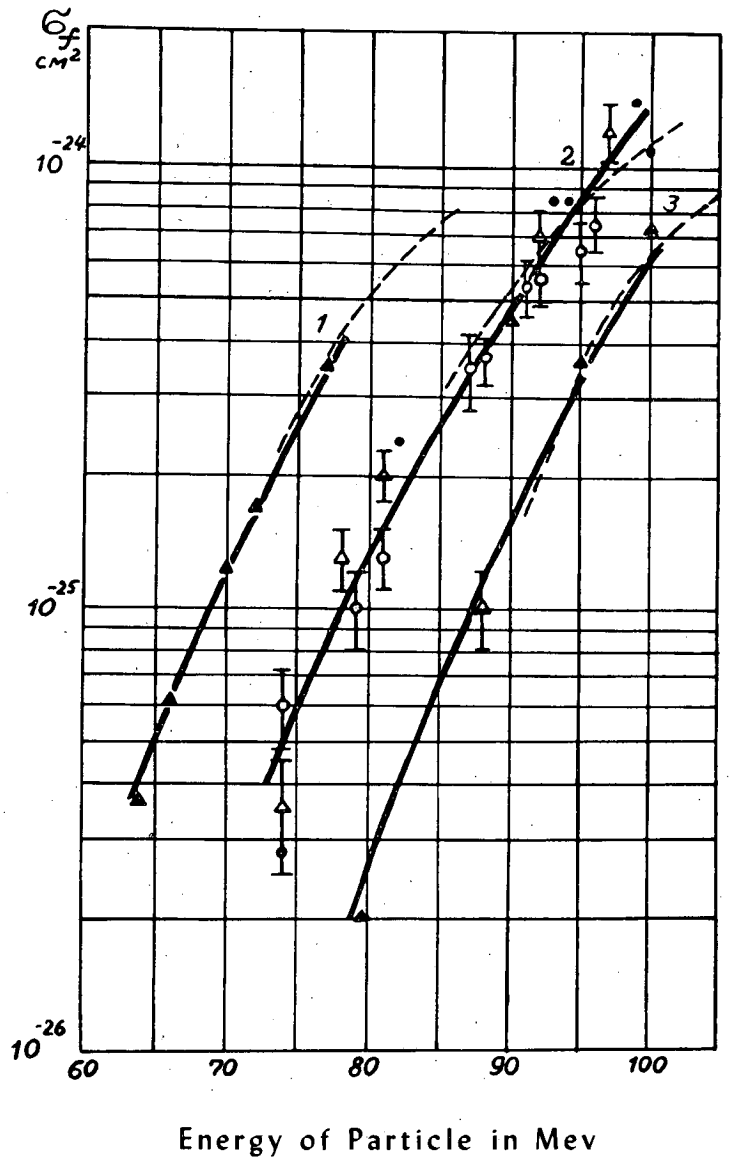

Fig. 12.36 Dependence of cross section for fission of uranium on energy of ions of carbon (1), nitrogen (2), oxygen (3). Reference 102.
Solid curves - experimental.
Broken curves - theoretical for $r_o = 1.4f$ (1), $r_o = 1.45f$, $r_o = 1.52f$ (3).
Δ - data of chamber for U^{238}.
o - data of chamber for U^{235}.
●▲ - activation data for U^{238}.

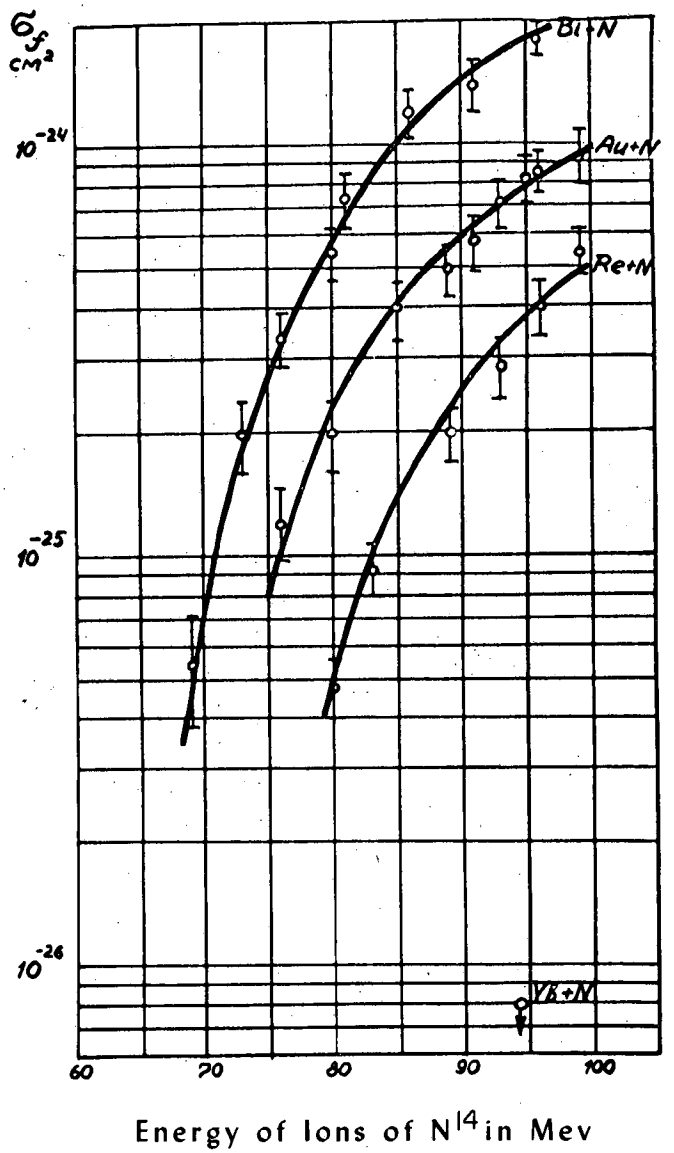

MU-19423

Fig. 12.37 Dependence of cross section for fission of bismuth, gold, rhenium and ytterbium on energy of nitrogen ions. Reference 102.

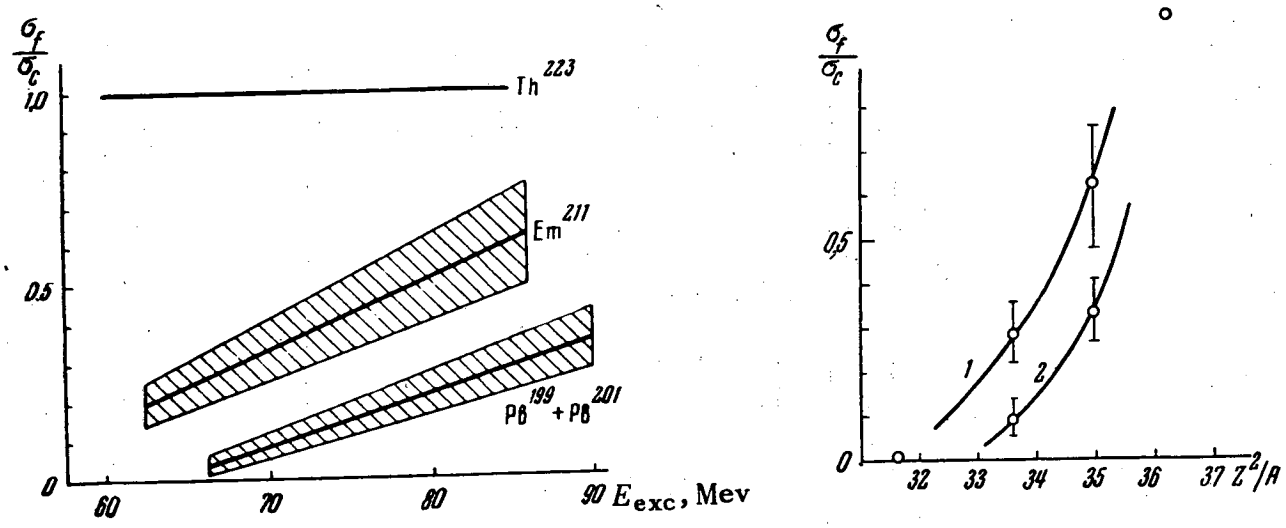

MU-19451

Fig. 12.38 Dependence of the ratio of fission to total cross section on energy of excitation for compound nuclei resulting from the amalgamation of nitrogen with bismuth, gold, and rhenium. From Druin, Polikanov and Flerov.[104]

conclude that there is a strong dependence of Γ_f/Γ_n on Z(or Z^2/A) and on the excitation energy.

Other measurements of fission cross sections are summarized in Table 12.14 [illegible] GILMORE[104a] has studied the influence of angular momentum by measuring the fission cross section of a selected compound nucleus prepared by two different heavy ion reactions. For example the compound nucleus Tl^{197} can be prepared by the reactions

$$Ta^{181} + O^{16} \longrightarrow [\,Tl^{197}\,]$$
$$Re^{185} + C^{12} \longrightarrow [\,Tl^{197}\,]$$

By suitable choice of energy of the bombarding heavy ions the Tl^{197} can be prepared at the same level of excitation but with widely different angular momenta in the two cases owing to differences in Coulomb barrier and in the masses and radii of the targets and the incident particles. In the top portion of Fig. 12.39 the maximum angular momentum ℓ_{max} is shown as estimated from the classical expression

$$\ell_{max} = \sqrt{2\mu\,(r + R)^2\,(E-B)} \qquad (12.12)$$

where μ = reduced mass

R = radius of target

r = radius of projectile

E = Energy in center of mass

and B = Coulomb barrier

[illegible] GILMORE exposed a series of nuclear emulsions at various positions around targets of tantalum and rhenium and measured the fission fragments emerging from the targets at various angles to the incoming beam. He determined the angular distribution of the fragments and integrated over all directions to determine a total fission cross section. The results are shown in the bottom portion of the figure. The result is a striking demonstration that the same compound nucleus at the same level of excitation will fission more readily when its angular momentum is increased. This result is confirmatory evidence for the theoretical ideas of PIK-PICHACK† and of HISKES‡ which are mentioned in Section 11.2.1 on the theory of nuclear fission. See report UCRL-9036.

104a. [illegible] J. Gilmore, unpublished results, Berkeley, Calif.

† Pik-Pichack, Soviet Physics, J.E.T.P, 1, 238 (1958)

‡ J. Hiskes, unpublished results, Lawrence Radiation Laboratory, Berkeley, Calif.

Table 12.14 Fission Cross Sections from Heavy Ion Reaction Studies≠

Target and Projectile	Energy of Projectile (Mev)	$\sigma_{fission}$ (barns	Method of Measurement	Ref.
$Au + C^{12}$	120	0.90 ± 0.20	Radiochemistry	a
$Au + O^{16}$	160	2.2 ± 0.3	Counter	b
$Ta + O^{16}$	87.5	0.043 ± 0.007		
	89.2	0.096 ± 0.006		
	94.1	0.167 ± 0.014		
	98.0	0.333 ± 0.025	emulsion	c
	109.0	0.728 ± 0.025		
	122.5	1.12 ± 0.06		
	136.5	1.37 ± 0.05		
	150.0	1.59 ± 0.08		
	167.0	1.75 ± 0.08		
$Re^{185} + C^{12}$	87.5	0.043 ± 0.007		
	89.2	0.096 ± 0.006		
	94.1	0.167 ± 0.014		
	98.0	0.333 ± 0.025	emulsion	c
	109.0	0.728 ± 0.025		
	122.5	1.12 ± 0.06		
	136.5	1.37 ± 0.05		
	150.0	1.59 ± 0.08		
	167.0	1.75 ± 0.08		
$Au + C^{12}$	69.	0.102 ± 0.009		
	86	0.514 ± 0.039	counter	d
	107	0.988 ± 0.072		
	124.5	1.28 ± 0.095		

≠ Russian work is summarized in figures 12.35 through 12.37

a. H. M. Blann, unpublished results, Berkeley 1959
b. Quinton, Britt, Knox and Anderson, Bull. Am. Phys. Soc. II, 414 (1959), and paper in publication in Nuclear Physics, 1960.
c. J. Gilmore, unpublished results, Berkeley 1959; uncertainties on standard deviations.
d. G. Gordon, Larsh, Sikkeland and Walton, unpublished results, Berkeley 1959.

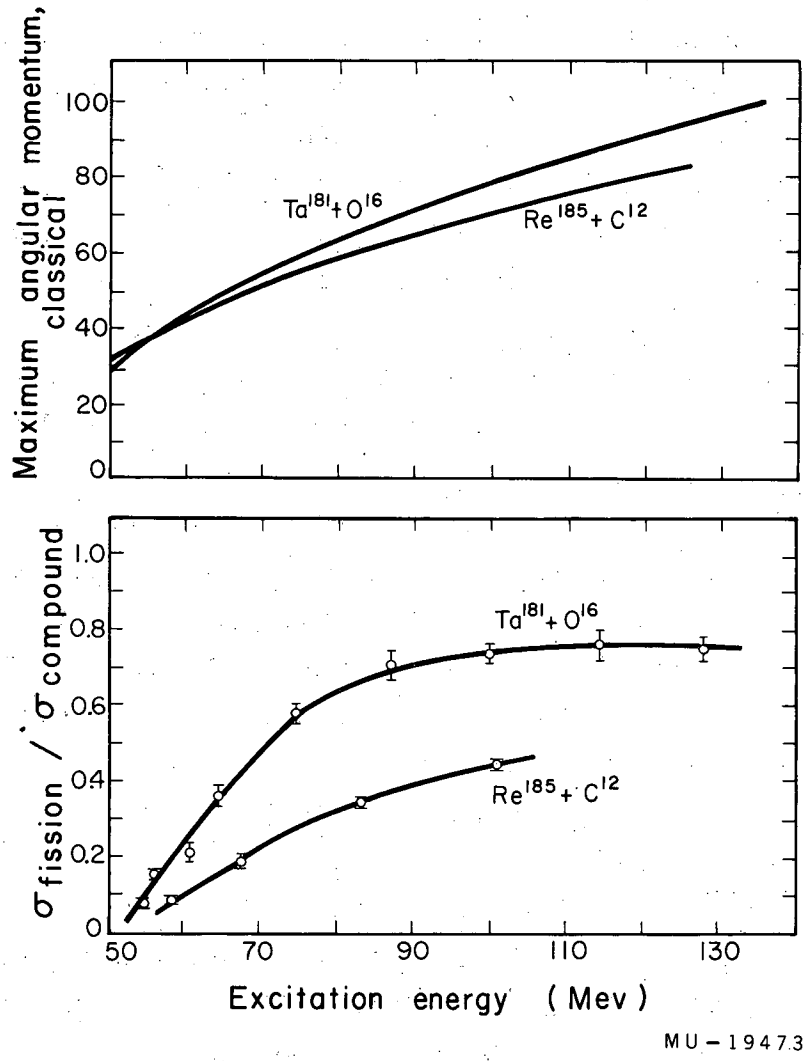

Fig. 12.39 Experimental study by GILMORE[104a] showing the importance of angular momentum on fission probability. The top portion of the figure shows the maximum angular momentum computed classically of the compound nucleus, Tl^{197}, as a function of the excitation energy of the compound nucleus prepared by two different heavy ion reactions. The bottom portion shows the ratio $\sigma_{fission}/\sigma_{compound\ nucleus}$ as a function of excitation energy. A square well approximation was used in computing $\sigma_{compound\ nucleus}$. $\sigma_{fission}$ was measured by a nuclear emulsion technique.

The mass yield distribution of fission products appears to have a symmetric distribution in the few cases in which it has been studied radiochemically. TARANTIN AND CO-WORKERS[105] studied the $Au^{197} + N^{14}$ case and found the peak of the distribution at about mass 100 and a width of about 20 mass units at the points where the yield curve was at half its maximum height. The narrow distribution resembles that observed by FAIRHALL[105a] in the fission of bismuth with 22 Mev deuterons. In a similar radiochemical study of the fission of gold with 120 Mev C^{12} ions BLANN[106] obtained a similar narrow mass distribution. He obtained a full width at half maximum of 25 mass units. The peak of the yield distribution fell at mass number 101 indicating a value of 7 for $\bar{\nu}$, the average number of neutrons emitted in fission plus prefission neutron evaporation. By integration under the mass yield curve he estimated a fission cross section of 0.90 ± 0.20 barns.

TARANTIN[105] showed that in the case of the bombardment of U^{238} with N^{14} ions the fission mass spectrum is quite broad (width at half maximum $\geq$ 50 units) remaining roughly constant from mass 90 to mass 145. The great width of the "symmetric" distribution probably is the result of a mixture of symmetric and asymmetric fission modes. BROWN, PRICE AND WILLIS[107] radiochemically analyzed the products of the fission of U^{238} with C^{13}. The 17 nuclides chosen for study defined a symmetric distribution centered at mass 120 with a full width at half maximum of about 55. The position of the maximum indicates a $\bar{\nu}$ value of eleven. This $\bar{\nu}$ value includes neutrons emitted during fission and before fission.

The kinetic energy distribution of the fragments has been measured by several techniques. GORDON, LARSH AND SIKKELAND[108] used an argon gas scintillation cell and a solid state detector to measure the kinetic energy and the angular distribution of fragments from fission of gold with C^{12} ions. The small solid state detector was particularly useful in measuring fragments at small angles to the beam. The detectors were calibrated with a Cf^{252} spontaneous fission

---

105. Tarantin, Gerlit, Guseva, Miasvedor, Filippova and Flerov, JETP (USSR) 34 316 (1958); Soviet Physics, JETP, 7, 220, (1958).

105a. A. W. Fairhall, Phys. Rev. 102, 1335 (1956)

106. H. M. Blann, unpublished results

107. F. Brown, M. R. Price and H. H. Willis, J. Inorg. Nucl. Chem. 3, 9 (1956)

108. G. E. Gordon, A. E. Larsh and T. Sikkeland, University of California Radiation Laboratory Report, UCRL-9003, December 1959, Submitted for publication in Phys. Rev. Letters, 1960.

source. The analysis of their results led to a value of 73±3 Mev for the most probable energy of the fragments in the center-of-mass system when the bombardment energy was 123 Mev. When 93 Mev carbon ions were used the kinetic energy was 71±3 Mev. These data and other unpublished data by the same experimenters indicate that there is very little dependence of the fragment energy on the energy of the bombarding carbon ions.

QUINTON, BRITT, KNOX AND ANDERSON[108a] used a proportional counter detector to measure the fragment energy release in the fission of gold with 160 Mev oxygen ions. In the center-of-mass system the kinetic energy distribution was symmetric about 75±5 Mev with a full width of 30 Mev at half the maximum peak height. The center-of-mass energy distribution was independent of the angle of the detector with respect to the beam.

The two research groups just quoted measured the distribution of fragments as a function of the laboratory angle between the fragments and the incoming beam. These distributions were corrected for the center-of-mass motion of the compound nucleus and recalculated as a center-of-mass angular distribution which was then compared with the theoretical curves given by HALPERN AND STRUTINSKI[94] and by GRIFFIN[95] discussed in section 12.1.7 immediately above. A similar study was carried out by VIOLA AND THOMAS[91] in the case of gold targets caused to fission with 125 Mev C^{12}, 146 Mev N^{14} and 167 Mev O^{16}. VIOLA AND THOMAS[91] carried out their measurements by counting the gross activity of fission recoil products collected on a series of catcher foils placed at various angles to the beam.

A typical result taken from the work of GORDON, LARSH AND SIKKELAND[108] is given in Figures 12.40 and 12.41. The first shows the angular distribution in the laboratory system. The second shows the distribution in the center-of-mass system after correcting for a η value of 0.223±0.01 and of 0.190±0.01 for the 123 Mev and 93 Mev bombardments respectively. The quantity η is defined as v/V where v is the velocity of the compound nucleus in the direction of the beam and V is the velocity of the fragment in the moving system. Within experimental error the η values represent full momentum transfer by the bombarding projectile to the fissioning nucleus; i.e. true compound nucleus formation.

108a. A. R. Quinton, H. C. Britt, W. J. Knox and C. E. Anderson, Bull. Amer. Phys. Soc. II 4, 414, 1959.

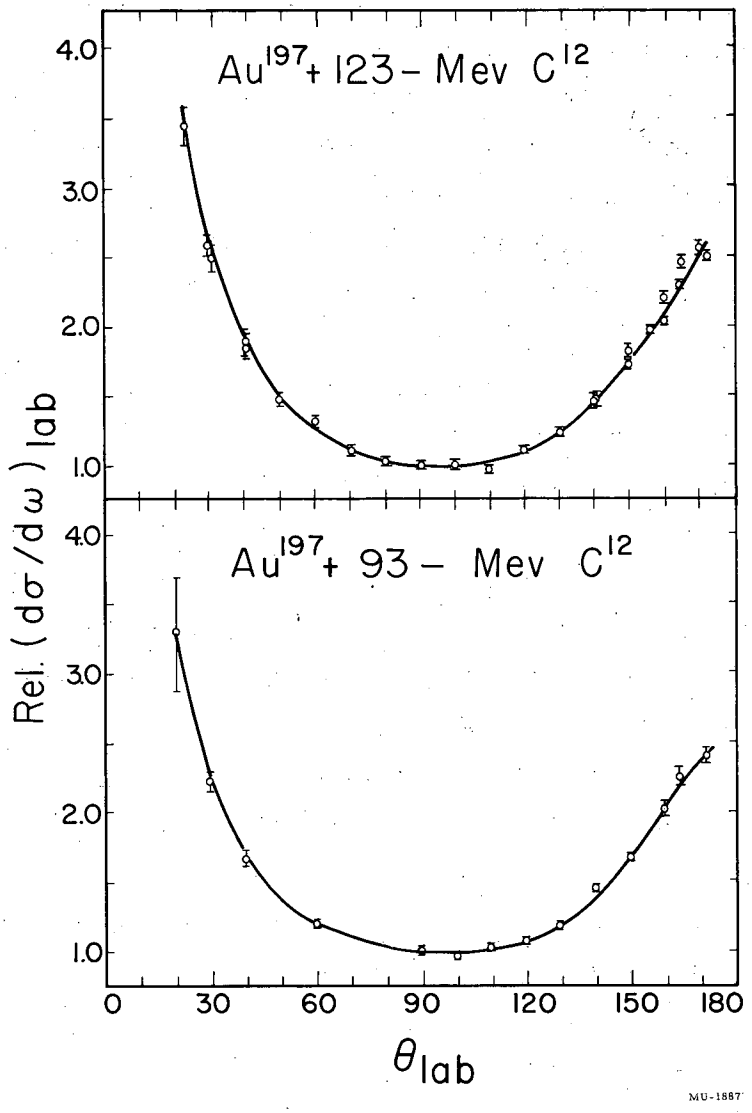

Fig. 12.40 Angular distribution of fission fragments in the laboratory system as measured by GORDON, LARSH AND SIKKELAND.[108] Upper curve, Au^{197} + 123 Mev C^{12}; lower curve, Au^{197} + 93 Mev C^{12}.

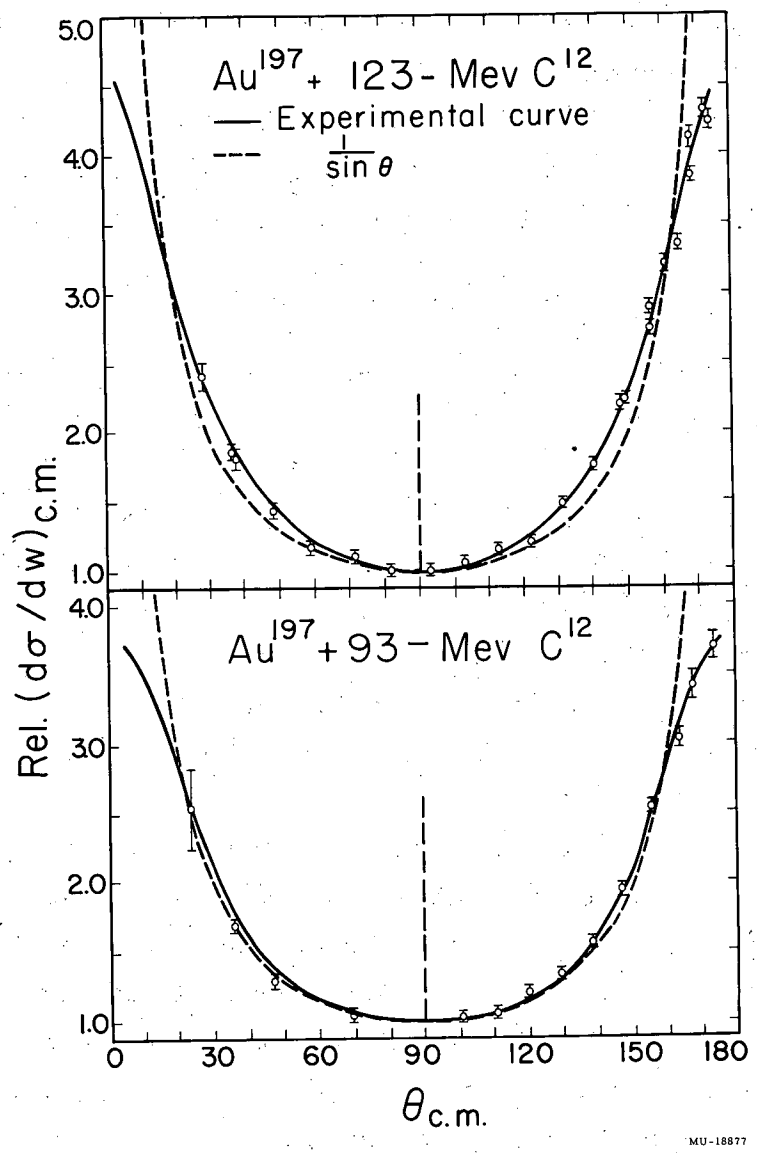

Fig. 12.41 Angular distribution of fission fragments in the center-of-mass system as determined by GORDON, LARSH AND SIKKELAND[108]. Upper curve, Au^{197} + 123 Mev C^{12}; lower curve, Au^{197} + 93-Mev C^{12}.

The following details of the results may be noted:

(a) The center-of-mass angular distributions are symmetric about 90° within experimental error.

(b) Between 15° and 165° on the 123 Mev curve the points lie somewhat above $1/\sin\theta$, in fair agreement with GRIFFIN'S [95] predictions.

(c) The shape of the angular distribution for the 93 Mev C^{12} ions near 0° and 180° is in better agreement with the predictions of HALPERN AND STRUTINSKI[94] than with those of GRIFFIN[95].

A similar curve taken from the radiochemical study of VIOLA AND THOMAS is shown in Figure 12.42

Heavy ions with kinetic energy below the Coulomb barrier might possibly be able to induce fission via the Coulombic excitation process. The cross section for the excitation of a heavy nucleus to an energy above the fission threshold would probably be extremely low but under certain conditions it might be measurable. JONES AND ZUCKER[109] made a search for the fission of U^{238} nucleus by a Coulomb excitation process induced by 28 Mev nitrogen ions. No positive effect was observed and an upper limit of 10^{-28} cm^2 was set for the cross section.

FLEROV[108a] reviewed Russian work on heavy ion reactions in a 1958 Geneva Conference paper. He reported that one interesting consequence of the high angular momentum of the fissioning nucleus is the enhanced yield of high spin isomers among the fission products. For example, it was found that the yield of Cadmium-115 (spin 11/2) relative to Cadmium-115 (spin 1/2) was 20 times larger in the case of gold induced to fission with oxygen ions than it is during the fission of Uranium-235 by thermal neutrons.

108a. G. N. Flerov, Paper P/2299 Volume 15, Proceedings of the Second U.N. International Conference on the Peaceful Uses of Atomic Energy, Geneva, 1958.

109. W. H. Jones and A. Zucker, Oak Ridge National Laboratory Report, ORNL-CF-58-3-38.

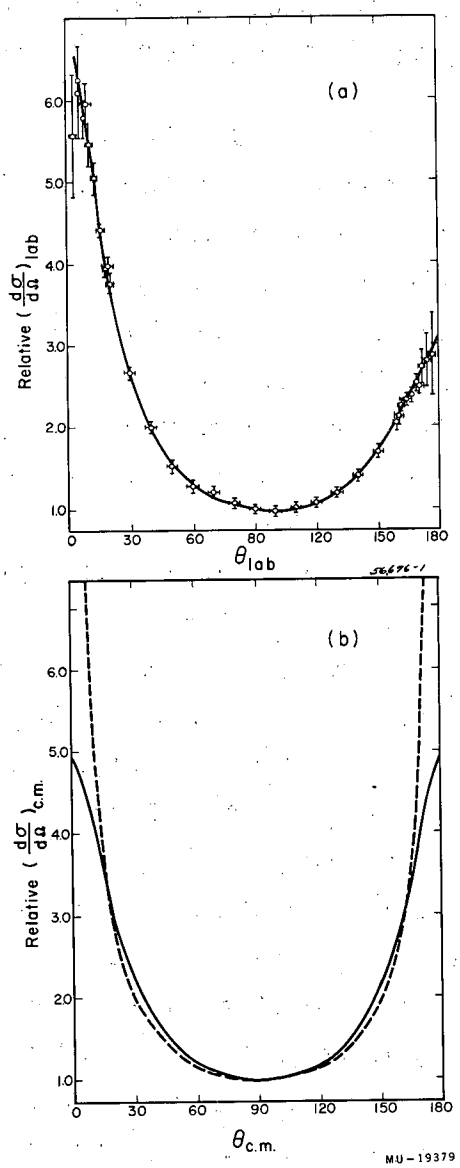

Fig. 12.42 Angular distribution of fission fragments (a) in the laboratory system and (b) in the center-of-mass system as determined by counting the fission fragments recoiling out of a thin target by Viola and Thomas. 125 Mev C^{12} + Au^{197}. Target 0.75 mg/cm^2. The dotted line in part (b) shows a $1/\sin\theta$ distribution. The η value used in the transformation to the center-of-mass system was 0.228.

12.2 NUCLEAR REACTION PHENOMENA INCLUDING FISSION AT HIGH BOMBARDMENT ENERGY

12.2.1 The Serber Model. It will simplify our discussion of the experimental data on high energy fission and spallation of heavy element targets if we first describe the prevailing view on the mechanism of high energy reactions. It is well known that the BOHR[111] compound nucleus theory ceases to be a satisfactory model for nuclear reactions when the energy of the bombarding particle becomes very high. For example with 50 Mev protons as the incident particles only about half of the nuclear reactions go by the initial formation of a compound nucleus for a heavy nucleus target. SERBER[112] pointed out that at higher energies the collision time between the incident particle and a particle in the nucleus is short compared to the time between collisions of the particles in the nucleus. Thus, the first step in the reaction can be considered to be the collision of the incoming particles with a single nucleon in the nucleus. This collision will not be exactly analogous to the interaction of nucleons in free space since the Pauli principle will exclude those encounters with small momentum transfers; hence the allowed collisions will result in somewhat higher momentum transfers. At high energies there is even a finite probability that the bombarding particle will traverse the nucleus without any interaction i.e. the nucleus begins to be transparent to the bombarding particles. When collisions do occur the average momentum transferred to the struck nucleon is small, perhaps of the order of a few tens of Mev. Since the struck particles have much lower energy and shorter mean free paths it is rather likely that they in turn will undergo further collisions and that this energy will be distributed over many nuclear particles thus contributing to the excitation of the nucleus. The incident particle in most cases will still retain most of its energy after its initial encounter and is likely to emerge from the nucleus without a second collision. However, if the first collision occurs near the center of the target nucleus there is a chance that the bombarding particle will make a second, a third, or even more collisions before it is finally captured or escapes with much-reduced energy.

---

111. N. Bohr, Nature 137, 344 (1936).

112. R. Serber, Phys. Rev. 72, 1114 (1947).

This first part of the reaction is referred to as the nucleonic cascade, the "knock-on" cascade, or simply as the cascade. It may consist of a single collision or of many collisions including those made by the original particle and those made by the struck particles while escaping or being captured by the nucleus.

By the end of the cascade, which takes place in a very short period of time ($\sim 10^{22}$ seconds), the interacting target nuclei will be converted to a distribution of product nuclei excited to a variety of excitation energies. There are a variety of possibilities ranging from the bombarding particle emerging with most of its energy intact to the loss of the entire incident energy to the nucleus.

The subsequent disposition of the energy of excitation can be described in terms of some evaporation model in which the nuclear excitation energy is dissipated by successive boiling off of particles each with a few million volts of kinetic energy. For heavy element targets the evaporation of neutrons will be much more probable than the evaporation of protons or of positively charged clusters such as helium ions. In the cascade step the possibility of knocking out a proton is of the same order of magnitude as that for neutrons. For heavy element targets it is quite possible that fission will occur during the evaporation phase of the reaction. For targets such as thorium, uranium and heavier elements fission competition might be expected to be severe at each stage of the evaporation process. Because of this and because the cascade process leaves a mixture of nuclei at various levels of excitation, a complex varity of fissioning nuclei will contribute to the observed mixture of fission products. Radiochemical investigations can provide only an average picture of the results. Ionization chamber measurements of fission cross section also give only average values and reveal nothing of the fission cross section of specific nuclei at specific levels of excitation. Some experimental techniques do provide more specific information. For example, Russian workers have studied fission fragments made visible in nuclear emulsions loaded with uranium salts and by measurement of angular distributions, of cascade protons ejected from the target nucleus, and other characteristics they have been able to deduce considerable information about the excitation energy at the time of fission. This is discussed in Section 12.2.7.

Some simplification occurs when lighter targets such as bismuth and tantalum are bombarded. The fissionability of these elements is quite low and only a small fraction of the nuclear species produced by the cascade and subsequent evaporation processes will contribute to the observed fission products. In the absence of any clear-cut information one can postulate the two extreme mechanisms diagrammed in Fig. 12.43. It may be that fissionability is strongly determined by Z^2/A; in this case the evaporation process would proceed until, after emission of many neutrons, an isotope of high Z^2/A is produced which readily fissions although it has rather low excitation energy. For example, GOECKERMANN and PERLMAN[113] explained their results for the fission of bismuth with 190 Mev deuterons by postulating the evaporation of about 10 neutrons leading to the production of Po^{199}, or a few nuclei around Po^{199}, (with $Z^2/A \sim 35.5$) which then fission with a high cross section. An alternate extreme explanation is that fissionability of nuclides in this region is a strong function of excitation energy and that fission widths increase much faster than neutron evaporation widths at high excitation energy. If this is the case, fission will occur immediately upon completion of the "knock-on" cascade when the excitation energy is the greatest. The fission fragments will be much more highly excited than in low energy fission and will then proceed to evaporate many neutrons. It is possible to consider mechanism lying between these two extremes, i.e. competition of neutron evaporation and fission in a few or in all stages of neutron evaporation. In many experimental investigations the observable end results will be the same whether neutron emission occurs before or after fission so that two cases are difficult to distinguish. Various experimental observations which seem to favor one mechanism or the other are discussed below.

12.2.2 Monte Carlo Calculations of Nuclear Cascade. The SERBER formulation of the initial cascade step of high energy nuclear reactions lends itself to quantitative calculation by the Monte Carlo method of ULAM and VON NEUMANN.[114] GOLDBERGER[115] outlined the application of the Monte Carlo calculation to this

113. R. Goeckermann and I. Perlman, Phys. Rev. 76, 628 (1949).

114. S. Ulam and J. Von Neumann, Bull. Am. Math. Soc. 53, 1120 (1947).

115. M. L. Goldberger, Phys. Rev. 74, 1269 (1948).

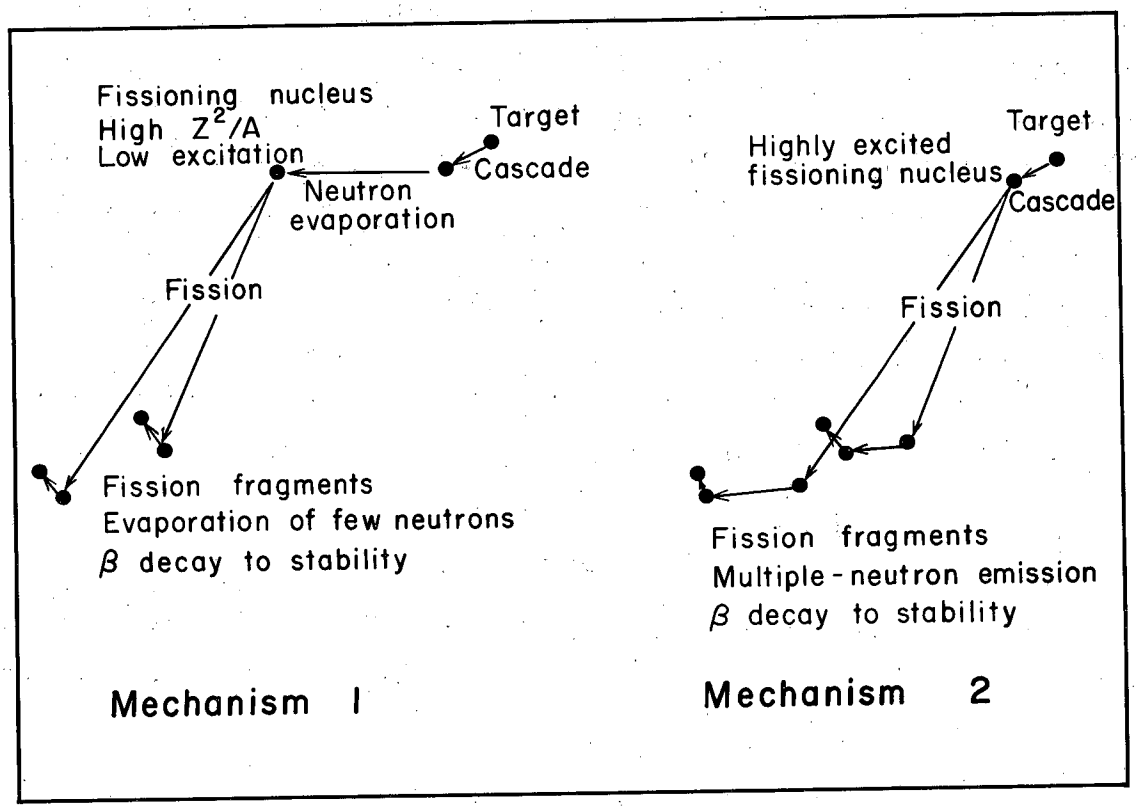

MU-19413

Fig. 12.43 Two extreme mechanisms of high energy fission.

problem. Many other authors[116-124] have used the method for a variety of reaction conditions and each has added some refinements to the technique. Most of the early published calculations involved laborious hand or desk top computor calculation of a few hundred cascade events. The first serious attempt to program the calculation for a high speed electronic computer was carried out by METROPOLIS, BIVENS, STORM, MILLER, FRIEDLANDER, and TURKEVICH[124] with the Maniac digital computor at Los Alamos. We shall outline their calculation as an illustration of the method and quote some of their results.

The target nucleus was represented by the Fermi gas model. According to this representation the ground state of the nucleus is considered to be composed of ideal zero-temperature, non-interacting fermion gases of neutrons and protons bound in a uniform potential well:

$$\begin{aligned} &-|V| \text{ for } r \leq \text{nuclear radius} \\ &\quad 0 \text{ for } r > \text{nuclear radius.} \end{aligned} \tag{12.13}$$

The Fermi-momentum distribution depends upon the effective density of nuclear matter and on the temperature. In a simple potential well the solution for the maximum Fermi momentum is

$$P_{max} = \left(\frac{3h}{8\pi}\right)^{1/3} \left(\frac{N}{V}\right)^{1/3} \tag{12.14}$$

where N = number of nucleons and V = the nuclear volume. The nuclear radius is given by $R = r_o A^{1/3}$ where r_o is evaluated as 1.3×10^{-13} cm. For uranium the

---

116. G. Bernardini, E. T. Booth and S. J. Lindenbaum, Phys. Rev. 85, 826 (1952); ibid 88, 1017 (1952).
117. J. Combe, Nuovo Cimento 3, 182 (1956).
118. P. Cuer and J. Combe, J. Compt. rend. 238, 1799 (1954); 239, 351 (1954).
119. J. W. Meadows, Phys. Rev. 98, 744 (1955).
120. H. McManus, W. T. Sharp and H. Gellman, Phys. Rev. 93, 924 (1954).
121. G. C. Morrison, H. Muirhead, and W. G. V. Rosser, Phil. Mag. 44, 1326 (1953).
122. H. Muirhead and W. G. V. Rosser, Phil. Mag. 46, 652 (1955).
123. G. Rudstam, "Spallation of Medium Weight Elements" Thesis, Uppsala (1956).
124. N. Metropolis, R. Bivens, M. Storm, A. Turkevich, and J. M. Miller, and G. Friedlander, Phys. Rev. 110, 185 (1958); 110, 204 (1958).

Fermi energies of the protons and neutrons are 24.0 and 32.7 Mev respectively. The ideal zero-temperature Fermi gas distribution of nucleons is assumed during the development of the internal nucleonic cascade. The Fermi gas model supplies data on the momenta of struck particles and specifies which collisions are forbidden. Experimental data on total scattering cross sections for reactions of the pn, pp or nn type were computed from formulae of the type

$$\sigma_{pn} = \frac{A}{\beta^2} + \frac{B}{\beta} + C \qquad (12.15)$$

$$\text{where } \beta = \frac{\text{velocity of particle}}{\text{speed of light}}$$

and A, B, and C are empirical constants adjusted to give the best fit to experimental data for the particle-particle cross sections.[125]

The angular variation of the nucleon-nucleon cross section was expressed by the relation,

$$\frac{d\sigma}{d\Omega} = K(A \cos^4\theta + B \cos^3\theta + 1) \qquad (12.16)$$

where A, B, C, are empirical constants chosen to give the best fit over the energy region studied. The constants were put into the computor in the form of a table.

Binding energy was taken into account by using an average binding energy; for bismuth and uranium targets average binding energies of 6.4 and 6.1 Mev, respectively, were used for the loosest nucleons. This corresponds to the binding energy of a particle within the nucleus with the maximum Fermi energy. An incoming particle increases its kinetic energy while an outgoing particle (neutron or proton) decreases its energy by this amount.

For incident protons or neutrons below 300 Mev in energy the only collision processes considered were elastic nucleon-nucleon collisions. Above 300 Mev inelastic collisions leading to meson production become increasingly important and serious errors would be made by ignoring their existence. Data on meson production cross sections, meson multiplicities, angular correlations, charge exchange reaction probabilities, reabsorption probabilities, etc. are not well

---

125. A good general summary of high-energy nucleon-nucleon cross section data is given by W. N. Hess, Rev. Modern Phys. 30, 368 (1958).

known so that it is hard to program an accurate computation of the cascade process for this energy region. Nonetheless, the computations were extended to cover the energy region 300 Mev to 3 Bev because of the interest in radiochemical analysis of targets bombarded with such high energy particles. Meson effects were allowed for in the following simplified way. Simplified cross section formulas as a function of energy were introduced for one pion and two pion production – neutral and charged; no higher multiplicities were considered. In pp or np collisions in which mesons are produced the momentum was assumed to be shared equally among the 3 or 4 particles. The cross section for the elastic collisions of mesons with nucleons in the nucleus, for reabsorption of the mesons, and for charge exchange reactions were introduced in the form of simple tables.

The sequence of operations in the Monte Carlo machine calculation is diagrammed in Fig. 12.44 for the case of incident proton energy below π-meson production threshold. The incident particle parameters are input data choices. The point of entry of the incident particle into the nucleus is chosen randomly. The distance of travel is next chosen by random number selection with the possible distances appropriately weighted by the mean free path expression obtained from the free nucleon cross sections. The collision site must then be examined to see whether it is still within the nucleus. If it is not, the event is tabulated as contributing to the nuclear transparency cross section. If it is, the characteristics of the struck particle and the relativistic kinematics of the collision must be computed. The collision is then examined to see whether it is permitted by the Pauli principle. If it is not, the particle is returned to the collision site and given another chance to escape the nucleus or to undergo another collision. If the collision is allowed the individual nucleons or pions emerging from the collision are allowed in turn to undergo additional collisions until they escape from the nucleus or are so reduced in energy that they are captured by the nucleus. It is necessary to decide how far the energy degradation of any particle should be followed before the particle may no longer be regarded as a cascade particle. This so-called "death energy" was taken arbitrarily in these calculations to be that kinetic energy a proton would need to escape the potential barrier. For uranium the coulomb barrier is 16.5 Mev for a nuclear radius

Fig. 12.44

1. Point of entry into nucleus chosen.

2. Distance of travel chosen on basis of total cross sections and nuclear composition, i.e. position of collision established.

3. Position of collision examined to see if it is inside the nucleus or not.

4. If inside, the partner is chosen:
   (a) N or P
   (b) its energy
   (c) its direction of motion (μ,ϕ)

5. Collision mechanics are carried out relativistically choosing an appropriate angle, Θ, for the collision and calculating out energies and directions of motion of resulting particles in the laboratory system.

6. "Forbiddenness" of collision is examined, i.e. whether either of the resulting particles have energies less than the corresponding Fermi energy.

7. If "allowed", one particle is stored for later treatment and the other is followed.

4b. A new stored particle is selected (see 7). If no stored particles are left, a new cascade is started with a fresh incident particle (box 1.)

4a. If outside the nucleus, the nucleon has "escaped". Energy and direction of motion of escaping nucleon are noted.

7a. If the collision is "forbidden" a new distance of travel is calculated (from point of forbidden collision) for the cascade particle (box 2)

Block diagram showing sequence of operations in the Monte Carlo calculation of the high energy knock-on cascade performed on the Maniac by Metropolis et al.[124] This diagram is for incident neutron or proton energies below the π meson production threshold.

parameter of 1.3×10^{-13} cm. To this must be added the Fermi energy and the binding energy, totaling in all 50.9 Mev in the case of uranium. The same cut-off energy was used for neutrons. When the energy of any particle is reduced to the cut-off value it is assumed to be captured and the kinetic energy is considered to contribute to the excitation energy of the residual nucleus. The final excitation energy of the residual nucleus is a summation of the kinetic energy of cascade particles at the time of capture and of the "hole energies" of ejected particles.

In the case of incident particle energies above the meson threshold the block diagram for the calculation took on an additional complexity. At each nucleon-nucleon collision site it was necessary to make a random selection from properly weighted choices of alternate collision processes; elastic scatter, single meson production or double meson production. If a meson was produced it was necessary to determine its fate by the possible processes of elastic scatter from nucleons, charge exchange with a nucleon, reabsorption, or escape. A two-dimensional representation of a typical nuclear cascade involving meson production is shown in Fig. 12.45.

Even from this abbreviated description it is easy to realize that a complete cascade calculation is a very complicated process. Each step in the calculation is relatively simple but the numerous steps and the necessity for recording and correlating information for the many cascade particles developed in the cascade makes the overall computation quite involved. The average length of time taken for each event by the MANIAC computor was about 5 seconds.

Let us now consider the information which is obtained from the computation; it is the following:

1. The nature and energy of the particle going into the nucleus.
2. The number of collisions inside the nucleus.
3. The nature and number of the outgoing particles.
4. The energy and the angular distribution of the outgoing particles.
5. The atomic number and mass number of the residual nucleus.
6. The excitation energy of the residual nucleus.
7. The momentum of the residual nucleus both forward and transverse.

These Monte Carlo calculations were run for several representative target elements and for many choices of bombardment energy. One thousand cascades

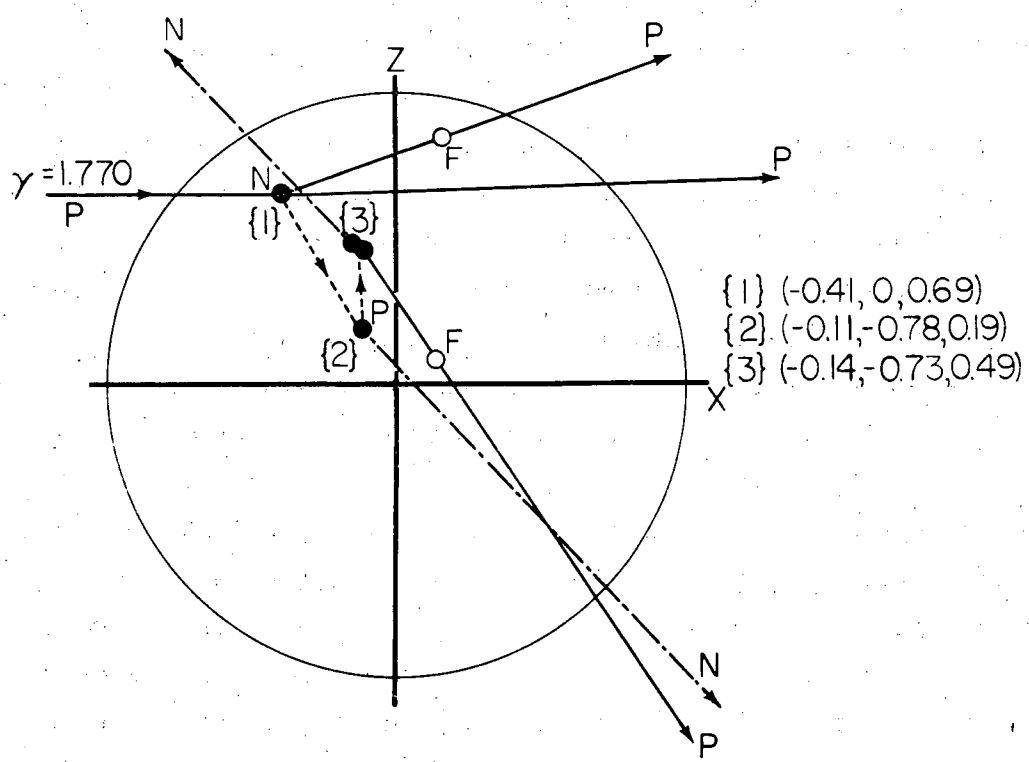

MU-19380

Fig. 12.45 Typical cascade for a high energy proton, $\gamma = 1.77$, striking a heavy nucleus. $\gamma = 1/\sqrt{1-\beta^2}$ Collision {1} is an allowed collision (indicated by black circle) with a neutron of the type $P + N \rightarrow \pi^- + P + P$. Both protons escape although one collision is considered but rejected as forbidden (open circle labelled F). The pion encounters a proton {2} and charge exchange occurs. $\pi^- + P \rightarrow N + \pi^+$. The neutron escapes while the pion is reabsorbed at site {3} · $\pi^+ + (N+N) \rightarrow N + P$. A collision is considered for the outgoing proton and rejected as forbidden.

were calculated for each combination so that good statistical accuracy could be obtained. The element ruthenium was chosen as a "stand-in" for AgBr so that the numerous emulsion data could be compared with the Monte Carlo calculations.

A complete tabulation of all the results would have been too lengthy for journal publication so METROPOLIS and CO-WORKERS[124] published only average results of a number of important quantities. We now consider a sampling of these.

Nuclear transparency is defined as the difference from unity of the ratio of the experimental inelastic cross section to the geometrical cross section. Calculated transparencies for bismuth and uranium nuclei are listed in Table 12.15. While these transparencies are appreciable, they lie within the error of most experimental measurements and hence are hard to verify. This difficulty stems not only from the experimental errors involved in a measure of total inelastic cross sections but also from the uncertainties in the choice of nuclear radius in estimating the geometrical cross section.

The calculated characteristics of the cascade particles can be compared with experimental measurement of the same quantities made by emulsion or counter techniques. The important characteristics are: the number of emerging cascade particles per cascade event, the neutron to proton ratio of these particles, their energy and angular distribution. For incident proton or neutron energies below the range of significant meson production the agreement of the calculated and experimental values is rather good and provides one with some confidence that the basic assumptions of the cascade calculation are correct. For higher energy cases the agreement with the very limited experimental data is only fair which suggests that the input data and/or the approximations used for the Monte Carlo calculations need improvement.

The calculated variation in the average number of escaping nucleons as a function of target nucleus and energy of the bombarding protons is presented in Figs. 12.46(a), (b) and (c) for proton energies below 300 Mev. Figure 12.47 shows the calculated average number of cascade nucleons per inelastic event for three target elements across the whole range of proton energies.

The calculated neutron-to-proton ratios of the outgoing cascade particles are presented in Table 12.15. We note that this ratio increases with the size

Table [illegible] Calculated Nuclear Transparencies

Target nucleus	Energy of incident protons (Mev)					
	82	235	286	460	940	1840
Bismuth	0.06		0.105	.08	.05	.03
Uranium	0.06	.08		.07	.03	.04

Table 12.15 Calculated Neutron/Proton Ratio of Emerging Cascade Particles

Bombarding energy(Mev)	Al	Cu	Ru	Ce	Bi	U
			Incident protons			
82	0.84	1.04	1.20	1.82	1.67	2.08
158	--	0.96	1.15	--	--	1.96
239	0.74	0.93	1.10	1.43	--	1.61
290	--	1.00	1.12	--	1.64	--
365	--	1.00	--	1.33	--	--
460	0.79	1.02	1.16	1.43	1.59	1.89
690	--	1.02	--	--	--	--
940	--	1.16	1.22	--	1.89	2.00
1840	0.92	1.18	1.25	1.56	1.75	2.08
			Incident neutrons			
82	1.82	2.43	2.80	--	--	4.15
156	--	1.93	--	--	--	--
236	1.72	2.11	2.23	--	--	3.28
286	--	2.04	--	--	--	--

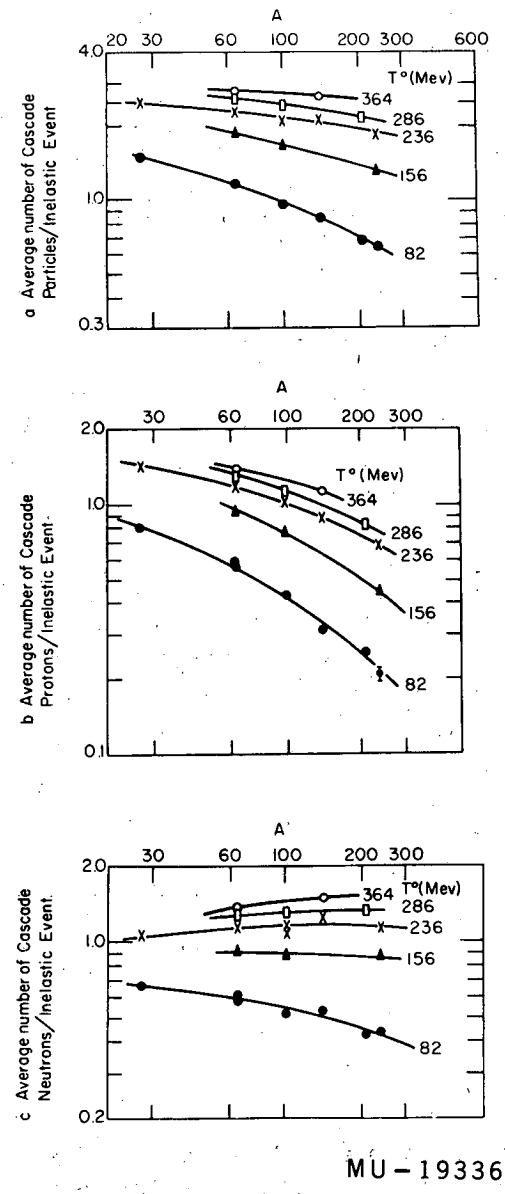

MU-19336

Fig. 12.46 Calculated average number of
(a) Cascade nucleons
(b) Cascade protons
(c) Cascade neutrons
per nuclear interaction as a function of the target nucleus in proton bombardments at various bombarding energies up to about 300 Mev. From METROPOLIS et al.[124]

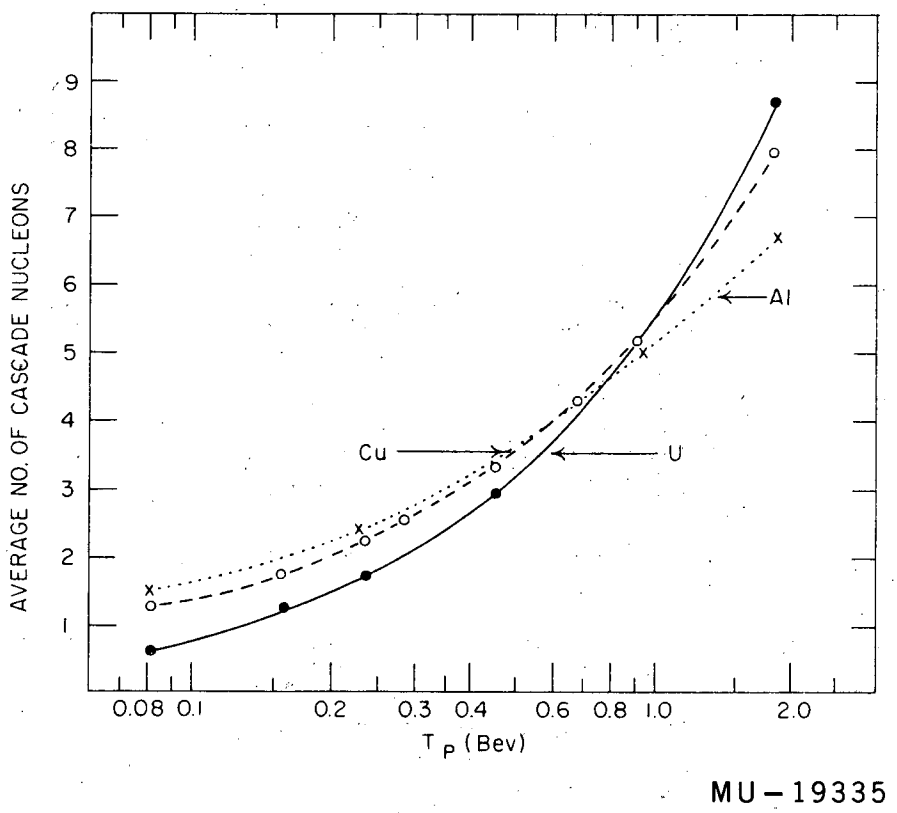

MU-19335

Fig. 12.47 Average number of cascade nucleons per inelastic event plotted as a function of incident proton energy for three target elements. From METROPOLIS et al.[124]

of the target nucleus. It is interesting to note that for uranium, where the cascade has the best chance to develop, the average ratio of neutron emission to proton emission is, over the whole energy range greater than the neutron to proton ratio in the target nucleus.

The calculated average number of cascade pions emitted per inelastic event is shown in Fig. 12.48. Pion production is strongly dependent upon the bombardment energy but only weakly dependent on the mass number of the target nucleus probably because the increase in pion production with increasing nuclear size is compensated by the decrease in the probability for escape of the pions. There are very few experimental data available to compare with the values given in Fig. 12.48. Probably the absolute values are somewhat inaccurate because of the crudeness of the input data on pion production but the general trends should not be significantly changed by more refined input data. We shall not review here the many details given by METROPOLIS and CO-WORKERS[124] on the proportion of the various pion charge states, and on the angular and energy distributions of the emerging pions, protons and neutrons.

The calculated distribution in numbers of cascade particles can be used to prepare curves on the relative frequency of different changes in mass number of the target nucleus at the end of the cascade part of the high energy interaction. Data on uranium targets are presented in Fig. 12.49. The curve for $A_2 = 239$ gives the fraction of cascade leading to compound nucleus formation. This fraction decreases sharply with energy. One-particle cascades, $A_2 = 238$, are the dominant mode of interaction from 90 to 200 Mev incident particle energy. Above 200 Mev cascades with two or more particles out become quite important.

The energy of excitation of a residual nucleus at the end of the fast cascade can be designated as E^* and computed by summing the "hole" energies in the degenerate nucleon gas and the kinetic energy of the excited nucleons. This is equivalent to calculating it via the formula

$$E^* = T_o^o - \sum_{i=0}^{m} T_i^o - (m-1)B \qquad (12.17)$$

where T_o^o is the energy of the incoming particle (lab system), T_i^o is the energy of an outgoing cascade particle, m is the number of outgoing particles and B

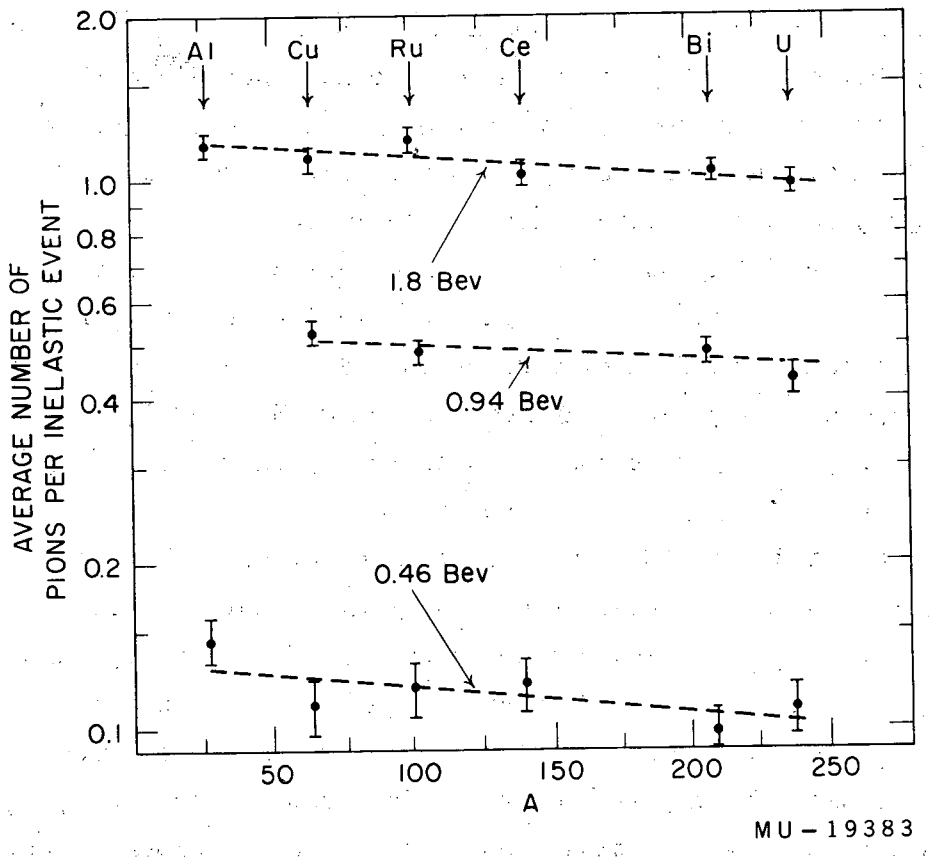

Fig. 12.48 Average number of pions (of all charge states) emitted per inelastic proton interaction with various target nuclei.

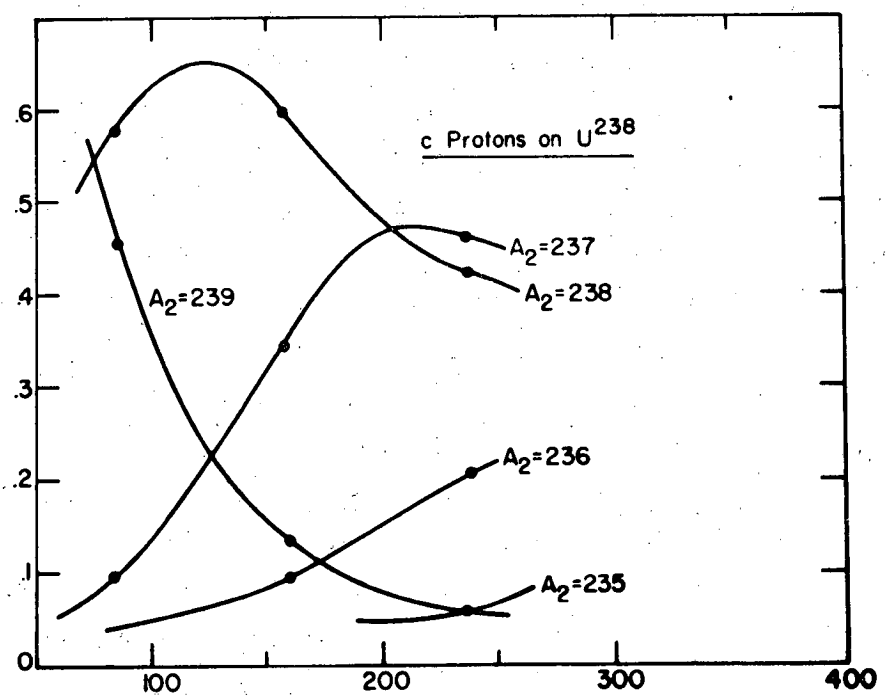

MU-19334

Fig. 12.49 Calculated yields of a given mass, A_2, as a result of proton-initiated nuclear cascades in uranium targets. From METROPOLIS.[124]
Ordinate: fraction of total inelastic cross section.
Abscissa: proton bombarding energy in Mev.

is the average binding energy of the m outgoing nucleons. The average excitation energy as calculated by this formula is given in Fig. 12.50.

Four striking features are apparent from this figure.

(1) Incoming protons (or neutrons) with greater than 100 Mev kinetic energy leave on the average only a fraction of their kinetic energy as excitation energy in the residual nucleus. This is perhaps the single most striking feature of the whole cascade model of the initial step in high energy nuclear reactions. This effect is most noticeable in the light elements but even for uranium less than half the energy of the incident particle is transferred to the target nucleus.

(2) The average excitation energy at any given bombarding energy increases with the mass number of the target nucleus.

(3) The average excitation energy increases only slowly with the incident particle energy for energies below 350 Mev.

(4) The average excitation energy increases relatively rapidly with incident energy for incident energies above about 400 Mev.

The last feature is a result of the onset of meson production. The meson interactions with the nucleus provide a more efficient energy transfer mechanism than the purely elastic nucleonic cascade because in nuclear matter the scattering mean free path of a pion created in a nucleon-nucleon collision is generally shorter than that of the nucleon that produced the pion. Furthermore, the pion has an appreciable probability of being reabsorbed. There is some evidence that the energy deposition as given by Fig. 12.50 is overestimated at the highest proton energies which again is a reflection of the uncertainties in the input data. There is no question however that meson processes play a significant role in the energy deposition process for the higher energies.

Another characteristic feature of the cascade model is that there is a broad distribution in excitation energies around the average value of Fig. 12.50. One can get some idea of the breadth of this distribution by an examination of Fig. 12.51 which shows the calculated gross distribution of excitation energies $N(E^*)$ for various elements at different proton bombarding energies.

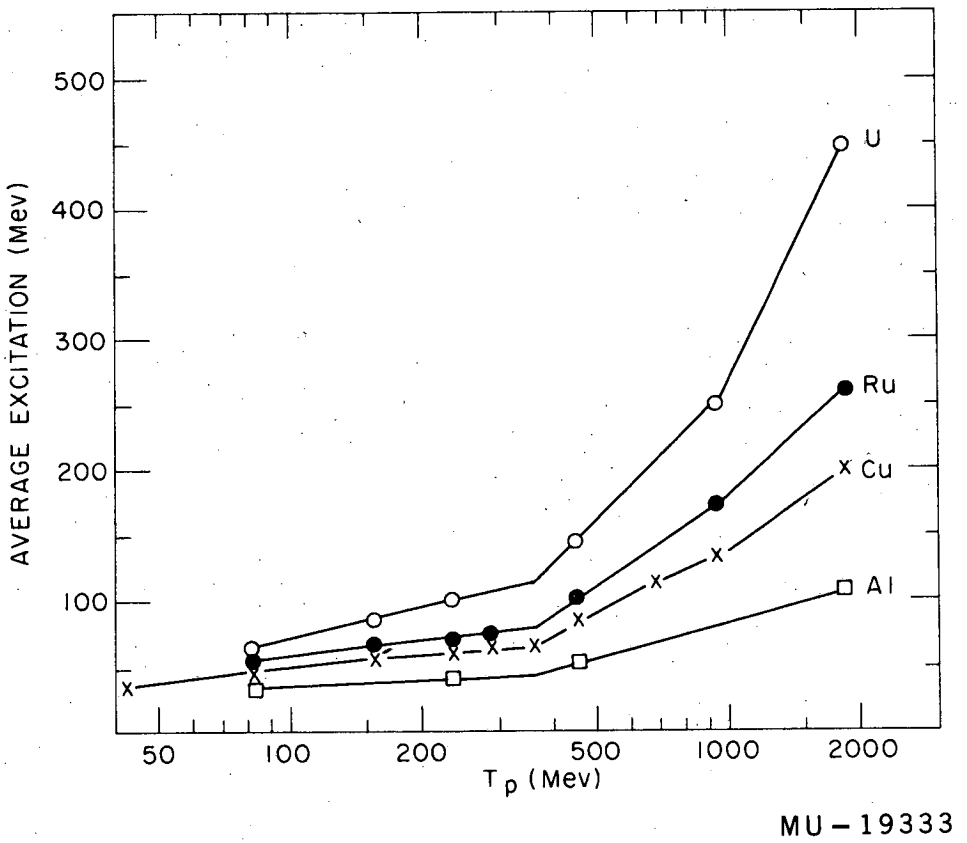

Fig. 12.50 Calculated average excitation energy $\overline{E}^*$ in various target nuclei as a function of proton bombarding energy T_p.

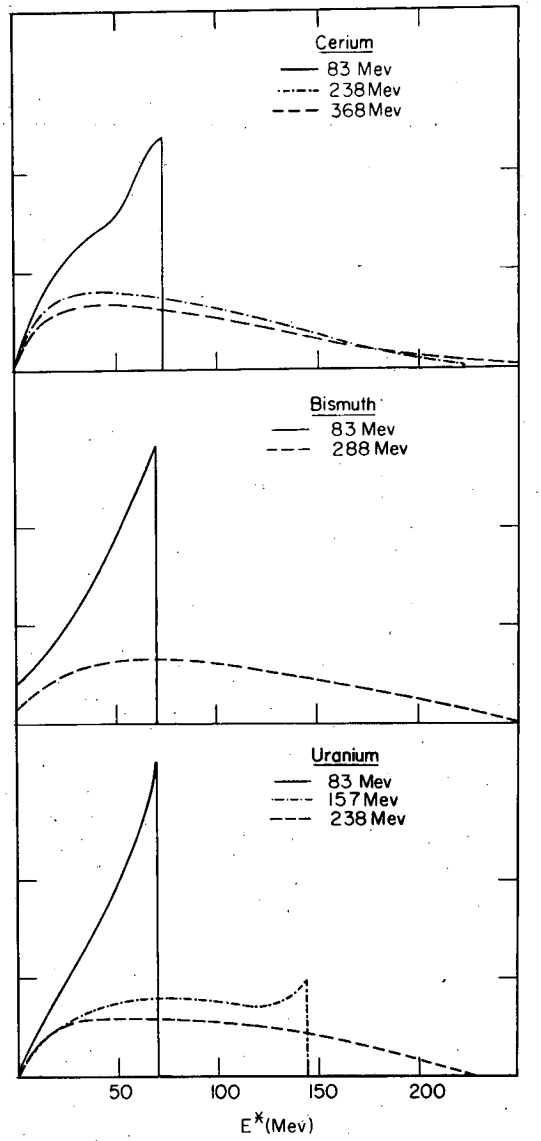

MU-19385

Fig. 12.51 Calculated gross distribution of excitation energies, $N(E^*)$, for cerium, bismuth and uranium at different proton bombarding energies. (Compound nucleus cases not included.) From METROPOLIS et al.[124]
Ordinate: $N(E^*)$ in units of $(10\ \text{Mev})^{-1}$
Abscissa: Excitation energies, E^*, in Mev.

12.2.3 Monte Carlo Calculations of the Evaporation Cascade. At the end of the nucleonic cascade the target nucleus has been converted to a highly-excited nucleus with a different composition of neutrons and protons. We now turn to the task of considering how this excitation energy is disposed of in the slower, second stage of the reaction. We consider first the evaporation of nucleons or groups of nucleons.

Most treatments of evaporation are derived from WEISSKOPF'S[126,127] original treatment of the problem. An important contribution to the theoretical analysis of the evaporation de-excitation of very highly excited nuclei was made by LE COUTEUR[128] who was interested in explaining photo emulsion data taken on high energy cosmic rays. He treated the de-excitation of nuclei excited to the range 300-800 Mev. FUJIMOTO and YAMAGUCHI[129-130] also contributed to this analysis. Since excitation energies of the same order of magnitude are now achieved in target nuclei bombarded in laboratory accelerators, the analysis of the evaporation de-excitation of highly excited nuclei has taken on a new importance.

Evaporation treatments usually start with the WEISSKOPF expression

$$\omega_j(E)\ dE = \frac{\sigma(E) g_j m_j}{\pi^2 \hbar^3} \frac{E\ \rho_f(E_f)}{\rho_i\ (E_i)}\ dE \qquad (12.18)$$

where

$\omega_j(E)$ is the probability of emission of particle j with an energy between E and E + dE.

E_i is the excitation energy of initial nucleus

E_f is the excitation energy of final nucleus after emission of particle j

g_j is the angular momentum degeneracy

---

126. V. Weisskopf, Phys. Rev. 52, 295 (1937).

127. Blatt and Weisskopf, Theoretical Nuclear Physics, John Wiley and Sons, New York, 195

128. K. J. Le Couteur, Proc. Phys. Soc. (London) 63A, 259 (1950); ibid. 65A, 718 (1952).

129. Y. Yamaguchi, Prog. Theor. Phys. 5, 142 (1950).

130. Y. Fujimoto and Y. Yamaguchi, Prog. Theor. Phys. 4, 468 (1949); ibid. 5, 76, 787 (1950).

m_j is the mass of the particle

$\rho_f(E_f)$ is the level density of the nucleus after evaporation when the nucleus is left with excitation energy E_f.

$\rho_i(E_i)$ is the level density of the initial nucleus at excitation energy E_i.

$\sigma_{(E)}$ is the cross section for the reverse reaction. For neutron evaporation $\sigma_{(E)}$ is equated with the geometrical cross section σ_{geom}. For charged particle emission $\sigma_{(E)}$ is set equal to zero for $E < V_j$, where V_j is the potential barrier for particle J. For $E > V_j$ the quantity $\sigma_{(E)}$ may be set equal to σ_{geom} $(1-V_j/E)$. The selection of a proper value of V_j is influenced by barrier penetration effects and by possible lowering of the barrier at large excitation energies.

Crucial quantities in the above expression are the level densities $\rho_f(E_f)$ and $\rho_i(E_i)$. To evaluate them it is necessary to assume some nuclear model. If the Fermi gas model is chosen, a suitable expression for the level density may be the familiar Weisskopf expression,

$$\rho\ (E) = C \exp\ [2(aE)^{1/2}] \tag{12.19}$$

where C and a are constants to be evaluated empirically. Odd-even effects may be included by using different values of C for different nucleon types or by computing the excitation energy from a corrected ground state which is displaced upward by varying amounts from the true ground state.

If one selects explicit level density expressions and a set of constants for the calculation of $\sigma_{(E)}$, it is a simple matter to calculate the probability of emission of a neutron, a proton, an alpha particle or some other group of nucleons for a given initial excited nucleus. Since we are discussing very high excitation energies, the emission of a single particle will leave the resultant nucleus with still sufficient energy to continue the evaporation process. In practice then, what one really wishes to know is the integrated probability for the emission of various particles or particle groups over a whole sequence of successive evaporations until the excitation energy is reduced below the point where any more particles can be lost. For a particle, j, of a given type, the total emission probability will be

$$P_j = \int_{V_j}^{E_i-Q} \omega_j(E)\, dE = \int_{V_j}^{E_i-Q} \frac{\sigma(E)\; g\; m\; (E-V_j)\; \rho_f(E_f)}{\pi^2\, \hbar^3\; \rho_i(E_i)}\, dE \qquad (12.20)$$

Where the limits of integration are set by

V_j the potential barrier, corrected for penetration of the particle j

E_i the excitation energy of the initial nucleus

Q the separation energy of the particle j

This integration over the entire de-excitation process can be done analytically or by a Monte Carlo type method. LE COUTEUR[128] and FUJIMOTO and YAMAGUCHI[129-130] used the first approach but found it necessary to use some severe approximations and to assume stationary values for some of the variables in order to reduce the calculation to tractability. RUDSTAM[131], DOSTROVSKY, RABINOWITZ and BIVENS[132], and FRIEDLANDER, FRAENKEL and DOSTROVSKY[133] decided on the other hand that the Monte Carlo method was ideally suited to this problem since the various probabilities can be calculated afresh after the emission of each individual particle, and the necessary nuclear constants can be adjusted to the most appropriate values for each step of the evaporation cascade. Let us examine briefly how the Monte Carlo method is applied and what information it provides.

At each stage of the evaporation sequence we have two questions to ask: (1) What particle is evaporated? (2) With what energy is that particle evaporated?

---

131. G. Rudstam, "Spallation of Medium Weight Elements", Thesis, Uppsala, 1956.

132. I. Dostrovsky, P. Rabinowitz and R. Bivens, Phys. Rev. 111, 1659 (1958).

133. G. Friedlander, Z. Fraenkel and I. Dostrovsky, Phys. Rev. 116, 383, (1959). This paper is a continuation of the work described in reference 132 and represents a more sophisticated treatment of the evaporation equations and of the parameters used therein. The calculations were compared with about 60 excitation functions for nuclear reactions in the mass range Cr^{50} to Se^{74} and the energy range < 50 Mev. While both the mass and energy range are much lower than we are discussing here, this paper is highly pertinent in that it establishes the general validity of the statistical evaporation model.

To answer the first question we may use expressions of the following type for the relative probability of emission of two particles i and j. This equation is given by DOSTROVSKY, RABINOWITZ and BIVENS[132] who base it on the work of LE COUTEUR.[128] The expression is based on the statistical model of a degenerate Fermi gas and on the WEISSKOPF level density formula.

$$\frac{P_i}{P_j} = \frac{g_i m_i}{g_j m_j}\left(\frac{R_i}{R_j}\right) \frac{a_j}{a_i} \exp\left\{2 \left[(a_i R_i)^{1/2} - (a_j R_j)^{1/2}\right]\right\} \qquad (12.21)$$

In this expression the constants a_j are defined by the WEISSKOPF expression given above as Eq. (12.19) and R_j is the maximum value of the excitation which a nucleus may possess after evaporating a particle j

$$R_j = E_o - Q_j - V_j \qquad (12.22)$$

where E_o is the excitation energy of the nucleus before evaporation,

Q_j is the binding energy of particle j to the residual nucleus, and

V_j is the coulomb barrier for particle j suitably corrected for barrier penetration.

The Q_j's can be evaluated for each case in various ways. The most suitable is to use experimental values when they are available and to use some appropriate semi-empirical mass formula when they are not.

The evaluation of the constant, a, is perhaps the most important and most difficult step in the use of the above equation. It would take too much space to discuss critically all the experimental data relating to an evaluation of this level density parameter; the reader should consult DOSTROVSKY[132] and the papers cited therein for more information. Let us just say that one choice that seems as appropriate as any on the basis of present information is the following:

Let a be equal to A/10, that is to one-tenth the mass number. Then correct this for the neutron excess of the nucleus. LE COUTEUR formulates this dependence in this way:

$$\left.\begin{aligned}
a_n^{1/2} &= a^{1/2}\,(1 - 1.3\,\Theta/A) \\
a_p^{1/2} &= a^{1/2}\,(1 + 1.3\,\Theta/A) \\
a_d^{1/2} &= a^{1/2}\,(1 - 1/2\,A) \\
a_t^{1/2} &= a^{1/2}\,(1 - 1/A - 1.3\,\Theta/A) \\
a_{He^3}^{1/2} &= a^{1/2}\,(1 - 1/A + 1.3\,\Theta/A) \\
a_\alpha &= a^{1/2}\,(1 - 3/2\,A) \\
&\text{where } \Theta = \text{neutron excess} = \frac{N-Z}{A}
\end{aligned}\right\} \qquad (12.23)$$

To answer the second question concerning the energy of the evaporated particle, we turn again to WEISSKOPF[126] who has shown that the kinetic energy of neutrons emitted from a given nucleus follow approximately a Maxwellian distribution determined by an appropriate nuclear temperature. The evaporated charged particles will also have a Maxwellian energy distribution but an additional energy equivalent to the Coulomb barrier must be included.

The sequence of steps in the Monte Carlo calculation is the following: An initial nucleus with a definite excitation energy is chosen. The appropriate parameters for the probability equations (12.19) given above are chosen for this particular nucleus and the relative probability for the emission of neutrons, protons, deuterons, tritons, etc. are computed. The sum of these probabilities is normalized to the value 1 and by a random number selection between 0 and 1 it is decided which particle is emitted. The energy of the emitted particle is then selected by a random number selection from possibilities which are properly weighted to conform with the expected Maxwellian distribution of the energy. Then new values of Z, A and excitation energy are computed, an adjustment is made, if necessary, in the choice of the evaporation parameters and a new decision is made by random number selection on the type of particle to be emitted and on its energy. This process is repeated until the initial excitation energy is almost all removed. At the very end of the cascade it might happen that some particles are eliminated as evaporation possibilities because their R_j values (Eq. 12.22) are no longer positive. It also might happen that the random number choice of particle energy might be

greater than that available from the residual excitation. This choice is then rejected and new random number choices are tried until a combination is found which permits the last evaporation to take place. This entire sequence constitutes one evaporation cascade event. To achieve any statistical significance, it is necessary to carry through such operations for hundreds of cascade events.

RUDSTAM[131] used simple roulette wheels for his random number selections and by a combination of graphical techniques and hand calculations, carried through evaporation calculations for a series of medium weight nuclei excited to a series of initial energies ranging from 25 to 165 Mev. DOSTROVSKY, RABINOWITZ and BIVENS[132] coded the whole problem for the high speed electronic computor called the WEIZAC and were able to compute 1000 cases each for a wide variety of initial nuclei. They were also able to investigate the effect of different choices of the evaporation parameters. It is beyond the scope of this chapter to give a summary of these results and we wish only to state what type of information is obtained.

The most complete tabulation would show for each cascade event and for each iteration step the nature of the outgoing particle, its kinetic energy and the residual excitation energy of the new nucleus. For most purposes this is more detailed than is needed and a more manageable and useful tabulation simply summarizes for each series of cascades

1. the average number of each type of evaporated particle,
2. the average energy spectra for each type of particle, and
3. the A, Z distribution of the residual nuclei.

An example of a typical summary is given in Table 12.16.

In principle, all three of these items can be compared with experimental data. However, the calculation refer to the idealized case of a given nucleus with a definite unique excitation. In almost every real high-energy experiment, we must deal with a range of nuclei, each with a distribution of excitation energies. The most detailed comparison of theory and experiment can be made if the Monte Carlo calculations of the high energy cascade and the evaporation stage are combined. This can be done by applying the evaporation calculation to the main group of excited nuclei previously calculated for the high energy cascade and combining the results with proper weighting factors. One can thus predict the number, angular distribution, energy distribution, and nature

Table 12.16 Typical Summary of Evaporation Calculation for a Heavy Element (from Ref. 132)

Case: Pa^{231} with initial excitation 450 Mev	
Average Number of Specified Particle per 100 Cases	
n	23.4
p	3.6
d	1.0
t	0.5
He^3	0.05
α	1.8
Average Quantities per 100 Cases	
Aver. number particles evap.	30.4
Aver. mass number change	37.9
Aver. number charged particles	6.9
Aver. change in Z	8.8

(neutrons, protons, deuterons, etc.) of the knock-on particles and of the evaporated particles. The evaporated particles will have isotropic distributions in the center of mass system of the struck nucleus and much lower average energies so that they can often be distinguished from the cascade particles in emulsion studies. One can also predict the yields of the end products of the two stage process. These in general will be radioactive nuclei whose yields can be determined radiometrically. We have mentioned above the fact that emulsion studies of the high energy protons agree remarkably well with the predictions of the knock-on cascade. Many studies have also been made of the low energy protons in cosmic ray stars or in accelerator experiments. LE COUTEUR[128] found rather good agreement between his calculations and the energy distribution of protons from high energy cosmic ray stars. BARKAS and his co-workers[134-138] have made a careful study of charged particles ejected from various targets bombarded with high energy protons, deuterons and helium ions in the Berkeley 184-inch cyclotron. In these experiments the particles emerging from an internal cyclotron target traveled in different spiral paths in the magnetic field of the cyclotron before entering nuclear emulsions. The particle trajectories as defined by a slit system, the position of the track on the plates, and the characteristics of the tracks themselves were used to distinguish protons from deuterons, tritons, helium-three nuclei, alpha particles, and heavier aggregates and to measure the energies of each. Neutron abundances and energies were also recorded by proton recoil tracks in emulsions. These studies provide a wealth of detailed information on the identity, populations, momentum distributions and angular distributions of light particles which can be compared with the predictions of the model just reviewed.

---

134. W. Barkas and H. Tyren, Phys. Rev. 89, 1 (1953).

135. R. W. Deutsch, Phys. Rev. 97, 1110 (1955).

136. E. Bailey, Thesis, University of California Radiation Laboratory Report, UCRL-3334 (1956), unpublished.

137. E. Gross, University of California Radiation Laboratory Reports, UCRL-3330 and UCRL-3337 (1956), unpublished.

138. Gilbert, University of California Radiation Laboratory Report, UCRL-2771, unpublished.

DOSTROVSKY, FRAENKEL and WINSBERG[139] made just such a comparison with the experimental data of BAILEY[136] and GROSS[137] for targets of nickel, silver and gold bombarded with 190 Mev protons. For computational purposes, the spectra of excited nuclei produced in the knock-on cascades were estimated from the calculations of METROPOLIS and co-workers.[124] These distributions in Z in A and in excitation energy were then used as a starting point for an evaporation calculation of the charged particle emission using the detailed approach developed by DOSTROVSKY, FRAENKEL and FRIEDLANDER.[133] Table 12.17 compares the experimental cross sections for neutrons, protons, deuterons, tritons, helium-3 nuclei and helium-4 nuclei and the theoretical values based on several choices of the nuclear radius and level density parameters. The experimental values for the forward hemisphere include cascade as well as evaporated particles so that the particles observed in the backward hemisphere should be compared with the calculations. The agreement is not spectacular but it is impressive that the order of magnitude of the predicted cross sections is about right. However, the predicted energy spectra of the evaporated particles is not in good agreement with the experiment. The shapes of the spectra are similar, but the whole theoretical spectrum is displaced many Mev in the direction of higher energies. Figure 12.52 is a sample comparison taken from the many published in the cited reference. This predominance of low-energy charged particles has been observed in other elements by FULMER and COHEN[139a] and by others. This disagreement cannot be patched up by any reasonable change in the radius and level density parameters. It may be that the replacement of the square well nuclear potential by one with a gradual drop off will improve matters somewhat. Another needed major correction to the theoretical calculation is based on the recognition that the inverse reaction cross section, which is an important factor in the basic evaporation equation (see Eq. 12.16), should be calculated for the interaction of a charged particle and an <u>excited</u> nucleus. Several authors[139,139a] have discussed this point. In the work cited here, DOSTROVSKY, FRAENKEL and WINSBERG recalculated their results with an energy dependent Coulomb barrier of the form

---

139. I. Dostrovsky, Z. Fraenkel and L. Winsberg, submitted for publication Phys. Rev. (1960). See also Report UCRL-8963, Nov. 1959.

139a. C. B. Fulmer and B. L. Cohen, Phys. Rev. <u>112</u>, 1672 (1958).

Table 12.17 Comparison of experimental and calculated cross sections for the emission of neutrons, protons, deuterons, He^3 and He^4 upon the bombardment of Ni, Ag and Au with 190 Mev protons

Ni + 190 Mev protons			n mb/ster	p mb/ster	d mb/ster	t mb/ster	He^3 mb/ster	He^4 mb/ster
Experimental*		Forward		120	9.25	2.06	1.93	17.4
			109.5					
		Backward		69	4.43	0.98	0.92	9.65
Calculated	Prompt Cascade***		52.3	55				
Evaporation cascade calculated various parameter choices**	$r_o = 1.5$ F | $a = A/10$		65.9	90.5	6.57	0.70	0.92	5.75
	$r_o = 1.5$ F | $a = A/20$		51.6	76.5	11.2	1.72	2.16	10.0
	$r_o = 1.7$ F | $a = A/20$		45.7	80.6	11.5	1.87	2.62	13.95
	$r_o = 1.7$ F | $a = A/20$	(Corr)	36.1	81.8	12.85	1.93	3.95	26.0
Ag + 190 Mev protons								
Experimental*		Forward		128	13.7	4.53	1.76	23.2
			412					
		Backward		65.8	5.84	1.97	0.64	14.1
Calculated	Prompt Cascade***		75	67				
Calculated Evaporation cascade various parameter choices**	$r_o = 1.5$ F | $a = A/10$		394	49.05	8.69	1.52	0.28	9.07
	$r_o = 1.5$ F | $a = A/20$		321.5	46.2	17.6	6.18	1.18	17.67
	$r_o = 1.7$ F | $a = A/20$		320.8	42.05	18.0	5.62	0.997	20.25
	$r_o = 1.7$ F | $a = A/20$	(Corr)	255.7	53.4	22.5	6.87	3.02	58.35
Au + 190 Mev protons								
Experimental*		Forward		136				15.0
			1085					
		Backward		34				9.91
Calculated	Prompt Cascade***		131	80				
Calculated Evap. Cascade**	$r_o = 1.5$ F | $a = A/10$		980	12.31				2.40

Table 12.17 (cont'd.)

*Results of L. E. Bailey[136] and E. Gross[137] the experimental neutron cross sections do not include prompt-cascade neutrons, according to Gross.

**Calculations of Dostrovsky, Fraenkel and Winsberg.[139]

***The value given here is that of Metropolis et al.[124] divided by 2π, since it is assumed that the prompt neutrons go into the forward hemisphere. F refers to the Fermi unit, 10^{-13} cm. The letter, a, is a level density parameter.

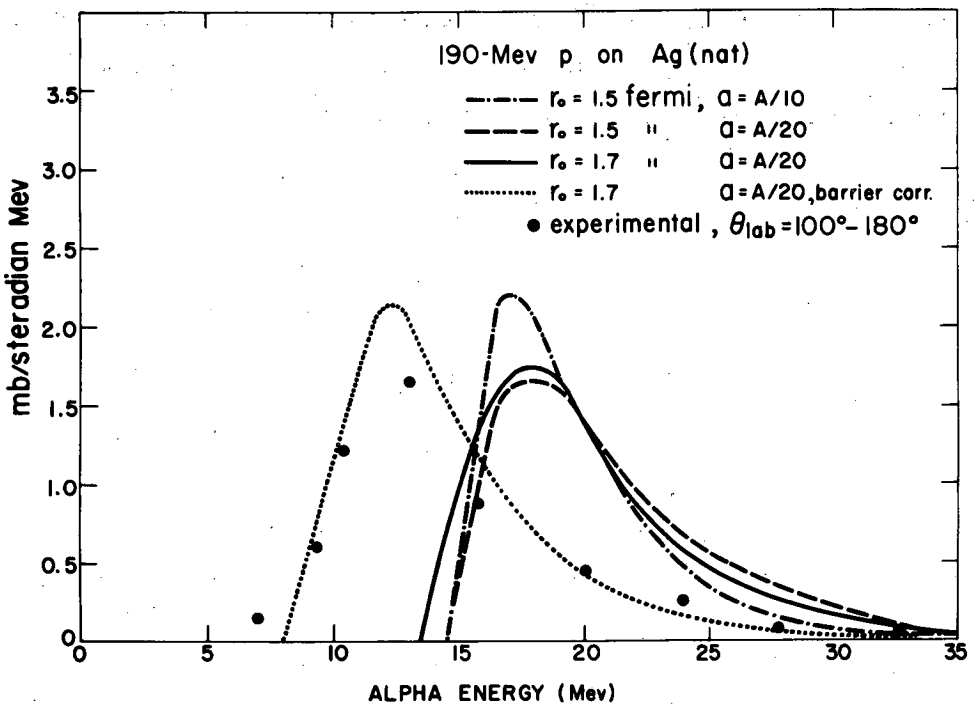

MU-18602

Fig. 12.52 Data of Bailey on the alpha particles emitted in the backward hemisphere (θ_{lab} = 100 to 180°) from silver targets bombarded with 196 Mev protons. Theoretical curves based on the evaporation calculations of Dostrovsky, Fraenkel and Winsberg. Figure from ref. 139.

$$V = kV_o \,/\, (1 + \sqrt{\frac{E_r}{2A}}\,) \qquad (12.24)$$

where V_o is the classical Coulomb barrier and E_r, the residual excitation energy. The recalculated spectrum of alpha particles, shown as a dotted line in Fig. 12.52 gives a much better fit with experiment. The parameters which give this better fit to the energy data, however, result in a poorer fit to the experimental cross section values as shown by the entries in Table 12.16 labeled $r_o = 1.7$ F $\underline{a} = A/20$ (corr.) The calculated emission of deuterons, tritons, He^3 and He^4 is too high while with this correction that of the neutrons is too low.

Such difficulties show that closer attention to many of the explicit and implicit assumptions of the evaporation treatment is required if satisfactory agreement is to be obtained with experimentally determined quantities. On the other hand the general agreement is good enough to indicate the basic correctness of the statistical evaporation theory approach.

12.2.4 Spallation-Fission Competition in the Evaporation Cascade. In high energy reactions fission contributes significantly to the observed cross section not only for the heaviest elements but also for many elements much lower down in the periodic chart, such as gold, tantalum, or silver. Some of the pertinent cross section data for these moderate weight elements is mentioned in Section 12.2.6 below. In view of these facts the evaporation calculations will be incomplete and misleading for heavy and moderately-heavy elements unless the possibility for fission competition is included. It is very difficult to do this properly because there is no clear theoretical guidance on the fission widths of excited nuclei or for the Γ_f/Γ_n ratio particularly for excitation energies ranging up to hundreds of Mev. In the earlier section 12.1.4 the competition of fission with neutron emission for excitation energies ranging up to several tens of Mev is discussed and it is shown there that certain conclusions on the qualitative and quantitative features of this competition can be deduced from experimental data. For excitation energies of hundreds of Mev the situation is much less clear.

Two rather different approaches to this problem were taken in the two studies to be discussed next.

DOSTROVSKY, FRAENKEL and RABINOWITZ[139b] used a semi-theoretical approach. They went back to the BOHR-WHEELER[140] paper to find an expression of the following form for the fission width:

$$\Gamma_f = \frac{1}{2\pi\,\omega(E)} \int^{E-E_f} \omega^*(E-E_f-\epsilon)\, d\epsilon \qquad (12.25)$$

where $\omega(E)$ = level density of excited nucleus before fission

$\omega^*(E)$ = level density of nucleus at saddle point

E_f = fission barrier, given by $E_s A^{2/3} f(x)$ where E_s is surface energy, A is mass number and f(x) is a function of $(Z^2/A)/(Z^2/A)$ crit.

The width for neutron emission was taken by these authors from WEISSKOPF.[126]

$$\Gamma_n = \hbar \int_0^{E_A-E_n} \sigma(E_A,\epsilon)\, \frac{g\,m}{\pi^2\hbar^3}\, \epsilon \exp\left(\left(S_B(E_A-E_n-\epsilon) - S_A(E_A)\right)\right) d\epsilon \qquad (12.26)$$

where E_A = excitation energy of initial nucleus A

E_n = neutron binding energy

$\sigma(E_A,\epsilon)$ = cross section for the reverse process

g = statistical weight for spin states

m = neutron mass

S_A = entropy of initial nucleus = $\log \omega_A(E)$

S_B = entropy of residual nucleus

ϵ = kinetic energy of neutron

DOSTROVSKY, FRAENKEL and RABINOWITZ[139b] integrated these two equations and after some simplification obtained an expression for the ratio Γ_f/Γ_n. They then included this expression in a Monte Carlo calculation of the nuclear de-excitation so that fission as well as the emission of neutrons, protons, tritons, etc. would be properly accounted for. The goal of the calculation was to get an overall fission cross section which could be compared with experimental values. For a proper comparison it was necessary to use as input data in the evaporation calculation some data on the distribution of excited nuclei resulting from the nucleonic cascade step. The authors were able to find a set of parameters which gave excellent agreement of the total fission cross section (or more exactly of the ratio of the total fission cross section to the total inelastic cross section) with experimental data for uranium bombarded with protons in the range 100-460

139b. I. Dostrovsky, Z. Fraenkel and P. Rabinowitz, "A Monte Carlo Calculation of Fission-Spallation Competition", Paper P/1515, Vol. 15, Proceedings of the Second U.N. Conference on the Peaceful Uses of Atomic Energy, Geneva, 1958.

Mev. Other details such as the ratio of alpha particles to protons or the number of charged particles associated with fission events also appeared to be satisfactorily predicted.

The original paper gives considerable data on the variation of Γ_f/Γ_n with excitation energy and on the variation of $\sigma_f/\sigma_{inelastic}$ with initial excitation for many heavy element nuclei. However, the theoretical underpinnings of these calculations are not firm and the detailed predictions of this model will have to be used with reservations until more detailed experimental confirmation is obtained.

Another attempt to learn something about the variation of the ratio Γ_f/Γ_n as a function of excitation energy was made by LINDNER and TURKEVICH.[140a] These authors examined the data published by LINDNER and OSBORNE[141] on the yields of neptunium, uranium, protactinium and thorium isotopes produced in the bombardment of uranium with 340 Mev protons and on the yields of protactinium, thorium, actinium and radium isotopes in the bombardment of thorium with 340 Mev protons. (See Figs. 12.67 and 12.69 in Section 12.2.9). In these two bombardment cases the yields of the spallation products are greatly lowered by fission competition. LINDNER and TURKEVICH[140a] assumed the validity of the two-step high-energy reaction mechanism outlined in this chapter and carried through a calculation of the theoretical yields of the same nuclides for which experimental values were published, using various assumptions on the nature of the fission competition during the evaporation steps. The theoretical calculation involved the following steps:

(1) Determination of the yield distribution of the nuclides produced by the high energy cascade for 340 Mev protons incident on uranium and thorium targets. This distribution was obtained by interpolation of the results for 236 Mev and 460 Mev protons in the published Monte Carlo calculations of METROPOLIS et al.[124]

---

140. N. Bohr and J. A. Wheeler, Phys. Rev. 56, 426 (1939).

140a. M. Lindner and A. Turkevich, "Competition Between Fission and Neutron Emission in Heavy Nuclei", to be published, 1960.

141. M. Lindner and R. N. Osborne, Phys. Rev. 103, 378 (1956).

(2) Determination of the excitation energy distribution for each of the nuclides produced in the high energy cascade. This distribution was also obtained by a suitable interpolation of the published Monte Carlo calculation of METROPOLIS et al.[124]

(3) Calculation of neutron evaporation from each product of the cascade step, averaged over the excitation energy distribution. This was done with the evaporation model of JACKSON[28] mentioned earlier (Section 12.1.3), with a very similar model given by HECKROTTE,[142] and by the very simple assumption that one neutron was evaporated for each 10 Mev of excitation. All three evaporation models gave similar results as far as the main conclusions of the analysis were concerned.

(4) Inclusion at each evaporation step of a fission competition expressed as the ratio Γ_f/Γ_n. Four different assumptions on the variation of Γ_f/Γ_n with excitation energy were tested. These were:

(a) That Γ_f/Γ_n is a function only of nuclear type and does not vary with energy for the excitation $\leq$ 100 Mev.

(b) That $\Gamma_f/\Gamma_n = 0$ for high excitation, for say $E^* > 20$ Mev, but $\Gamma_f/\Gamma_n \neq 0$ for $E^* < 20$ Mev. According to this assumption fission competes only in the last stages of neutron evaporation.

(c) That fission occurs to the exclusion of neutron emission above some specific energy taken arbitrarily to be 40 Mev, i.e. $\Gamma_f/\Gamma_n = \infty$ at $E > 40$ Mev but Γ_f/Γ_n is finite below $E < 40$ Mev.

(d) That the ratio Γ_f/Γ_n is some smoothly varying function of excitation energy. The treatment of DOSTROVSKY, FRAENKEL and RABINOWITZ[139b] mentioned just above was used to test this assumption.

The application of this 4-step procedure including the 4 sets of assumptions in step 4 led to sets of predicted cross sections for the spallation products which could be compared with the experimental data. It was found that a satisfactory agreement could be obtained with assumption 4a. LINDNER and TURKEVICH[140a] used Γ_f/Γ_n values based on the summary of VANDENBOSCH and HUIZENGA[39,46] reviewed in Section 12.1.4 (See especially Fig. 12.18). Much poorer agreement was obtained

---

142. W. Heckrotte, University of California Radiation Laboratory Report, UCRL-2184 (revised).

with assumptions 4 (b), (c) and (d). See Table 12.17. Therefore, for nuclides of elements in the region of uranium it is strongly indicated that Γ_f/Γ_n does not change significantly with excitation energy.[143]

Some idea of the agreement of theory and experiment can be gotten from Fig. 12.53 and Table 12.18. The worst disagreement occurs in the case of U^{237} which is the end-product of the (p,pn) reaction. For this nuclide the experimental yield is twice what it is predicted to be and this discrepancy cannot be patched up by invoking a reduced fission competition. It is a basic fault of the cascade model used by METROPOLIS et al.[124] that (p,pn) reaction cross sections are underestimated, probably because of nuclear edge effects.

12.2.5 Summary Comments on Serber Model of High Energy Reactions. The calculation of the characteristics of the fast nucleonic cascade and of the slower evaporation phase of high energy reactions has now been carried through with the aid of high speed electronic computors for a large number of representative cases. It has been possible to make many tests of this reaction model by comparison of calculated experimental quantities. It is beyond the scope of our treatment to go into these comparisons in any detail and we shall make only a few general comments about them.[144]

The model is remarkably successful in describing the light cascade particles, the evaporated particles and the spectrum of residual heavy nuclei for those cases in which the energy of the bombarding particle is less than about 400 Mev.

---

143. A similar conclusion was obtained by BATZEL (report UCRL-4303) and by VANDENBOSCH and HUIZENGA[139] in earlier and somewhat cruder analyses of the same problem. On the other hand, V. P. Shamov [Doklady Acad. Nauk SSSR 103, 543 (1955)] also analyzed the data of LINDNER and OSBORNE and came to the conclusion that assumption 4(b) best fit the data. SHAMOV'S analysis was published before the Monte-Carlo cascade calculations of METROPOLIS et al.[124] His conclusions are based on the assumption that excited U^{237} and Pa^{237} nuclei were the sole precursors of the observed uranium and protactinium isotopes, respectively, and that the excitation distributions for U^{237} and Pa^{237} decreased linearly with excitation energy.

144. A review of high energy nuclear reactions is presented by J. M. Miller and J. Hudis in Vol. 9, pp. 159-202, Ann. Rev. Nuclear Sci. (1959).

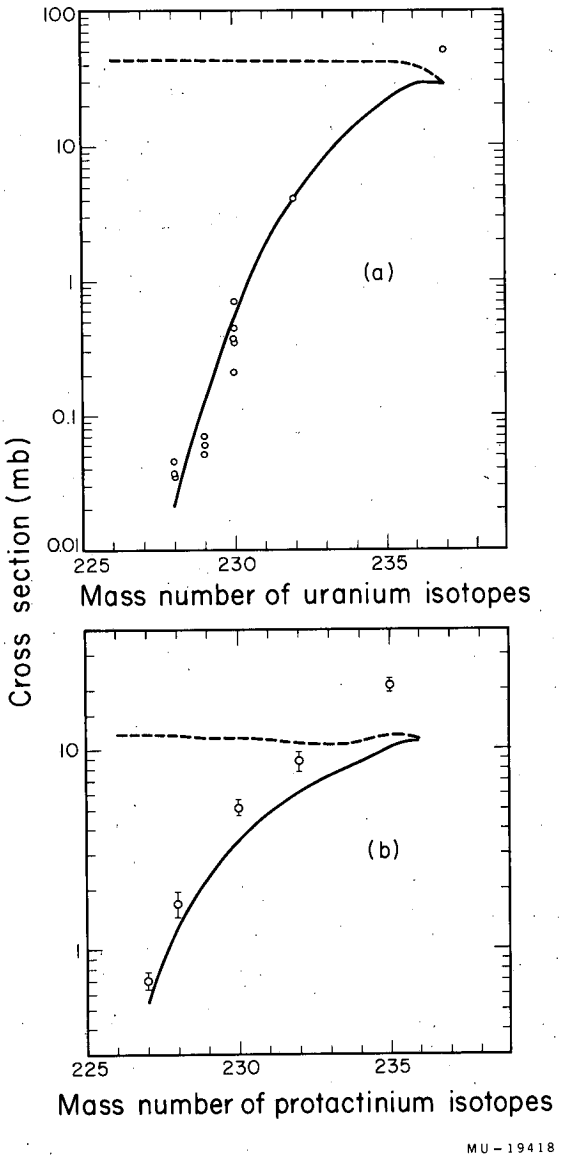

Fig. 12.53 Comparison of the spallation yield data of LINDNER and OSBORNE[141] with the calculations of LINDNER and TURKEVICH[140] for products of the bombardment of uranium with 340 Mev protons. Dotted lines show calculated yields assuming no fission competition. Solid lines show calculated yields assuming fission competition. x's are experimental points. Part (a) refers to uranium isotope end-products. Part (b) refers to protactinium isotope end-products.

Table 12.18 Final Cross-Sections (in mb) of Uranium Isotopes Produced by the Bombardment of U^{238} with 340 Mev Protons

Assumption used to evaluate Γ_f/Γ_n	Mass number of uranium										
	238	237	236	235	234	233	232	231	230	229	228
4 (a)	3.3	26.7	29	22	14.4	8.3	4.1	1.7	0.53	0.13	0.025
4 (b)	3.3	27	30	22	17	14	10.5	7.9	5.4	3.4	1.8
4 (c)	3.3	26.6	28	20	10	2.2	0.3	0.03	--	--	--
4 (d)							29				4.4
Experimental		~50					3		0.35	0.06	0.038

The agreement of theory and experiment is far from perfect, but with due allowance for the many approximations which had to be introduced to make the calculations possible there do not appear to be many serious discrepancies between prediction and measurement which cast doubt on the fundamental correctness of the reaction model. Some of the discrepancies do show the direction in which the simplifying assumptions and approximations need to be altered to make the calculations more realistic. For example, several authors[140,145,146] have noticed that experimental cross sections for such simple reactions as the (p,pn) and (p,2p) reaction types are two or three times higher than predicted by the Monte Carlo calculations of METROPOLIS.[124] This can be interpreted to mean that the square well nuclear potential assumed for the calculations should be replaced by some nuclear potential which drops off gradually at the nuclear edge.

As far as fission is concerned, it is probably correctly treated as a competition with particle emission in the evaporation stage. Present uncertainties on the variation of this competition with nuclear competition and particularly with nuclear excitation make it difficult to make a meaningful calculation for comparison with experimental results.

When the energy of the bombarding particle is raised above the threshold values of meson processes it is also difficult to make a meaningful calculation for comparison with experiment. In the METROPOLIS[124] calculations the input data for meson production cross sections, angular distribution, multiplicity, etc. were very rough and incomplete. Future calculations with more refined input data will be very helpful.

Radiochemical yield studies on the residual nuclei found in targets of copper[147], tantalum[148], lead[149], bismuth[150,151], and uranium[152,153], bombarded

145. A. A. Caretto and G. Friedlander, Phys. Rev. 110, 1169 (1958).

146. S. S. Markowitz, F. S. Rowland and G. Friedlander, Phys. Rev. 112, 1295 (1958).

147. D. W. Barr, Univ. of Calif. Radiation Laboratory Report, UCRL-3793, unpub.

148. J. R. Grover, Univ. of Calif. Rad. Lab. Report, UCRL-3932 (1957) unpub.

149. R. Wolfgang, et al., Phys. Rev. 103, 394 (1956).

150. P. Kruger and N. Sugarman, Phys. Rev. 99, 1459 (1955).

151. N. T. Porile and N. Sugarman, Phys. Rev. 107, 1422 (1957).

152. R. W. Shudde, Univ. of Calif. Rad. Lab. Report, UCRL-3419 (1956) unpub.

153. C. L. Carnahan, Univ. of Calif. Rad. Lab. Report, UCRL-8020 (1957) unpub.

with protons of greater than one Bev energy indicate that the reaction model as outlined above is not adequate to describe the results. This fact has given rise to speculation concerning "fragmentation" process to be considered as an alternative to fission or evaporation processes of nuclear de-excitation. "Fragmentation" refers to some process which leads to the breakup of the nucleus into two or more complex aggregations of nucleons. It occurs only when nuclear excitation is of the order of hundreds of Mev. An explicit but tentative formulation of the fragmentation process for lead targets has been given by WOLFGANG and co-workers[149] who interpret it as being intimately associated with the production and reabsorption of mesons in complex nuclei. Their hypothesis is outlined as follows.

The π mesons created in nucleon-nucleon collisions have been shown[154] to have energy spectra which are quite sharply peaked at low energies (at ~100 Mev in the center-of-mass system) and which shift only slightly with incident nucleon energy in the range of 1 to 3 Bev. Thus most of the pions produced inside a nucleus by incident protons in the Bev range have energies in the region of the large resonance peak[155] in the pion-nucleon cross section and therefore have short mean free paths in nuclear matter. For example, for a π^+ meson of 200 Mev kinetic energy (near the peak of the resonance) the mean free path in a lead nucleus is about one-tenth the nuclear radius. The probability that a pion produced inside a heavy nucleus escapes without additional scattering collisions is thus negligibly small and in most cases there will be several pion-nucleon scatterings. Because of the rather low kinetic energies of the pions the energy transfer in any such scattering collisions will be small (generally < 50 Mev) so that the struck nucleons will usually not escape but contribute to nuclear excitation.

In addition to the large scattering cross section, pions in nuclear matter will also have appreciable cross sections for absorption by pairs of nucleons and for this process too there appears to be a resonance at a pion energy of ~140 Mev. There is then a reasonable probability that the total energy of a pion created inside a complex nucleus (including its rest energy) is converted

---

154. L. C. L. Yuan and S. J. Lindenbaum, Phys. Rev. 93, 1431 (1954).

155. S. J. Lindenbaum and L. C. L. Yuan, Phys. Rev. 100, 306 (1955).

into nuclear excitation. These energy deposition mechanisms, particularly meson reabsorption, presumably lead to concentration of large amounts of energy in relatively small zones of the nucleus. Under such conditions it seems plausible that fragments of nuclear matter could be emitted before anything like equipartition of energy can be established. "Fragmentation" of this sort would take place in a large variety of modes according to the spatial and momentum distribution of the nucleons participating in the energy-deposition cascade. The rather broad spectrum of fragment sizes (with some favoring of small fragments) which would be expected from such a fast fragmentation mechanism is consistent with the observed yield pattern at Bev bombarding energies, particularly for heavy element targets.

One might think of fragmentation as proceeding by knock-on cascades which break numbers of neighboring nucleon-nucleon bonds and thus produce considerable local disturbances in the nucleus. Surface tension and Coulomb repulsion forces, as well as momentum imparted by the knock-on cascade would tend to separate clumps of still-cohering nucleons from each other. These are the progenitors of the final products.

The essential characteristic distinguishing the suggested fragmentation mechanism from the more familiar fission process is that it is fast compared to the life of a compound nucleus. The neutron-proton ratios in the initial fragments must then be essentially the same in the excited nucleus before breakup. These fragments are in general highly excited and may therefore evaporate a sizable number of nucleons after fragmentation.

This formulation of a fragmentation hypothesis is a tentative one and it may have to be seriously modified or rejected as more experimental data and better nuclear models become available. In this chapter we are concerned mostly with high energy fission phenomena, but it is necessary to make at least this brief mention of fragmentation because in high energy reactions it is difficult to distinguish the radioactive products of fission from the products of fragmentation events. PORILE and SUGARMAN[156] for example, conclude from their radiochemical studies of the high energy interaction of protons with bismuth that many of the products which would seem on first analysis to be fission products are in reality products of a fragmentation process.

156. N. T. Porile and N. Sugarman, Phys. Rev. 107, 1422 (1957).

We conclude our remarks on the Serber high energy reaction model by pointing out that detailed calculations of the model have so far been limited to simple particles like protons. It would be quite interesting to extend the calculations to cover reactions induced by helium ions and other particles. Also a number of possible interactions of the incoming particle with the nucleus which can be grouped together under the general terms pickup and stripping processes are not considered. It has been found[157-159] that high energy deuterons, tritons and helium ions are ejected in appreciable yields when complex nuclei are bombarded with 300 to 400 Mev protons in addition to the low energy isotropically-emitted evaporated particles. The observed angular distributions of these high energy particles suggest that they are produced during the cascade step of the reaction but no adequate theory of such events has been developed. LINDNER and TURKEVICH[140a] also call attention to the fact that the yields of products of the reactions written formally as (p,3pxn) are considerably higher than predicted by the cascade-evaporation model. It may be that such products are actually produced by reactions of the (p,αpxn) type in which the alpha-particle is knocked out of the nucleus during the cascade step.

WILLOUGHBY[160] examined the characteristics of stars and prongs in nuclear track emulsions bombarded with 380 Mev helium ions and found that stripping or splitting of the incident alpha particle changes the cascade particle distributions greatly from those obtained in bombardments with protons.

12.2.6 Fission Cross Sections at High Energy.‡ STEINER and JUNGERMAN[161] have measured the proton-induced fission cross sections for U^{238}, U^{235}, Th^{232}, Bi^{209} and Au^{197} in the energy range 100 to 340. A cancellation-type ionization chamber was used to detect the fission fragments above a background of ionization caused by the proton beam. A sampling of the results is given in Table 12.19.

157. J. Hadley and H. F. York, Phys. Rev. 80, 345 (1950).

158. R. W. Deutsch, Phys. Rev. 97, 1110 (1955).

159. E. Bailey, Univ. of Calif. Rad. Lab. Report, UCRL-3334 (1956).

160. D. S. Willoughby, Phys. Rev. 101, 324 (1956).

161. H. M. Steiner and J. A. Jungerman, Phys. Rev. 101, 810 (1956); see also H. M. Steiner, Thesis, Univ. of Calif. Report, UCRL-3258 (1956).

‡Fission cross sections at moderate excitation energy are covered in Section 12.1.2.

Table 12.19 Measurements of STEINER and of STEINER and JUNGERMAN[161] on fission cross sections of heavy elements. Energy range 100-400 Mev. Method - Cancellation type ionization chamber.

Bombarding particle	Energy (Mev)	Fission cross section in barns				
		U^{238}	U^{235}	Th^{232}	Bi^{209}	Au^{197}
Protons	114	1.37	1.68	0.89	--	--
	158	1.47	1.36	0.90	0.146	0.016
	216	1.31	1.28	0.82	0.173	0.038
	261	1.34	1.36	0.81	0.191	0.038
	336	1.35	1.30	0.82	0.198	0.051
Deuterons	88	1.84	1.90	1.23	0.096	0.010
	100	2.05	2.00	1.32	0.143	--
	159	1.98	1.90	1.22	0.198	0.037
	190	1.98	1.94	1.28	0.245	0.055
Helium ions	212	2.40	2.2	1.9	0.69	0.24
	252	2.4	2.5	1.7	0.76	0.24
	300	2.2	2.1	1.5	0.60	0.20
	380	2.2	2.2	1.6	0.62	0.19

These results supercede earlier results by JUNGERMAN[162] which were somewhat lower. Figures 12.54 and 12.55 show the ratio of the fission cross section to the total inelastic cross section. A glance at these data shows that the fission cross section for uranium isotopes is large and remains large over the entire range of energies studied. It can be expected that elements of higher atomic number will have an even higher percentage of the total reaction cross section going into fission. In the case of thorium, about half the inelastic cross section goes into fission and this percentage does not change over the range 100 to 400 Mev. Bismuth shows a marked change in fissionability as a function of energy. For excitation energies of a few tens of Mev the fission cross section is only of the order of microbarns.[163] (See Table 12.1 in Section 12.1.2). In the energy range 100 to 400 Mev fissionability rises steeply until the fission reaction takes about 13 percent of the total reaction cross section. This figure probably represents the maximum percent fissionability which bismuth ever achieves. PORILE and SUGARMAN[164] estimate that the bismuth fission probability reaches a peak of 0.17 for a deposition energy of 230 Mev. This sharp rise in fissionability at high energies makes it possible to use bismuth fission chambers as a convenient monitor for fluxes of high energy neutrons or protons.[165,166]

KELLEY and WIEGAND[166] used an ionization chamber technique to measure the fissionability of several elements relative to thorium for neutrons ranging in energy up to 84 Mev. At 84 Mev the fission yields relative to the standard element were: Bismuth(0.019), lead (0.0055), thallium (0.0032), mercury (0.0023), gold (0.0020) and platinum (0.0009). GOLDANSKII, PENKINA and TARUMOV[167] measured the fission cross section of several elements bombarded with high energy neutrons. Fission fragments emerging from thin foils of the fissionable material were counted in an ionization chamber. Results are summarized in Table 12.20.

---

162. J. Jungerman, Phys. Rev. 79, 632 (1950).

163. A. W. Fairhall, Phys. Rev. 102, 1335 (1956).

164. N. T. Porile and N. Sugarman, Phys. Rev. 107, 1422 (1957).

165. W. N. Hess, H. W. Patterson, R. Wallace, Proc. Health Phys. Soc. 1, 133-140 (1956).

166. E. L. Kelley and C. Wigand, Phys. Rev. 73, 1135 (1948).

167. V. I. Goldanskii, V. S. Penkina and E. Z. Tarumov, J.E.T.P. USSR 29, 778 (1955); Soviet Physics J.E.T.P. 2, 677 (1956).

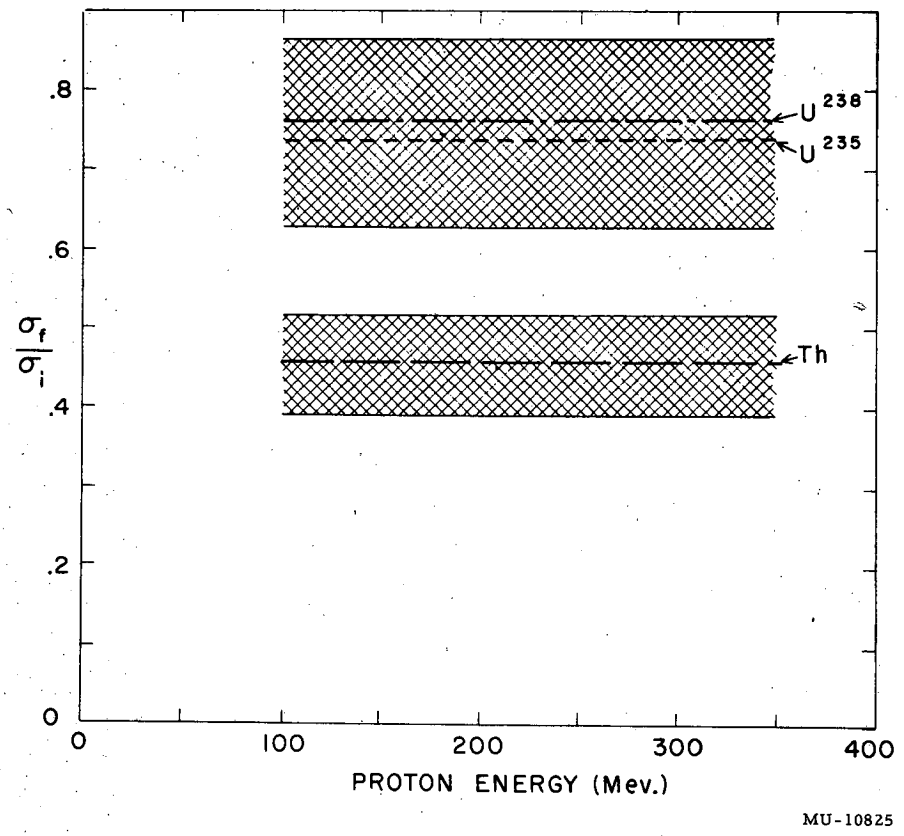

Fig. 12.54 Ratio of the fission cross section, σ_f, of U^{238}, U^{235} and Th^{232} to the total inelastic cross section σ_i of natural uranium. The total inelastic cross sections were obtained from the data of MILLBURN, BIRNBAUM, CRANDALL and SCHECTER, Phys. Rev. 95, 1268 (1954). The cross-hatched area indicates the limits of error.

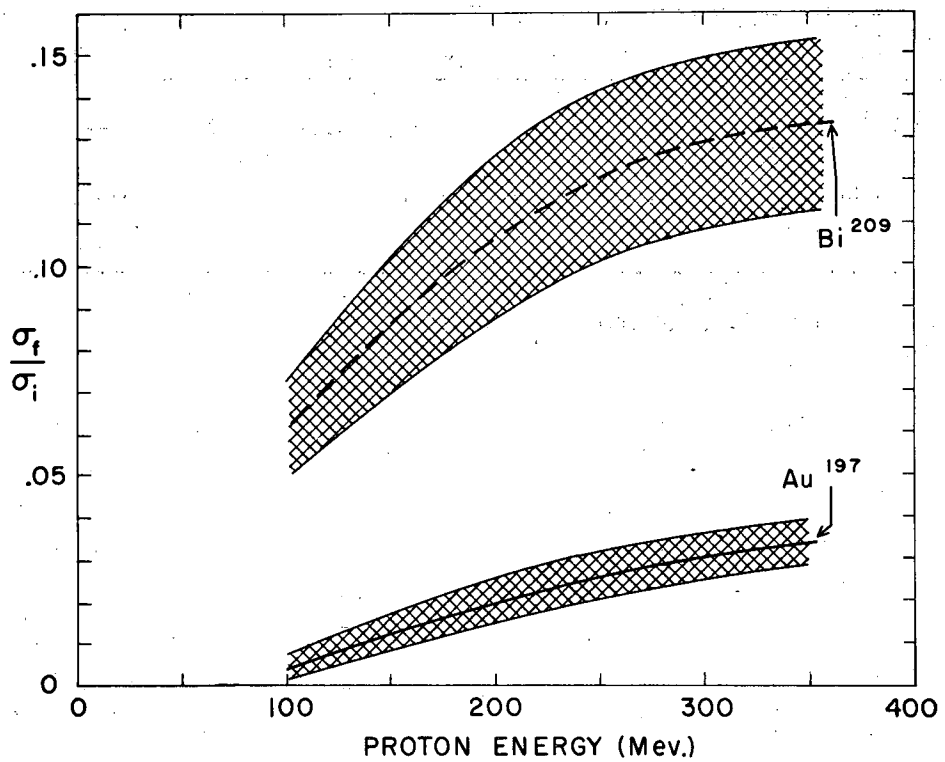

MU-10826

Fig. 12.55 Ratio of the fission cross sections, σ_f, of Bi^{209} and Au^{197} to the total inelastic cross section of lead, σ_i. The total inelastic cross sections were obtained from the data of MILLBURN, BIRNBAUM, CRANDALL and SCHECTER, Phys. Rev. 95, 1268 (1954). The cross hatched area indicates the limits of error.

Table 12.20 Cross sections for fission with high energy neutrons

Neutron energy (Mev)	σ_f(barns)									
	U^{235}	U^{238}	Th	Bi	Pb	Tl	Au	Pt	Re	W
120	1.5	1.14	1	.036	.020	0.01	01	--	.0017	.0011
380	1.24	1.03	0.9	.074	.033	0.019	020	012	--	.0038

Data from Goldanskii, Penkina and Tarumov.[167]

IVANOVA[168,169] measured fission cross sections by exposing nuclear emulsions loaded with uranium to protons with energies of from 140 Mev to 660 Mev with the results shown in Table 12.21. PERFILOV[170] reports measurements on uranium, bismuth and tungsten using the loaded emulsion technique. These are listed in Table 12.24 below.

Fission cross sections have been measured radiochemically by summation of the mass yield curve for targets bombarded at high energies. Some of these values are collected in Table 12.22. This table makes it apparent that there is a strong atomic number effect on fissionability even at high energies. Figure 12.56 shows the total fission cross section of uranium as a function of proton energy.

---

168. N. S. Ivanova, J.E.T.P. USSR 31, 413-415 (1956); Soviet Physics J.E.T.P. 4, 365 (1957). See also Proc. Acad. Sciences USSR 103, 573, 593 (1955).

169. N. S. Ivanova in Physics of Fission, an English translation of a Conference of this title published as Supplement I to the Soviet Journal of Atomic Energy, Moscow, 1957. English translation by Consultants Bureau, Inc., N. Y.

170. N. A. Perfilov in Physics of Fission (see Ref. 169).

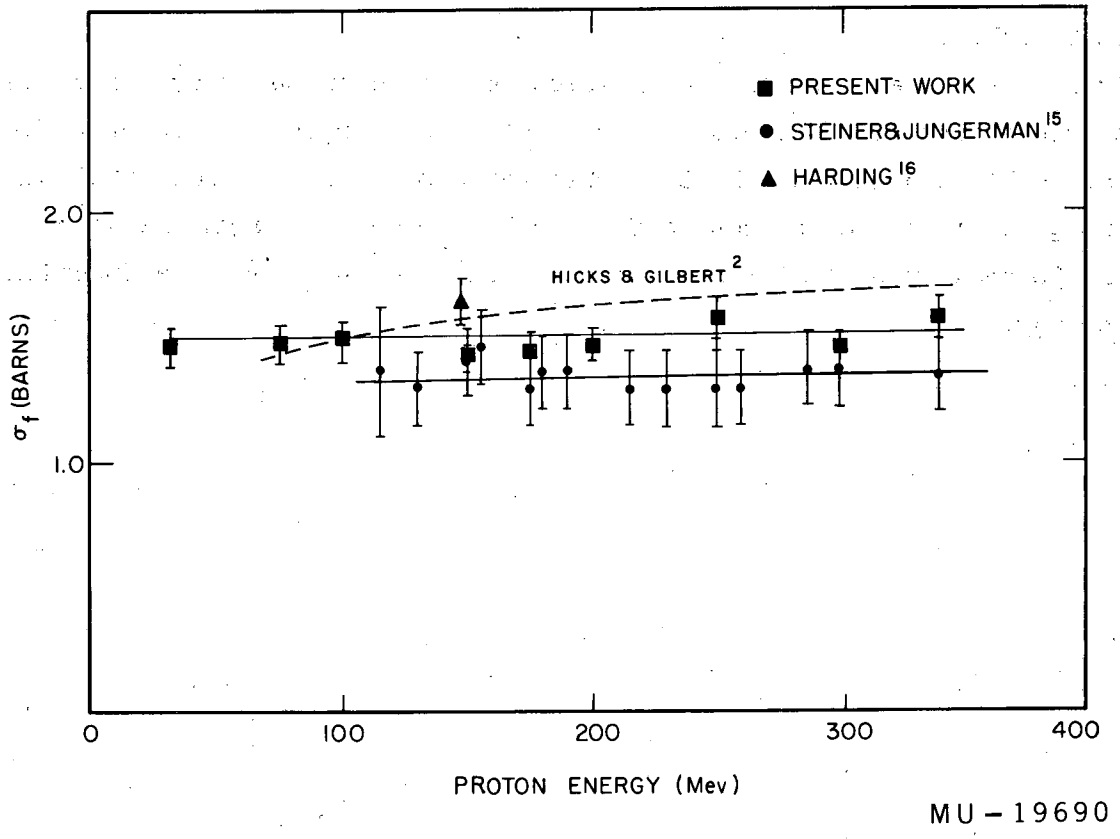

Fig. 12.56 Fission cross section of U^{238} bombarded with protons of various energies. The rectangles refer to the radiochemical data of Stevenson, Hicks, Nervik and Nethaway.

Table 12.21 IVANOVA'S measurements of uranium fission cross section by the emulsion technique

Energy of protons	$\sigma_{fission}$	Probability of fission‡
140	1.56	0.77
350	1.4	0.86
460	1.2	0.74
660	1.1	0.65
	0.97	
	1.01	

‡Ratio of $\sigma_{fission}$ to a calculated σ_{total}.

Table 12.22 Cross sections for fission determined by summation of mass yield curve

Target	Projectile	Energy (Mev)	Fission cross section (barns)	Mass number at peak of symmetrical mass yield curve	Assumed "fissioning" nucleus*	Target reaction*	Reference
Natural uranium	p	340	~2.0	114			1
"	α	380	~2.0				2
"	p	170	1.9				14
"	p	480	~geometrical				3
"	p	480	1.65				11
U^{238}	p	170	1.6	115			4
"	p	70	1.47				
"	p	100	1.49				
"	p	150	1.44				
"	p	200	1.47				12
"	p	250	1.58				
"	p	300	1.46				
"	p	340	1.59				
"	d	50	1.61				
"	d	75	2.13				
"	d	100	2.42				
"	d	125	2.45				12
"	d	150	2.39				
"	d	170	2.48				
"	d	190	2.49				
Th^{232}	p	450	0.67	103.5	$_{87}Fr^{207}$	p,4p 22n	5
Th^{232}	p	480	1.6				11
Th^{232}	p	480	~1.5				3
Bi	d	190	0.2		$_{84}Po^{199}$	d,12n	6
Bi	p	340	0.24			p,2p 18n	7
Bi	p	480	0.070	96	$_{80}Hg^{192}$	p,4p 16n	3
Bi	p	480	0.1		$_{82}Pb^{193}$	p,2p 15n	11
Bi	p	184	0.11	97	$_{82}Pb^{194}$	p,2p 14n	8

Table 12.22 (cont'd.)

Target	Projectile	Energy (Mev)	Fission cross section (barns)	Mass number at peak of symmetrical mass yield curve	Assumed "fissioning" nucleus*	Target reaction*	Reference
Bi	p	242	0.15	96.5	$_{82}Pb^{193}$	p,2p 15n	8
Bi	p	303	0.16	95.5	$_{81}Tl^{191}$	p,3p 16n	8
Bi	p	427	0.19	93	$_{80}Hg^{186}$	p,4p 20n	8
Bi	p	450	0.21	93	$_{80}Hg^{186}$	p,4p 20n	5
Au	p	450	0.061	87.5	$_{76}Os^{175}$	p,4p 19n	5
Re	p	450	0.019	83	$_{72}Hf^{166}$	p,4p 17n	5
W	d	280	~0.001				15
Ta	p	340	0.004	83	$_{71}Lu^{166}$, $_{72}Hf^{166}$	p,2p 14n	9
Ta	p	450	~0.005	80.5	$_{70}Yb^{161}$	p,4p 17n	5
Ho	p	450	~0.002	72	$_{64}Gd^{144}$	p,4p 18n	5
La	p	660	0.0006				13
Ag	p	340	10^{-4}-10^{-5}				10

*Based on assumption of prefission emission of neutrons. The fissioning nucleus is to be regarded as the most probable of a group of fissioning nuclei clustering around the one named. The target reaction is also be regarded as only a rough approximation since undoubtedly the radiochemical results are an average of many reactions.

1. Folger, Stevenson and Seaborg, Phys. Rev. 98, 107 (1955).

2. O'Connor and Seaborg, Phys. Rev. 74, 1189 (1948).

3. Vinogradov and co-workers, "Radiochemical Study of the Fission Products of Bismuth, Thorium and Uranium Upon Bombardment with 480 Mev Protons", Chemical Session of Conference of the Academy of Sciences of the USSR on the Peaceful Uses of Atomic Energy, July 1-5, 1955. English translation available from Superintendent of Documents, U.S. Government Printing Office.

4. Hicks and Gilbert, Phys. Rev. 100, 1286 (1955).

5. Kruger and Sugarman, Phys. Rev. 99, 1459 (1955).

6. Goeckermann and Perlman, Phys. Rev. 76, 628 (1949).

7. Biller, University of California Radiation Laboratory Report, UCRL-2067, January, 1953.

8. Jodra and Sugarman, Phys. Rev. 99, 1470 (1955).

9. Nervik and Seaborg, Phys. Rev. 97, 1092 (1955).

10. Kofstad, University of California Radiation Laboratory Report, UCRL-2265 (1953).

Table 12.22 (cont'd.)

11. A. K. Lavrukhina and L. D. Krasavina, J. Nuclear Energy 5, 236 (1957).

12. Stevenson, Hicks, Nervik and Nethaway, Phys. Rev. 111, 886 (1958).

13. Lavrukhina, Krasavina, Pozdnyaikov, Doklady Akad. Nauk. SSSR 119, 56 (1958).

14. A. Kjelberg and A. C. Pappas, Nuclear Phys. 1, 322 (1956).

15. Kurchatov et al., Division of Chemical Sciences in Proceedings of a symposium of the Academy of Sciences of the USSR on the Peaceful Uses of Atomic Energy, July 1-5, 1955, Moscow.

12.2.7 Photo Emulsion Studies of High Energy Fission. Photo emulsion techniques have many advantages for the study of many features of high energy fission. Russian scientists have contributed a great deal to the exploitation of this method and in particular the group associated with Professor N. A. Perfilov at the Radium Institute in Leningrad has pioneered many novel experimental techniques in this type of fission research.

A series of studies were carried out in which special emulsions impregnated with uranium, bismuth, and tungsten salts were exposed to protons having energies ranging up to 660 Mev. In some cases "relativistic" emulsions were used which were sensitive not only to fission fragments and low energy protons but also to high energy protons. Hence these emulsions give rather complete pictures of the individual fission events in contrast to the radiochemical method which can provide only average results. In other experiments P-9 type, thin-emulsion films were used which were not sensitive to protons of energy greater than 25 Mev. These emulsions can be exposed to greater beam currents than the "relativistic" emulsions.

In addition to cross section measurements the emulsion studies yield many results which confirm the basic correctness of the nuclear cascade model described above. The type of information which is obtained is the following:

1. The length of the fission fragment tracks; the ratio (asymmetry) of the ranges of the two fragments.
2. The deviation from 180° of the angle of the two fission fragments with respect to each other, from which the momentum of the fissioning nucleus can be deduced.
3. The anisotropy of the fission fragments with respect to the direction of the proton beam.
4. The number, energy, and angular distribution of high-energy charged particles (i.e. the knock-on particles) accompanying the fission event.
5. The number, energy and angular distribution of the low-energy charged particles, designated as evaporated protons and alpha particles.

The cascade particles were distinguished by their high energy and their pronounced forward peaking. The number of charged cascade particles (the great majority of them protons) which accompanied the fission events averaged one or two, but in some cases as many as seven or eight were observed. The average

number of such particles increased slowly with the energy of the bombarding particles. See Table 12.23. These observations are in good agreement with the Monte Carlo calculations of the nuclear cascade.

IVANOVA[169,171] compared the distribution of fission cases as a function of the number of charged cascade particles emitted by the fissioning uranium nucleus. He also examined the angular distribution of the cascade particles. Both distributions were in good agreement with some theoretical calculations by PYANOV.

In the emulsion method there are two ways of estimating the excitation energy deposited in the nucleus before fission. OSTRUOMOV[172] made the important observation that the fission fragments were often not directed in precisely opposite direction, but at an angle somewhat less than 180°, the vertex of which is generally directed toward the incident beam of protons. This is the result of the transfer of momentum to the target nucleus from the incoming proton. It can be concluded from this that the life of the excited nucleus before fission is less than the time it takes for the nucleus to be slowed down, i.e. $< 10^{-13}$ seconds. It is also possible to calculate the momentum and energy of the fissioning nucleus in the direction of the beam. To do this, one needs to know the angle between the fragments, the ranges of the fragments and the relationship between fragment velocity and range. Then with some plausible assumptions about the cascade process and straight-forward application of the laws of conservation of energy and momentum, the excitation energy of the fissioning nucleus can be found. It was later found that a relationship existed between the number of evaporated charged particles accompanying fission and the average value of the angle between the fragments. From this relationship it is possible to estimate the mean excitation energy of the fissioning nucleus also simply by counting the number of light charged particles accompanying fission.

PERFILOV and co-workers[170,173] used these techniques to gather the data presented in Tables 12.24 and 12.25. It is seen that the cross section for fission

---

171. N. S. Ivanova and I. I. Pyanov, J. Exp. Theor. Phys. 31, 416 (1956); english translation in Soviet Physics JETP 4, 367 (1957).

172. V. I. Ostroumov, Proc. Acad. Sci. USSR 103, 409 (1955).

173. Perfilov, Ivanova, Lozhkin, Ostroumov and Shamov, Proceedings of the Conference of the Academy of Sciences of the USSR on the Peaceful Uses of Atomic Energy, Moscow, July 1-5, 1955, english translation available from Superintendent of Documents, U. S. Government Printing Office, Washington.

Table 12.23 Average number of charged particles observed per fission event‡
(Studies of uranium-loaded emulsions)

Energy of primary protons (Mev)	Relativistic emulsion		P-9 emulsion		
	N^1_{Av}	$N(0^o)/N(180^o)$	N^2_{Av} E<25-30 Mev	$N(0^o)/N(180^o)$ E<25-30 Mev	$N_{p\text{-evap.}}$
140	0.4	4	0.25	2.6	0.14
350			0.56	1.6	0.43
460	1.65	3.3	0.86	1.3	0.66
660	3.06	3.1	1.05	1.3	0.81

‡Data quoted by N. S. Ivanova, Symposium on Physics of Fission, Supplement No. 1 to the Sovet Journal of Atomic Energy, Moscow, 1957.

N^1_{Av} average number of charged particles of all energies accompanying fission (chiefly cascade protons)

$N(0^o)/N(180^o)$ ratio of particles emitted in forward and backward hemispheres

N^2_{Av} average number of charged particles of energies less than 25-30 Mev accompanying fission

$N_{p\text{-evap}}$ number of charged particles showing isotropic distribution and presumed to be evaporated protons.

Table 12.24 Characteristics of high energy fission of uranium, bismuth, and tungsten deduced from emulsion studies by Perfilov and co-workers[170,173]

Element	$\bar{E}_f^*$		n_p-cascade		N_p-evap.		σ_f	
	E_p=460	E_p=660	E_p=460	E_p=660	E_p=460	E_p=660	460	660
Uranium	130	150	1.2-1.3	2.2-2.3	0.6-0.7	0.8-0.9	0.9±0.2	1.1±0.2
Bismuth	190	230			0.8	1.2-1.3	0.09±0.3	0.12±0.03
Tungsten	340	440			1.6	2.9-3.0	0.004±0.002	0.11±.003

$\bar{E}_f^*$ = mean excitation energy of the nuclei undergoing fission

E_p = energy of bombarding protons

n_p = cascade average number of charged particles ejected in cascade

n_p - evap. average number of charged particles evaporated

σ_f = fission cross section

Table 12.25 Excitation energy of nucleus undergoing fission as a function of number of low-energy charged particles

	Uranium			Bismuth			Tungsten		
$n_{\alpha p}$	E_p=460 %	E_p=660 %	$\bar{E}_f$, Mev	E_p=460 %	E_p=660 %	$\bar{E}_f$, Mev	E_p=460 %	E_p=660 %	$\bar{E}_f$, Mev
0	57.5	46.5	75	32	25.6	135	15	10.4	270
1	22.5	22.8	140	35.6	28.6	185	25	11.1	295
2	11	12.7	245	20.4	18.5	250	25	10.4	345
3	6.3	9.6	325	8.4	12.9	315	15	11.8	390
4	2.1	5.25	410	3.4	7.65	385	15	12.6	430
5		1.9	600		4	455	5	11.8	485
6		1	560		2.46	520		11.8	520
7		0.3			0.67	590		10.4	565
8		0.1			0.22			5.9	

E_p - energy of the bombarding particles (Mev)

$n_{\alpha p}$ - number of charged particles associated with one fission ($E_p \leqslant$ 30-35 Mev)

E_f - initial excitation energy of nucleus undergoing fission

% - the percentage of the cases of fission in which there is the given number of charged particles ($n_{\alpha p}$)

This table reproduced from reference 173.

drops rapidly as the atomic number of the fissioning nucleus decreases. Correspondingly, the excitation energy of the fissioning nuclei increases sharply even though the energy of the incoming protons is kept constant. In the case of uranium, there is probably not much difference in the distribution of excitation energy for all interacting nuclei whether these ultimately fission or not; in the case of bismuth and rhenium, the excitation energies of those nuclei which fission is considerably higher than that of those which de-excite in other ways.

An anisotropy of the fission fragment distribution with respect to the proton beam was first detected with the emulsion method by OSTROUMOV.[173] Some results of this type are quoted in Section 12.1.6 (see Tables 12.12 and 12.13). A distinct preference was found for emission of fragments in a direction perpendicular to the proton beam. This was the reverse of the anisotropy observed at lower proton energies and was a quite unexpected result.

Some interesting results have been obtained by measuring the ranges of the two fission fragments. The most probable range of the fragments decreases with increasing bombardment energy. This is a reflection of the fact that more particles are lost by the knock-on cascade or in particle evaporation at the higher energies. This corroborates other evidence that excitation energy does not get converted into fragment energy but that the latter is derived chiefly from the Coulombic repulsion of the fragments themselves. When the mass-splitting is symmetrical, the ranges are equal; conversely, a difference in the two ranges can be used as a measure of asymmetry in the mass division. It is possible to measure the distribution in the ratios as a function of the excitation energy of the fissioning nucleus; the latter can be determined by counting the number of evaporated protons or measuring the angle between the fragments. As the excitation energy of the fissioning uranium nucleus increases from 0 to 75 Mev, there is, as expected, an increase in the number of fission events having equal fragment ranges. At higher excitation energies, however, the number of asymmetric fragment ranges increases again. This effect is illustrated in Fig. 12.57.

The region of uranium excitation energy in which fission is most symmetric is estimated to be 60-100 Mev.

In the case of bismuth symmetric fission is favored at the lowest energies studied but the percentage of asymmetric fissions increases with excitation

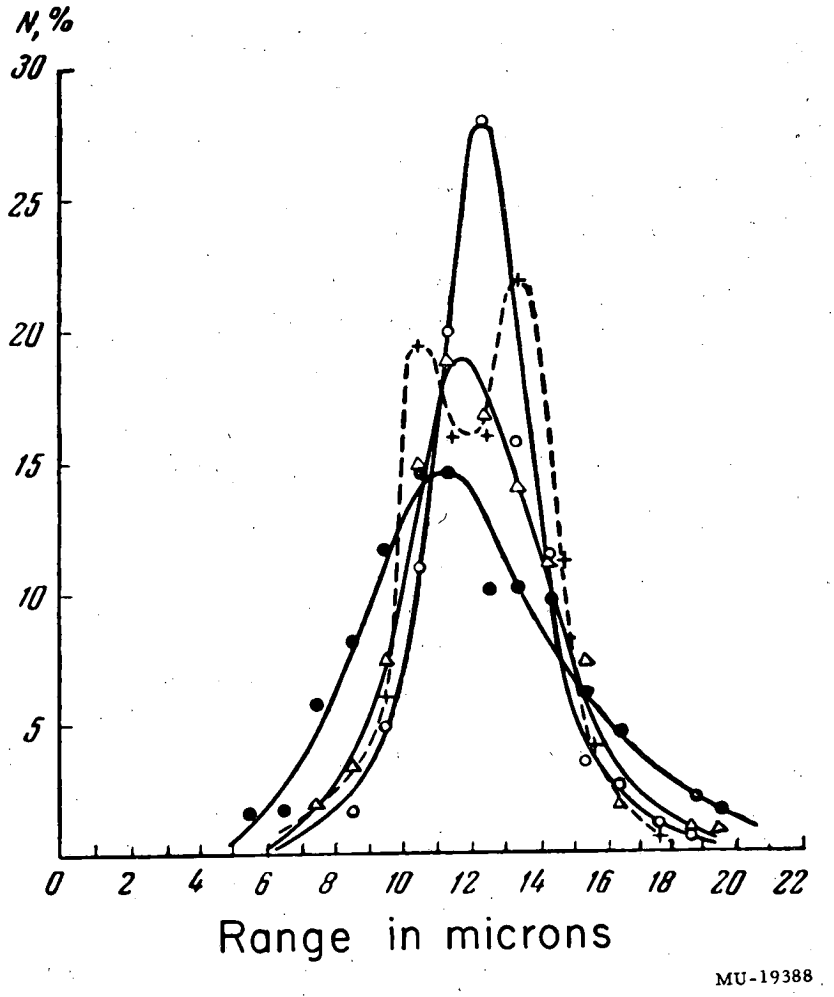

Fig. 12.57 Distribution of ranges (in emulsion) of uranium fission fragments at various excitation energies. N is the percentage of nuclei having a given range:
+ Fission of U^{235} with thermal neutrons
○ Fission of uranium at E_{excit} = 75 Mev
△ Fission of uranium at E_{excit} = 240 Mev
● Fission of uranium at E_{excit} = 540 Mev
From Perfilov.[173]

energy. SHAMOV AND LOZHKIN[174] conclude that the excitation energy at the end of the prompt nucleonic cascade rather than the energy remaining after the evaporation of many neutrons, is crucial for determining the character of the fission process. They conclude that neutron evaporation occurs after fission not only for uranium, but also for bismuth and tungsten.

DENISENKO and co-workers[175] have investigated some interesting triple-pronged events observed in the fission of uranium by 560-660 Mev protons. In this study they used extremely fine-grained emulsions which permitted excellent discrimination of tracks caused by particles of different charge. For every 300 cases of binary fission one disintegration is observed in which three multi-charged particles are emitted, often accompanied by protons and alpha particles. There are two general types of these triple-pronged fission events. In the more prominent type, one of the fragments has much greater range than the other two and hence much smaller mass. The second type is about one-fifth as numerous and consists of events in which the ranges and charges of all three particles are comparable. No explanation is offered for the second type of star. In the first type the authors suggest that the events do not represent tripartite fission but the superposition of two processes (1) emission of a small fragment with Z = 4 to 11 and (2) fission of the still excited residual nucleus. This conclusion is supported by the observation of fragments with similar Z-distribution, angular distribution, and frequency dependence on bombarding energy, when silver is bombarded with high energy protons. In the silver case,[176] these lighter fragments are not accompanied by fission fragments.

12.2.8 Radiochemical Study of Bismuth Fission Induced by High Energy Particles. PERLMAN, GOECKERMANN, TEMPLETON and HOWLAND[177] were the first to use the radiochemical method to call attention to the possibility of inducing fission in elements as light as tantalum, lead and bismuth by bombarding these

---

174. V. P. Shamov and O. V. Lozhkin, Soviet Physics, JETP 2, 111 (1956).

175. Denisenko, Ivanova, Novikova, Perfilov, Prokoffieva, and Shamov, Phys. Rev. 109, 1779 (1958); N. A. Perfilov and G. F. Devisenko, JETP 35, 631 (1958).

176. O. V. Lozhkin and N. A. Perfilov, J.E.T.P. USSR 31, 913 (1956). English translation; Sov. Phys. J.E.T.P. 4, 790 (1957).

177. I. Perlman, R. H. Goeckermann, D. H. Templeton, and J. J. Howland, Phys. Rev. 72, 352 (1947).

elements with charged particles of very high energy. These experiments were done soon after the Berkeley 184-inch cyclotron was put into service. The possibility of inducing fission in these elements with neutrons of 30-84 Mev energy was shown at the same time by KELLEY and WIEGAND[166] using an ion chamber technique. The neutrons were obtained by deuteron stripping in the 184-inch cyclotron. The first detailed radiochemical study of bismuth fission was published by GOECKERMANN and PERLMAN[178] in 1949. A number of additional studies have been published since.[179-188]

When GOECKERMANN and PERLMAN[178] measured the radiochemical yields of the radioactive products of bismuth bombarded with 190 Mev deuterons, they observed the distribution shown in Fig. 12.58 for products in the mass range 50 to 150.

---

178. R. H. Goeckermann and I. Perlman, Phys. Rev. 76, 628 (1949).

179. W. F. Biller, Ph.D. Thesis, University of California Radiation Laboratory Report, UCRL-2067.

180. P. Kruger and N. Sugarman, Phys. Rev. 99, 1459 (1955).

181. L. G. Jodra and N. Sugarman, Phys. Rev. 99, 1470 (1955).

182. A. P. Vinogradov, et al., Radiochemical study of the fission products of bismuth, tungsten, and uranium upon bombardment with 480 Mev protons. Session on Chemical Science, Conference of the Academy of Sciences of the USSR on the Peaceful Uses of Atomic Energy, July 1-5, 1955. English translation available from Superintendent of Documents, U.S. Government Printing Office.

182a. A. V. Kaliamin, A. N. Murin, B. K. Preobrazhenskii and N. E. Titov, Atomic Energy USSR (English translation) 4, 196 (1958).

183. N. T. Porile and N. Sugarman, Phys. Rev. 107, 1410 (1957); ibid. 107, 1422 (1957).

184. N. Sugarman, M. Campos and K. Wielgoz, Phys. Rev. 101, 388 (1956).

185. R. Wolfgang, E. W. Baker, A. A. Caretto, J. B. Cumming, G. Friedlander, and J. Hudis, Phys. Rev. 103, 394 (1956).

186. A. N. Murin, B. K. Preobrahensky, I. A. Yutlendov, and M. A. Yakimov. Chemical Session of Conference of the Academy of Sciences of the USSR, on the Peaceful Uses of Atomic Energy, July 1-5, 1955. English translation available from Superintendent of Documents, U.S. Government Printing Office.

187. F. I. Pavlotskaya and A. K. Lavrukhina, Soviet Journal of Atomic Energy, (English translation) 5, 791 (1956).

188. W. E. Bennett, Phys. Rev. 94, 997 (1954).

188a. E. T. Hunter and J. M. Miller, Phys. Rev. 115, 1053 (1959).

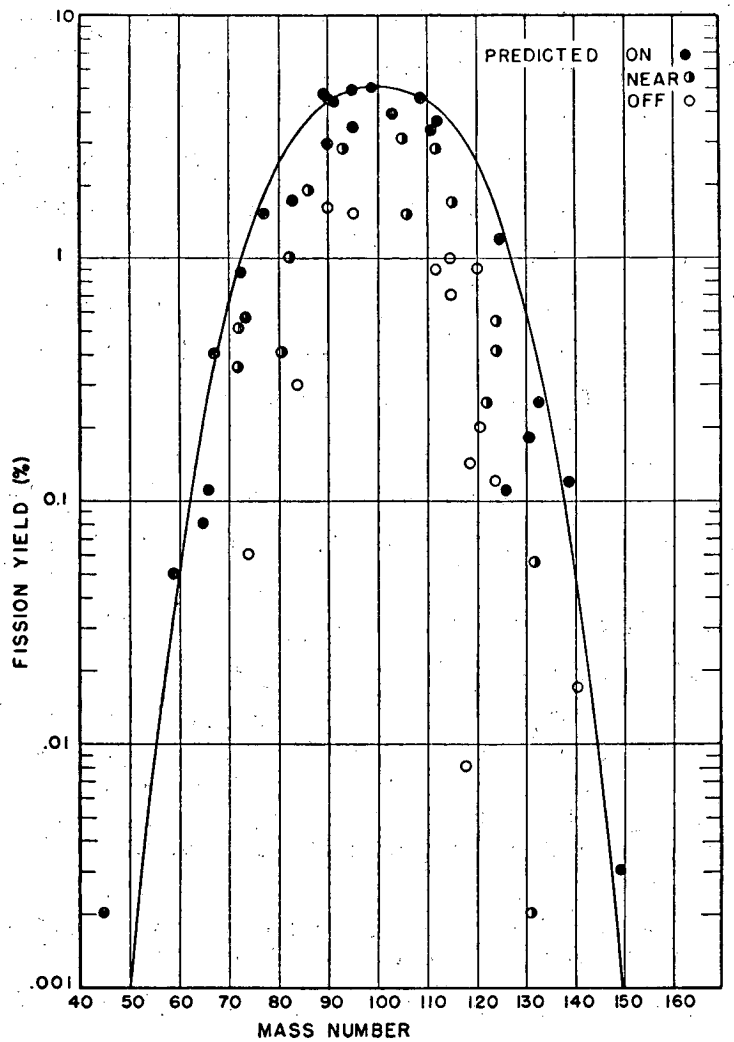

MU-19438

Fig. 12.58 Yields of products for the bombardment of bismuth with 190 Mev deuterons. Curve shows total yield at each mass number. Solid points are experimental yields expected to represent nearly the total chain yield. Open circles are experimental points expected to represent only a portion of the chain yield. The peak yield is about 10 millibarns. From Goeckermann and Perlman.[178]

A very similar distribution was observed by BILLER[179] when bismuth was bombarded with 340 Mev protons. The smooth line shows the total yield at each mass number when suitable allowance is made for the unmeasured yields in each isobaric chain. The peak yields are about 10 millibarns decreasing to a value less than one-thousandth of this at mass number 150. At higher mass numbers the yields increased rapidly again and largest reaction yields were found in the immediate neighborhood of the target.[‡] It is clear that at least two separate groups of products have been formed. The high energy cascade-evaporation mechanism has given rise to a group of products within a few mass numbers of the bismuth target with yields dropping off very sharply with decreasing mass number. Some of these products, however, are fissionable and during the course of their de-excitation, undergo fission, thus leading to the distribution of products in the mass range 50 to 150. These products cannot possibly be produced by evaporation of neutron, protons or other small particles since the energy of excitation required is too high. Furthermore, fission fragments corresponding to binary fission have been observed in photographic emulsions loaded with bismuth salts, the ionization caused by the fragments has been measured in ionization chambers and the high recoil energy of the fragments has been measured radiochemically using thin foil absorbers.

In many ways these fission products differ from those observed in the low energy fission of uranium. A single symmetric peak is observed. However, this peak is very broad compared to the peak observed by FAIRHALL[189] in the fission of bismuth with 16 Mev deuterons, indicating that an appreciable fraction of asymmetric divisions occur in the high energy fission of bismuth. This is in agreement with the emulsion studies of PERFILOV[173] cited above which showed that the ratio of the fragment ranges showed a broader distribution at the higher energies.

The light fission fragment are beta emitters and the high yield products in each mass chain definitely lie on the neutron-excess side of stability. However, many of the heavy fragments lie near stability or even on the neutron-deficient

---

189. A. Fairhall, Phys. Rev. 102, 1335 (1957); see Section 12.1.5.

‡E. T. Hunter and J. M. Miller, Phys. Rev. 115, 1053 (1959) made a careful study of the spallation products (mass number range 186-207) in the bombardment of bismuth with 380 Mev protons.

side of stability. In the case of barium, for example, the neutron-excess isotope Ba^{140}, which is a prominent fission product in the slow neutron fission of uranium, is produced here in very low fission yield while Ba^{133} is quite prominent. The neutron-to-proton ratio of the light and heavy fragments are nearly the same; the charge distribution does not follow the GLENDENIN hypothesis of equal charge displacement used to describe the fission product distribution in the slow neutron fission of uranium.

The peak in the mass yield distribution occurs at mass number 99 to 100 and at atomic number 42. GOECKERMANN and PERLMAN[178] formulated a mechanism to account for their results. See mechanism 1 of Fig. 12.43. They postulated that the excitation energy deposited in the nucleus during the knock-on cascade was dissipated chiefly in the emission of neutrons. In the most probable events leading to fission, about 10 neutrons are boiled out. The resulting nucleus, Po^{199}, has a much higher Z^2/A than does the Bi^{209} in the target, and some fraction of the Po^{199} nuclei undergo fission. This cleavage is further assumed to occur without charge redistribution so that each fragment retains the neutron/proton ratio of the parent nucleus. Because of the statistical nature of the cascade-evaporation process it is certain that a number of nuclei in the region of Po^{199} will be produced each with a distribution of excitation energy so that one probably should consider the observed products as resulting from the fissioning of a group of nuclei centered near Po^{199}. YAMAGUCHI[190] has considered this fission mechanism from a semi-theoretical point of view and finds it to be plausible.

The GOECKERMANN-PERLMAN hypothesis accounts neatly for the experimental observations, but our knowledge of the factors affecting fissionability for highly excited nuclei is too sketchy to decide whether it is in fact correct. Most of the results could just as easily be explained by a mechanism involving fission of a highly excited nucleus followed by evaporation of neutrons from the highly excited fragments. The GOECKERMANN-PERLMAN mechanism corresponds to mechanism 1 of Fig. 12.43 while the latter refers to mechanism 2 of the figure.

The total cross section for bismuth fission for incident particles of hundreds of Mev energy is about 200 millibarns or approximately one-tenth the

---

190. Y. Yamaguchi, Progr. Theoret. Phys. (Japan) 5, 143 (1950).

geometrical cross section. Experimental values are summarized in Tables 12.19, 12.20 and 12.22.

The recoil studies carried out by PORILE and SUGARMAN[183], and SUGARMAN, CAMPOS and WIELGOZ[184] have provided additional information on the fission of bismuth. Individual fission products were isolated from thin targets of bismuth and from recoil collector foils placed in front and in back of the target foil. From the amounts of activity found in the three foils the true range in the bismuth target and the relative velocity of the fragment and the struck nucleus were computed. The energy of the fragment was calculated from the range and by application of the principle of conservation of momentum the energy of the fission fragment partner was also derived. The kinetic energy release for many complementary fission fragments was computed and properly averaged according to the mass yield curve to obtain a value of the average total kinetic energy release. PORILE and SUGARMAN[183] report an average of 111 Mev for the case of bismuth bombarded with 435 Mev protons and 96 Mev for tantalum bombarded with the same particles. This can be compared with the 166 Mev released in the slow neutron fission of U^{235}. The largest error in these estimates is traceable to uncertainties in the range-energy relationships for fission fragments.

The momentum of the struck nucleus was derived by SUGARMAN[183,184] from the difference in the amount of recoil activity ejected in the forward direction over that ejected backward. This is the same quantity which PERFILOV and co-workers[173] obtain from the observed angle (lab system) of the fission fragment tracks with respect to each other. One can calculate the deposition energy of the struck nucleus from this provided one knows the momentum of the incoming proton and the number, energy and angle of ejection of the cascade particles. However, the deposition energy values one obtains are markedly dependent on the assumptions made about cascade nucleons. PORILE and SUGARMAN[183] found it possible to minimize these uncertainties by examining the Monte Carlo cascade calculations of METROPOLIS[124] which are referred to in Section 12.2.2. Several hundred cascade calculations were examined in detail to find the forward component of momentum of the struck nucleus as a function of the energy of excitation E^*. This examination led to the calibration curve shown in Fig. 12.59.

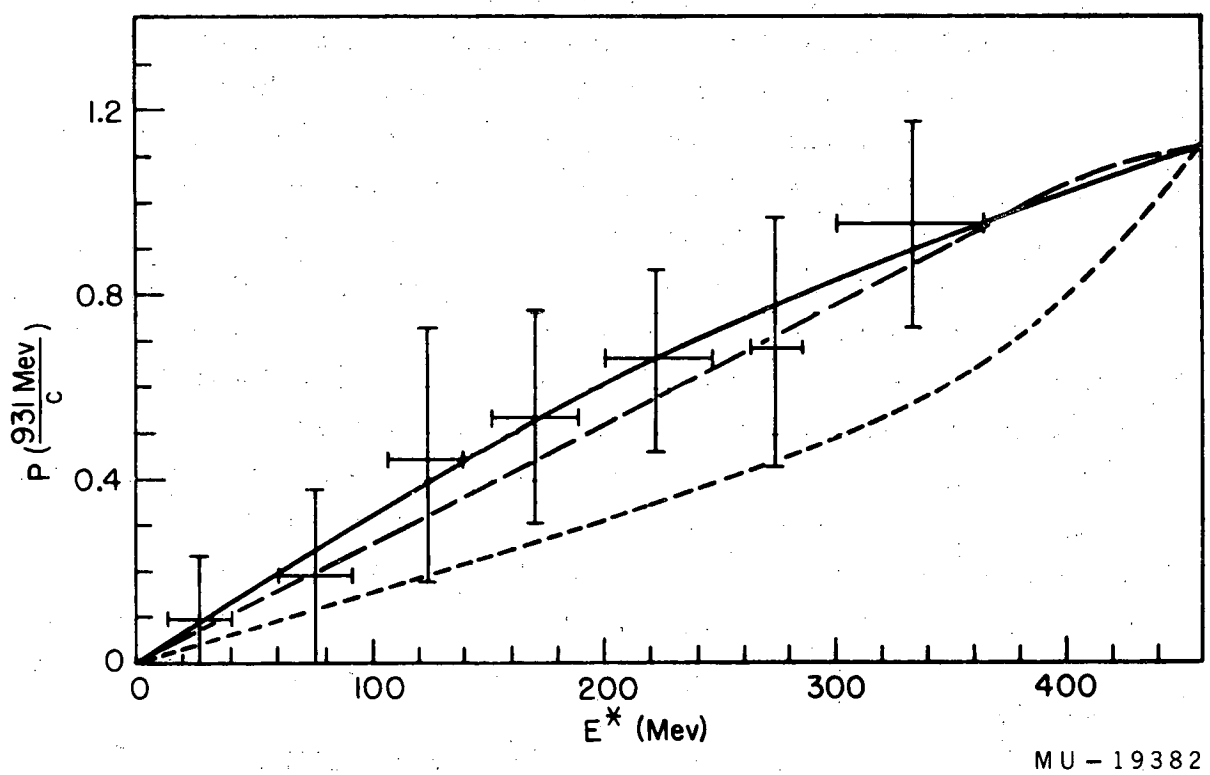

Fig. 12.59 Momentum of struck nucleus as a function of deposition energy for bismuth target bombarded with 458 Mev protons. From Porile and Sugarman.[183]

With this curve one needs only to know the momentum of the struck nucleus from emulsion or recoil data in order to know the excitation energy of this nucleus.

Some typical values of recoil ranges and deposition energies are listed in Table 12.26. One notes that the range values are substantial and of the magnitude expected for a fission product. It can also be noted that there is considerable variation in the deposition energy leading to different fragments; i.e. there is a wide spread in excitation energy for which fission occurs when a nucleus is bombarded with high energy particles. We also note that the fission of tantalum leading to a specific fragment requires on the average about 30 Mev more deposition energy than does the fission of bismuth. The recoil ranges of such typical spallation products as bismuth, lead and thallium isotopes were also studied and found to be much less; the effective range in the forward direction was of the order of 0.1 mg/cm^2 bismuth.

The average deposition energy in inelastic events leading to fission can be calculated from the deposition energies found for individual fragments provided that proper averaging is done using the mass yield curve as a weighting curve. This calculation leads to the results given in Table 12.27. The average deposition energy for all inelastic events is lower than the average deposition energy leading to fission reflecting the low branching ratio for fission for deposition energies below 75 Mev. The difference between the average deposition energy for all processes and for fission is greater for tantalum targets than for bismuth targets as might be expected from the higher effective fission threshold of tantalum. The values in this table are somewhat lower than the average values of deposition energy one would obtain from Perfilov's values quoted in Table 12.25, which were estimated by use of data obtained by the emulsion technique. (See PORILE and SUGARMAN[183] for a discussion of this discrepancy).

SUGARMAN, CAMPOS and WIELGOZ[184] state that the values of deposition energy leading to fission provide evidence against the fission mechanism involving pre-fission boil-off of neutrons, i.e. Mechanism 1 of Fig. 12.43. The values of deposition energy seem lower than would be required to produce the "fissioning" nucleus deduced from the radiochemical mass yield curve. For example, KRUGER and SUGARMAN[180] list $_{80}Hg^{186}$ as the "most probable fissioning

Table 12.26 Recoil data on fission products of bismuth and tantalum bombarded with 450 Mev protons. Porile and Sugarman.[183]

Nuclide	Range* in target material (mg/cm^2 Bi)	Kinetic energy of fragment** (Mev)	$\frac{R_eF}{R_eB}$ †	Anisotropy parameter ratio b/a, for $a + b \cos^2\theta$ distribution ‡	η	Kinetic energy of struck nucleus (Mev)	$\bar{E}^*_A$
			Bismuth + 450 Mev protons				
Mn^{56}	11.75	61.4	1.248	0.15	0.056	0.71	184
Cu^{67}	10.85	62.6	1.256	0.05	0.057	0.63	171
Sr^{89}	9.2	59.8	1.248	0.09	0.055	0.42	136
Sr^{91}	9.2	61.0	1.223	0.09_4	0.050	0.35	122
Sr^{92}	9.2	62.4	1.188	0.15	0.044	0.27	109
Pd^{109}	7.6	48.9	1.270	0.10	0.060	0.33	120
Ba^{133m}	5.8	31.1	1.536	0.11_4	0.108	0.56	162
			Tantalum + 450 Mev protons				
				Anisotropy parameter ratio b/a, for $a + b \sin^2\theta$ distribution			
$Sc^{47,48}$	10.50	47.6	1.383	0.30	0.078	1.10	223
Mn^{56}	10.58	56.5	1.379	0.08	0.079	1.12	224
Cu^{67}	9.4	54.1	1.346	0.03	0.074	0.79	179
Sr^{91}	7.4	45.6	1.412	0.03	0.086	0.66	162
Pd^{109}	6.1	35.7	1.499	0.07	0.100	0.59	152
$Ba^{128,129}$	3.0	9.2	2.787	0.37	0.241	0.75	174

*Range is calculated for target material rather than absorber material.

**Kinetic energy is obtained from the equation $E = KAR^2$ where R is range, A is mass number of fragment and K is a constant obtained from other recoil data.

†R_eF is activity recoiling forward from target foil, R_eB is activity recoiling backward from target foil.

$$\eta = \frac{\text{component of velocity of struck nucleus in direction of proton beam}}{\text{velocity of recoiling fragment in system of moving target nucleus}}$$

$\bar{E}^*_A$ is the most probable average deposition energy leading to this particular fragment.

‡The anisotropy parameter ratio is obtained by measurement of activity recoiling perpendicular to the beam.

Table 12.27 Some characteristics of the high energy fission of bismuth and tantalum

	Most probable deposition energy leading to fission	Average deposition energy all events
Bi + 450 Mev protons	155	147
Ta + 450 Mev protons	180	136

Data from Porile and Sugarman[183]

nucleus" for bismuth bombarded with 450 Mev protons. The minimum of 320 Mev required to make this nucleus is considerably more than the 155 to 180 Mev listed in Table 12.27. This suggests that post-fission boil-off is the more probable mechanism since this yields a somewhat lower energy value for the energy deposited.

Up to this point we have discussed the fission reaction in bismuth for bombardment energies of hundreds of Mev where the fission products form the dominant feature of the mass yield curve. It will be interesting now to consider the remarkable changes which occur when the energy of the incident particles is raised to the Bev range.

No group has made a general radiochemical yield study of bismuth targets, but the work of WOLFGANG and co-workers[185] on the interaction of 3 Bev protons with the neighboring element, lead, indicates rather well the pattern of reaction products for target elements around bismuth. That the pattern of yields observed at 3 Bev is completely different from that observed when bombardment energies fall in the region 100 Mev to 700 Mev, can be seen at once by an inspection of Fig. 12.60. The valley between the fission and spallation region is completely absent. The yields of products which at lower energies represented the peak yields of the fission spectrum have actually decreased. Also the yields of spallation products near the target have decreased. All other mass numbers are represented by isotopes produced in much higher yields than before. In fact, one is faced with the remarkable result that to a first approximation when a heavy element target is bombarded with 3 Bev protons, the total isobaric yields are invariant to mass number change.

To explain these results as well as others not discussed in detail here, it was necessary that there be some mechanism for the deposition of large amounts of excitation energy which is qualitatively different from the simple nucleon-cascade-followed-by-nuclear-evaporation model as developed to account for energy transfers from incident particles of a few hundred Mev. The new mechanism is called fragmentation. A possible description of fragmentation in terms of meson production and reabsorption as developed by WOLFGANG et al.[185] is outlined in Section 12.2.5.

It is interesting to consider the excitation functions for selected products. The cross sections for medium-mass nuclides such as Mo^{99} which

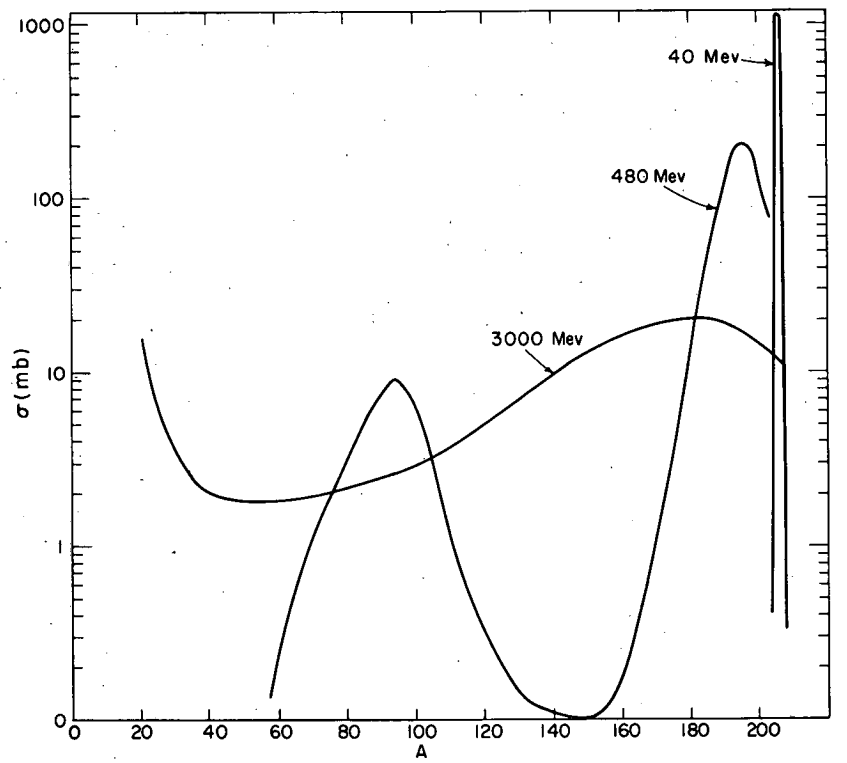

MU-19534

Fig. 12.60 Cross sections as a function of product mass number for the interaction of lead or bismuth with protons of various energies. Total cross sections for each mass number are given but in the case of the 3 Bev results the curve is based on incomplete experimental data and is presented as a schematic representation of the results. The 3 Bev curve is for a lead target. The other three curves are for bismuth targets. From Miller and Hudis, Ann. Rev. Nuclear Science 9, (1959).

fall at the peak of the fission product distribution at lower energies are observed to decrease with increasing proton energy in the energy range 0.6 Bev to 3.0 Bev (Fig. 12.61). For heavy, neutron-deficient isotopes such as $Ba^{128-131}$ there is, on the other hand, a steep rise in yield as the energy increases from 0.5 Bev to 3 Bev. (Fig. 12.62). This increase in yields is due partly to evaporation of more particles at the higher energies, and to the onset of the fragmentation process. Some of the most interesting behavior is shown by the low-mass species P^{32}, Mg^{28}, Na^{24} and F^{18}. (Fig. 12.63). The steep rise of these products at the higher energies shows that their production must be associated with some process which becomes prominent in the Bev range of energies.

SUGARMAN and co-workers[183-184] applied a recoil range method to specific radioactive products to see whether recoil data would reveal changes in the production processes in changing from 400 Mev protons to 2.2 Bev protons. Consider, for example, the results given in Table 12.28. The data for Sr^{91} undergo no great change indicating that the fission process is probably responsible for the major part of its production cross section throughout the energy range studied. In the case of $Ba^{129,133m}$ however, large changes are noted as though a change in the nature of the process producing this nuclide were occurring. At 450 Mev bombarding energy, the barium isotopes are typical fission products. At 2.2 Bev bombarding energy a sizable fraction of the barium isotopes are produced by fragmentation.

PORILE and SUGARMAN[183] have made an interesting speculative analysis of the relative contribution of fission and fragmentation to the production of representative radioactive products in the bombardment of bismuth over the whole range of energies. The analysis is based on the excitation functions for selected products and on the deposition energy of the struck nucleus as predicted by the Monte Carlo calculations of the knock-on cascade. They conclude that a true fission product is produced over a wide range of deposition energies, but the maximum probability for fission occurs at a deposition energy of 100 to 200 Mev. At higher deposition energies the cross section for fission drops markedly. PORILE and SUGARMAN[183] estimate that the branching ratio for fission achieves a peak value of 0.17 at a deposition energy of 190 Mev and then decreases. The maximum value for the branching ratio for the fission of tantalum

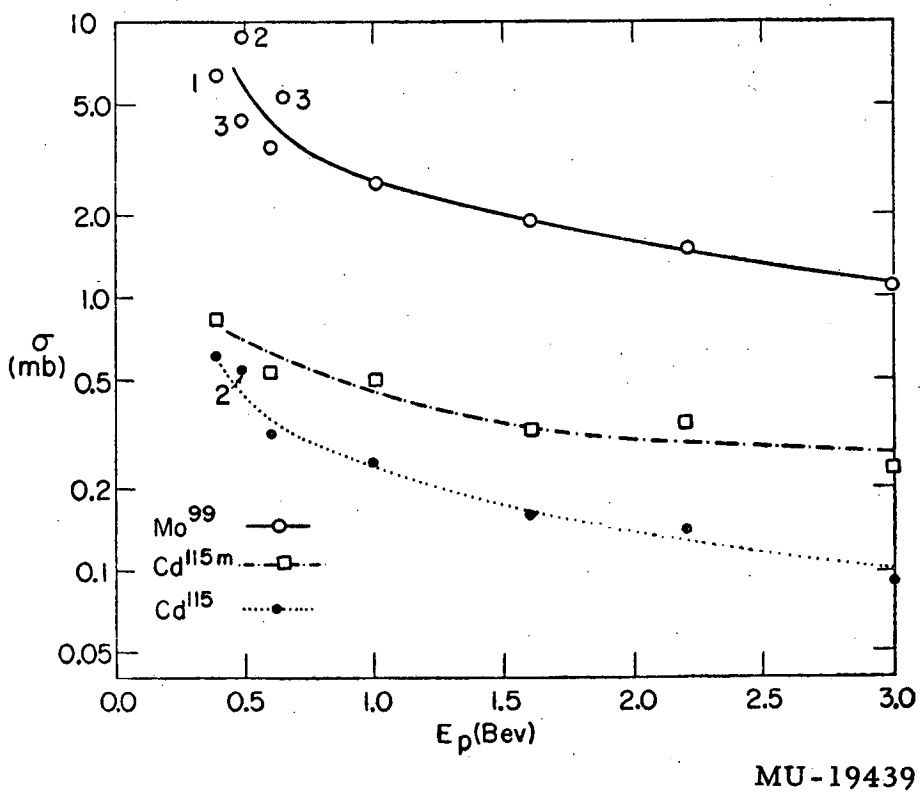

Fig. 12.61 Excitation functions for the production of some typical fission products in proton bombardments of lead. From Wolfgang et al.[185]

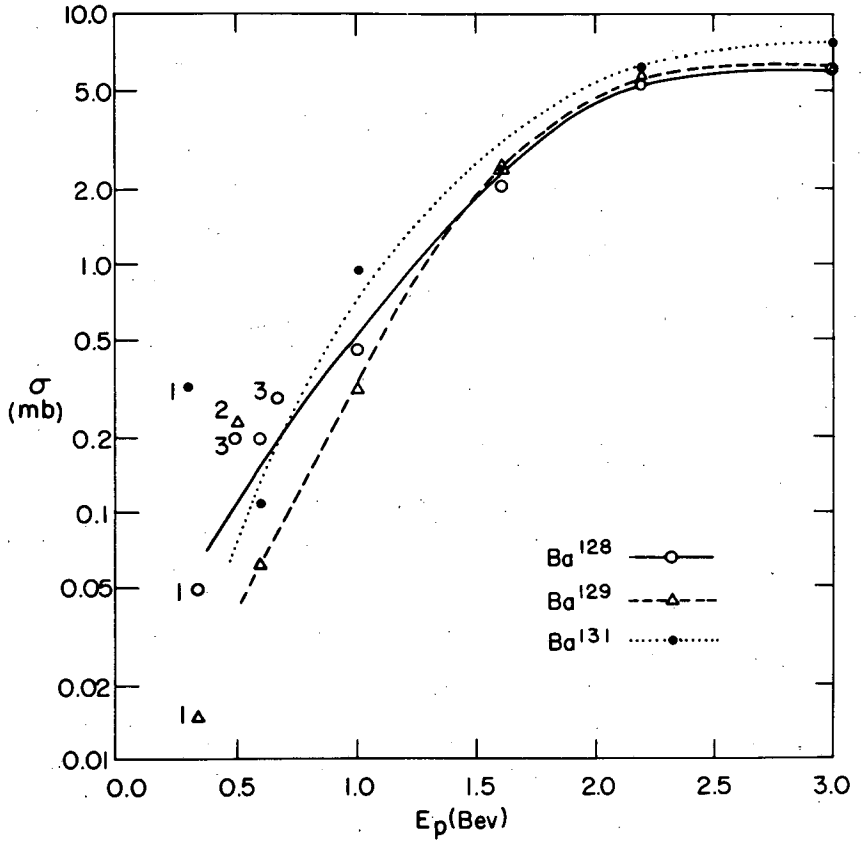

Fig. 12.62 Excitation functions for the production of neutron-deficient barium isotopes in proton bombardments of lead. From Wolfgang et al.[185]

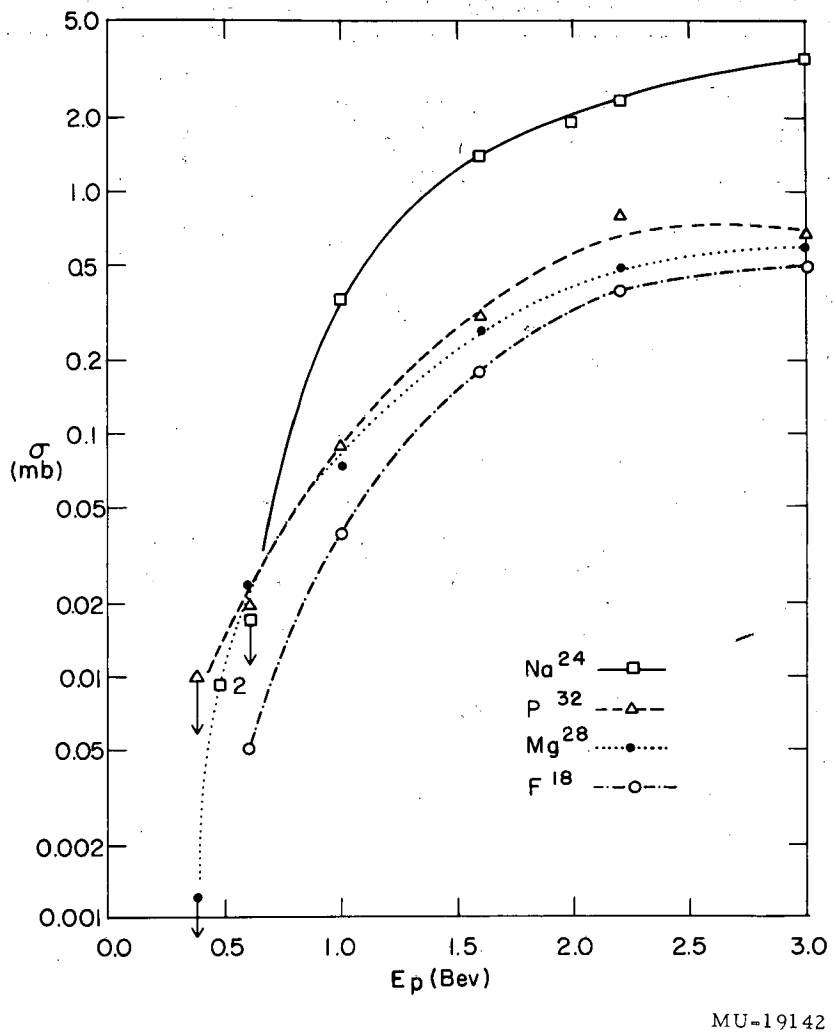

Fig. 12.63 Excitation functions for the production of light nuclei in proton bombardments of lead. These nuclides are believed to be fragmentation residues. From Wolfgang et al.[185]

Table 12.28 Changes in recoil characteristics of Sr^{91} and $Ba^{129,133m}$ from bismuth targets when proton energy is changed from 450 Mev to 2.2 Bev

Proton energy (Mev)	Recoiling product	$\frac{R_eF}{R_eB}$	Range in bismuth (mg/cm^2)	Energy of recoiling product (Mev)	Deposition energy of struck nucleus (Mev)
450	Sr^{91}	1.22	9.2	61	122
450	$Ba^{129,133m}$	1.54	5.8	31	162
2200	Sr^{91}	1.24	10	70	144
2200	$Ba^{129,133m}$	3.8	3.0	7	265

$$\frac{R_eF}{R_eB} = \frac{\text{recoil activity forward}}{\text{recoil activity backward}}$$

Data from Sugarman and co-workers.

is only 0.007 at a deposition energy of 230 Mev. At no deposition energy is fission the predominating process for either bismuth or tantalum. The bombardment energies for which the average deposition energy equals the values most favorable for fission are 750 Mev for bismuth and 1.5 Bev for tantalum.

The fragmentation process begins to make appreciable contributions for bombardment energies of 500 Mev and contributions of fission and fragmentation are about equivalent for many products in the "fission product region" when the bombardment energy is about 1.5 Bev. Fragmentation according to this analysis makes substantial contributions to the observed yield of products over a mass region covering selected products as low as mass 24 and as high as 131.

12.2.9 Radiochemical Study of Uranium and Thorium Fission Induced by High Energy Particles. We consider first a range of energy for the bombarding particles of 100 to 700 Mev. The first radiochemical study of this type was carried out by O'CONNER and SEABORG[191] who measured yields of radioactive isotopes produced in the bombardment of uranium with 380 Mev helium ions. The dominant feature of the yield distribution was a broad symmetric peak of fission products centered at a mass number about half the mass of the heavy target nucleus. Others who have made a rather complete determination of the mass-yield curve of the fission products are FOLGER, STEVENSON and SEABORG[192] (uranium plus 340 Mev protons), VINOGRADOV and co-workers[193] (uranium and thorium plus 480 Mev protons), and STEVENSON, HICKS, NERVIK and NETHAWAY[194-196] (uranium plus 10-340 Mev protons; uranium plus 20-190 Mev deuterons).

Figure 12.64 taken from the paper of the last-named authors reveals most of the significant features of the fission product distribution. The changes in

---

191. P. R. O'Conner and G. T. Seaborg, Phys. Rev. 74, 1189 (1948).

192. R. L. Folger, P. C. Stevenson, and G. T. Seaborg, Phys. Rev. 98, 107 (1955).

193. A. P. Vinogradov, et al., reported in Chemical Session of Conference on Peaceful Uses of Atomic Energy, Academy of Sciences, USSR, July 1-5, 1955. English translation available from Superintendent of Documents, U.S. Government printing office.

194. P. C. Stevenson, H. G. Hicks, W. E. Nervik, and D. R. Nethaway, Phys. Rev. 111, 886 (1958).

195. H. G. Hicks, P. C. Stevenson, R. S. Gilbert and W. H. Hutchin, Phys. Rev. 111, 886 (1958).

196. H. G. Hicks and R. S. Gilbert, Phys. Rev. 100, 1286 (1955).

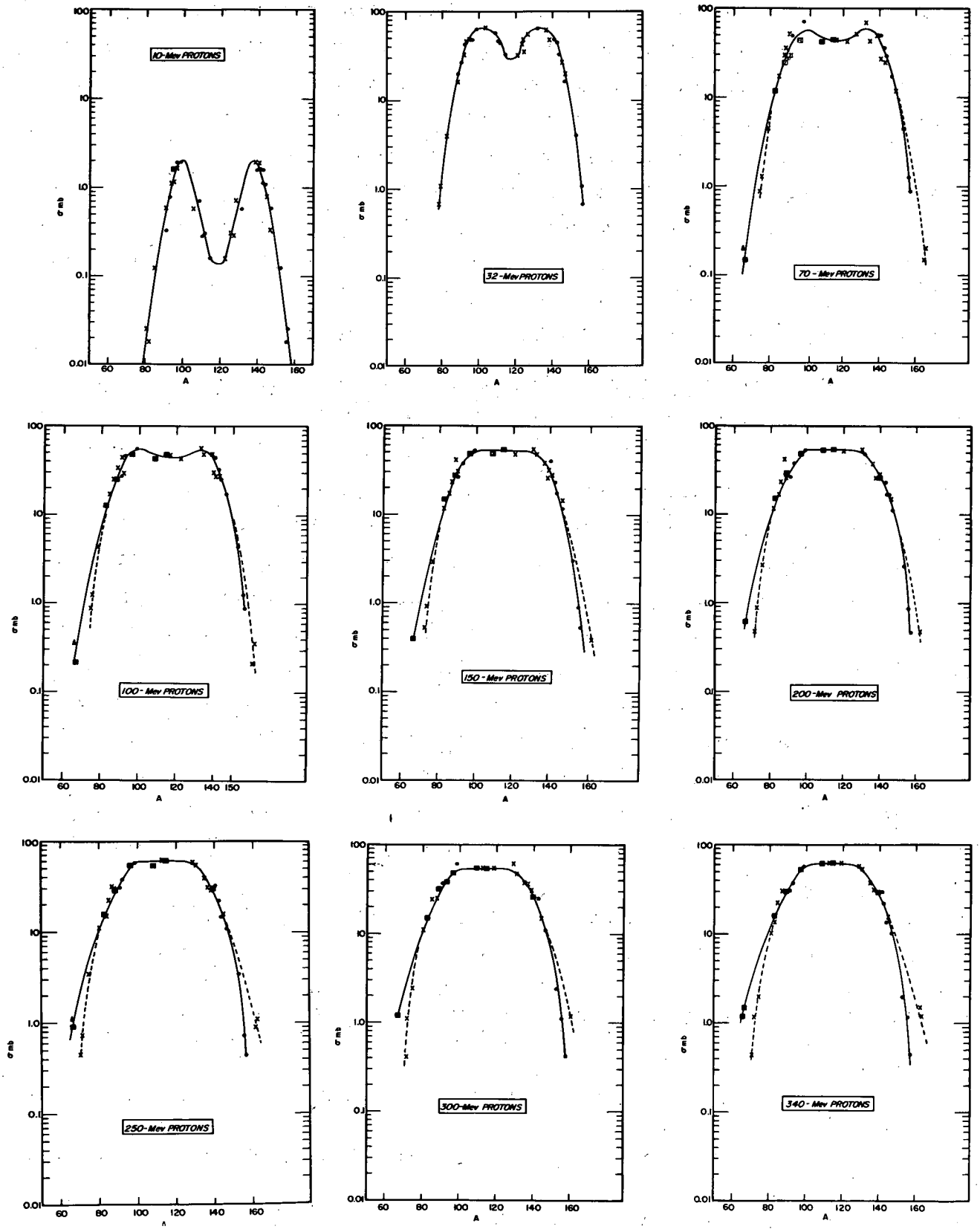
10-Mev PROTONS
32-Mev PROTONS
70-Mev PROTONS
100-Mev PROTONS
150-Mev PROTONS
200-Mev PROTONS
250-Mev PROTONS
300-Mev PROTONS
340-Mev PROTONS
σ mb
A

Fig. 12.64 Fission-product distributions of U^{238} bombarded with protons of various energies. The symbol ● denotes work by Stevenson et al.[194]; ■ denotes previous work by Hicks et al.[195-196]; ▲ denotes work by Lindner and Osborne[197]; and X denotes reflection points. A similar figure for deuteron bombardments is given in reference 194.

the fission product distribution for the most part just continue the trends observed at lower bombarding energies and discussed in Section 12.1.5. The distribution is nearly symmetric, but it is quite broad indicating that a major fraction of the mass splits are unequal. This fraction increases as the bombardment energy goes up. The mass number of the peak of the yield distribution is substantially less than one-half the mass number of the target nucleus. This proves that a large number of nucleons, chiefly neutrons, are emitted during the sequence of events leading to the fission products which are chemically isolated. This number may be as large as 20, as can be seen in the next-to-the-last column of Table 12.22 above.

STEVENSON and co-workers[192] noted at the higher bombarding energies that the mass yield curves are not completely symmetrical. Reflection of the heavy rare earth cross-sections through the "apparent center of the fission yield curve" as estimated from the higher-yield products gives points that fall well below the observed values on the low-mass-number wing of the curve. This effect can be seen in Fig. 12.64 as the deviation of the solid curve from the dotted (reflection) curve.

The fission products of low atomic number are of the neutron-excess type. On the high atomic number side of the fission product distribution many of the products are in the region of beta stability or even on the neutron-deficient side. The charge distribution in the high energy fission of uranium approaches more closely the GOECKERMANN and PERLMAN[178] hypothesis of unchanged charge-to-mass ratio than the equal charge displacement hypothesis which describes the mass distribution for thermal fission of uranium.

FOLGER, STEVENSON and SEABORG[192] found that their analysis of the radiochemical yields did not lead to a choice of a single "most probable fissioning nucleus" but to a group of fissioning species. DOUTHETT and TEMPLETON[197] reached a similar conclusion from a study of the recoil ranges of specific fission products.

The recoil studies of these last authors revealed the interesting fact that the recoil ranges of fission fragments in high energy fission are less than the corresponding ranges (reviewed in Section 11.6.4, Chapter 11) for thermal fission. The energy brought into the nucleus by the high-energy incoming particle

197. E. M. Douthett and D. H. Templeton, Phys. Rev. 94, 128 (1954).

does not appear in the kinetic energy of the fission fragments; the fragments apparently get their kinetic energy only from their mutual Coulombic repulsion. The lowered energy of Coulombic repulsion derives from the fact that the mass and charge of the fissioning nucleus is lessened by prefission loss of neutrons or protons. Or, if fission occurs before excess energy is dissipated by neutron evaporation, the separating fragments instantly lose many neutrons by evaporation and the fragments are observed to have correspondingly lower kinetic energies.

The radiochemical method has been applied to the determination of yields of specific fission products as a function of the energy of the bombarding particles.[196,198,199] LINDNER and OSBORNE[198] found that neutron-rich products such as Ba^{139}, Zr^{97} and Ag^{111} which are prominent among the fission products at low energy increase in yield only slightly as the energy of the protons increases and eventually decrease in yield. See Fig. 12.65. The neutron-deficient nuclides Ni^{66}, Ba^{131} and Ba^{128} were taken as representative of the products of high energy fission. The yields of these products rise steeply for energies above 50 Mev. See Fig. 12.66.

There is a pronounced minimum in the mass yield curve between the heaviest of the fission products and the spallation products which lie within a few mass numbers of the target isotope. The entire range of products in this mass region has not been measured as carefully as it should, but there is a considerable amount of cross section data for the isotopes of such elements as uranium, protactinium, thorium, actinium, etc. The yields of these products would be much larger if nuclear fission did not occur. The differences between the actual yields and those predicted by the Monte Carlo calculations with fission competition ignored (or included according to varying assumptions on the fission probability) are important in the evaluation of the true nature of fission competition. This point is discussed in Section 12.2.4. These yields are also important in a practical way because many isotopes of these elements can only be made, or can be made most conveniently, by high-energy bombardment of heavy element targets. We summarize some of the important measurements of

---

198. M. Lindner and R. N. Osborne, Phys. Rev. 94, 1323 (1954).

199. M. Lindner and R. N. Osborne, Phys. Rev. 103, 378 (1956).

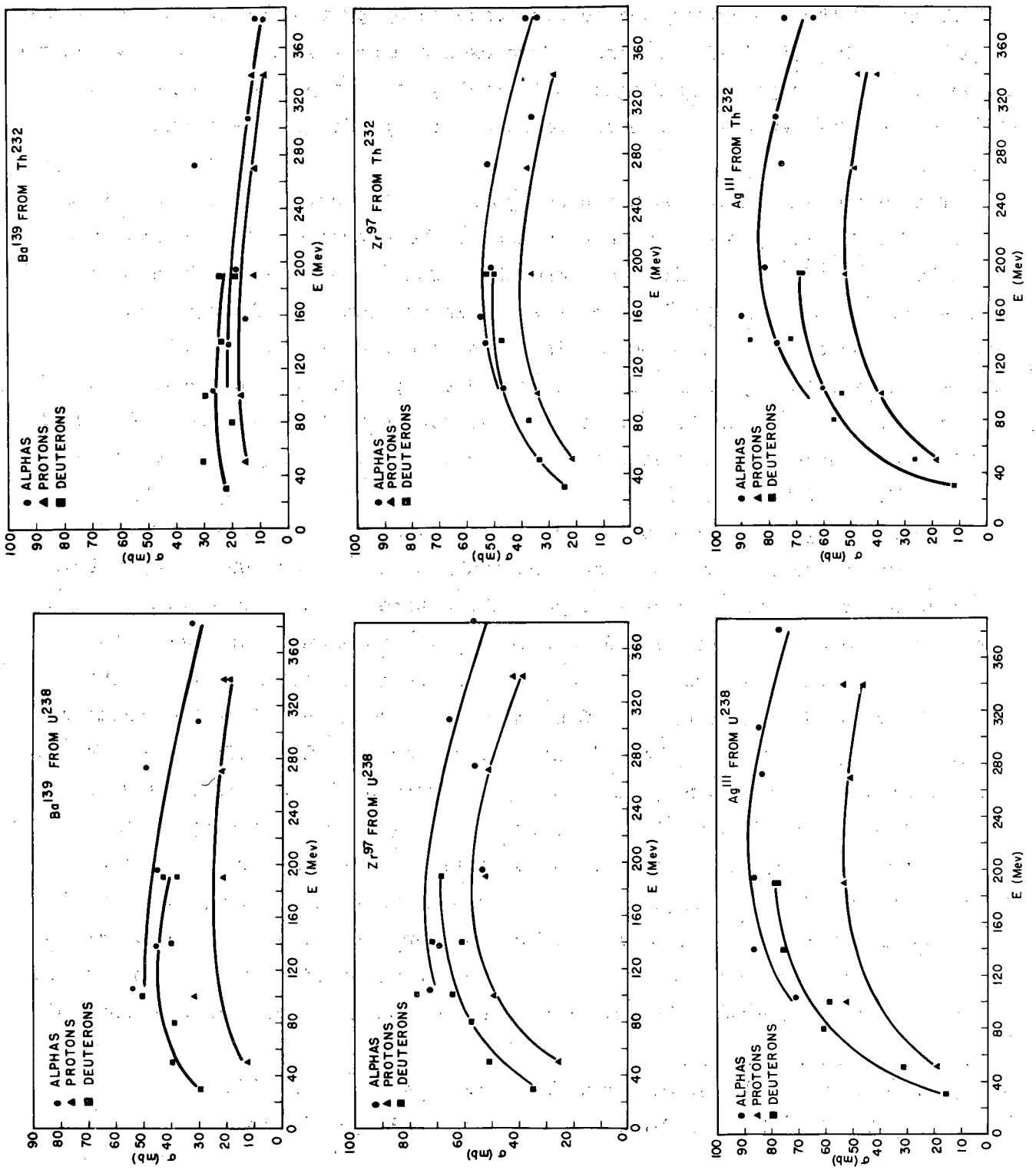
Ba139 FROM Th232
Zr97 FROM Th232
Ag111 FROM Th232
Ba139 FROM U238
Zr97 FROM U238
Ag111 FROM U238
ALPHAS
PROTONS
DEUTERONS
σ (mb)
E (Mev)

MUB-376

Fig. 12.65 Energy dependence of cross sections for formation of certain neutron-rich fission products of U^{238} and Th^{232}. The abscissa gives the energy of the bombarding particle. From Lindner and Osborne.[198]

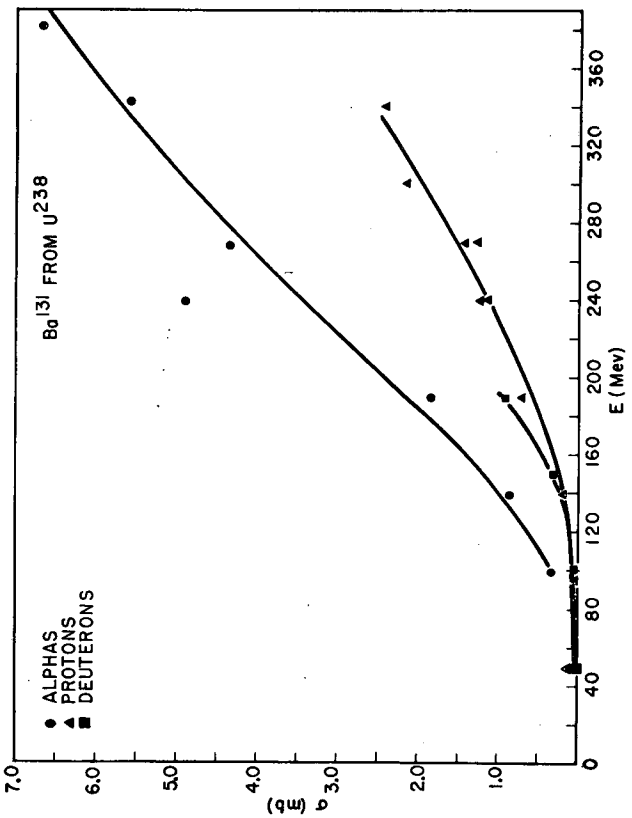
Ba131 FROM U238
ALPHAS
PROTONS
DEUTERONS
σ (mb)
E (Mev)

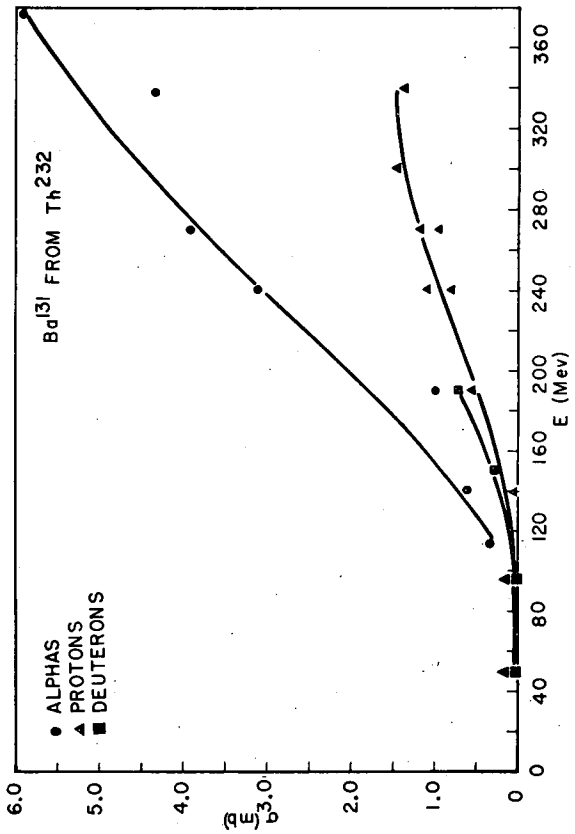
Ba131 FROM Th232
ALPHAS
PROTONS
DEUTERONS
σ (mb)
E (Mev)

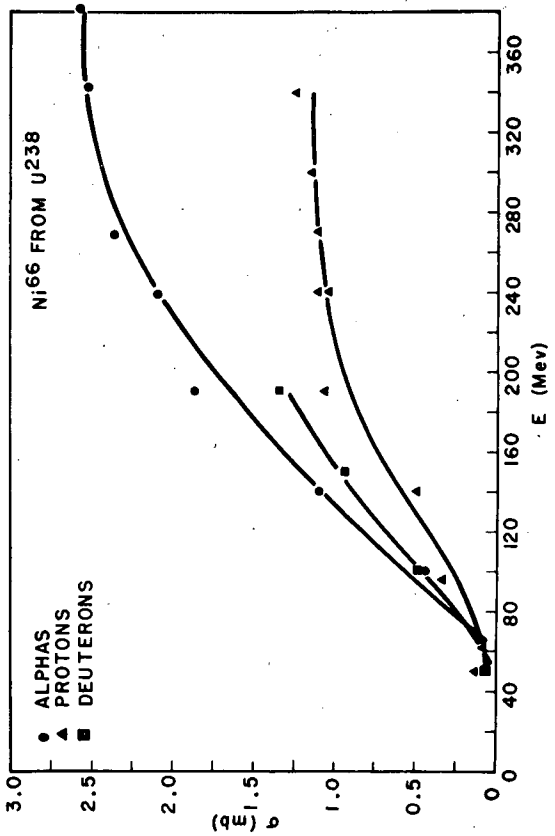
Ni66 FROM U238
ALPHAS
PROTONS
DEUTERONS
σ (mb)
E (Mev)

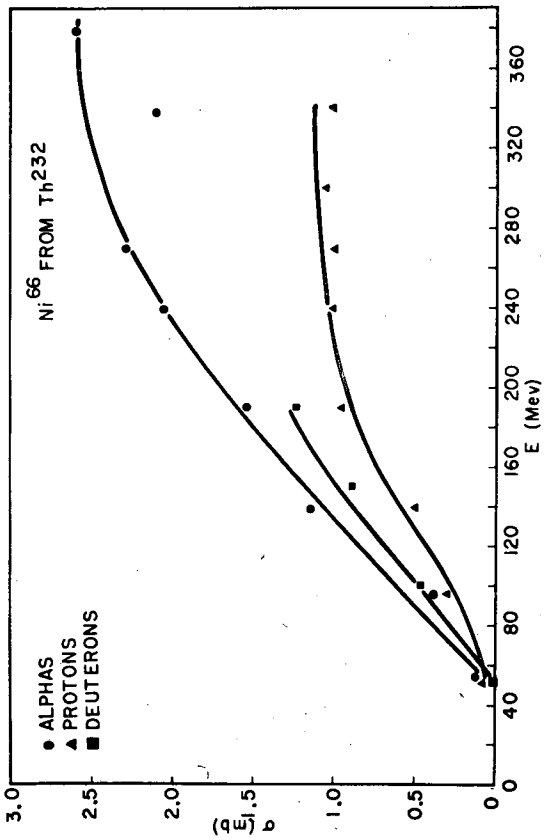
Ni66 FROM Th232
ALPHAS
PROTONS
DEUTERONS
σ (mb)
E (Mev)

MUB-377

Fig. 12.66 Dependence of the formation of certain neutron-deficient fission products of U^{238} and Th^{232} on the energy of the bombarding particles. From Lindner and Osborne.[198]

LINDNER and OSBORNE[199] in Table 12.29 and Figs. 12.67-12.69. PATE and POSKANZER[200] have also studied the yields of principal spallation products at very high bombardment energies.

Let us now consider the reaction of uranium with protons accelerated to billions of electron volts energy. Experimental studies in this energy region are very incomplete since very few laboratories have accelerators capable of delivering protons of such great energy and since the beam intensities of these accelerators are rather low for radiochemical research. We cannot report here anything approaching a complete mass-yield curve. Many other important features of the reaction are imperfectly mapped out. Nonetheless, it is clear from the preliminary studies which have been made that the reaction is qualitatively different from that which was just discussed.

SHUDDE[201] and CARNAHAN[202] measured the yields of about sixty radioactive nuclides in uranium targets bombarded with 5.7 Bev protons in the Berkeley Bevatron. See Table 12.30. DOSTROWSKY[203], and PATE and FRIEDLANDER[204] measured such products as astatine, protactinium and radium in uranium targets bombarded with 1-3 Bev protons in the Brookhaven Cosmotron. FRIEDMAN and GORDON[205] overcame many experimental difficulties and succeeded in applying the mass spectrometric techniques to the measurement of the yields of cesium isotopes at proton energies of 1-3 Bev. ALEXANDER and GALLAGHER[206] made a detailed study of the yields and recoil ranges of iodine isotopes in uranium targets exposed to protons in the range 0.5 to 6.4 Bev.

---

200. B. Pate and A. Poskanzer, unpublished results.

201. R. H. Shudde, Ph.D. Thesis, University of California Radiation Laboratory Report, UCRL-3419, 1956.

202. C. L. Carnahan, Thesis, University of California Radiation Laboratory Report, UCRL-8020, 1957.

203. I. Dostrowsky, unpublished results.

204. B. D. Pate and G. Friedlander, Bull. Am. Phys. Soc. II 2, 198 (1957) and unpublished results.

205. L. Friedman and B. M. Gordon, unpublished results.

206. J. Alexander and M. F. Gallagher, unpublished results.

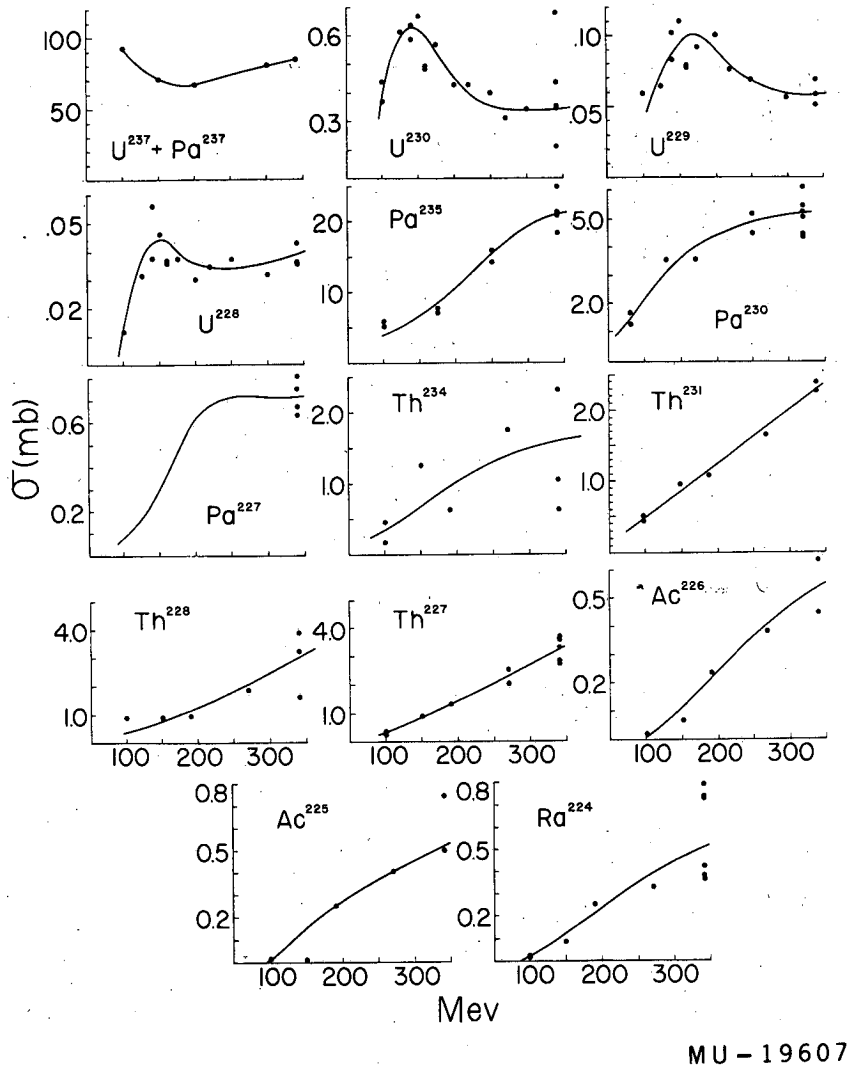

Fig. 12.67 Dependence of formation cross sections of spallation products of U^{238} on the energy of the incident protons. Lindner and Osborne.[199]

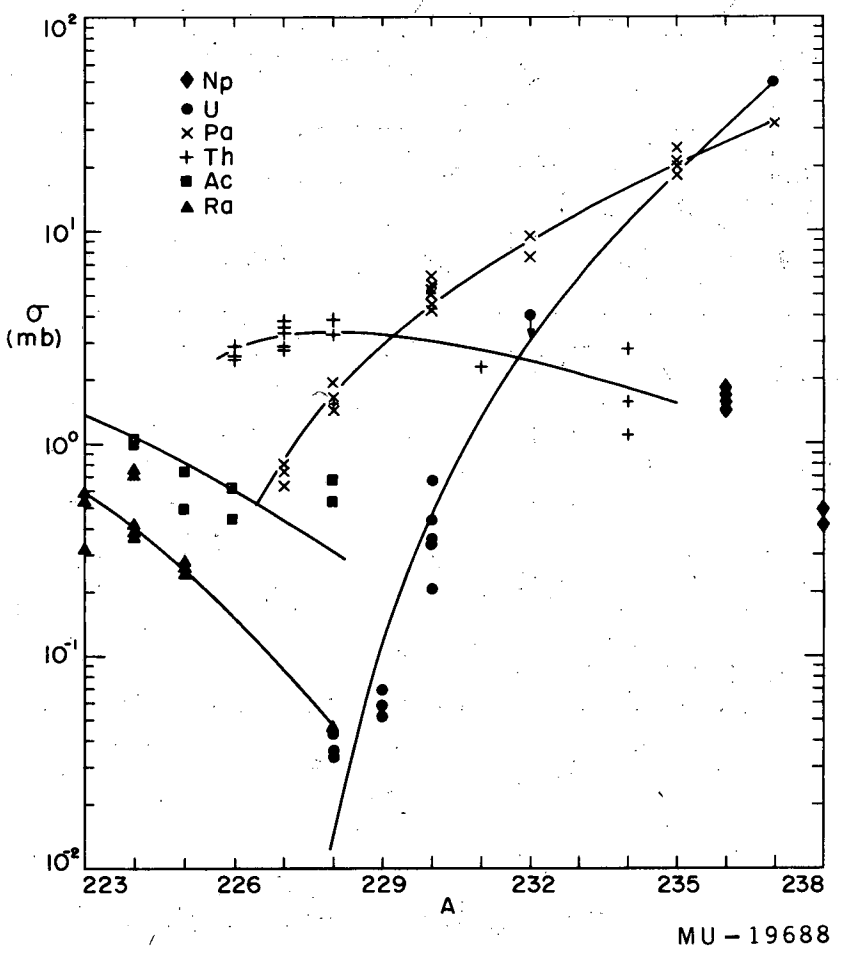

Fig. 12.68 Formation cross sections of disintegration products of U^{238} bombarded with 340 Mev protons. Lindner and Osborne.[199]

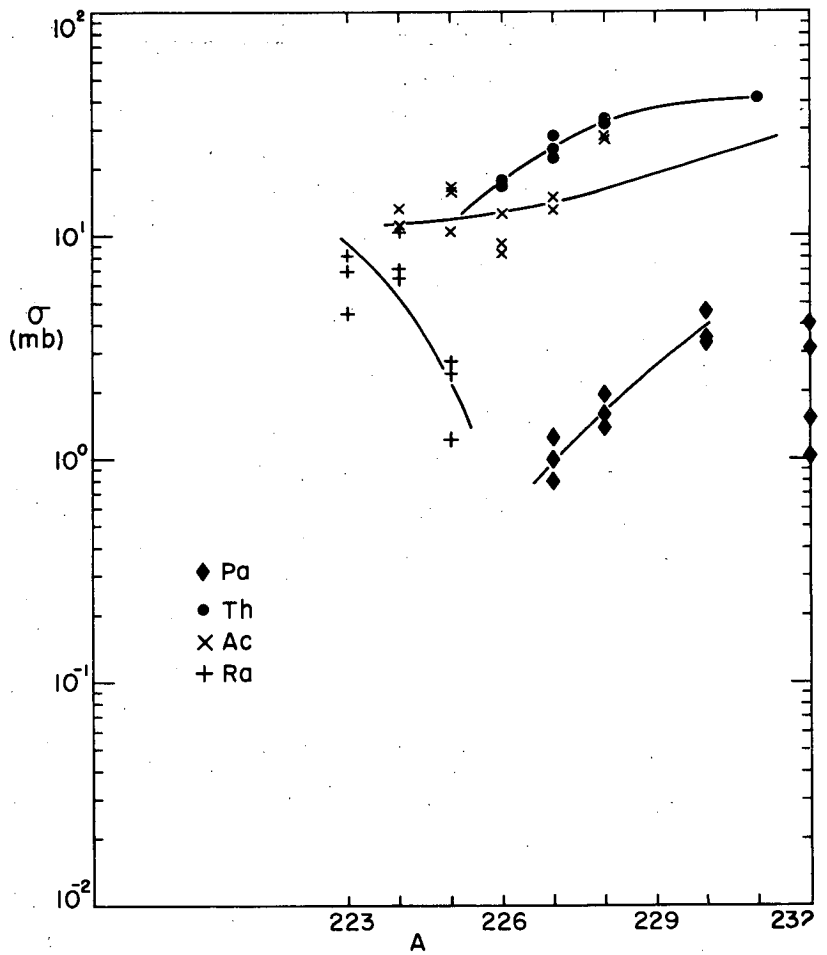

Fig. 12.69 Formation cross sections of disintegration products of Th^{232} bombarded with 340 Mev protons. Lindner and Osborne.[199]

Table 12.29 Yields (in millibarns) of the chief spallation products from the bombardment of uranium and thorium with 340 Mev protons Lindner and Osborne[198]

Nuclide	Yield from uranium target	Yield from thorium target
Np^{238}	0.46 ± 0.05	
Np^{236}	1.7 ± 0.1	
U^{237}	85	
U^{232}	< 4	
U^{230}	0.35 ± 0.12	
U^{229}	0.060 ± 0.005	
U^{228}	0.038 ± 0.002	
Pa^{235}	21 ± 2	
Pa^{232}	8.7 ± 1	2.6 ± 1.2
Pa^{230}	5.1 ± 0.5	4.2 ± 0.3
Pa^{228}	1.7 ± 0.2	1.7 ± 0.2
Pa^{227}	0.71 ± 0.06	1.0 ± 0.2
Th^{234}	1.8 ± 0.7	
Th^{231}	2.4 ± 0.1	68 ± 3
Th^{228}	2.9 ± 0.9	30 ± 3
Th^{227}	3.3 ± 0.4	22 ± 5
Th^{226}	2.7 ± 0.2	17 ± 0.3
Ac^{228}	0.62 ± 0.08	28 ± 0.1
Ac^{227}		14 ± 0.8
Ac^{226}	0.54 ± 0.09	10 ± 1.6
Ac^{225}	0.62 ± 0.13	14 ± 3
Ac^{224}	1.05 ± 0.05	12.5 ± 0.9
Ra^{228}	0.043	
Ra^{227}		> 0.7
Ra^{225}	0.26 ± 0.02	2.1 ± 0.5
Ra^{224}	0.58 ± 0.18	8.0 ± 1.5
Ra^{223}	0.48 ± 0.11	6.7 ± 1.4
At^{210}	1.2	2.4
Pb^{210}	1.7	13
Bi^{210}	1.6	26

Table 12.30 Cross sections for production of nuclides from uranium bombarded by 5.7-Bev protons

Nuclide	Cross section* (millibarns)	Type of yield**
Be^{7}	15.	C
Na^{22}	2.4	C
Na^{24}	12.	C
Mg^{28}	3.8	C
Si^{31}	2.4	C
P^{32}	1.8	I
P^{33}	0.87	C
S^{35}	3.7	C
S^{38}	0.77	C
Cl^{34m}	1.1	C
Cl^{38}	4.5	I
Cl^{39}	2.5	C
K^{42}	7.3	I
K^{43}	4.5	C
$K^{44,45}$	2.9	C
Ca^{45}	5.6	C
Ca^{47}	1.6	C
Mn^{52}	1.3(ground state only)	~I
Mn^{56}	7.1	C
Fe^{52}	0.045	C
Fe^{59}	3.7	C
Co^{61}	6.5	C
Ni^{65}	2.8	C
Ni^{66}	1.6	C
Cu^{61}	0.53	C
Cu^{64}	5.4	I
Cu^{67}	4.0	C
Zn^{69m}	2.0	C
Zn^{72}	0.68	C
Ga^{68}	7.1	I

Table 12.30 (cont'd.)

Nuclide	Cross section* (millibarns)	Type of yield**
Ga^{72}	5.4	~I
Ga^{73}	6.1	C
Mo^{99}	42.	C
Ru^{103}	28.	C
Ru^{105}	28.	C
Ru^{106}	25.	C
Pd^{109}	23.	C
Pd^{111m}	2.7	C
Pd^{111}	7.2	C
Pd^{112}	1.1_5	C
Ag^{110m}	3.0	I
Ag^{111}	$21._5$	C
Ag^{112}	9.5	~I
Ag^{113}	15.	C
Ag^{115}	7.3	C
Cd^{115m}	9.5	C
Cd^{115}	28.	C
Cd^{117m}	13.	C
In^{111}	5.9	C
In^{114m}	4.8	I
Ba^{128}	20.	C
Ba^{140}	32.	C
La^{140}	0.9	I
$La^{132,133,141}$	29.	-
Ta^{178}	5.9	I
Ta^{183}	8.6	C
Pb^{204m_2}	15.	~I
Pb^{209}	3.9	C
Pb^{212}	0.47	C
Bi^{210}	3.0	C

*Cross sections are based on a value of 10.5 mb for the monitor reaction $Al^{27}(p,3pn)Na^{24}$.

**C and I are used to designate cumulative yields and independent yields, respectively.

The yield of isotopes across the entire range of mass numbers is of the order of a few millibarns or higher. There still remains a maximum centered roughly at mass 110 indicating the importance of binary fission, but the fission product region is not at all definitely separated from lighter and heavier mass products by valleys of low yields. Yields in the mass region 100-140 are lower at 5.7 Bev than at 340 Mev while the yields below mass 100 and above mass 140 have risen markedly. The yield of Na^{24} at 5.7 Bev is 200 times as high as it is at 340 Mev; the P^{32} yield is 250 times as high as at 480 Mev; the Fe^{59} yield is 20 times higher than at 340 Mev; the yield of Ba^{210} is about 10 times as high as at 340 Mev; etc.

CARETTO, HUDIS and FRIEDLANDER[207] measured the cross sections for the production of Na^{24} and F^{18} in uranium targets bombarded at a series of proton energies ranging up to 6 Bev. They compared these numbers with similar determinations in other target elements. These excitation functions rise steeply above a threshold value of roughly 0.5 Bev proton energy and level off at values of the magnitude of millibarns for incident protons above a few Bev. The threshold value of ~0.5 Bev suggests that meson production may play a significant role in the mechanism leading to these products. Figures 12.70 and 12.71 show the production cross sections for Na^{24} and F^{18} as a function of target number. The striking feature of these curves is the rise in the cross section with target mass number above a minimum at mass 170. It may be that this effect is meson-related; i.e. in a heavy target the mesons produced in the high energy cascade have a greater probability of being reabsorbed and making their kinetic and rest energy available for fragmentation of the nucleus. The high yields from the lightest targets are most likely end products of the normal cascade-evaporation mechanism.

In the mass region where the typical fission products are found a characteristic feature is a very flat variation in cross section over the isotopes of a given element. SHUDDE[201] found that the yield of the neutron-deficient Ba^{128} was almost the same as that of neutron-rich Ba^{140}. ALEXANDER and GALLAGHER[206] measured the yield of 10 iodine isotopes stretching from I^{121} to I^{135} and found them all to lie in the narrow range of 2.3 to 6.0 millibarns. It may be that some of the yield of the products with great neutron deficiency may be contributed by a fragmentation rather than a fission process, but clear evidence on the nature of this contribution is lacking.

207. A. A. Caretto, J. Hudis and G. Friedlander, Phys. Rev. 110, 1130 (1958).

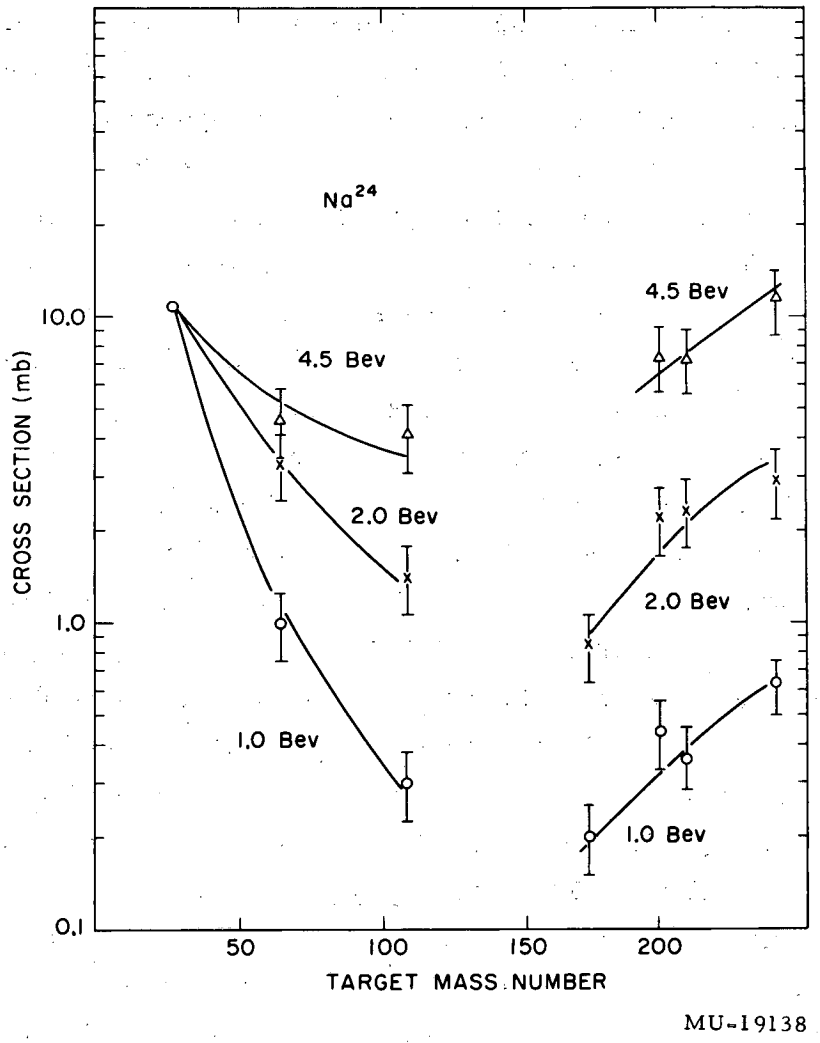

Fig. 12.70 Formation cross section of Na^{24} versus target mass number. Uranium points are at extreme right. Caretto, Hudis and Friedlander.[207]

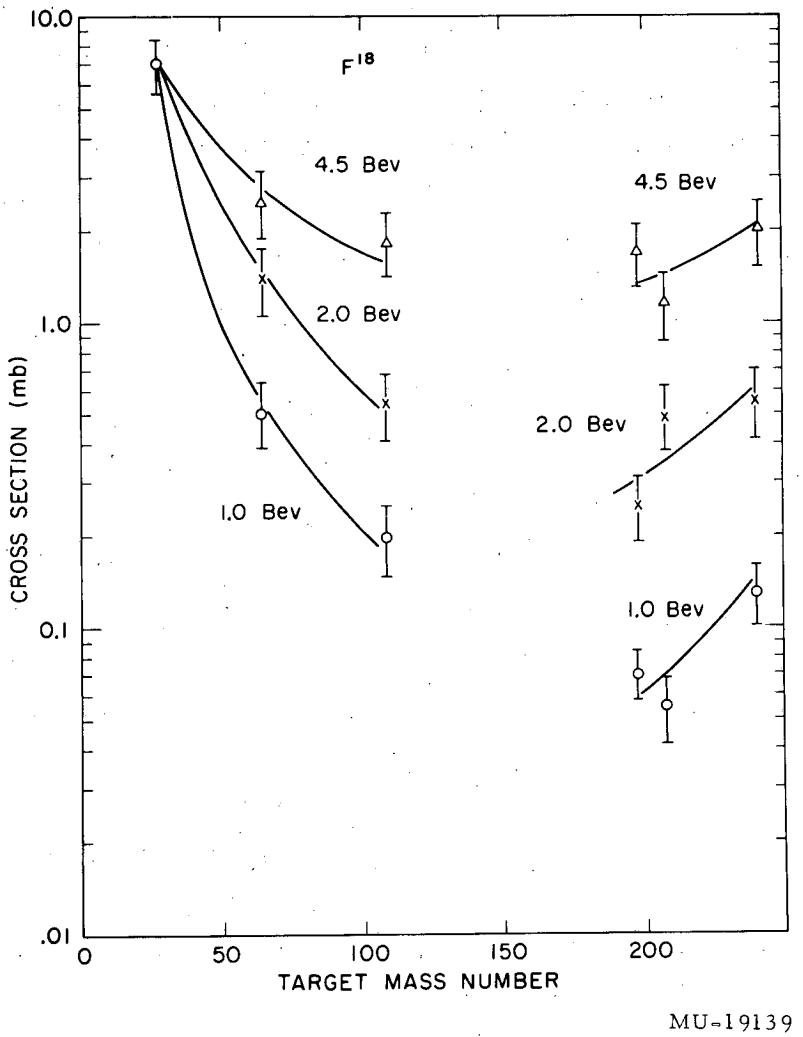

Fig. 12.71 Formation cross section for F^{18} versus target mass number. Uranium points on extreme right. Caretto, Hudis, and Friedlander.[207]

12.3 FISSION INDUCED BY MESONS

Slow negative π-mesons are absorbed by heavy nuclei with high probability and this absorption is followed by fission in a high percentage of cases. In this respect pions have a superficial resemblance to slow neutrons, but the mechanism of pion reactions is distinctly different. The negative meson is first captured into one of the Bohr orbits around the nucleus. It then interacts with a pair of nucleons as follows:

$$\pi^- + N + P \longrightarrow N + N + 140 \text{ Mev}$$

or

$$\pi^- + P + P \longrightarrow N + P + 140 \text{ Mev.}$$

The rest energy of the pion is nearly all converted into the kinetic energy of the two nucleons, which may escape from the nucleus or may undergo collisions with other nucleons (nuclear cascade) resulting in the deposition of considerable amounts of excitation energy in the nucleus.[209] It has been suggested that the nucleon pair absorption of the pion occurs close to the nuclear surface and that one of the resulting two 70 Mev particles has a high probability of escape without further interaction. Aside from this, the distribution of excitation energies might be expected to resemble that left in targets bombarded with 140 Mev protons. According to Fig. 12.50 above, the average excitation energy deposited in uranium targets is about 80 Mev for this case. Even if this should turn out to be somewhat overestimated for the pion case, it is clear that the excitation energy is high enough to cause fission to be a prominent process in the de-excitation stage of the reaction. With target elements lower in atomic number, this will, of course, not be so true. This model for the fission of heavy elements bombarded with π^- mesons is in accord with the experimental data which have been collected.

It might be expected that fission induced by muon capture in heavy nuclei would be somewhat different since in muon capture most of the rest

---

209. A Monte Carlo calculation of the interaction of zero energy mesons with uranium, including the development of the nucleonic cascade, is reported by Metropolis and co-workers, Phys. Rev. 110, 205, 1958. The basic assumptions of a simplified model of the interaction are given, but many of the detailed results are unpublished.

mass is expected to be carried off in the form of neutrino energy leaving only a small amount of energy for nuclear excitation.

Most work on meson-induced fission has been done with nuclear emulsions impregnated with heavy element compounds. Radiochemical studies have been difficult because of the low beam intensities available. Fission induced by slow π^- mesons was first noted in the Soviet Union in 1951 by two groups, working independently, one led by PERFILOV[210-215] and another by BELOVITSKII and FRANK.[216] Simultaneously, in the United States, studies of this kind were initiated by AL-SALAM[217] and by JOHN and FRY.[218] In later years the Russian publications have been more numerous and detailed.

Independent evaluations of the probability of fission of uranium upon capture of a π^- meson have centered around a value of 0.5. This value is not precise because of uncertainties in measuring the flux of mesons, the concentration of the uranium in the emulsion, the distribution of the uranium within the emulsion and the relative absorption of mesons in uranium compared to the light elements in the emulsion. A radiochemical determination which will be mentioned below,[221] gave a value of 0.48 ± 0.09. Emulsion studies of the probability of fission of bismuth and tungsten resulted in the lower values of ~0.02 and ~0.002, respectively.[210-212]

---

210. N. A. Perfilov, N. S. Ivanova, O. V. Lozhkin, V. I. Ostroumov, and V. P. Shamov, pp. 79-96. Meetings of the Division of Chemical Sciences, Session of the Academy of Sciences of the USSR on the Peaceful Uses of Atomic Energy, July 1-5, 1955, Moscow. English translation available from Superintendent of Documents, U.S. Government Printing office.

211. N. A. Perfilov, O. V. Lozhkin and V. P. Shamov, J.E.T.P., USSR 28, 655 (1955); Soviet Physics, JETP 1, 439 (1955); Dokl. Akad. Nauk. SSSR 103, 417 (1955).

212. N. A. Perfilov and A. S. Ivanova, J.E.T.P., USSR 29, 551 (1955); Soviet Physics JETP 2, 433 (1956).

213. O. V. Lozhkin and V. P. Shamov, J.E.T.P., USSR 28, 739 (1955); Soviet Physics JETP 1, 587 (1955) letter.

214. N. S. Ivanova, Soviet Physics JETP 7, 955 (1958).

215. N. S. Ivanova, Soviet Physics JETP 4, 597 (1957).

216. Belovitskii, Romanova, Soukhov and Frank, J.E.T.P. USSR, 28, 729 (1955) and 29, 537 (1955). Soviet Physics JETP 2, 249 (1956) and 2, 493 (1956).

217. Sue Gray Al-Salam, Phys. Rev. 84, 254 (1951).

218. W. John and W. Fry, Phys. Rev. 91, 1234 (1953).

Fission tracks in uranium-loaded emulsions have ranges of the same magnitude as those from slow neutron induced fission. Thus, as in other high energy fission processes, the energy of excitation is not converted into kinetic energy of the fragments. The ranges of the two fragments in the majority of cases is equal indicating a preference for fission into two fragments of equal size. The distribution of the ranges around a mean value of 12 microns is nearly the same as that found when high energy protons are used as the bombarding particles in agreement with the fission mechanism just outlined. This distribution does not undergo much change with energy providing the energy is high. DENISENKO and co-workers[219,220] get the identical distribution of ranges whether slow pions, 300 Mev pions, 140 Mev protons, 350 Mev protons or 460 Mev protons are used.

DENISENKO and his co-workers[219] studied fission of uranium induced by 300 Mev π^+ mesons. The results are consistent with a fission mechanism consisting of interaction of the meson with a pair of nucleons (N,P) in the nucleus which must scatter with high kinetic energy at an angle close to 180°. These particles may escape or may initiate a nucleon-nucleon cascade. Excitation energy left in the initial interaction or in the cascade excites the nucleus above the fission threshold. The average number of charged particles per fission event is 1.03 compared to 0.56 observed when fission is induced with 350 Mev protons. The angular distributions of the ejected protons <u>with respect to each other</u> when 2 or 3 ejected protons are observed tends to peak at 180° and at 0° whereas in proton induced fission this distribution is isotropic. Both observations are in accord with the proposed mechanism. Fragment ranges show that symmetric fission is favored. IVANOVA[214] studied the fission of uranium by 280 Mev π^+ mesons using "relativistic" emulsions sensitive to very high energy protons. He found an average of 2.1 charged particles per fission event, a high percentage of these being protons of > 50 Mev energy. He saw π^+ mesons of considerable energy accompanying fission in many cases and concludes that about 10% of the fission events are preceded by π^+ meson scattering with

---

219. Denisenko, Ivanova, Novikova, Perfilov, Prokoffieva and Shamov, Phys. Rev. <u>109</u>, 1779 (1958).

220. N. S. Ivanova in Physics of Fission, an English translation by Consultants Bureau Inc., of Supplement No. 1 to the Soviet Journal of Atomic Energy, 1957.

large energy transfer while the rest follow meson absorption by nucleon pairs, mostly n,p pairs. The estimated fission cross section is $(1.0 \pm 0.2) \times 10^{-24}$ cm^2. Further details of this study are given in a Geneva paper by IVANOVA, OSTROUMOV and FILOV.[220a]

RUSSELL and TURKEVICH[221] have performed a radiochemical study of the fission of U^{238} caused by capture of slowed π^- mesons. The fission yields of about 40 species were determined. The results are plotted in Fig. 12.72. For comparison purposes, the same authors also determined the mass-yield curve for fission of U^{238} induced by 134 Mev protons. The results are shown in Fig. 12.73. These curves are remarkably similar. π^- - fission of uranium is typical high-energy fission with the broad symmetric distribution of fission products. The average neutron multiplicity in this form of fission is 10-14; the value differs slightly whether one refers to symmetric mass splits ($\bar{\nu} \sim 14$) or to moderately asymmetric mass splits ($\bar{\nu} \sim 10$-11). The excitation energy was estimated to be about 77 Mev which can be compared with the ~90 Mev estimated by emulsion techniques[210] and ~80 Mev calculated by Monte Carlo methods.[209] RUSSELL and TURKEVICH[221] measured the fission probability per pion stopped in uranium and obtained a value of 0.48 ± 0.09.

The Monte Carlo calculations[209] indicate that the primary result of the meson capture in uranium and the subsequent cascade initiated by two high energy nucleons is the production of an assemblage of protactinium nuclei with a broad distribution in excitation energy from 0 to 140 Mev. Thorium nuclei are also produced with a broad distribution in excitation energy, but not in such large numbers. The excitation energy of this assemblage of excited nuclei is dissipated by neutron evaporation with some high-energy fission occurring at each stage of evaporation.

The fission product distribution observed in radiochemical experiments can give only a composite picture of end-results of a variety of fissioning systems. Thus pion-induced fission is closely analogous to fission induced by charged particles of high energy.

220a. N. S. Ivanova, V. I. Ostroumov and R. A. Filov, Paper P/2039, Volume 15, Proceedings of the Second U.N. Conference on the Peaceful Uses of Atomic Energy, Geneva, 1958.

221. Russell and A. Turkevich, unpublished results; I. J. Russell, Ph.D. Thesis, University of Chicago, December, 1956, unpublished.

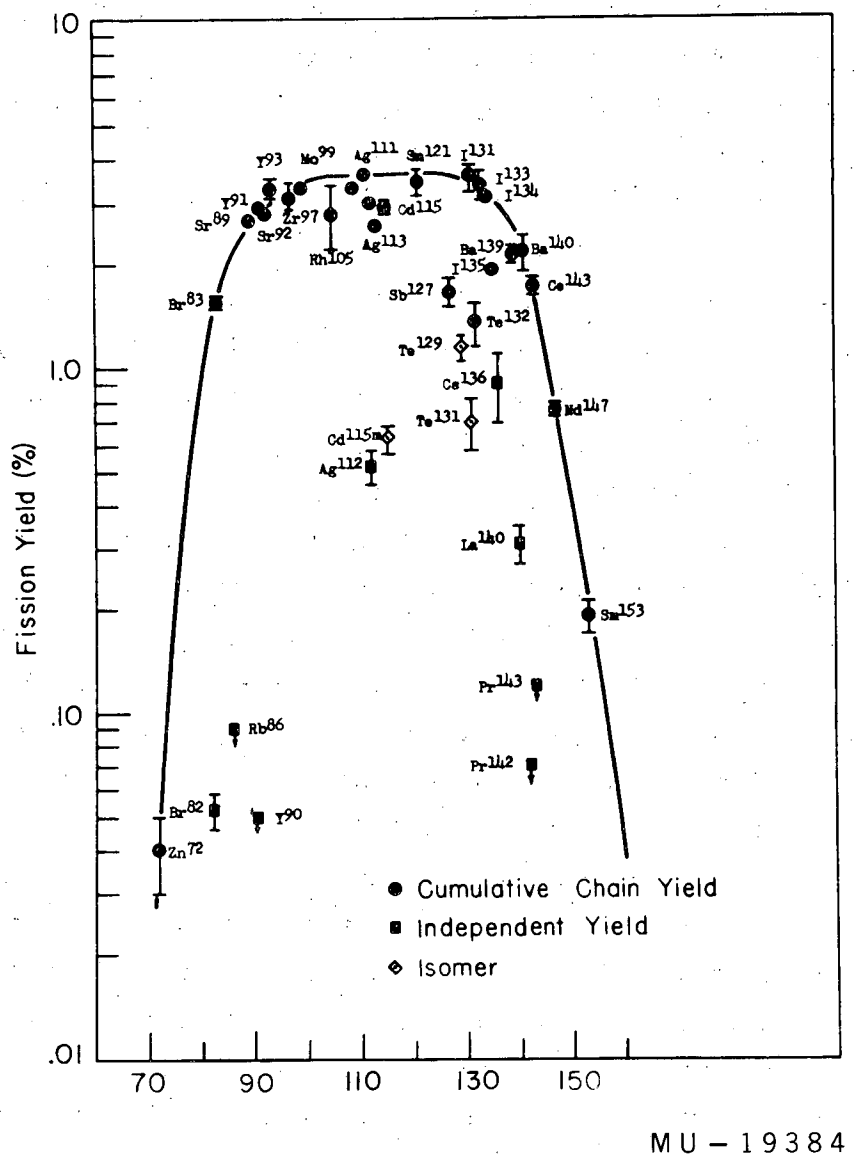

Fig. 12.72 Distribution of products from the fission of natural uranium induced by slow π^- mesons (Russell and Turkevich)[221]

The ordinate is the absolute fission yield in percent obtained by normalizing the envelope of the distribution to two hundred fission yield percent. The abscissa represents the mass of the fission product. Circles represent cumulative chain yields; solid squares represent independent chain yields; open squares rotated through ninety degrees represent cumulative chain yields of isomeric products.

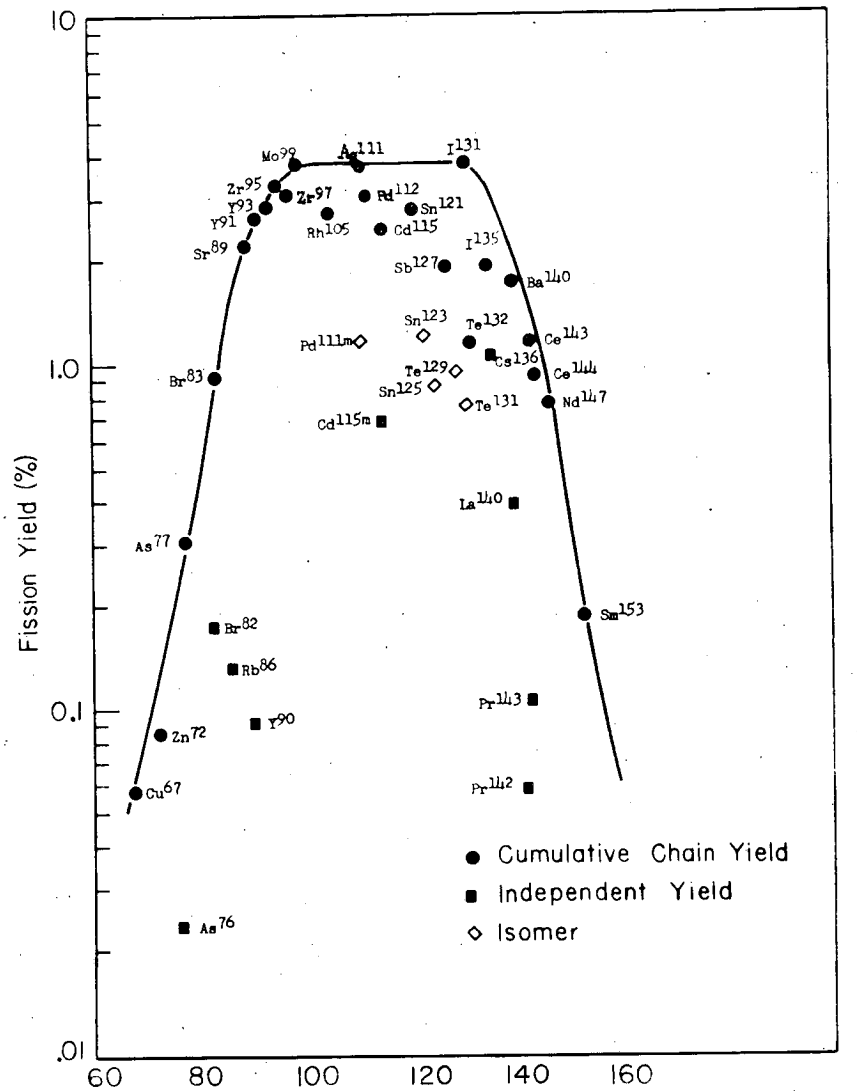

MU-19381

Fig. 12.73 Distribution of products from the fission of natural uranium induced by 134 Mev protons (Russell and Turkevich).[221]

The ordinate represents the absolute fission yield in percent, obtained by normalizing the envelope of the distribution to two hundred fission yield percent. The abscissa represents the mass of the fission product. Circles represent cumulative chain yields; solid squares represent independent chain yields; open squares rotated through ninety degrees represent cumulative chain yields of isomeric products.

The possibility of the induction of nuclear fission by muons has been mentioned by WHEELER[222] but has received scant experimental attention. There are two ways in which muons could induce fission.

(a) By capture of a μ^- particle in an outer Bohr orbit followed by transitions down through the 2s - 2p - 1s states. During these transitions an energy of about 7 Mev is released in a heavy element which is greater than the photofission threshold. In an appreciable fraction of cases, which in principle can be calculated, this 7 Mev will be transferred to the nucleus by a non-radiative transition.

(b) By nuclear capture according to the reaction

$$\mu^- + p \longrightarrow n + \nu .$$

In this process about 15 Mev is released. ZARETSKY[223] has attempted to calculate the nuclear excitation from non-radiative capture into mesonic orbits in order to evaluate the possibility of fission catalysis by mesons; the results were only qualitative.

An experimental attempt to detect uranium fission by μ^- mesons in cosmic rays was negative.[224] JOHN and FRY[225] using uranium-loaded nuclear emulsions observed 7 sets of fission tracks at the end of μ^- tracks and calculated a fission-to-capture ratio of about 0.15. MIHUL and PETRASHCU[226] repeated the experiment with considerably better statistics. 26,975 μ^- meson endings were considered in uranium-loaded nuclear plates and 59 fission events were found. A fission-to-capture ratio of 0.08 was estimated. These two studies do not distinguish between fission mechanisms (a) and (b). They are furthermore, subject to considerable error because of assumptions on the microscopic distribution of uranium in the plates and particularly on the relative absorption of mesons by uranium and by the other elements present.

---

222. J. A. Wheeler, Rev. Modern Phys. 21, 133 (1949).

223. D. F. Zaretsky, Proceedings of the Second International U.N. Conference on the Peaceful Uses of Atomic Energy, Geneva, 1958, (United Nations, New York, 1958), Volume 15, p. 175.

224. W. Galbraith, W. J. Whitehouse, Phil. Mag. 44, 77 (1953).

225. W. John and W. F. Fry, Phys. Rev. 91, 1234 (1953).

226. A. K. Mihul and M. G. Petrashcu, Dubna Report, Joint Institute for Nuclear Research, 1958, unpublished.

DIAZ, KAPLAN, MacDONALD and PYLE[227] used multiple scintillation counters in a delayed coincidence experiment to obtain the relative probabilities of the two fission mechanisms. The fission induced by BOHR orbit atomic transitions of the μ^- meson should occur promptly ($\tau \ll 10^{-9}$ sec), whereas those due to nuclear capture of the μ^- meson should occur with the characteristic mean lifetime of a μ^- meson stopped in uranium ($8.8 \pm 0.4 \times 10^{-8}$ sec). This experiment gave a strong indication that the nuclear capture mechanism (b) was dominant. The percentage of fissions due to non-radiative atomic capture was set at 5.6 ± 2.7 percent.

227. J. Diaz, S. N. Kaplan, B. MacDonald, and R. V. Pyle, Phys. Rev. Letters 3, 234 (1959).

12.4 PHOTOFISSION

12.4.1 Photofission Probability. The nuclear fission of heavy elements following the nuclear absorption of electromagnetic energy was predicted by BOHR and WHEELER[228] in their famous 1939 paper. The first evidence for a photofission process was obtained in 1941 by HAXBY, SHOUPP, STEPHENS and WELLS[229] who bombarded uranium and thorium with 6.1 Mev gamma rays originating in the reaction, $F^{19}(p,\alpha\gamma)O^{16}$. They estimated cross sections of 3.5 and 1.7 millibarns, respectively, for the fission of the two elements. Their results were confirmed by ARAKATSU and co-workers.[230]

All research in photonuclear reactions is hampered by the very limited numbers of monochromatic gamma rays which are available in sufficient intensity for significant experimental work. This shortage of monochromatic gamma sources has forced experimentalists to use the high intensity bremsstrahlung beams obtained from betatrons, synchrotrons and electron linear accelerators. The continuous distributions of photon energy up to the maximum energy of the electrons is an unavoidable disadvantage in the use of bremsstrahlung beams.

The pioneer study of this type was carried out by BALDWIN and KLAIBER[231] using the General Electric Company 100 Mev betatron. Fission was detected in uranium and thorium samples by observing the ionization pulses produced by fission fragments in an ionization chamber. It was necessary to blank out the pulses of ionization caused by the huge x-ray beam by using a double ion chamber. The fissionable material was placed on the inner walls of only one of the two chambers. Only when the ionization in this chamber was much greater than in the second was a fission event registered. This double chamber technique has been standard practice in subsequent photofission measurements in many other laboratories. BALDWIN and KLAIBER[231] found an appreciable fission cross section in both uranium and thorium, the fissionability of the former being about twice that of the latter.

---

228. N. Bohr and J. A. Wheeler, Phys. Rev. 56, 426 (1939).

229. R. O. Haxby, W. E. Shoupp, W. E. Stephens and W. A. Wells, Phys. Rev. 59, 57 (1941).

230. Arakatsu et al., Proc. Phys. Math. Soc., Japan 23, 440 (1941).

231. G. C. Baldwin and G. S. Klaiber, Phys. Rev. 71, 3 (1947).

The raw experimental data in such an experiment show the cross section as a function of the maximum energy of the bremsstrahlung beam, which in itself is not a very revealing correlation. The cross section so observed may be expressed:

$$\sigma_{integrated} = \int_{0}^{E_{max}} \sigma(E)\, N_{(E_{max},E)}\, dE \qquad (12.26)$$

where E_{max} is the maximum energy of the bremsstrahlung beam

$\sigma_{(E)}$, the desired quantity, is the cross section for monoenergetic γ-rays of energy E

$N_{(E_{max},E)}$ is the number of photons with energy E in the bremsstrahlung spectrum of maximum energy E_{max}.

If $N_{(E_{max},E)}$ and $\sigma_{integrated}$ are known exactly as a function of E_{max}, one can in principle, calculate σ_E over a range of E up to E_{max}. The function $N_{(E_{max},E)}$ has been calculated by BETHE and HEITLER.[232] The exact expressions for the photon distributions are complex but to a first approximation $N_{(E_{max},E)}$ can be evaluated from the expression

$$E\, N_{(E_{max},E)}\, dE = \text{constant}. \qquad (12.27)$$

Using this approximate expression or the more exact expressions for the bremsstrahlung spectrum and using many experimental values of the integrated cross section taken at a series of values of E_{max} one can proceed to calculate $\sigma_{(E)}$ by the "photon difference" method described by KATZ and CAMERON.[233] The application of the photon difference method has been simplified by the work of PENFOLD and LEISS[234] who developed an inverted matrix method for such computations.

BALDWIN and KLAIBER[231] published their work before these mathematical techniques of KATZ and CAMERON[233] or PENFOLD and LEISS[234] were developed, but they were able to deduce a $\sigma_{(E)}$ curve for the photofission of uranium and thorium

---

232. H. A. Bethe and W. Heitler, Proc. Roy. Soc. London, A146, 83, 1934; W. Heitler, Quantum Theory of Radiation, Oxford University Press, New York, 1944, 2nd Ed; for an extensive review of the radiative processes occurring during the slowing of electrons in matter, see Bethe and Ashkin, Part II, Vol. I. "Experimental Nuclear Physics", E. Segrè, editor, Wiley, 1953.

233. L. Katz and A. G. W. Cameron, Can. J. Phys. 29, 518 (1951).

234. A. S. Penfold and J. E. Leiss, Phys. Rev. 114, 1332 (1959).

by an approximate calculation method similar in principle. Their most significant finding was that the cross section rose rapidly from a threshold value near 5 Mev to a maximum at 18 or 20 Mev and then dropped steeply. Above 30 Mev the fission cross section was quite low. More recent work has located the peak of the cross section at somewhat lower values, but otherwise has amply confirmed this result. Furthermore, measurements on photoneutron emission in thorium and uranium has shown a similar maximum yield at a broad resonance centered near 15 Mev. These results show that the photonuclear processes in the heaviest elements are characterized by the "giant" dipole resonance which is the dominant feature of photonuclear reactions in all target elements throughout the Periodic System of the Elements. A clear explanation of the fundamental nature of this high frequency gamma resonance has not been developed. In the light elements there has been considerable success in applying the independent particle model to explain the photonuclear resonance. As theorists learn more about the nature of the residual interactions between particle outside of closed shells and are better able to handle independent particle model calculations when many particles beyond closed shells are present in the nucleus there is hope that the calculation of photonuclear absorption may be extended satisfactorily to more complex nuclei. WILKINSON[235,236] has made many contributions in this direction. GOLDHABER and TELLER[237] became interested in the giant resonance phenomenon in the heavy elements when BALDWIN and KLAIBER[231] published their photofission results. They advanced a tentative explanation based on the notion that the nucleus as a whole received a dipole vibration, consisting of the motion of the bulk of the protons in a direction opposite to the motion of the neutrons at a fixed resonance frequency.

---

235. D. H. Wilkinson, "Nuclear Photodisintegration", Ann. Rev. Nuclear Sci. 9, 1 (1959).

236. D. H. Wilkinson, Proceedings of the Amsterdam Conference, Physica (1956).

237. M. Goldhaber and E. Teller, Phys. Rev. 74, 1046 (1948).

It is beyond the scope of our review to discuss the interesting theoretical developments in photonuclear processes. We refer the reader to several excellent reviews.[235-241]

The excitation energy brought into a heavy nucleus like U^{238} by photoabsorption is disposed of by neutron emission or fission with the possibility of a fission-evaporation competition at each step of an evaporation chain. If this view is correct, the following definitions supply some useful terminology:

$$\sigma_{total} = \sigma_{\gamma,\gamma'} + (\sigma_{\gamma,n} + \sigma_{\gamma,2n} + \dots) + (\sigma_{\gamma,f} + \sigma_{\gamma,nf} + \sigma_{\gamma,2nf} + \dots) \tag{12.28}$$

where $\sigma_{(\gamma,nf)}$ refers to fission which occurs after the emission of one neutron, and the meaning of the other terms is plain.

$$\sigma_{\gamma,F} = \sigma_{\gamma,f} + \sigma_{\gamma,nf} + \sigma_{\gamma,2nf} + \dots \tag{12.29}$$

$$\sigma_{\gamma,N} = (\sigma_{\gamma,n} + 2\,\sigma_{\gamma,2n} + 3\,\sigma_{\gamma,3n} + \dots) + \bar{\nu}\,\sigma_{\gamma,f} + (1 + \bar{\nu})\sigma_{\gamma,nf} + (2 + \bar{\nu})\sigma_{\gamma,2nf} + \dots \tag{12.30}$$

where $\bar{\nu}$ is the average number of neutrons emitted in fission, a number about 2.5. This $\bar{\nu}$ value should not be confused with the average number of neutrons obtained for every one fission that takes place in a bulk of irradiated material.

This terminology was introduced by GINDLER, HUIZENGA and SCHMITT.[242]

Most experimental work provides a measure of $\sigma_{\gamma,F}$ or $\sigma_{\gamma,N}$ while the other cross sections must be deduced by an indirect analysis. Let us discuss some recent data, starting first with measurements of $\sigma_{\gamma,F}$. Three general methods have been used. The first is the differential ion chamber method of

---

238. G. R. Bishop and R. Wilson, "The Nuclear Photoeffect", Vol. 42, Handbuch der Physik, Springer-Verlag, 1957, S. Flugge, Editor.

239. K. Strauch, "Recent Studies of Photonuclear Reactions", Ann. Rev. Nucl. Sci. 2, 105 (1953).

240. J. S. Levinger, "Theories of Photonuclear Reactions", Ann. Rev. Nucl. Sci. 4, 13 (1955).

241. Titterton, Photodisintegration Experiments with Nuclear Emulsions, Progr. Nucl. Phys. 4, 1 (1958).

242. J. Gindler, J. Huizenga and R. Schmitt, Phys. Rev. 104, 425 (1956).

BALDWIN and KLAIBER.[231] This has been used also by OGLE and McELHINNEY,[243] by LAZAREVA and co-workers[244] and by KATZ, BAERG and BROWN.[245] A second general method is the collection of fission fragments recoiling out of a heavy element foil and the analysis of the radioactive fission products, a method which has been exploited by McELHINNEY and OGLE,[246] by ANDERSON and DUFFIELD,[247] and WINHOLD and HALPERN.[248] The third general method is the radiochemical analysis of fission products present in a heavy element target after irradiation with a known flux of protons. This approach has been used by DUFFIELD and HUIZENGA,[249] by KATZ and co-workers,[250] by GINDLER, HUIZENGA and SCHMITT,[242] by SCHMITT and DUFFIELD[251] and others. The agreement between these various authors has been satisfactory.

Typical results are shown in Fig. 12.74 taken from the ion chamber measurements of KATZ, BAERG and BROWN.[245] Figure 12.75 shows the results of the transformation of these data into a photofission cross section versus proton energy curve, by the photon difference calculation cited above. It is customary to compare cross section data for the giant resonance by specifying the location of the cross section maximum, the width at half maximum and the integrated cross section $\int_0^E \sigma \, dE$. These values as derived from the analysis of KATZ, BAERG and BROWN[245] are listed in Table 12.31 together with similar data taken from the work of other authors.

---

243. W. E. Ogle and J. McElhinney, Phys. Rev. 81, 344 (1951).

244. Lazareva, Gavrilov, Valuev, Zatsepina, and Stravinsky, Conference of the Academy of Sciences of the USSR on the Peaceful Uses of Atomic Energy, July 1-5, 1955, Session of the Division of Physical and Mathematical Sciences (Consultants Bureau, New York, 1955), p. 217.

245. L. Katz, A. P. Baerg, and F. Brown, Paper P/200 in Volume 15, Proceedings of the Second U.N. International Conference on the Peaceful Uses of Atomic Energy, Geneva, 1958.

246. J. McElhinney and W. E. Ogle, Phys. Rev. 81, 342 (1951).

247. R. E. Anderson and R. B. Duffield, Phys. Rev. 85, 728 (1952); R. E. Anderson, B.S. Thesis, University of Illinois, 1951 (unpublished.)

248. E. J. Winhold and I. Halpern, Phys. Rev. 103, 990 (1956).

249. R. B Duffield and J. R. Huizenga, Phys. Rev. 89, 1042 (1953).

250. Katz, Kavanagh, Cameron, Bailey and Spintz, Phys. Rev. 99, 98 (1955).

251. R. A. Schmitt and R. B. Duffield, Phys. Rev. 105, 1277 (1957).

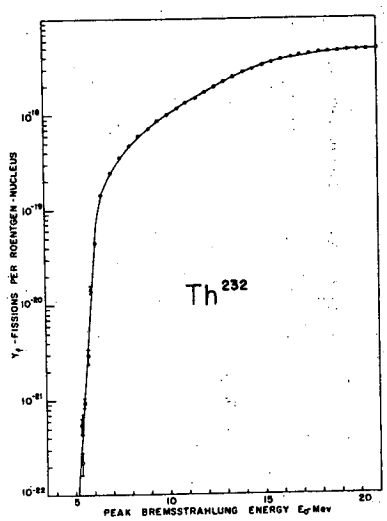
Th232
γf - FISSIONS PER ROENTGEN - NUCLEUS
PEAK BREMSSTRAHLUNG ENERGY E0, Mev

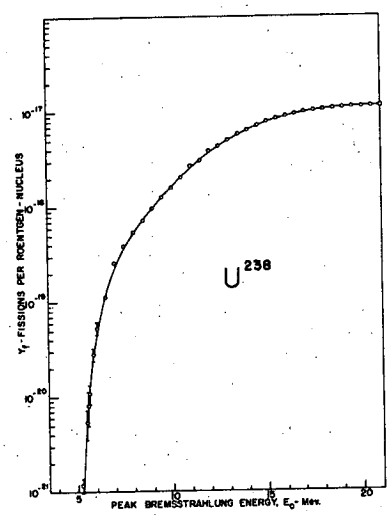
U238
γf - FISSIONS PER ROENTGEN - NUCLEUS
PEAK BREMSSTRAHLUNG ENERGY, E0 - Mev.

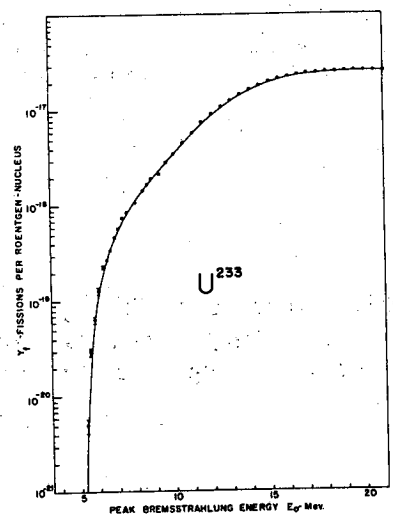
U233
γf - FISSIONS PER ROENTGEN - NUCLEUS
PEAK BREMSSTRAHLUNG ENERGY E0, Mev.

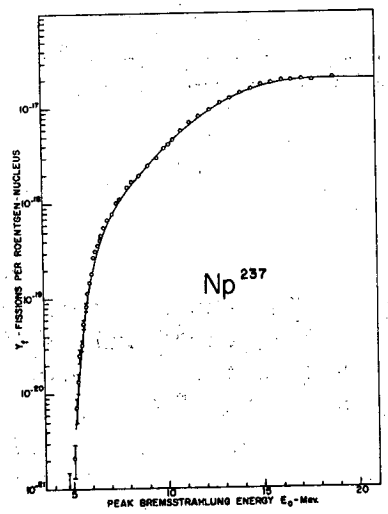
Np237
γf - FISSIONS PER ROENTGEN - NUCLEUS
PEAK BREMSSTRAHLUNG ENERGY E0 - Mev.

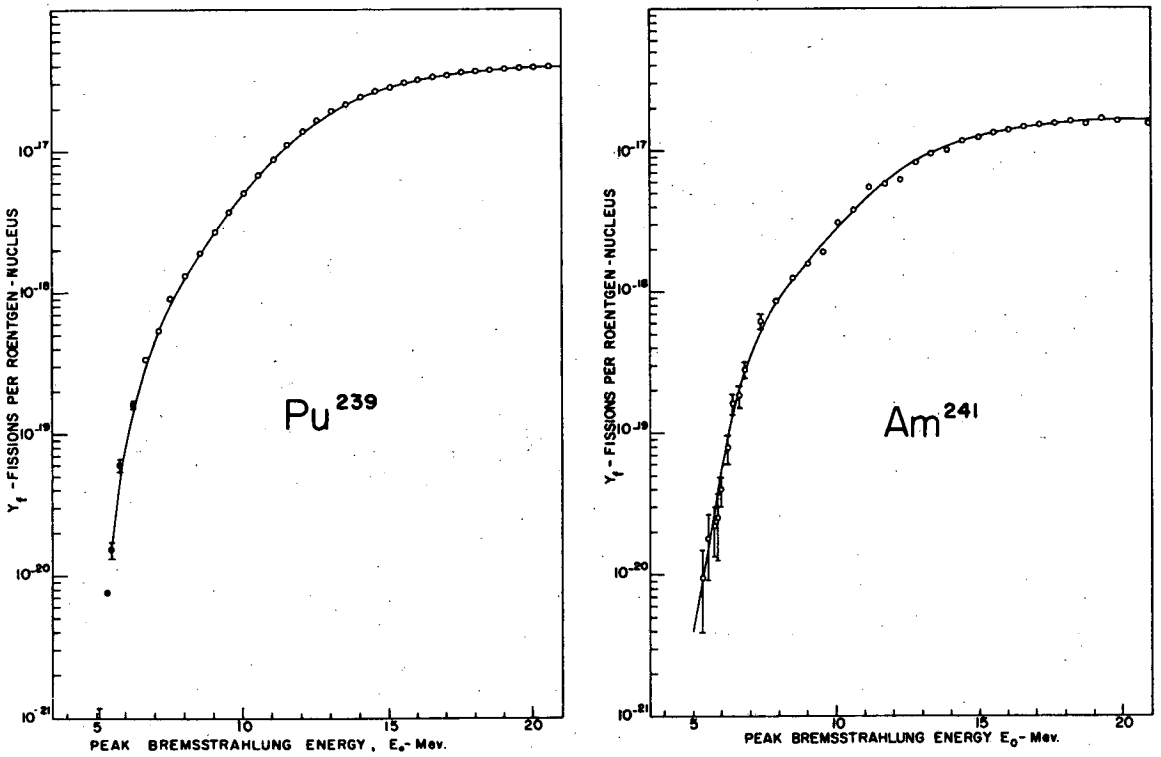

MU-19277

Fig. 12.74 Photofission yield curves for Th^{232}, U^{238}, U^{233}, Np^{237}, Pu^{239} and Am^{241}. Fissions per roentgen-nucleus versus maximum bremsstrahlung energy. From Katz, Baerg and Brown.[245]

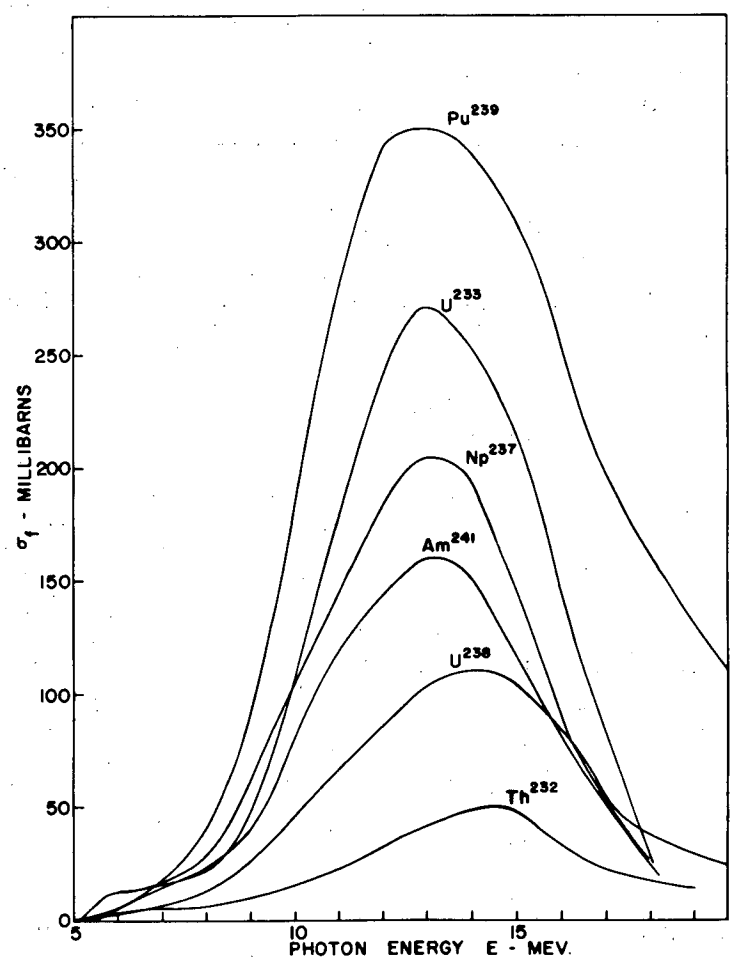

MU-19276

Fig. 12.75 Photofission cross sections versus photon energy for the 6 nuclei shown in the previous figure. From Katz, Baerg and Brown.[245]

Table 12.31 Characteristics of the giant resonance in photofission and photoneutron emission for heavy element nuclides

Reaction	σ_{max} (barns)	$E(\sigma_{max})$ (Mev)	Half width[c] (Mev)	$\int \sigma\, dE$ Mev-barns[d]	Reference
$Th^{232}(\gamma,F)$	0.051	14.1	7.0	0.64±0.06 (0-28)	a
$Th^{232}(\gamma,F)$	0.045	13.5	7.7	0.35 (0-20)	b
$Th^{232}(\gamma,F)$	0.048	14.5	6.0	0.32 (0-19)	c
$Th^{232}(\gamma,n)Th^{231}$	0.490	12.2	4.2	2.2 (0-20)	b
$Th^{232}(\gamma,N)$	0.80	14.5	5.6	6.61 (0-28)	a
$Th^{232}(\gamma,N)$	0.99	14.2	6.0	7.15 (0-22)	d
$U^{238}(\gamma,F)$[a]		16	5		e
$U^{238}(\gamma,F)$		15	8		f
$U^{238}(\gamma,F)$		14.6	6.8		g
$U^{238}(\gamma,F)$	0.18	14	7.6	1.2 (0-20)	h
$U^{238}(\gamma,F)$	0.125	14	8.8	1.1 (0-24)	i
$U^{238}(\gamma,F)$	0.20	14.0	6.7	1.7 (0-28)	a
$U^{238}(\gamma,F)$	0.160	13.7	5.8	1.0 (0-20)	b
$U^{238}(\gamma,F)$	0.110	14.0	6.4	0.76 (0-19)	c
$U^{238}(\gamma,n)U^{237}$	0.53	11	3.6	2.6 (0-20)	h
$U^{238}(\gamma,n)U^{237}$	0.400	12.0	5.0	2.1 (0-20)	b
$U^{238}(\gamma,N)$[b]		15.8	7.1		g
$U^{238}(\gamma,N)$	1.8	13	(5)	11.4 (0-27.5)	j
$U^{238}(\gamma,N)$	0.96	14	6.4	7.1 (0-25)	k
$U^{238}(\gamma,N)$	1.18±0.15	14.9	6.8	12.9±1.0(0-28)	a
$U^{238}(\gamma,N)$	1.29	15.2	6.4	9.74	d
$U^{233}(\gamma,F)$	0.27	13.0	5.6	1.62 (0-19)	c
$U^{233}(\gamma,N)$	1.67	14.0	6.0	11.2(0-22)	d
$Np^{237}(\gamma,F)$	0.205	13.0	5.7	1.26 (0-19)	c
$Pu^{239}(\gamma,F)$	0.350	13.0	7.4	2.65 (0-19)	c
$Pu^{239}(\gamma,N)$	1.58	13.6	6.3	11.6 (0-22)	d
$Am^{241}(\gamma,F)$	0.160	13.5	6.0	1.01 (0-19)	c

Table 12.31 (cont'd.)

a. (γ,F) indicates all processes initiated by a photon in which fission occurs i.e. $\sigma\gamma F = \sigma(\gamma,f) + \sigma(\gamma nf) + \sigma(\gamma 2nf) + \ldots$

b. (γ,N) indicates the total number of neutrons produced by the nuclear absorption of a photon. Because of the low probability of charged-particle emission, the cross section for the (γ,N) process may be represented by $\sigma(\gamma,N) = \sigma(\gamma,n) + 2\sigma(\gamma,2n) + 3\sigma(\gamma,3n) + \ldots \bar{\nu}\,\sigma(\gamma,F)$, where $\bar{\nu}$ represents the average number of neutrons produced by a gamma excited nucleus which eventually fissions. These neutrons may be emitted before fission occurs, may be a result of the fission process, or may be a combination of the two.

c. Half width is defined as the full width at half maximum.

d. Integration limits in Mev are given in parentheses following the integrated value.

References:

a. Lazareva et al., Moscow Conference, 1955.

b. Gindler, Huizenga and Schmitt, Phys. Rev. 104, 425 (1956).

c. Katz, Baerg and Brown, Geneva Conference, 1958.

d. Katz, et al., Can. J. Phys. 35, 470 (1957).

e. Baldwin and Klaiber, Phys. Rev. 71, 3 (1947).

f. Ogle and McElhinney, Phys. Rev. 81, 344 (1951).

g. Anderson and Duffield, Phys. Rev. 85, 728 (1952).

h. Duffield and Huizenga, Phys. Rev. 89, 1042 (1953).

i. Katz et al., Phys. Rev. 99, 98 (1955).

j. Jones and Terwilliger, Phys. Rev. 91, 699 (1953).

k. Nathans and Halpern, Phys. Rev. 93, 437 (1954).

We shall examine some details of the photofission curves after we discuss photoneutron measurements. Photoneutron yields can be measured by neutron counting or by radiochemical analysis for the heavy element product resulting from neutron emission. The first method determines the cross section $\sigma_{\gamma,N}$ whereas the second measures $\sigma_{\gamma,n}$ or $\sigma_{\gamma,2n}$ depending on the nuclide chosen for analysis. To count neutrons some research groups[244,252] use BF_3 counters with massive amounts of paraffin surrounding the target and detector system to reduce the energy of the neutrons to thermal energy. Calibration of the counting efficiency and elimination of background neutrons are severe experimental problems. WINHOLD and HALPERN[248] used neutron activation analysis to measure the neutron yields. The experimental neutron yield curves have the same shapes as those for photofission and the derived cross section curves show the same giant resonance. The cross sections for neutron production are, however, greater than for fission.

The $\sigma_{\gamma,N}$ curves have a different appearance in the threshold region than is the case for a bismuth or lighter target. In the latter case no neutrons are emitted for an incident gamma ray lower in energy than the neutron binding energy. A heavy element target can fission at a photon energy below the neutron binding energy and contribute neutrons to the observed $\sigma_{\gamma,N}$ via the $\bar{\nu}\,\sigma_{\gamma,f}$ term.

Radiochemical measurements of the $U^{238}(\gamma,n)U^{237}$ cross section have been made by DUFFIELD and HUIZENGA[240] and measurements of this cross section plus that of the $Th^{232}(n,\gamma)Th^{231}$ reaction have been made by GINDLER, HUIZENGA and SCHMITT.[242] Characteristics of the giant resonance for the photoproduction of these products are included in Table 12.31.

The photofission branching ratio, defined as

$$\frac{\sigma_{\gamma,f}}{\sigma_{\gamma,f} + \sigma_{\gamma,n}},$$

is of some interest. The most straightforward data come from radiochemical measurements of the $\sigma_{\gamma,n}$ yields compared to $\sigma_{n,f}$ measured by ion chamber measurements or radiochemistry. Some values for U^{238} and Th^{232} are listed in

---

252. L. Katz, K. G. McNeil, J.M. LeBlanc and F. Brown, Can. J. Phys. 35, 470 (1957).

Table 12.32, for photon energies of 7-11 Mev. The table also includes branching ratio data deduced from neutron counting determinations[244] of $\sigma_{\gamma,N}$. In this case the photofission branching ratio is known with less certainty because of uncertain corrections for the $\bar{\nu}$ neutrons contributed per fission. At photon energies of 7-12 Mev which lie between the γ,n and γ,2n thresholds, the photofission branching ratio can be taken as a measure of $\frac{\Gamma_n}{\Gamma_f}$ whose importance is stressed in Section 12.1.4. In that section neutron-emission-to-fission-width ratios derived from photonuclear data are listed in Table 12.6. A comparison of these data with $\frac{\Gamma_n}{\Gamma_f}$ ratios deduced from charged-particle induced reactions (Table 12.4) and 3 Mev neutron cross sections (Table 12.5) shows that the values derived from photofission are in line with those deduced from other data (see Fig. 12.18).

(γ,n) and (γ,f) cross sections and photofission branching ratios undergo some strong changes between 5 and 7 Mev which can be correlated satisfactorily with photofission and photoneutron threshold values. A good discussion of these changes and correlations for U^{238} and Th^{232} targets is given by GINDLER, HUIZENGA and SCHMITT.[233]

Photofission branching ratios and Γ_f/Γ_n ratios can be calculated for other elements besides thorium and uranium from published measurements of fission cross section relative to those of U^{238}. BALDWIN and KLAIBER[231] set an upper limit of 10^{-2} millibarns for the photofission cross sections of gold, bismuth, lead, samarium, thallium and tungsten targets. McELHINNEY and OGLE[246] measured the relative photofission yields of several fissionable materials with respect to U^{238} by a fission product catcher method. For photons in the energy region 12-22 Mev the following results were obtained: U^{238} (1.00, standard), U^{235} (1.49), U^{233} (2.49), Pu^{239} (2.51), Th^{232} (0.26) and Th^{230} (0.85). HUIZENGA, GINDLER and DUFFIELD[253] measured relative photofission yields at betatron energies of 12, 17 and 20 Mev. Fission rates were determined by counting scintillation flashes in a zinc sulfide screen deposited on the front surface of a photomultiplier tube. The relative fission rates at 17-20 Mev are the following: U^{238} (1), Th^{232} (0.31), U^{236} (1.43), U^{235} (2.40), U^{234} (1.82), U^{233} (2.54), Np^{237} (2.40) and Pu^{239} (3.17). These results check

---

253. J. R. Huizenga, J. E. Gindler and R. B. Duffield, Phys. Rev. 95, 1009 (1954).

Table 12.32 Photofission branching ratio for thorium and uranium

	U^{238}				Th^{232}		
E(Mev)	Ref. a	Ref. b	Ref. c $\bar{\nu} = 2.5$	Ref. c $\bar{\nu} = 3$	Ref. a	Ref. c $\bar{\nu} = 2.5$	Ref. c $\bar{\nu} = 3$
7			0.24	0.28		0.18	0.20
8	0.21	0.25	0.22	0.24	0.10	0.14	0.15
9	0.17	0.21	0.19	0.21	0.08	0.10	0.11
10	0.18	0.16	0.23	0.26	0.08	0.08	0.08
11	0.20	0.18	0.23	0.26	0.08	0.08	0.08

References:

a. Gindler, Huizenga and Schmitt, Phys. Rev. 104, 425 (1956).

b. Duffield and Huizenga, Phys. Rev. 89, 1042 (1953).

c. Lazareva et al.[244]

those of McELHINNEY and OGLE[246] except that corresponding to the point for Pu^{239} point. The results for 12 Mev energy were converted to Γ_n/Γ_f to give the results shown in Table 12.6 of Section 12.1.4. All these data point to a strong influence of Z or Z^2/A on the photofission probability. There does not seem to be anything special about relative probabilities of neutron emission and fission in compound nuclei excited by photoabsorption compared to deexcitation of similar compound nuclei produced in other ways. Hence the detailed discussion of nuclear structure effects on fissionability which is given in Section 12.1.4 is believed to be valid for photofission.

DUFFIELD, SCHMITT and SHARP[254] report a Γ_f/Γ_{total} value of 0.003 for Ra^{226} by comparing its fissionability with U^{238}, both targets irradiated with 23-Mev bremsstrahlung. This gives a value of Γ_n/Γ_f of 330. SUGARMAN[255] reported a photofission cross section for bismuth of about 1/1000 of the U^{238} cross section for an 85 Mev bremsstrahlung beam.

Let us now examine some of the details of the photofission and photoneutron curves. Several investigators[247,231,248,251] have noted a small bump in the photofission cross section of thorium and uranium centered at about 6 Mev. At first it was not certain that this bump was not a fiction resulting from errors and uncertainties in deriving cross sections by the photon difference method. The bulk of evidence now indicates that this "resonance" is a real effect although small compared to the giant resonance at 14 Mev. A particularly strong piece of evidence comes from an experimental study by CLARKE and HUIZENGA[256] and an extension of it by HUIZENGA, GINDLER and VANDENBOSCH.[257] In this work, heavy element targets were irradiated with gamma rays produced by the $F^{19}(p,\alpha\gamma)O^{16}$ reaction. A mixture of three monochromatic gamma rays of 6.14, 6.91 and 7.11 Mev energy is produced in this reaction, but the intensity ratio $I_{6.14}/(I_{6.91} + I_{7.11})$ can be varied over a large factor by changing the energy

---

254. R. B. Duffield, R. A. Schmidt, and R. A. Sharp, Paper P/678, p. 202, Vol. 15, Proceedings of the Second U.N. International Conference on the Peaceful Uses of Atomic Energy, Geneva, 1958.

255. N. Sugarman, Phys. Rev. 79, 532 (1950).

256. K. M. Clarke, Thesis, Argonne National Laboratory Report, ANL-5853, July, 1958; K. M. Clarke and J. R. Huizenga, Bull. Am. Phys. Soc. II (2), 377 (1957). A similar measurement was also made by J. Hartley, Ph.D. Thesis, University of Pennsylvania, 1955, unpublished.

of the protons striking a thin CaF_2 target. Some results of this study are given in Table 12.33. The important result is the higher cross section at 6.14 Mev than at 7.0 Mev for U^{236} and the near-equivalence of the cross sections at these energies for Th^{232} and U^{238}. The difference in all these cases is outside the probable error. Hence there can be little doubt that a local maximum occurs in the photofission curve below 7 Mev, at least for some nuclei. The size of the bump is not large, as can be seen in Fig. 12.75. (See also Fig. 12.78 below).

Several possible explanations for a local maximum at about 6 Mev have been proposed but none of them is completely satisfactory. The neutron binding energy falls at about this point and the onset of neutron emission as a competitor to fission could account for the dip in fission cross section. In a nuclide like Th^{232} the (γ,n) reaction competes strongly and for a constant photon absorption cross section the fission cross section must drop when the neutron emission commences. In heavier, more fissionable nuclides the effect would be less. From the atomic mass tables the neutron binding energies can be estimated rather accurately. However, there does not seem to be a clear correspondence between the neutron binding energy and the occurrence or non-occurrence of a drop in cross section for the nuclides in Table 12.33. The binding energy of the last neutron in U^{234} and U^{236} for example lie at 6.84 Mev and 6.46 Mev respectively; yet the fission cross section of the first rises while that of the second drops between 6.14 and 7.0 Mev.

A second possible explanation is a change in the mechanism of photon-absorption. It is possible that quadrupole absorption is larger than dipole absorption near 6 Mev. Since the nuclei considered here are spheroidal nuclei with large quadrupole moments such a mechanism is plausible. This possibility is discussed in the text by BLATT and WEISSKOPF.[258] Some Russian

---

257. J. R. Huizenga, J. E. Gindler and R. Vandenbosch, Bull. Am. Phys. Soc. II (4), 234 (1959) and unpublished work.

258. J. M. Blatt and V. F. Weisskopf, "Theoretical Nuclear Physics" John Wiley and Sons, Inc., New York, 1952.

Table 12.33 Photofission cross sections at 6.14 Mev and 7.0 Mev

Nuclide	$\sigma_{6.14}(\gamma,f)$ (millibarns)	$\sigma_{7.0}(\gamma,f)$ (millibarns)	$\sigma_6(\gamma,f)/\sigma_7(\gamma,p)$
Th^{232}	9	9	0.99
U^{233}	13	44	0.31
U^{234}	5	52	0.10
U^{235}	16	33	0.49
U^{236}	35	28	1.26
U^{238}	13	15	0.89
Np^{237}	31	45	0.69

Unpublished results of Clarke, Gindler, Vandenbosch and Huizenga.

experiments[244,259,260,261] on the angular distribution of fission fragments for photofission of U^{238} at 9.4 Mev indicated a distribution of the form

$$I(\theta) = a + b \sin^2\theta + c \sin^4\theta \qquad (12.31)$$

where the constant c was significant compared to b. This would indicate quadrupole absorption. However, KATZ, BAERG and BROWN[245] later made a careful study of the angular distribution of the fission fragments of U^{238} and Th^{232} and found no necessity to invoke quadrupole effects to explain their results. They state, however, that quadrupole contributions are not conclusively ruled out.

Further research is required before the true nature of the photofission process in the region of 5-7 Mev will be resolved.

We have mentioned the angular distribution of fragments from nuclei induced to fission with photons. One of the most interesting discoveries[239] about photofission was the fact that the even-even nuclei U^{238} and Th^{232} show a pronounced peaking of fragment emission at 90° to the incident photon beam. This anisotropy is at a maximum at the photofission "threshold" and washes out rapidly at higher photon energies. These angular effects are fully discussed in Section 12.1.7 of this chapter.

The determination of photofission thresholds has been a matter of some interest since this threshold might provide a direct measure of the activation energy for fission. The first major investigation was carried out by KOCH, McELHINNEY and GASTEIGER[262] who detected fission events in a differential ion chamber and reported the threshold values listed in Table 12.34. These results did not agree well with the predictions of the classical liquid drop model. FRANKEL and METROPOLIS[263] made calculations on the ENIAC computer based on the liquid drop model of BOHR and WHEELER[264] of classical fission thresholds,

259. Lazareva and Nikitina, Physics of Fission, Suppl. No. 1 Sov. J. Atomic Energy, Atomic Press Moscow, 1957(trans. Consultants Bureau, New York,1957)p.125.

260. A. I. Baz, et al., Paper P/2037, Vol. 15, Proceedings of the Second U.N. Conference on the Peaceful Uses of Atomic Energy, Geneva, 1958.

261. Bannik, Kulikova, Lazareva and Yakovlev, Physics 22, 1186A (1956).

262. H. W. Koch, J. McElhinney and E. L. Gasteiger, Phys. Rev. 77, 329 (1950).

263. S. Frankel and N. Metropolis, Phys. Rev. 72, 914 (1947).

264. N. Bohr and J. A. Wheeler, Phys. Rev. 56, 426 (1939).

Table 12.34 Photofission thresholds*

Nucleus	Threshold value (Mev) Koch, McElhinney and Gasteiger[262]	Threshold value (Mev) Katz, Baerg and Brown[245]
Th^{232}	5.40	5.16
U^{233}	5.18	4.82
U^{235}	5.31	--
U^{238}	5.08	4.60
Np^{237}	--	4.74
Pu^{239}	5.31	4.73
Am^{241}	--	5.31

*"Threshold" means here the lowest photon energy for which fission could be detected.

defined as the energy difference between the initial spherical equilibrium shape of the drop and the saddle point shape. In all cases except Pu^{239} the calculated thresholds were higher and furthermore these showed a much stronger variation with Z^2/A than the experimental results. Experimental values of fission threshold deduced from the behavior of the cross sections for neutron-induced fission show a similar disagreement with the calculated values.

Two things can be said about this comparison. In the first place, as is strongly emphasized in Section 11.2 of the review of low energy fission, (Report UCRL-9036) our knowledge of the classical liquid drop model is incomplete so that we really are uncertain about the true locations in deformation space of all the low-lying saddle points and about the potential energy of these saddle points. Furthermore, the liquid drop model by its very nature is a gross oversimplification which ignores the details of the individual particles and of possible shell structure in the nucleus. We know that shell structure effects are quite important. The strong equilibrium deformations in the nuclear ground states of uranium and other heavy element nuclei is quite strong proof of this. Hence it is certain that a more realistic model for the nucleus would lead to different saddle point potential energies than those calculated by FRANKEL and METROPOLIS[263] or any other authors who base their computations on the idealized liquid drop.

The second comment is that, in the quantum-mechanical description of fission there can be no such thing as a true threshold since a nucleus excited to some point below the classical threshold has a definite (if small) probability of penetrating a potential barrier and dividing. This is shown schematically in Fig. 11.16 of the last chapter. Below-the-barrier fission would be expected to have an exponential dependence upon energy. The experimental "threshold" would then be merely a measure of the limits of fission detectability. Recent experiments have amply confirmed this. KATZ, BAERG and BROWN[245] increased the sensitivity of the ion-chamber method and showed that fission was occurring at measurable rates at gamma ray energies as low as those listed in column 3 of Table 12.34. These values are much lower than the earlier ones of KOCH, McELHINNEY and GASTEIGER.[262] More important than these numbers is the shape

---

265. R. A. Schmitt and R. B. Duffield, Phys. Rev. 105, 1277 (1957).

of the yield curves and of the cross section curves derived from them which indicate strongly that photofission is occurring by barrier penetration at these low energies. There seems little doubt that fission could be detected at even lower energies if greater sensitivity were achieved — by use of higher current electron accelerator for example. There appears to be a decrease in fission cross section of about a factor of 1000 for each 1.0 Mev decrease in energy. The fission cross sections for Th^{232} and U^{238} are less than one microbarn at the threshold values quoted by KATZ, BAERG and BROWN.[245] Complete cross section curves in the barrier penetration energy region are given for Th^{232}, U^{233}, U^{238}, Np^{237}, Pu^{239} and Am^{241} in Fig. 12.74.

SCHMITT and DUFFIELD[265] have investigated the yields of specific fission products of U^{238} and Th^{232} in the threshold energy region by radiochemical techniques. Their results corroborate those of KATZ, BAERG and BROWN in showing that fission can be detected below 5.0 Mev. Consider, for example, Fig. 12.76 which shows the yields of some typical products of asymmetric fission as a function of maximum x-ray energy. The sensitivity of the radiochemical method makes it possible to cover an enormous range of fission yield; for example the asymmetric photofission of U^{238} was found to increase by a factor of 10^4 as the betatron energy was increased from 4.8 to 6.0 Mev. The authors also studied the yield of Cd^{117} which was selected as a monitor for symmetric fission probability; Cd^{117} lies near the bottom of the trough in the thermal neutron fission of U^{235}. The results are shown in Fig. 12.77. It is noteworthy that some symmetric fission occurs at quite low gamma ray energies. SCHMITT and DUFFIELD[265] also examined the percentage of fission events leading to Cd^{117} as a function of betatron electron energy. This percentage was well below one percent in the energy range 0-24 Mev but from its variation in energy it could be seen that (1) the probability of symmetric fission in Th^{232} is vanishingly small at betatron energies below 7 Mev; for example at a betatron energy of 6.5 Mev the yield of Cd^{117} is less than 0.0003%. This is considerably lower than the yield (0.01%) from thermal-neutron induced fission of U^{235}; (2) the probability of symmetric fission in U^{238} is higher than in Th^{232} at energies below 10 Mev; and (3) the probability of symmetric fission in U^{238} has a local maximum of about 0.05 percent at 6 Mev. There is no theoretical interpretation for this result although it might bear some relation to a possible quadrupole photoabsorption mechanism near 6 Mev.

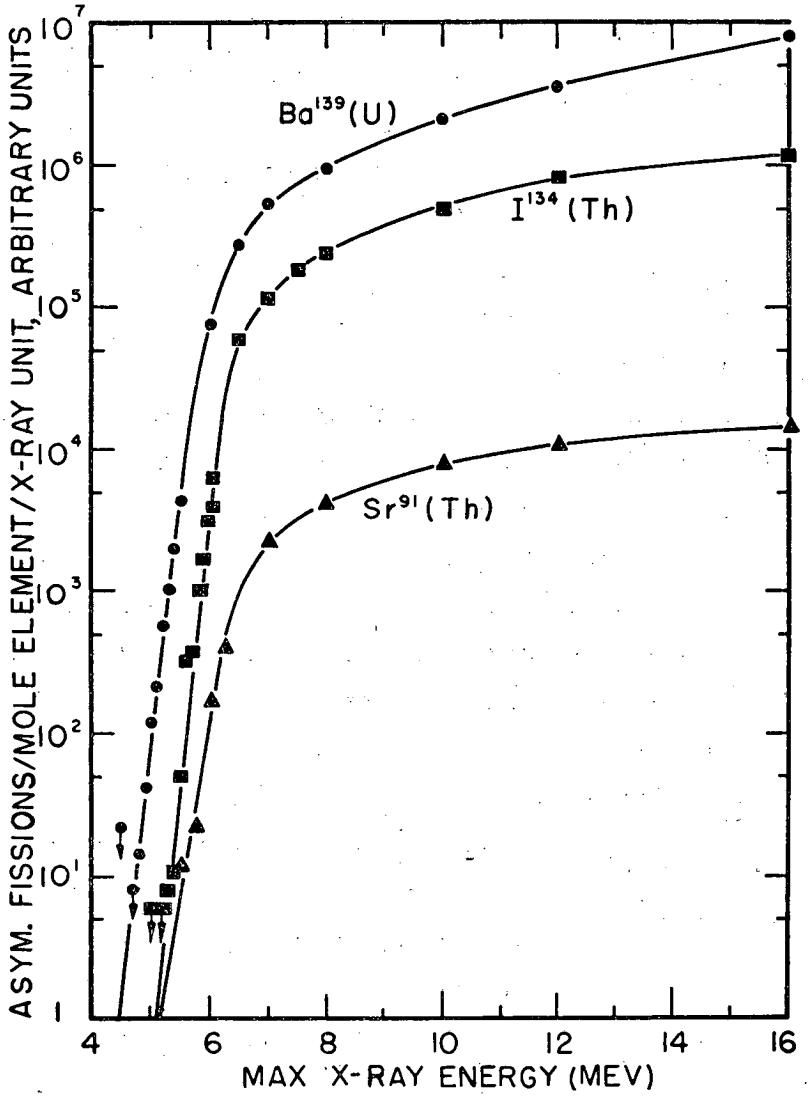

MU-19434

Fig. 12.76 Relative yield of some typical products of asymmetric fission of natural uranium and thorium as a function of increasing betatron energy. Ordinates for Ba^{139}, Sr^{91} and I^{134} are unrelated. From Schmitt and Duffield.[265]

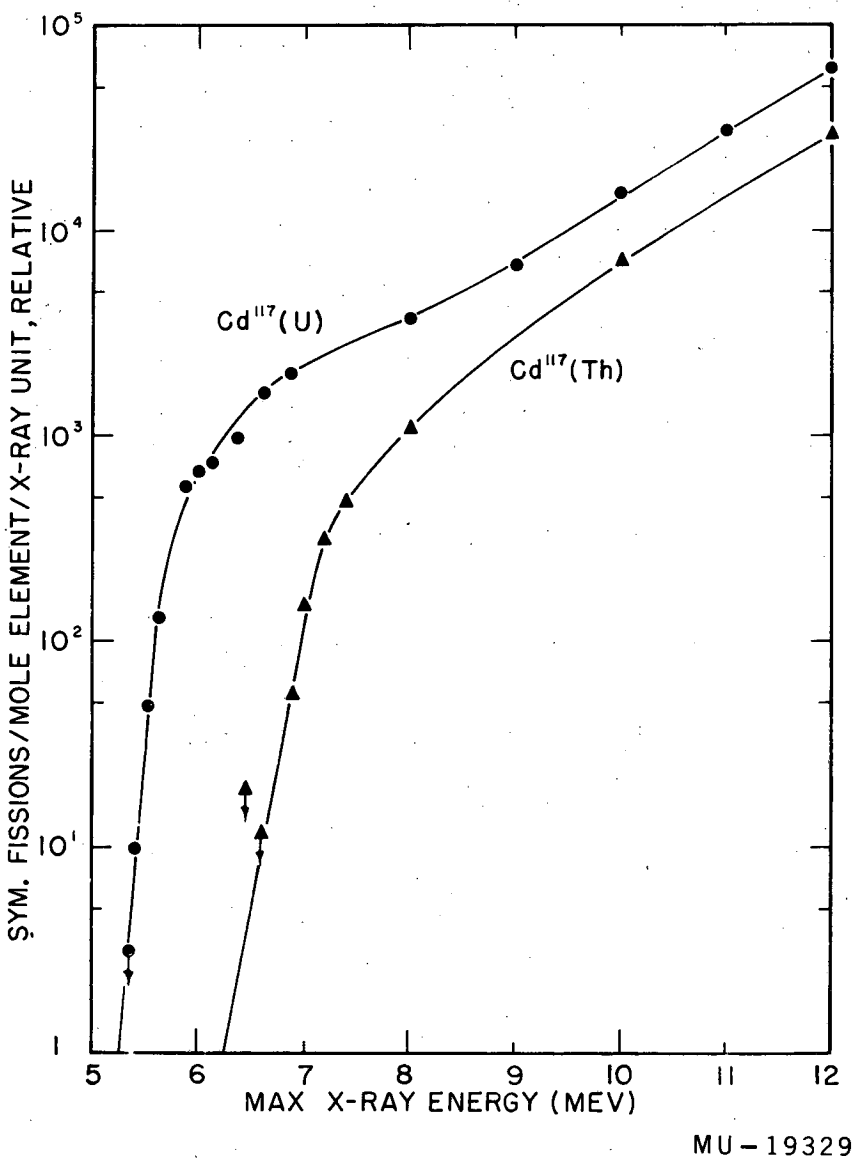

Fig. 12.77 Relative yield of Cd^{117} (used as a representative of symmetric fission) as a function of increasing betatron energy. From Schmitt and Duffield.[265]

SCHMITT and DUFFIELD applied the photon difference method to their Ba^{139} and Cd^{115} yields from U^{238} fission in order to calculate the cross section versus photon energy curves shown in Fig. 12.78. The interesting feature is the confirmation of the small resonance at about 6 Mev which had been observed previously in ion chamber measurements. (See above).

12.4.2 Fission Product Yield Distribution in Photofission. From the dominance of the giant resonance in the excitation function for photofission it is clear that the majority of the fissioning nuclei are excited to about 14 Mev even when the maximum energy of the bremsstrahlung beam is considerably greater. We may expect then that the mass yield curve will resemble those observed in charged particle bombardment when the compound nucleus is excited to about 14 Mev. This expectation is borne out by the facts.

SCHMIDT and SUGARMAN[266] studied the yield of 26 fission chains for uranium targets irradiated with bremsstrahlung beams with maximum energy 48, 100 and 300 Mev. In addition they measured the yields of selected peak and trough products for products for photon beams of 7, 10, 16 and 21 Mev. RICHTER and CORYELL[267] used a uranium salt sample as the target of the 16 Mev electrons in the M.I.T. linear accelerator so that the uranium target served simultaneously as the x-ray source and absorber. Radiochemical determinations were made of the yields of 19 chains. Some products were also isolated from targets bombarded with 10 Mev electrons. KATZ and co-workers[268] measured the yield of 12 fission products of uranium at betatron energies of 12, 18, and 22 Mev. In addition, the yield of Ba^{139} (used as a monitor of asymmetric fission) and of Cd^{115} (used as a monitor of symmetric fission) were determined at 1 Mev intervals from 8 Mev to 24 Mev. DUFFIELD and co-workers[269] isolated many products from uranium targets struck with electron beams at several energies between 5.5 and 8.0 Mev. DAHL and PAPPAS[270] studied uranium fission product yields at 31 Mev.

---

266. R. A. Schmidt and N. Sugarman, Phys. Rev. 95, 1260 (1954).

267. H. G. Richter and C. D. Coryell, Phys. Rev. 95, 1550 (1954).

268. L. Katz, T. M. Kavanagh, A. G. W. Cameron, E. C. Bailey and J. W. T. Spinks, Phys. Rev. 99, 98 (1955).

269. R. B. Duffield, L. E. Glendenin, R. A. Schmitt and E. P. Steinberg, unpublished data, 1955, cited in reference 272.

270. J. B. Dahl and A. C. Pappas, University of Oslo, Norway, 1955, unpublished data cited in reference 272.

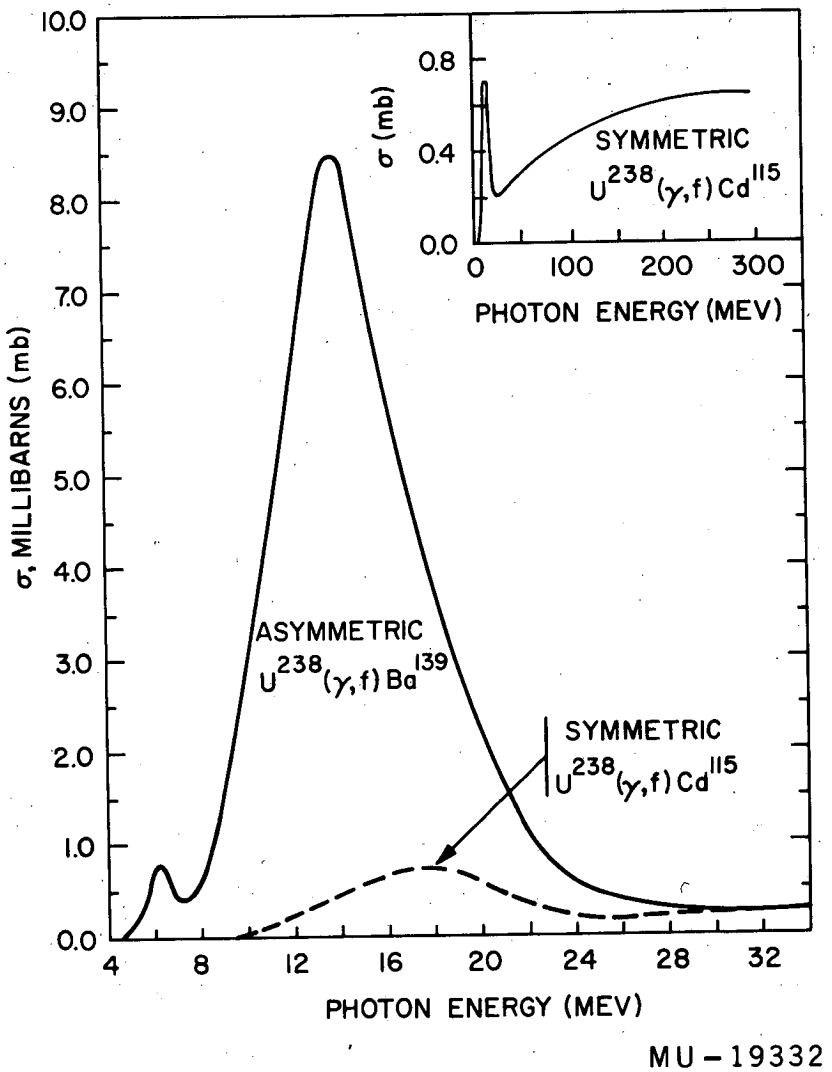

Fig. 12.78 Cross section for Ba^{139} and Cd^{115} chosen as representative fission products for asymmetric and symmetric fission of U^{238}. The curves were derived by the photon difference method from the yield curves as function of maximum betatron energy. From Schmitt and Duffield.[265]

SPENCE[271] measured some yields of 20 Mev photofission of U^{235}.

A complete tabulation of the results of these studies and an interpretation of the results is given in an excellent summary report by DUFFIELD, SCHMITT and SHARP.[272] We shall present only a sampling of the results.

Figure 12.79 shows the general shape of the mass-yield distribution over a wide range of maximum bremsstrahlung energies. The distribution has the typical two humps. The principal comments which need to be made are the following:

(1) The yields of nuclides with mass numbers 77 through 84 which represent very asymmetric mass divisions are substantially higher than the corresponding yields in the fission of U^{235} induced by slow neutrons. Masses 83 and 84 increase by factors of 2 or 3 as the x-ray energy is increased from 5.5 Mev to 300 Mev.

(2) The yields in the neighborhood of the light and heavy peaks are approximately equal to the corresponding yields when U^{238} is fissioned with fission-spectrum neutrons, or when U^{235} is fissioned with 14 Mev neutrons.

(3) Fine structure which has been shown to be present in the thermal-neutron fission of U^{235} at masses 100 and 134 (see Section 11.4 in Chapter 11) appears also to be present in photofission. RICHTER and CORYELL[267] also report a spike in their fission yields near mass number 133.

(4) Construction of smooth mass yield curves suggests the following average number of neutrons, $\bar{\nu}$. At 8.0 Mev $\bar{\nu}$ is 2.0 for asymmetric modes and 1.0 for symmetric modes. At 10 and 16 Mev $\bar{\nu} = 3$ while at 48 Mev it is 4.

(5) The yields of products of symmetric fission (mass number 112 through 126) are considerably greater than those of thermal neutron fission of U^{235}. The change in the peak-to-trough ratio as a function of the maximum photon energy is given in Table 12.35. There is some scatter in the experimental ratios but the general trend is clearly in the direction of filling in the valley as excitation energy is increased. In a careful study of Cd^{117} yields as a function of x-ray energy between 5.3 and 8.0 Mev with points spaced at 0.2 Mev

---

271. R. W. Spence and co-workers, unpublished results cited in reference 258.

272. R. B. Duffield, R. Å. Schmitt and R. A. Sharp, Paper P/678, p. 202, Vol. 15, Proceedings of the Second U.N. Conference on the Peaceful Uses of Atomic Energy, Geneva, 1958.

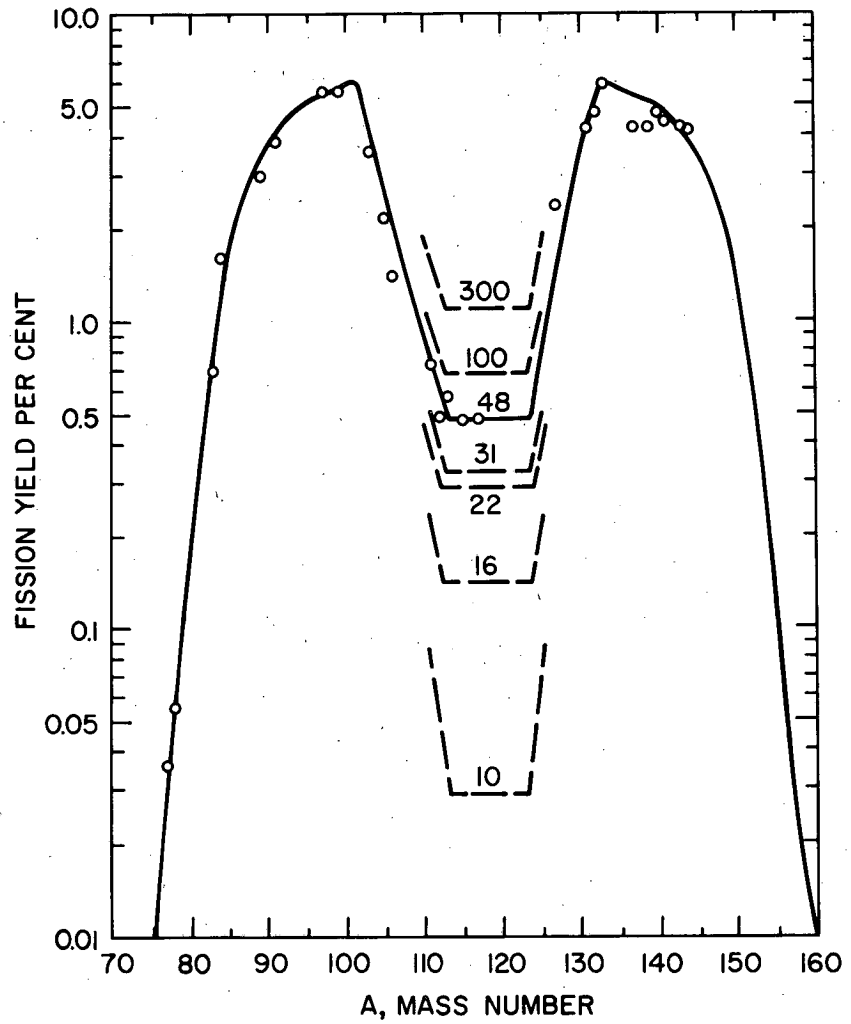

MU-19331

Fig. 12.79 Photofission mass-yield distributions of U^{238} as a function of maximum x-ray energy. The circles and the solid line represent yields at 48 Mev. Dashed curves have been drawn through the 10, 16, 22, 31, 100 and 300 Mev symmetric photo yields, all normalized to 5.6% mass-yield at mass 99. Figure taken from Duffield, Schmitt and Sharp.[272]

increments SCHMITT and DUFFIELD[265] found evidence for a local maximum at ~6.0 Mev x-ray energy. Such a local maximum was not seen in a comparable study of Th^{232} fission product yields.

KATZ and co-workers[268] analyzed their radiochemical yield data in an interesting and illuminating way. The yields of a given mass were plotted as a function of the maximum energy E_o of the bremsstrahlung distribution. The curve so obtained was similar to the usual yield curve in photonuclear reactions, and was analyzed by the photon difference method[233] to yield the corresponding cross section curve as a function of photon energy; this derived curve can be represented as $[\sigma_{\gamma f}(h\nu)]_A$. It has the "resonance" shape characteristic of photonuclear reactions and is interpreted as the cross section leading to the mass chain A in the photofission induced by monoenergetic photons of energy $h\nu$. It was then possible with the aid of several such $[\sigma_{\gamma f}(h\nu)]_A$ curves to construct a three-dimensional surface, $S(\sigma,A,h\nu)$. This surface is shown in Fig. 12.80. A cut through this surface at constant A is simply one of the $[\sigma_{\gamma f}(h\nu)]_A$ curves. A cut through this surface at constant $h\nu$ results in a σ-A (yield-mass curve which is readily seen to be the mass yield curve which would be obtained with monochromatic photons. Yield-mass curves of this type are of the most fundamental interest. The area under such a σ-A curve is the total photofission cross section for monochromatic photons of that energy. A comparison of the yield of a representative peak product to a representative trough product gives the peak-to-trough ratio as a function of photon energy. This comparison is more meaningful than the ratios quoted in Table 12.35 which are averages over the bremsstrahlung spectrum. For fission induced by monochromatic 24 Mev gamma rays the true peak-to-trough ratio is about 3.

The cross sections for asymmetric fission and for symmetric fission both go through a maximum in the region of the giant dipole resonance. Beyond this energy region the cross section for symmetric fission goes through a gradual rise with increasing gamma energy. At a photon energy of 300 Mev the cross section for symmetric fission has increased to about the same value it had at the dipole resonance peak. It is an interesting question whether the cross section for asymmetric fission goes to zero for photon energies above the resonance. The analysis of SCHMITT and SUGARMAN[266] and of KATZ[268] indicates rather clearly that it does not. There is a high energy tail on the excitation function

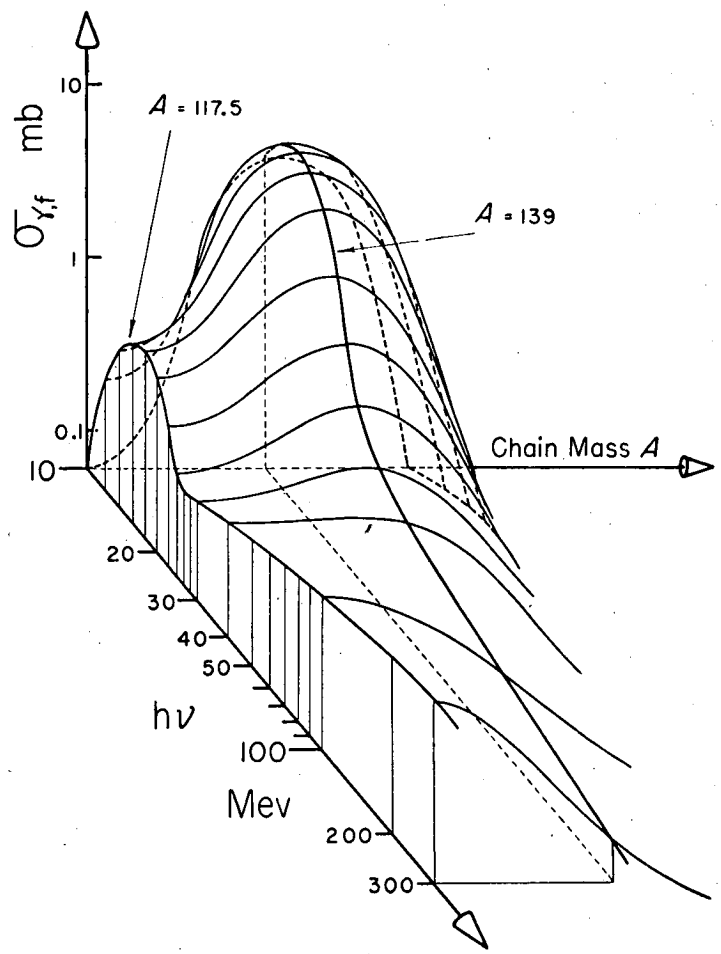

MU-19432

Fig. 12.80 The S(σ,A,hν) surface published by KATZ et al.[268] The target element is uranium. The surface is symmetric about mass number 117.5 but only the higher mass side is shown. Note that the energy scale starts at 10 Mev on the low energy side so that the A = 139 curve cuts the σ-A plane at a finite value. The shape of this surface up to 24 Mev is quite well established but above this energy only the A = 117.5 curve is known with any accuracy.

Table 12.35 Peak positions and peak-to-valley yield ratios in the photofission of uranium and thorium

Fissioning nucleus	Maximum energy x-ray or electron beam (Mev)	Average mass number at half height: Light peak	Average mass number at half height: Heavy peak	Ratio of peak-to-valley yields	Reference
Cf^{252}	Spon. fission	108	139	>600	
U^{235}	Slow neutron	95	139	650	
U^{238}	Fast neutron (fission spectrum)	98	139	200	
Th^{232}	69	91	138	10	a
U^{238}	5.5	98	138	200	b
U^{238}	8.0	98	138	310	b
U^{238}	10.0	97	137	200	c
U^{238}	12.0			64	d
U^{238}	16	97	137	125,[e] 43[c]	
U^{238}	22	95	139	16,[d] 20[c]	
U^{238}	48	97	138	13	c
U^{238}	100	97	138	9	c
U^{238}	300	97	137	6	c

(a) Hiller and Martin, Phys. Rev. 90, 581 (1953).

(b) Duffield, et al., unpublished data cited in Geneva Paper P/678, p. 202, Volume 15, Geneva Proceedings, 1958.

(c) Schmitt and Sugarman, Phys. Rev. 95, 1260 (1954).

(d) Katz, et al., Phys. Rev. 99, 98 (1955).

(e) Richter and Coryell, Phys. Rev. 95, 1550 (1954).

amounting to a few millibarns out to 300 Mev and farther. Asymmetric and symmetric fission are equally probable at about 50 Mev of excitation; above this energy symmetric fission is more probable. However, the ion-chamber measurements cited below do not agree with this but indicate that asymmetric fission is still dominant between 200-500 Mev. The total photofission cross section at 300 Mev is about 7 millibarns. It must be emphasized that these energy figures refer to the photon energy and to the initial nuclear excitation energy and not necessarily to the energy of excitation when fission occurred; multiple neutron emission may occur first followed by fission from a relatively unexcited nucleus. BELOVITSKII and co-workers[273] obtained evidence in emulsion experiments that the cross section for photofission is not negligible for photons well above the giant dipole reasonable energy.

HILLER and MARTIN[274] studied the distribution of 13 chain yields in the fission products from the photofission of thorium induced by a 69 Mev synchrotron bremsstrahlung beam. The results were quite similar to the uranium fission results just reviewed. The peak-to-valley ratio was 10. Symmetry of the curve about nucleon numbers of 114.5 indicated the average emission of approximately 3 neutrons.

SUGARMAN[275] measured the yields of 14 products of the photofission of bismuth induced by the photon beam from a 69 Mev betatron. The principal result is that the photofission of this element is predominantly symmetric. This is in agreement with the latter results of FAIRHALL[276] on the fission of bismuth with 22 Mev protons reviewed in Section 12.1.5. The yield-mass curve outlined by SUGARMAN'S results has a half-width of ~20 mass units which is considerably narrower than that found in the fission of bismuth with 190 Mev deuterons by GOECKERMANN and PERLMAN,[277] and more in agreement with FAIRHALL'S low energy study.

---

273. G. E. Belovitskii, T. A. Ramanova, L. V. Sukhov and I. M. Frank, Soviet Physics JETP 1, 586 (1955).

274. D. M. Hiller and D. S. Martin, Jr., Phys. Rev. 90, 581 (1953).

275. N. Sugarman, Phys. Rev. 79, 532 (1950).

276. A. Fairhall, Phys. Rev. 102, 1335 (1956).

277. R. N. Goeckermann and I. Perlman, Phys. Rev. 76, 628 (1949).

DUFFIELD, SCHMITT and SHARP[272] reported some preliminary radiochemical studies of the fission products of radium induced to fission with a 23 Mev x-ray beam. As expected, the total fission cross section was quite low, namely about one percent of the U^{238} fission cross section at the same x-ray energy. The interesting feature of the mass-yield distribution was that the yields seemed to conform to the three-peaked distribution (equal contributions from asymmetric and symmetric fission) which JENSEN and FAIRHALL[278] had observed in the fission of Ra^{226} with 11 Mev protons.

12.4.3 Photofission Probability at Very High Photon Energies – Photomesonic Fission. When the energy of the photons is greater than the photomeson threshold of 140 Mev, it is necessary to consider the photoproduction of π-mesons and the reabsorption of the mesons in the nucleus as a possible mechanism for transfer of energy into the nucleus. Much data exists on the photoproduction cross section for mesons in hydrogen targets, in deuterium and in complex nuclei. Many observations have been made of star formation and fast neutron and proton production in complex nuclei when bombarded with high energy photons; these observations give indirect evidence for the reabsorption of mesons before escape from the nucleus. It is out of place in this book to review the details of those photomesonic processes. We wish only to call attention to this general phenomena which undoubtedly contributes to the photofission process in all heavy elements for high photon energies.

JONES and TERWILLEGER[279] measured the photoneutron yield for eleven representative elements as a function of photon energy from 13.5 Mev to 320 Mev. The photoneutron excitation function for each element showed a strong peak in the region of 10-30 Mev corresponding to dipole absorption of the photon. Just above this energy range the cross section was quite low. At the higher energy range, however, the cross section increased again. The major part of this increase in the region beyond 140 Mev can probably be attributed to photomeson effects.

---

278. R. C. Jensen and A. W. Fairhall, Phys. Rev. 109, 942 (1958).

279. L. W. Jones and K. M. Terwilliger, Phys. Rev. 91, 699 (1953).

The photofission cross section for uranium shows an analogous behavior, as was pointed out by SCHMITT and SUGARMAN[266] and by KATZ.[268] The excitation curves can be seen in Fig. 12.80. Photofission at these high energies should have many resemblances to fission induced by high energy protons or by π^--meson capture. The first step may consist of a reaction of one of the following types with one of the bound nucleons.

$$\begin{aligned} h\nu + p &\longrightarrow n + \pi^+ \\ h\nu + n &\longrightarrow p + \pi^- \\ h\nu + p &\longrightarrow p + \pi^0 \end{aligned} \qquad (12.32)$$

The nucleon product of these reactions will have energy transferred to it and can be considered a cascade particle having a certain probability of escaping from the nucleon and a certain probability of transferring its energy to the nucleus by nucleon-nucleon collisions. The pion may escape or it may be captured as in the following process.

$$\begin{aligned} \pi^- + [P + P] &\longrightarrow P + N + 140 \text{ Mev.} \\ \pi^- + [P + N] &\longrightarrow N + N + 140 \text{ Mev.} \end{aligned} \qquad (12.33)$$

The outgoing nucleons in this step have 70 Mev of kinetic energy. One or both may escape without further interaction, or one or both may transfer part or all of their kinetic energy to the nucleus by an elastic collision cascade.

This picture of high energy photofission makes it quite understandable why the fission product distribution and other features of high energy photofission resemble those seen in fission induced by charged particles or π mesons. One would also predict that elements at or below the bismuth-lead region would show appreciable cross sections for photofission at high photon energies. This is borne out by experiment. GINDLER and DUFFIELD[280] used scintillation detectors to detect fission recoils and measured relative fissionability in bremsstrahlung beams of maximum energy 125 to 300 Mev. For a maximum energy of 275 Mev the following relative results were obtained: Ta^{181}(0.34), W(0.60), Au(1.2), Tl(1.7), Pb(2.9), Bi(6.3), Th(240) and U(570). The absolute cross section for bismuth is about 8 millibarns so these relative numbers are roughly

280. J. Gindler and R. B. Duffield, Phys. Rev. 94, 759 (1954); J. Gindler, Ph.D. Thesis, University of Illinois, 1954, unpublished.

equal to the observed cross section in millibarns. For bismuth and elements of lower Z the cross section drops off sharply as the photon energy decreases.

BERNARDINE, REITZ and SEGRÈ[281] studied the photomesonic fission of bismuth by counting fission events in a nuclear emulsion loaded with bismuth. The maximum energy of the betatron beam ranged from 100 to 319 Mev. The data were analyzed by the photon difference method. The principal result of interest was that the number of fission events was very low below 150 Mev and increased rapidly with energy above 150 Mev. The authors attributed the observed fission events to photomesonic fission.

This work was extended by JUNGERMAN and STEINER[282] who measured with considerable care the photofission yield of uranium, thorium, bismuth and gold over the range 150 to 500 Mev.[283] The energy range from 150 to 335 Mev was covered with the synchrotron of the Lawrence Radiation Laboratory at Berkeley while the higher energy data were obtained with the synchrotron at the California Institute of Technology. A cancellation-type, double-ionization chamber was used to measure fission rates while a calibrated ionization chamber was used to measure the beam intensity. The results are given in Table 12.36 and in Figs. 12.81 and 12.82.

JUNGERMAN and STEINER[282] made an approximate analysis of their yield curves by the photon difference method. In the case of the uranium and thorium targets they conclude that most of the yield observed in these high energy bremsstrahlung beams is actually contributed by photons in the giant resonance region around 14 Mev and that contributions from meson effects are masked. The derived cross section curves indicate a constant fission cross section of about (25 to 50) millibarns in the energy region 200 to 500 Mev for U^{238}, U^{235} and Th^{232}. This particular result does not agree well with the published results of MINAREK and NOVIKOV[283] who got higher cross sections and a much more sensitive

---

281. G. Bernardine, R. Reitz and E. Segre, Phys. Rev. 90, 573(1953).

282. J. A. Jungerman and H. M. Steiner, Phys. Rev. 106, 585 (1957).

283. E. V. Minarek and V. A. Novikov, Soviet Physics JETP 5, 253 (1957); carried out a similar study with the 250 Mev synchrotron of the Institute of Physics, Academy of Sciences, USSR. Their results for the Th and U are rather different than Jungerman and Steiner's but their results for bismuth agree within the experimental errors.

Table 12.36 Fission cross section per equivalent quantum for 100 to 500 Mev bremsstrahlung beams (in units of 10^{-27} cm^2). From Jungerman and Steiner.[282]

Maximum energy E of bremsstrahlung spectrum in Mev	U^{238}	U^{235}	Th^{232}	Bi^{209}	Au^{197}
500[a]	--	247±10	65.8±2.0	6.82±0.14	1.57±0.09
480[a]	159±5	--	64.7±1.5	6.17±0.29	--
476[a]	--	257±15	63.9±1.5	6.16±0.20	--
471[a]	--	--	63.4±1.3	--	--
466[a]	--	--	--	6.25±0.20	--
451[a]	--	--	--	6.10±0.18	1.42±0.14
431[a]	152±3	252±7	57.8±1.2	5.48±0.17	--
408[a]	--	--	--	5.09±0.17	--
400[a]	--	--	--	--	1.23±0.11
389[a]	--	--	60.5±2.0	--	--
385[a]	151±2	--	51.0±1.1	4.71±0.14	--
362[a]	--	--	--	4.00±0.09	--
350[a]	--	--	--	--	0.86±0.10
335	181±1	274±1	58.5±0.5	3.06±0.06	--
335[a]	146±2	235±6	50.5±1.1	3.12±0.13	--
300	163±2	244±6	53.0±1.1	--	0.72±0.08
291	168±5	276±5	61.2±1.8	--	--
285	173±5	--	55.7±1.3	1.85±0.13	0.78±0.06
285[a]	--	--	--	2.26±0.18	--
250	151±3	239±6	50.2±1.4	--	--
250[a]	--	--	--	1.78±0.22	0.33±0.07
244	170±5	270±7	51.3±1.3	--	--
232	--	239±4	--	--	--
208	154±4	244±8	42.8±1.2	1.18±0.28	--
200[a]	--	--	--	1.30±0.24	0.31±0.09
180	154±3	238±5	44.2±0.8	0.68±0.09	--
150[a]	--	--	--	0.61±0.12	--
143	147±4	226±6	43.3±1.4	--	--

[a]Data obtained at the California Institute of Technology.

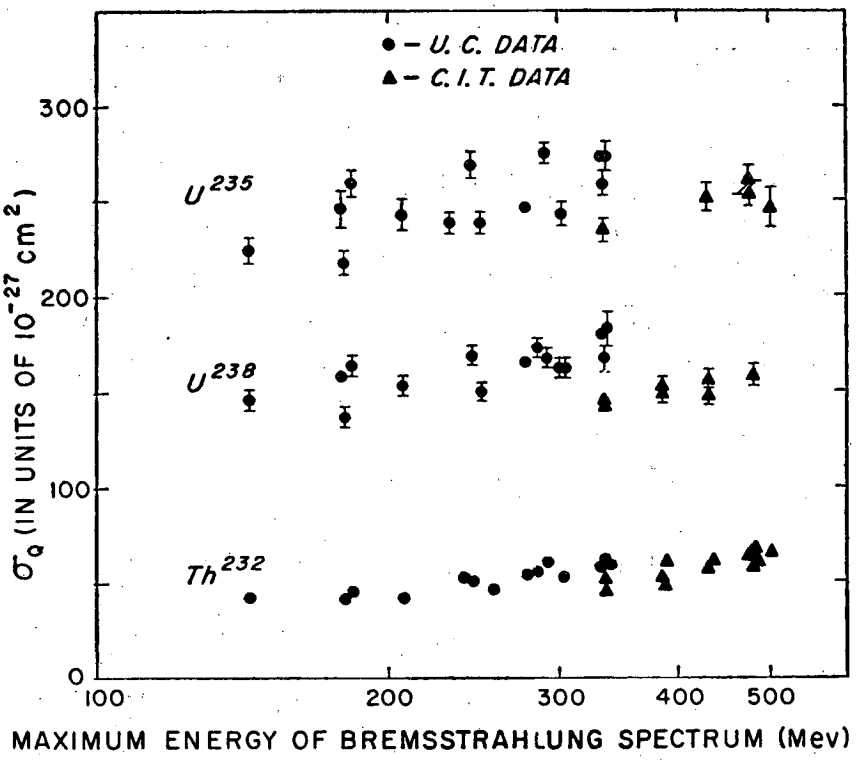

MU-19431

Fig. 12.81 Photofission cross section per equivalent quantum, σ_Q versus maximum bremsstrahlung energy for U^{235}, U^{238} and Th^{232}. The errors indicated on the points are standard deviations due to counting statistics only. From Jungerman and Steiner, Phys. Rev. 106, 585 (1957).

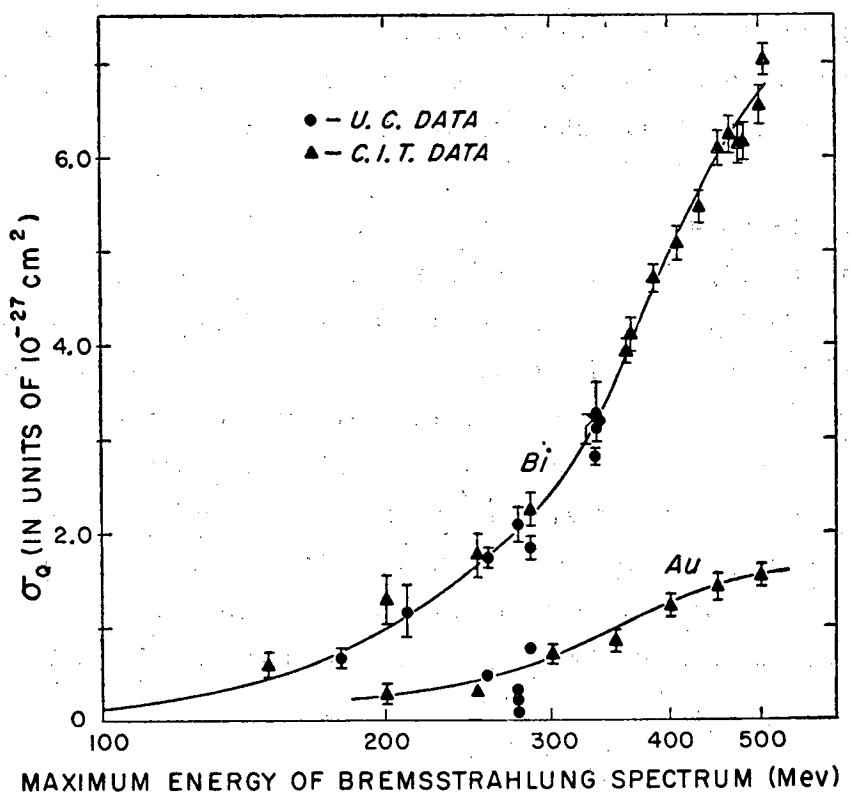

MU-19429

Fig. 12.82 Photofission cross section per equivalent quantum, σ_Q versus maximum bremsstrahlung energy for Bi^{209} and Au^{197}. The errors indicated on the points are standard deviations due to counting statistics only. From Jungerman and Steiner, Phys. Rev. 106, 585 (1957).

dependence on the proton energy. The radiochemical studies of KATZ et al.,[268] and of SCHMITT and SUGARMAN[266] indicated a cross section of 7-8 millibarns for symmetric fission modes at 300 Mev. If this figure as well as JUNGERMAN's and STEINER's figure for total fission are accepted then the ratio of asymmetric to symmetric fission is about 3-6 at 300 Mev. KATZ et al.[268] has earlier tentatively concluded that symmetric fission events would outnumber the asymmetric at 300 Mev.

Figure 12.83 shows cross section curves for bismuth and gold derived from the yield data of Fig. 12.82. In these cases there is a very definite increase above 100 Mev continuing up at least as far as 400 Mev. The curves indicate a resonance centered at ~400 Mev with a decreasing cross section above, but uncertainties in the data and in the analysis are such that this decrease may be fictional. Further experiments are needed to clarify this point. The form of the photofission curves for bismuth and gold strongly suggests a meson production and reabsorption sequence as the basic mechanism of the reaction, but the exact nature of this mechanism remains to be learned. Interesting comments on photomesonic fission are made by MINAREK and NOVIKOV[283] and by LAZAREVA and NIKITINA.[259]

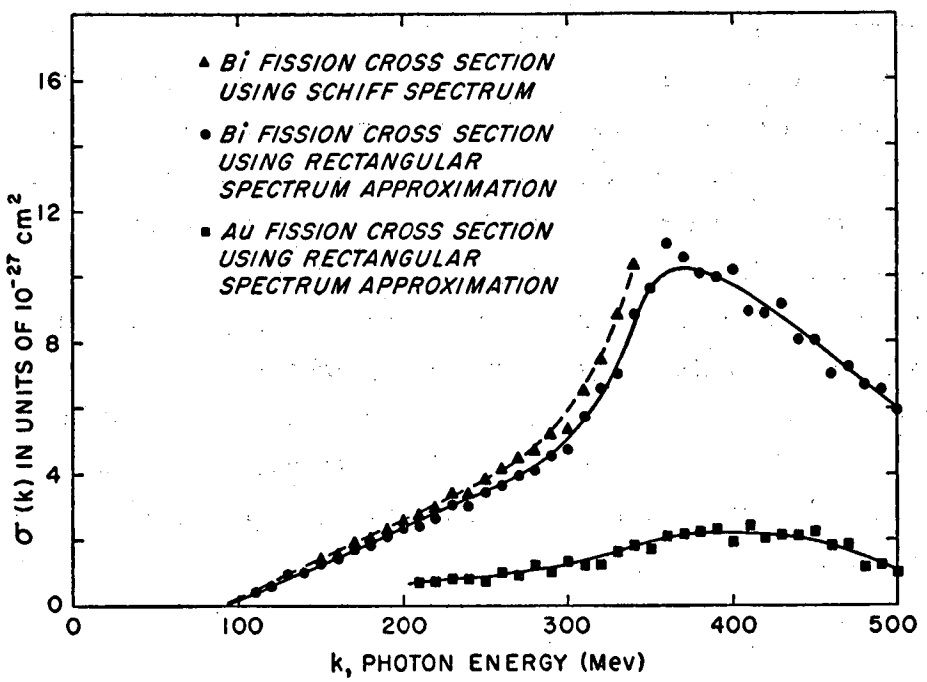

MU-19430

Fig. 12.83 Photofission cross section σ(k) of Bi and Au as a function of photon energy. These curves were obtained from a smoothed plot of the data in Fig. 12.76. The dotted curve was calculated by assuming a Schiff bremsstrahlung spectrum that varied with energy, using the photon difference method of KATZ and CAMERON.[233] The solid curves were calculated in a rectangular spectrum approximation. From Jungerman and Steiner, Phys. Rev. 106, 585 (1957).

Acknowledgements: The author wishes to thank his many colleagues at the Lawrence Radiation Laboratory who have made helpful suggestions regarding matters discussed in this report. Among others, he would like to mention J. Alexander, G. Gordon, T. D. Thomas, V. Viola, J. Gilmore, R. Vandenbosch and L. Winsberg.

He wishes to give special thanks to Professor G. T. Seaborg for a critical reading of the entire manuscript. Mrs. Susanne E. Vandenbosch and Miss Eileen Carson devoted a great deal of time to the assembly of data, preparation of tables, checking of references and preparation of figures and other details involved in the preparation of a manuscript of this size. Expert assistance in the typing of several drafts of this report was given by Miss Yoshi Uchida, Mrs. Lily Hirota and Mrs. Libbi Brecher.

Many individuals from other laboratories were generous in supplying figures from their publications. For this, thanks are extended to R. E. Bell, J. P. Butler, F. Brown, B. L. Cohen, R. B Duffield, A. W. Fairhall, G. Friedlander, I. Halpern, R. L. Henkel, J. Huizenga, J. D. Jackson, L. Katz, R. B. Leachman, M. Lindner, J. M. Miller, R. A Schmitt, P. C. Stevenson and N. Sugarman.

This report was prepared as an account of Government sponsored work. Neither the United States, nor the Commission, nor any person acting on behalf of the Commission:

A. Makes any warranty or representation, expressed or implied, with respect to the accuracy, completeness, or usefulness of the information contained in this report, or that the use of any information, apparatus, method, or process disclosed in this report may not infringe privately owned rights; or

B. Assumes any liabilities with respect to the use of, or for damages resulting from the use of any information, apparatus, method, or process disclosed in this report.

As used in the above, "person acting on behalf of the Commission" includes any employee or contractor of the Commission, or employee of such contractor, to the extent that such employee or contractor of the Commission, or employee of such contractor prepares, disseminates, or provides access to, any information pursuant to his employment or contract with the Commission, or his employment with such contractor.